LA-12022-PR
Progress Report

Accelerator Technology Division

Annual Report
FY 1990

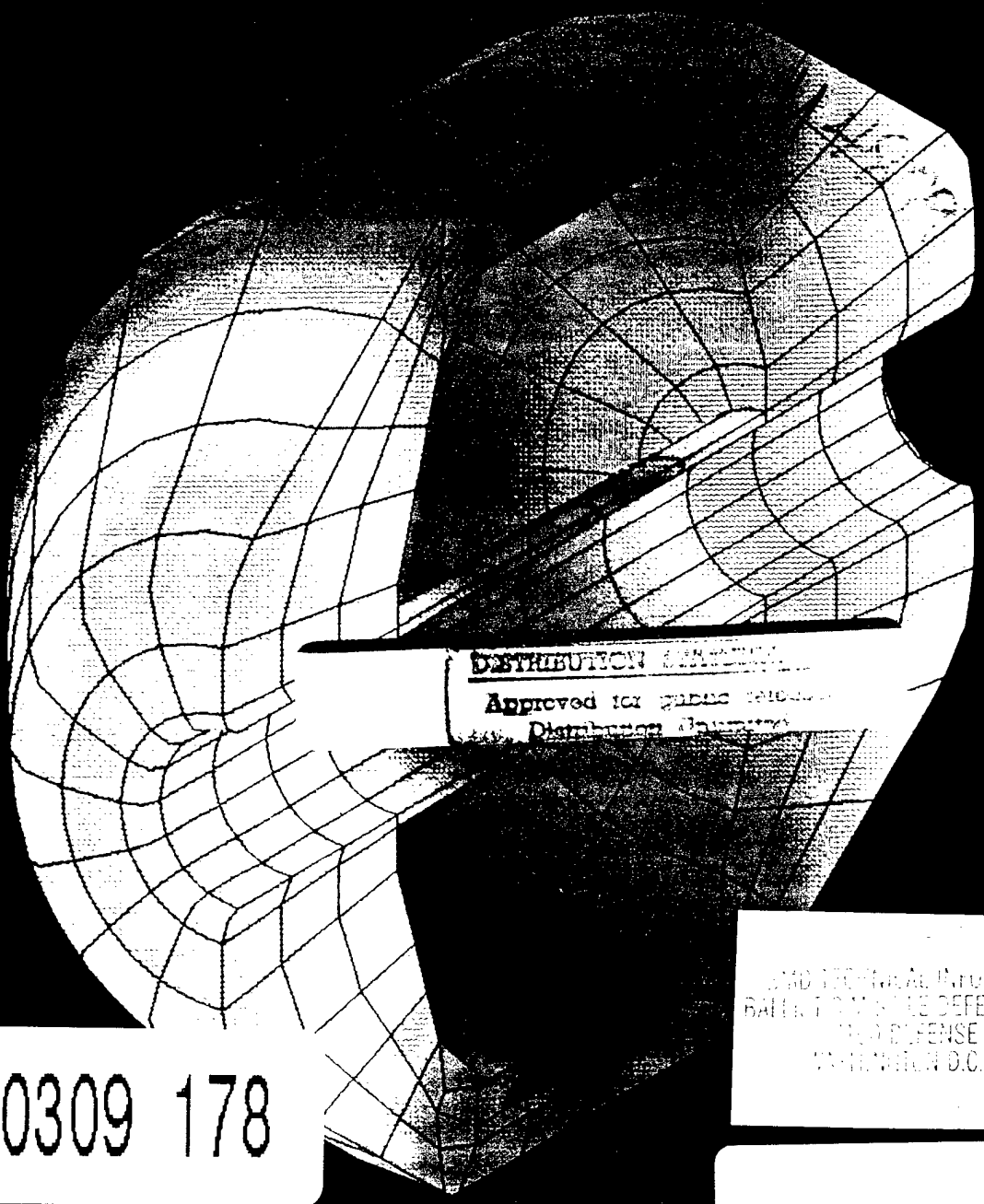

Los Alamos
NATIONAL LABORATORY

Los Alamos National Laboratory is operated by the University of California for the United States Department of Energy under contract W-7405-ENG-36.

Produced by AT and IS Divisions

Production coordination by Carolyn Beckmann, AT-DO
Art layout and design by Pete Sandford, IS-12
Printing coordination by Guadalupe Archuleta, IS-9

Acknowledgment: Special thanks to Anita Rodriguez and Barbara Maes

Front cover: Temperature contours of a cryogenic GTA drift tube resulting from the combination of power dissipation and gaseous helium cooling. Red indicates temperatures above 44 K, and yellow, green, and blue indicate progressively cooler regions. Drawing by Stephen Black.

The four most recently published reports in this series, unclassified, are LA-10719-SR, LA-10809-SR, LA-11295-SR and LA-11838-PR.

An Affirmative Action/Equal Opportunity Employer

Accession Number: 4879

Publication Date: May 01, 1991

Title: Accelerator Technology Division: Annual Report FY 1990

Personal Author: Schriber, S.O.; Hardekopf, R.A.

Corporate Author Or Publisher: Los Alamos National Laboratory, Los Alamos, NM 87545 Report Number: LA-12022-PR

Descriptors, Keywords: Ground Test Accelerator GTA Los Alamos Free Electron Laser Base GBFEL Neutral Particle Beam NPB Nuclear Waste ATW DEW FEL Conversion

Pages: 00122

Cataloged Date: Feb 10, 1994

Document Type: HC

Number of Copies In Library: 000001

Record ID: 28612

LA-12022-PR
Progress Report

UC-910
Issued: May 1991

Accelerator Technology Division

Annual Report FY 1990

Stanley O. Schriber, Division Leader
Robert A. Hardekopf, Deputy Division Leader

Los Alamos
NATIONAL LABORATORY
Los Alamos, New Mexico 87545

Contents

Foreword

S. O. Schriber, Division Leader; R. A. Hardekopf, Deputy Division Leader

The Accelerator Technology (AT) Division continued in fiscal year 1990 to fulfill its mission of developing accelerator science and technology for application to research, defense, energy, and other problems of national interest. Highlights for the year included

■ Successful operation of the first cryogenically cooled radio-frequency quadrupole (RFQ). The RFQ accelerated a beam of negative hydrogen ions to the design energy of 2.5 MeV with high transmission and beam quality. This is the first acceleration stage for the Ground Test Accelerator (GTA), being developed for the Neutral Particle Beam (NPB) program sponsored by Strategic Defense Initiative Organization (SDIO) and the US Army Strategic Defense Command.

■ Completion of a conceptual design for a high-current, continuous-wave linear accelerator for application to accelerator production of tritium (APT). The concept was reviewed by a Department of Energy Energy Research Advisory Board panel that found the APT proposal and the accelerator design to be technically sound.

■ Initial operation of the High Brightness Accelerator FEL (HIBAF), designed to produce an intense electron beam for free-electron laser (FEL) research. First acceleration of the high-current beam from a photoelectric injector to 17 MeV produced exceptional brightness that verified the design codes. This will lead the way to a new generation of high-efficiency FELs.

■ Organization and hosting of the Conference on Computer Codes and the Linear Accelerator Community in Los Alamos, January 22-25, 1990. This conference is described further in Group AT-6 Section of this report.

■ Hosting of the 1990 Linac Conference, a biennial international conference dedicated to advances in linear accelerator technology. This 5-day conference, held in Albuquerque, attracted 325 participants from 15 countries.

These accomplishments and others are discussed further in both the program and group sections that follow.

Organizationally, we formed a new group, AT-10, to concentrate on installation, operation, and commissioning of GTA. Group AT-2, the accelerator experiment and injector group, was combined with the operations section from AT-4 to form this new group.

Rebecca Montoya, Sue Nicol, Jan Barbe, Rhondda Bradbury, Marilyn Thomas
Division Office Administrative Staff

John Dussart, Property Management; Sharon Brock, Budget Fiscal Specialist;
Wayne VanderHam, Financial Section Leader

AT Division's staffing level at the end of FY 1990 was 242, a decrease of about 8 people from FY 1989. Of the 242, 120 were staff members, 91 were technical support personnel, and 31 were administrative support personnel. The staff members were balanced between science and engineering disciplines, with the engineers having expertise in mechanical, electrical, and computing science. In addition to Laboratory employees, we continued to employ a large number of technical support personnel from contracting organizations and from our GTA industrial partner, the Grumman Aerospace Corporation.

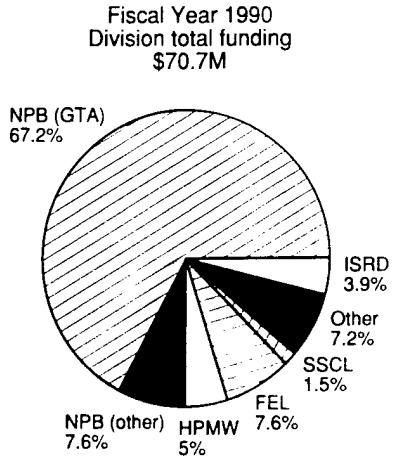

Programmatically, AT Division increased the funding level approximately 9% over FY 1989. The chart on this page indicates that about 67% of the division was engaged in the GTA program, the same percentage as FY 1989. As the program development section of this report describes, we are continuing a strong effort to diversify the division's funding with new programs.

For FY 1990, the Division was successful in obtaining Laboratory Institutional Supported Research and Development (ISRD) funds for fabrication of superconducting cavities, development of a large-orbit gyrotron, and investigation of neural networks for accelerator control. In addition, we coalesced several related ISRD-funded projects into a major new Laboratory Special Supporting Research Initiative (SSRI) to develop advanced free-electron lasers. This initiative is further described in the program section that follows.

During FY 1990 the Division submitted 16 proposals for FY 1991 ISRD funding in three categories: engineering and base technologies; mathematics and computational sciences; and plasmas, fluids, and particle beams. We were successful in obtaining approval for 4 of these initiatives, in addition to continuation of the SSRI.

A listing of unclassified publications by AT-Division staff appears in Appendix A, and internal technical notes are included in the group sections. In addition to contributions at the 1990 Linac Conference and other international meetings, division members contributed strongly to meetings held by the sponsors of the SDIO NPB and FEL programs.

On the following pages, we describe FY 1990 progress with summaries of our major programs, program development initiatives, and group accomplishments.

Susie Scoggins, Security; Carolyn Beckmann, Publications; John Graham, Safety

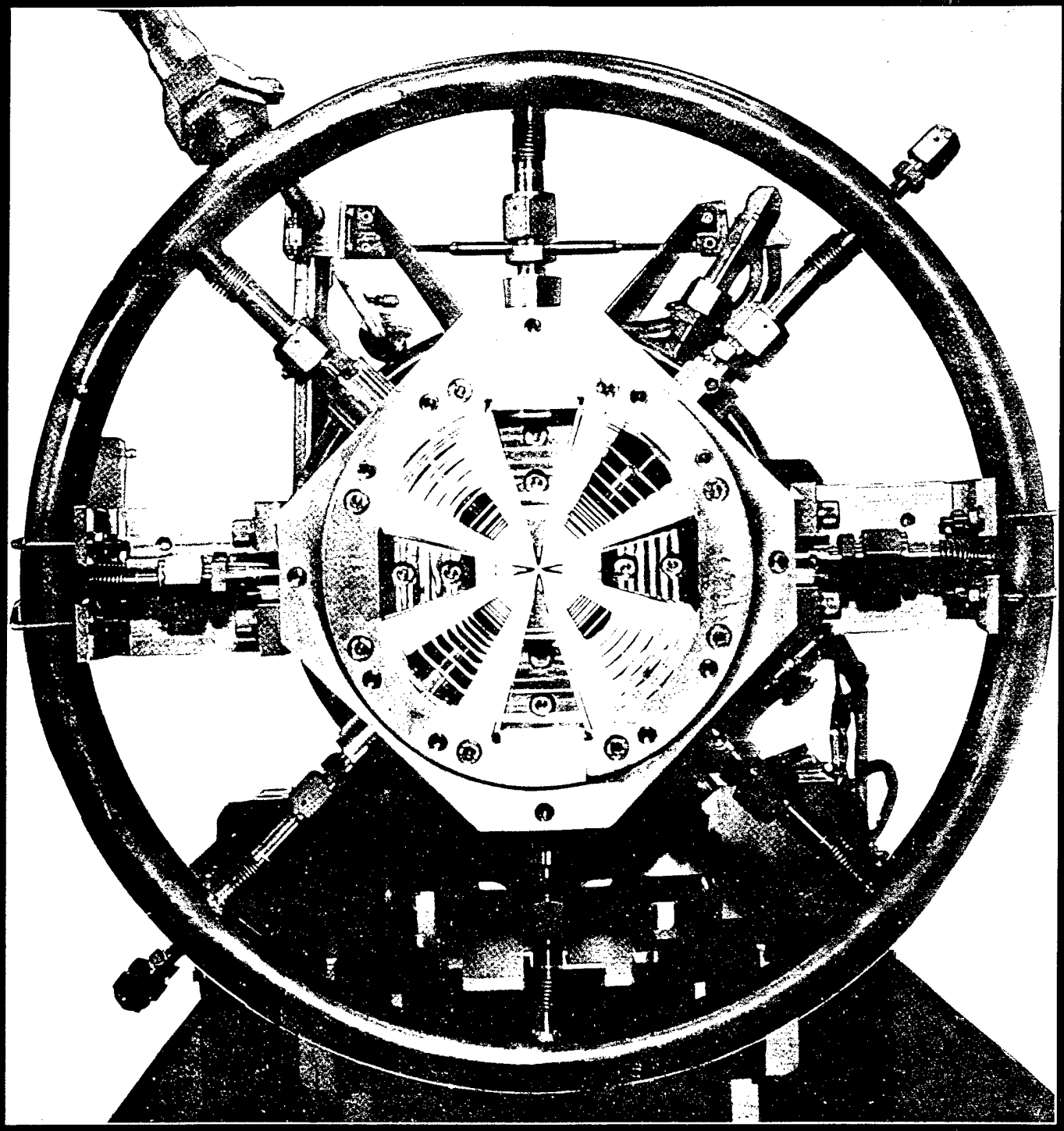

End view of the GTA RFQ core tank.

Major Programs

Jorg Jansen, GTA Program Manager, Ed Heighway, Technical Program Manager for GTA

Kenneth McKenna, GBFEL Project Office Leader

Larry Warner, Program Manager for High-Power Microwaves

The Ground Test Accelerator (GTA) Program

Introduction

The Ground Test Accelerator (GTA) program made rapid progress throughout the past year. Emphasis shifted from design and procurement to installation and commissioning. The injector was installed and commissioned in the GTA tunnel. The radio-frequency quadrupole (RFQ) was fully assembled and installed in its cryostat. On 15 October, a 25-mA, low-emittance ion beam was accelerated for the first time to 2.5 MeV through the cryogenically cooled RFQ.

Another success was the demonstration that two low-energy ion beams can be funneled without emittance growth. During this experiment we also tested the GTA diagnostics extensively. In parallel with the installation and commissioning efforts, the final design and fabrication of the first drift-tube linac (DTL) tanks continued. A 425-MHz tetrode radio frequency driver was built and tested. A two-hole klystron modulator was built and tested with two 850-MHz klystrons. Controls are now operational for the injector and RFQ.

A dedicated team of about 220 people worked hard and long hours to make these successes possible. Approximately 170 Los Alamos people cooperated very closely with 20 engineers and scientists from Grumman Aerospace Company and with 30 people from several contract houses.

The industrial partnership with Grumman, a first on this scale for the Laboratory, has been very successful. The symbiosis of Grumman and Los Alamos talents has strengthened the entire neutral particle beam program (NPB). The intended transfer of technology to industry has been exemplary.

The experimental program has been divided into several stages. The objectives and performance goals of each stage have to be met before the next stage is undertaken. The 24-MeV GTA milestone is achieved via stages 1A, injector; 1B, RFQ; 1C, intertank matching section (IMS); 2A, first DTL tank; 2D, DTL tanks 2 through 10; 3A/B, optics; and 3C, beam sensing. The 100-MeV milestone is achieved by addressing the 24-100 MeV accelerator portion and doubling the magnet field strength in the optics.

Injector

In January the GTA injector was installed in the tunnel of Building MPF-365. Initial tests were conducted with the small angle ion source (SAS) in earlier tests in MPF-18. This source is limited to a 0.5% duty factor. Our plans are to upgrade this source for ultimate use at the design 2% duty factor. We have produced currents up to 92 mA. However, the emittance at the intermediate diagnostic station in the low-energy beam transport (LEBT) is 50% higher than the desired emittance. At the RFQ match point, it has grown to 300% of design emittance. For an apertured current of 20 mA, the proper beam match was obtained at the RFQ match point with the design emittance. Efforts continue to produce a current with less noise (upgrade of the SAS source or 4X source), to improve the design of the extractor geometry, and to shorten the LEBT, all with the intent to obtain the design emittance at 55 mA.

A full complement of beam diagnostics is used to commission the injector. A permanent diagnostic station is located in the center of the LEBT, between the two solenoid lenses. The station contains two emittance scanners, a viewing screen, a four-grid energy analyzer, a large-area faraday cup, a beam plug for the personnel safety system, and collimating apertures to produce pencil beams for RFQ and DTL tests. In addition to the permanent diagnostics, an auxiliary diagnostic station is in use at the end of the LEBT with two additional emittance scanners, a viewing screen, and another faraday cup. A beam-current toroid just after the first solenoid lens measures the beam current for on-line operation. Neutralizing gas pressure and hydrogen flow from the ion source are also monitored.

An interesting new diagnostic tool was used during the injector performance testing. Fluorescent viewing screens were installed in both diagnostic stations to measure the intensity distribution of the beam. The screen employed a thin film of Al_2O_3 sprayed onto an aluminum plate by a plasma jet. A charge-coupled device TV camera recorded the data, which were displayed on a computer screen. The intensity distributions at design perveance are generally uniform with rounded edges, but they quickly evolve into peaked or hollow distributions for conditions where a perveance match is not obtained. Thus, this diagnostic can rapidly establish or check the tune of the injector.

The emittance diagnostic employed on GTA is an improved version of the accelerator test stand (ATS) system. A number of improvements in the program and in the plotting options were incorporated into the new software package. The diagnostic was calibrated with a double-slit collimator placed in front of the scanner. The beam was steered and focussed to fill the admittance of the double-slit collimator and the resulting emittance distribution was measured with the scanner. The scanners were independently checked by moving the beam centroid in specified steps. This calibration confirmed the correctness of emittance software and motor pulse calibrations. We estimate that the absolute emittance error is less than 5% and is due primarily to the finite angular resolution of the slits in the scanner.

Radio-Frequency Quadrupole (RFQ)

The manufacturing of the GTA RFQ was completed very successfully. The mechanical structure met all performance requirements. One major design change was incorporated. Cryogenic bead pulls indicated that end-wall tuners were sufficient to stabilize the RFQ. Therefore, the eight complex azimuthal stabilizers were replaced by simple end-wall tuners.

One major problem was successfully solved. Commercially available fittings called trision fitings provided the transition between the stainless steel cryogenic manifolding and the aluminum structure of the RFQ. In spite of extensive initial testing, these fittings started to leak after the machining of the RFQ. It was found that the silver braze at the joint interface was not bonding properly to the aluminum. We pursued a variety of solutions, e.g., other brazes, explosive bonding, mechanical joining, etc. A Pb-In braze was found that exhibited the desired ductile behavior during failure at room and cryogenic temperatures. This braze was extensively tested and then used to join the fittings. The RFQ has been operational since the beginning of October without a leak in any of the 16 fittings. Explosively bonded fittings and mechanical joints have been prepared and tested as back-ups.

The copper plating of the RFQ was very successful. Adhesion has remained excellent after many cryo cycles, and plating thickness accuracies of ±0.3 mil were achieved on the vane tips — a remarkable achievement. Room and cryogenic temperature tuning resulted in a field flatness and a dipole component each of <1%.

The RFQ has been power conditioned to 130% of design power at a macro pulse length of 1 ms. It has operated repeatedly with reduced beam under vacuum and at cryo temperatures in the GTA tunnel. The performance meets predictions in terms of transmission, emittance growth, phase, and energy output. This was an extraordinary success, as these results were achieved immediately during the first few days of opertation.

Intertank Matching Section (IMS)

We have completed the design, fabrication and assembly of the IMS. The cavities have been tuned, and subassemblies such as the dynamic tuner have been tested at cryo temperatures. The fully assembled IMS is presently under high-power test in the fusion materials irradiation test (FMIT) tank.

One interesting component is the variable-field permanent-magnet quadrupole (PMQ). Four of these magnets are used in the IMS to provide maximum flexibility for matching the RFQ to the DTL. The magnets are designed to operate at room temperature. The field strength of each magnet may be varied by rotating a ring-shaped yoke around the magnet assembly. This varies the integrated field strength from about 2 T to about 6 T. The harmonic components of the magnetic field were measured throughout the operating range. They were less than the 2% allowable harmonic component tolerance.

Drift-Tube Linear Accelerator (DTL)

The GTA-24 DTL is subdivided into ten 1-m-long modules. Each cavity comprises an open tank with a cover lid incorporating a rectangular waveguide flange. Each module incorporates a variety of auxiliary components, including drift tubes with PMQs, drift-tube positioners, post couplers, rotary tuners, monitor loops, temperature sensors, and steering magnets and their positioners. In addition, a complex array of parallel and series cooling loops cools the components to cryo temperatures. The drift tubes in each module are aligned to a tolerance of ±0.05 mm at room temperature and to ±0.125 mm at cryogenic temperature. Steering magnets are aligned to a comparable tolerance but with a position repeatability of 0.025 mm. Each module can operate independent of the other DTL modules.

The design, machining, and brazing of the first two tanks is complete. Drift-tube PMQs have been manufactured and field mapped and are being assembled into the drift tubes. After assembly, each drift-tube lid is E-beam welded to the drift-tube body. Postcouplers, monitor loops, slug tuners, etc., are in various stages of completion.

Several interesting developments took place this year in support of the DTL design. An automated cryogenic mapping device was built for the measurement of drift-tube magnets. Field strength and spatial harmonics of the DTL PMQs were measured at both room and cryogenic temperatures. This required the development of a precision mapping coil that rotates at a constant velocity inside the bore of the small PMQs and guarantees high accuracies from room to cryo temperatures. In a qualification program, Westinghouse Hanford and Grumman Aerospace Corporation developed a low-cost method for electron-beam welding the drift-tube bodies. This is a departure from the traditional brazing of drift-tube bodies because the samarium cobalt permanent magnets cannot tolerate the high brazing temperatures. The drift-tube cover must be assembled to the drift tube with an electron-beam weld to avoid exceeding the maximum supportable temperature (100°C) of the enclosed permanent magnet material. Both companies demonstrated that electon-beam welding of the GTA drift tubes is feasible.

A taut-wire alignment technique was developed to locate the magnetic center of an array of permanent magnet drift tubes. In an earlier experiment four drift tubes were successfully aligned at room and cryo temperatures. Recently, 39 drift tubes were aligned with the same technique over a length of approximately two meters. This technique is so accurate that we will be able to align all drift tubes of a single DTL module at cryogenic temperature to an accuracy of ±0.125 mm.

Remotely controlled positioners were developed which permit the positioning of each DTL module under vacuum and at cryogenic temperatures. Electromagnetic proximity probes determine the precise position of the module. The independent scissor jacks provide a total range of movement of ±5 mm with six degrees of freedom. Each DTL module is mounted on an independent pedestal to negate the effect of temperature variation along the axis of the machine. The waveguide is enclosed within the pedestal.

Radio-Frequency (rf) Power

GTA's radio-frequency power is supplied by three 300-kW 425-MHz tetrode drivers, by four 50-kW 850-MHz tetrode drivers; two solid state 10-kW 1700-MHz solid state drivers; and ten 1-MW 850-MHz klystron drivers. The system is fully integrated and controlled by a central low-level reference generating subsystem. With the use of feedback loops proper amplitude and phase control is maintained for each accelerator structure. The system is located on the mezzanine of the GTA building outside the tunnel.

The first low-level control system, a VXI production unit, was tested with a cavity to demonstrate ±0.5% amplitude and ±0.5° phase control. The first 425-MHz tetrode driver was completed and tested first into a water load, then into a cavity. The driver finally operated with the RFQ as part of experiment 1B. Resonance is controlled with a six-port reflectometer. This unit was successfully tested with a cavity and is now operational on experiment 1B.

The exacting requirement for phase and amplitude control requires a phase stabilized rf transport system with a phase shift of <0.1°. This was achieved with the use of a diplexer developed to replace an expensive and cumbersome temperature-compensated cable system.

We presently own seven single-socket modulators that were bought for the original 425-MHz ballistic missile early warning system klystrons for GTA-1 (50 MeV). To save cost, we decided to convert these modulators to two-socket, 850-MHz operation. One two-socket modulator is now operational with a modified Clinton P. Anderson Meson Physics Facility klystron and a Varian prototype klystron both driving water loads.

Earlier in the year, we placed an order with Thomson Tubes Electroniques for 12 klystrons, each with a peak power of 1.25 MW, a frequency of 850 MHz, and a duty factor of 6%. The first klystron passed the acceptance test successfully and was delivered to Los Alamos in October. The next two klystrons will be tested in December.

Optics

The optics physics design was completed at the beginning of the year with a final design review in February. The engineering design is now in progress.

The first telescope objective magnet has been mapped at its final location in the tunnel to determine the field quality *in situ*. The magnet itself was specified to have harmonic amplitudes for n = 3 to 6, less than 2.5 mT at 40 cm. This high purity requirement results from an improved understanding of large-bore magnet construction and measurement derived from our magnet development program. The first magnet does not have a built-in octupole correction field. It will be used as part of the second telescope magnet in a revised scheme to reduce costs. All subsequent magnets will have an appropriate built-in octupole. Corrector magnets are employed between the four objective lenses to correct multipole harmonics. The design consists of several layers of Lambertson coil style coils placed on top of each other. Each layer, composing a given multipole, is made up of accurately constructed panels, with each panel corresponding to a single coil of the multipole. The panels are made by (1) bonding the appropriate thickness (either 22.35 mm or 0.49 mm) of copper onto a 0.254 mm glass-epoxy substrate, (2) etching or (for the thick copper) machining, (3) rolling to a precise radius, and (4) joining the two layers of each coil by pins in the coil center. Tabs on the panels ensure alignment. With some difficulty we found a manufacturer for the coils. The assembly must dissipate over 35 kW and hence requires water cooling.

The requirements on the GTA steering magnet are very demanding in terms of field uniformity under rapid cycling conditions. Eddy current effects must be minimized. We have constructed a half-scale prototype steering magnet to develop construction techniques and to evaluate concepts that will be used on the full-size magnet. The prototype magnet is 0.5 m in diameter and 1.0 m long. A thin-walled square cross section stainless tube is wound into 5-mm-wide grooves machined in a glass-epoxy mandrel. Water for cooling is run through the tubing in several parallel paths, with ports exiting through tees which pass through the mandrel. The channel winding was the most difficult part of the effort, requiring careful brazing of the tube sections and water ports. We used stainless steel to minimize eddy current effects. The winding is made from Litz wire, again, to avoid eddy current effects. The Litz wire of rectangular cross section is placed in contact with the cooling tube into the grooves of the glass-epoxy mandrel. The prototype steering magnet is now fully assembled and ready for field measurement with a point mapper. Final precision adjustments of the wire will be made to optimize field uniformity.

The ambient field in the GTA tunnel appreciably perturbs the beam. The dipole component deflects the beam up to 17 cm in its passage through the telescope. This will be corrected by a "Helmholtz corrector" scheme involving two single-wire coils in each plane extending over the telescope length. To measure the tunnel field we constructed a simple mapper, placed it in the tunnel, and took data. The mapper consisted of a radial magnetometer probe mounted on a motor-driven boom. A single rotation took

data at a finely spaced series of locations in the tunnel. Results confirm the desirability of dipole correction as well as the desirability of an easily compensable multipole structure.

Diagnostics

A large variety of permanent and temporary beam diagnostics had to be developed and built to support experiments 1 and 2. This list includes microstrip probes, toroids, slit and collector emittance scanners, LINDA code, residual gas fluorescent devices, faraday cups, a four-grid analyser, a flying wire scanner, harps, and beam loss monitors.

The single-beam funnel experiment served as the ideal test bed at room temperature for testing these devices in a realistic environment. Subsequently, final designs were made of the devices and their associated complex electronics.

A large number of these devices are now operational in the LEBT and RFQ and in the diagnostic station at the RFQ output.

Controls

The top priority this year was the implementation of a supervisory control system to support experiment 1. Eleven input/output controllers (IOCs), three operator interfaces (OPIs), two servers, and several data analysis work stations, with a secure support network have all been installed in MPF-365.

These first IOCs are the basis of the entire control system for 24-MeV and higher energy GTA. For 24-MeV, 17 of the remaining 27 IOCs are copies of those already implemented, thus simplifying the implementation and configuration control tasks. To further expedite the control hardware production, we have developed a convenient and powerful tool that has been incorporated into the IOC configuration process: the definition of functional devices. Standardized device descriptions simplify wiring, documentation, and database configuration tasks and reduce control system complexity. Instead of tracking large numbers—about 8000 components and about 160,000 wire, cable, and termination descriptions—we have grouped channels and their wiring into functional units called devices. Once defined, they can be replicated at low cost and easily documented. This results in the need to track only about 35 device types for GTA. This standardization speeds hardware configuration and implementation and improves documentation. We have used the device definition process on the vacuum system, RFQ/IMS, DTL, and diagnostics IOCs. This process resulted in a completely configuration-controlled implementation of the controls for these subsystems through the definition of about 20 device types.

We placed significant emphasis on demonstrating integrated control. Injector and LEBT controls and the emittance data acquisition and analysis codes were completed and validated. A VXI-based rf controlled IOC was installed and auto resonance control was demonstrated. The vacuum and RFQ controls were installed, and integrated RFQ controls screens were developed and tested to support commissioning and experiment 1B.

The backbone of the control system, the Ethernet network, was installed in building MPF-365 and successfully tested. The full network will support 8 OPIs and an IOC in the control room; 16 IOCs, an OPI, and a Sun in the equipment area; and 19 IOCs, an OPI, and a Sun in the mezzanine. The Suns modify the configuration of the control database, access the system documentation, and provide data analysis. The network is based on a system of hubs and stars. A number of multi-media access centers form the hubs. Attached to the same control network, in building MPF-31, a variety of machines support the network. These include a Sun and IOC server and the OPI servers.

There are also connections to buildings MPF-18 and MPF-409 to support subsystem and component development.

Single-Beam Funnel Experiment

A major success was achieved in January: we demonstrated on ATS that one of ultimately two beams can be funneled with little emittance growth, a primary requirement for a high-current NPB device.

The buncher cavities successfully confined the longitudinal bunch and restricted longitudinal emittance growth, an issue of unique importance to the NPB system. The confined geometry of GTA requires the use of movable PMQs for beam steering. These PMQs were successfully tested on the funnel experiment thus qualifying this technology for GTA. The deflector is the most crucial funnel device since it is the final active element combining the beams onto a single axis. The deflector worked flawlessly, providing optimum performance (deflection, minimum emittance growth) at the design parameters.

A second objective of the funnel experiment was to combine rf power, controls and diagnostics into an integrated operation. The achievement of this objective was very important because it served as a model of the GTA subsystem and system integration.

A third objective was to demonstrate that a large fraction of the GTA diagnostics will work in the real environment of an integrated system. This objective was also achieved. The results served as final design inputs for the GTA diagnostics.

GTA Facility

The GTA facility is now functional and houses a number of GTA assembly and operational activities. All the building laboratories are occupied and functional. The structures tuning and alignment laboratories are functional. The majority of the rf power equipment on hand is installed in the facility and is being checked out in place. A new 750-W cryogenic refrigerator is installed and is in use for the RFQ cryo test. Construction of the 40-kW liquid hydrogen and gaseous helium cryo system is underway. The cooling water system (through experiment 2A) is functional. Many safety modifications and upgrades identified and mandated by safety inspections have been completed, such as correct labels, alarms, O_2 monitors, and correct door operation. We have installed a large number of the required wire trays, conduits, coaxial cable, and waveguides. The entire beam tunnel has been surveyed, and alignment markers and monuments have been set in place. Many equipment and instrumentation racks have been installed and are operational.

A computer-aided theodolite system is used for the precision alignment of GTA hardware. Many alignment targets are permanently installed on strategic parts of the GTA equipment. Other targets can be installed into mounting holes when needed. An IBM personal computer is the processor for the encoded angle information from each theodolite. This computer serves as the operator interface, data archiver, and calculator for determining absolute space location for each target.

The tuning laboratory is the primary facility for the low-power rf checkout of all rf structures. Bead-pull apparatus and precision rf measuring instruments are the chief tools. Off-line modeling and measurements are compared with SUPERFISH simulations. Low-power measurements are used to predict tuning sensitivity, dipole suppression, and longitudinal tilt. The cavity resonance frequencies and resulting Q are measured after each modification. Calibration and precise low-power tailoring of rf pickup loops and the rf drive loops are made at low power.

The high-power structures laboratory is the facility for the measurement of cavity Q gain under high-power conditions, for the fundamental studies of field breakdown and development of surface preparation procedures, and for power-conditioning cavities. Final matching of the rf drive lines, pickup loops, tuners, and stabilizers is achieved under high-power conditions. We calibrate field pickup loops against the absolute measurement of the gap potential by observing peak x-ray energies and final cavity conditioning under beam-current conditions.

Summary

The GTA team can look back with pride for having accomplished so much during 1990. The injector and RFQ are operating in the tunnel with rf power, all necessary controls, and beam diagnostics. The IMS is under test in the FMIT tank, several DTL tanks have been machined, klystrons and modulators have been tested, designs for the optics are being completed, drift-tube PMQs are under test at cryogenic temperatures, the prototype steering magnet is ready for field mapping and integration is in full swing.

Our plans for 1991 are to complete the integration of the first ten DTL tanks with the injector, RFQ, and IMS. We will characterize the low-energy portion of GTA up to 3.2 MeV and 100 mA. A DTL assembly line will produce most of the remaining nine tanks up to 24 MeV. The telescope will be fabricated, the matching section will be readied for installation, and beam diagnostics will be prepared for the commissioning of the entire DTL in 1992. The 850-MHz klystron modulators will be partially assembled and installed. And, tying it all together, the integrated control system will permit system-wide control from the new control room.

Los Alamos Ground-Based Free-Electron Laser (GBFEL) Program

The Ground-Based Free-Electron Laser (GBFEL) program represents a critical step in the development of ground-based lasers for ballistic missile defense. Ultimately, the powerful light beams generated by the ground-based laser will be directed by relay mirrors in space toward adversary ballistic missiles, destroying these missiles in their boost phase. The objective of the first phase of the GBFEL program is to build a laser at White Sands Missile Range to verify the feasibility of the laser system. Subsequent experiments will explore the laser beam's ability to propagate through the atmosphere without excessive degradation. Following these demonstrations, the laser system's performance will be upgraded to address the feasibility of an actual free-electron laser ballistic missile defense system.

In 1989, the Army Strategic Defense Command selected Los Alamos and its industrial partner, the Boeing Aerospace and Electronics Company, for the design, development, and construction of the laser system for the GBFEL demonstration experiment at White Sands. This selection concluded a several-year competition between Los Alamos/Boeing and Lawrence Livermore National Laboratory/TRW, Inc.

Los Alamos and Boeing each has over 10 years of experience in successful free-electron laser research and development, and a FEL is operating at each site. The division of GBFEL program tasks between Los Alamos and Boeing reflects the strengths of each organization. Los Alamos is developing the GBFEL science and technology base, providing the system physics design and verifying much of the engineering design, conducting concept-validation experiments, and developing many of the GBFEL system components. Boeing is providing the overall program management and engineering development. Boeing is also addressing issues associated with the integration and demonstration of relatively high-average-power systems.

The Los Alamos Accelerator Technology (AT) Division has traditionally been at the leading edge of FEL science and technology development. For example, researchers with AT invented the photoelectric injector, a system capable of generating electron beams far brighter than those generated by conventional means. This injector enables compact and efficient FELs, and it will be an integral part of the GBFEL device at White Sands. A major fraction of the Los Alamos GBFEL research and development effort is carried out within AT Division. Specific tasks include basic FEL research and validation experiments on the High-Brightness Accelerator FEL (HIBAF) facility; the design, development, and demonstration of the GBFEL accelerator cavities; the adaptation and enhancement of computer-control techniques and software developed for the NPB program to the GBFEL device; and the design and fabrication of the GBFEL electron-beam transport system.

The HIBAF facility has been specifically designed to allow the resolution of critical issues associated with the design and development of the GBFEL system. HIBAF is a very high beam-brightness FEL design using an integrated set of computer codes called INEX (integrated numerical experiment); it is highly instrumented for detailed investigation of GBFEL physics. The HIBAF accelerator operates at the GBFEL design value of micropulse charge, emittance, peak current, and macropulse average current. Accordingly, experiments on HIBAF provide the input required to verify and refine the predictive capability of INEX in the high-performance GBFEL regime. This verification and refinement process is essential, since the final physics design of the GBFEL device is critically dependent on the INEX code predictions. The most recent accomplishment on HIBAF is the long-term demonstration of a high-current photoinjector functioning in the environment of a routinely operating accelerator.

The GBFEL accelerator cavities are being designed and optimized to satisfy stringent physics parameter requirements, such as electron-beam quality, and engineering requirements; such as thermal and frequency control. The combined efforts of AT Division accelerator physicists and engineers are being directed toward the physics/engineering design, prototyping, cold modelling, and hot testing of these GBFEL accelerator structures. Throughout this detailed process, outstanding technological issues associated with the development of these unique structures will be identified and resolved.

The GBFEL control system hardware and software architecture is based on the control system developed by AT Division for the NPB GTA that is currently under construction at Los Alamos. By using an extension of the GTA control-system technology, we reduce the GBFEL program cost and risk. The GBFEL control system will incorporate the common run-time environment (CORE) system software developed at Los Alamos. Functionally, the CORE software supports low-level input/output through a distributed run-time database, systemwide access to the database, sequential and continuous system control, data logging and archiving, and supervisory control of the GBFEL device. The CORE software will be complemented by an extensive Toolkit that provides a powerful applications development capability.

The principal goal of the electron-beam transport task is to design and construct an achromatic bend system for transport of the electron beam to the beam dump after the beam has given up a portion of its energy producing laser light. This is a complex design project because the spent beam consists of a double-peaked beam-energy distribution. High-order magnetic-optics codes are being enhanced and utilized for the design of this system. This task also encompasses magnet construction and measurement, beam-diagnostics fabrication and implementation, and a beam-expansion system design for safely dissipating the beam energy on the beam dump.

These GBFEL development projects in AT Division are being integrated with ongoing GBFEL activities in other Laboratory divisions, combining the resources and expertise of an extensive portion of the Laboratory in the development and enhancement of FEL technology. Other divisions participating in the GBFEL program are Chemical and Laser Sciences (CLS), Materials Science and Technology (MST), Physics (P), and Applied Theoretical Physics (X).

The High-Power Microwave (HPM) Program

AT Division maintains a program management and program development effort in high-power microwaves (HPM) coordinated with HPM program management in the Conventional Defense Technology office of the Defense Research and Applications Directorate. At present, the same individual occupies both positions. This section presents an overview of that effort, which is described in detail under AT-9 activity since virtually all Division work in this area is conducted in that Group.

It has been recognized from the earliest days of radio that electromagnetic radiation (EMR) at rf wavelengths has potential as a weapon. Although technology did not effectively support this application of EMR until recently because of limitations on rf power at appropriate wavelengths, it has now become feasible to disrupt or destroy military electronics at useful ranges. Vulnerability considerations have shown that the appropriate wavelengths are in the microwave regime. Various agencies of the Department of Defense (DoD) have active programs to develop HPM weapons. The Laboratory and Division have participated for a number of years because of the unique capability here and because of potential synergism with accelerator applications within the Laboratory mission, as noted below.

The DoD has long been concerned about the *accidental* adverse effect of HPM on military systems, such as that aboard modern naval ships where nearby systems can interfere with one another. With the growing possibility of *intentional* interference or destruction by a microwave weapon, this concern has multiplied and has resulted in extensive programs to understand the vulnerability of US military systems to HPM. A related interest in HPM effects resulted in funding by the DOE and its predecessor agencies as well as the DoD because of the importance of the "electromagnetic pulse" from nuclear weapons. Again because of the availability of unique rf sources, instrumentation, and facilities, the Laboratory and Division have for many years participated in these vulnerability programs.

Future generations of high-performance rf accelerators will require amounts of rf power well beyond that available through a reasonable number of current technology sources. Thus, a strong source-development effort is an important part of the nation's rf accelerator program. Work on advanced sources for this application has also been an important part of the Division's past HPM activity.

The main thrusts of HPM program development have been to participate actively in national HPM program management and to detect and pursue opportunities to apply the Division's unique capabilities to HPM problems of national importance. HPM program management is intended to ensure effective technical and financial execution of programs, once funded, and to conduct sponsor liaison. To learn about the technical work performed in this area, the reader is invited to review the section of this report that covers Group AT-9.

Electron beam image from the high-brightness accelerator shows an extremely bright and laminar electron beam. A photo cathode was illuminated with laser light and was masked to produce electron emission in the form of the letters "FEL." Seven meters from the photo cathode, after having been accelerated to 17MeV, the beam was imaged. This demonstrates an extremely linear machine.

Program Development

Brian Newnam, Robert Jameson (standing); Don Reid, and George Lawrence, Program Development (seated)

Neutral Particle Beam (NPB) Power Systems Highlights

AT Division at Los Alamos has continued to be involved in developing technology that has the capability of generating large amounts of rf power in space in support of the Laboratory NPB and space-based free-electron laser (SBFEL) efforts. Each of these devices requires MW of rf power for operation. Since both devices are intended for space deployment, the power system necessary to drive them must be very lightweight and very efficient. AT Division has been directly responsible to the Strategic Defense Initiative Organization for managing the development of high-efficiency, lightweight rf amplifiers for this application.

One of the major accomplishments during the past year was the completion by Varian/Eimac of the 425-MHz Klystrode rf amplifier shown in Fig. 1.1. The Klystrode has an input similar to a gridded tube amplifier and a conventional klystron output. The amplifier has excellent potential for space applications because it is much smaller than a klystron at equivalent power levels and has a beam efficiency greater than 70%. This amplifier achieved an output power of 550 kW at a pulse length of 10 ms and a duty of 10%. The gain was 21 dB. Of significant interest is the efficiency vs rf drive characteristic, which is very flat with an input rf drive variation of 3 dB. Efforts are now under way to duplicate or improve this performance at 850 MHz.

Work has also been conducted during the past year to develop solid-state devices to operate at high-power levels at 850 MHz. GTE have been working to extend their static induction transistor (SIT) technology from 425 MHz to 850 MHz and have succeeded very well. They are still working at the chip level but have achieved 300-W continuous wave (cw) from a two-chip set at 850 MHz, with greater than 75% drain efficiency when the chips are cooled to about 80 K. More significantly, they have proven that the devices work just fine at 30 K, which is a significant accomplishment for application in the NPB and SBFEL programs. Based on this work, it now appears that the technology is available to make a transistor capable of 500-W cw at 850 MHz.

Los Alamos has also been heavily involved in the power system demonstrator (PSD), a program managed by the United States Army Strategic Defense Command. The intention of this program is to integrate all of the NPB power-system technologies into a fully operational ground demonstration. This demonstration will show that an efficient, lightweight, and space-qualifiable NPB power system can indeed be designed, built, and tested. During the past year, the two competing contractors have designed an NPB power system and are now extracting from that design the PSD. A down-select is expected in the March–April 1991 time frame.

Figure 1.1. The 425-MHz Klystrode body.

Materials Testing Facilities

Introduction

During 1990, the magnetic fusion and inertial confinement fusion programs were thoroughly reviewed by the National Academy of Science (NAS) and by a DOE Fusion Power Advisory Committee (FPAC). The reports of these two groups emphasized that materials testing is a major issue in the continued progress toward operational fusion devices, that materials testing is a long lead time area, and that new testing facilities are urgently needed to make any real progress. It is now generally agreed within the world community that the D-Li (deuteron bombarding a lithium target) intense neutron source is the best technology for a near-term facility. In this source, an intense deuteron linear accelerator drives a molten target, producing neutrons that bombard material specimens in a test chamber. An internationally funded facility, called the International Fusion Materials Irradiation Facility, is under discussion.

AT Division has been a prime mover in bringing the required deuteron accelerator technology to the materials testing application since the FMIT program, accomplished between 1978 and 1984.

Achievements

During this fiscal year, no funding was available. However, we carried out a number of interactions with the materials testing community as both as a continuing service and an effort to establish an initiative according to the NAS and FPAC recommendations. These included providing input to the FPAC committee deliberations and continuing our consultative involvement with the Japanese Energy Selective Neutron Source program. In view of shrinking fusion budgets and a broad array of basic materials development beyond fusion's specific requirements, the Japanese have proposed a smaller scale, but technically advanced, basic materials testing research facility that they could finance themselves, without international participation.

Future Plans

During FY 1991, we will interact strongly with the DOE and the international community to help execute the NAS and FPAC recommendations. We expect to develop a specific proposal when the parameters and ground rules for the materials testing facility are worked out. We will continue to be involved in the Japanese activities and will engage in efforts to determine if an internationally funded testing facility of larger scope can be arranged.

Accelerator Transmutation of Nuclear Waste (ATW)

In late 1989 and early 1990, an ad hoc panel of the DOE's Energy Research Advisory Board (ERAB) reviewed a Los Alamos/Brookhaven proposal for accelerator production of tritium (APT).[1] This proposal was based on the use of a very high-power proton linac with a 1.6-GeV, 250-mA cw beam driving a high-intensity spallation neutron source. The accelerator design concept developed in the summer of 1989 by an AT Division led team was found to be technically sound by the ERAB/APT panel.

Stimulated by the positive ERAB finding on the credibility of a high-power linac, our colleagues in P and T Divisions opened an investigation into the potential of applying a high-flux, accelerator-driven neutron source to the transmutation of the long-lived actinides and fission products in the accumulated defense nuclear wastes of Hanford, Savannah River, and other sites. The cleanup of these wastes has become a matter of intense public concern and is now one of the most critical problems facing the DOE.

A working group, consisting of members of AT, P, T, N, and A Divisions, formed in early 1990 to study accelerator transmutation of nuclear waste (ATW) concepts. The group quickly discovered that, by directing the high-intensity proton beam to a lead-bismuth target surrounded by a region of moderating material (D_2O), very high fluxes of thermal neutrons (>10^{16} n/cm^{2}s) could be obtained in a large working volume. C. Bowman (P-17) observed that in such unprecedented thermal neutron fluxes it would be possible to rapidly burn higher actinides such as ^{238}Np in a two-step process and also to rapidly convert long-lived fission products (such as ^{99}Tc) to stable or short-lived products. The general ATW concept is illustrated in Fig. 1.2.

A laboratory-wide effort involving many technical Divisions (AT, P, N, A, T, NMT, MST, MP, and X) assembled under the leadership of Ed Arthur (T-DO) to study ATW and related concepts and to develop a broadly based program involving many of the Laboratory's capabilities. A particularly exciting variant of the ATW scheme is the idea of using an accelerator-driven thermal neutron source to burn fertile materials such as ^{232}Th and ^{238}U in a subcritical assembly. This plan would efficiently generate fission power while at the same time continuously burning up the nuclear waste produced with the excess neutrons available in the process. This idea, denoted "Energy Production Without a Long-Term Waste Stream," has caught the imagination of many people inside and outside the Laboratory.

In the latter part of 1990, efforts of the ATW team have focussed on developing a coherent reference concept matched to DOE waste cleanup requirements, particularly addressing the long-lived fission product wastes at Hanford. Briefings on ATW and the energy production scheme were given to all levels of DOE, including the Secretary of Energy, and to several important management and advisory bodies inside and external to the Laboratory. We have sought DOE funding for an expanded ATW program. At present, it appears that up to $3 million will be available for more detailed ATW studies in FY1991. Ideas have evolved rapidly and have stimulated much interest laboratory-wide as well as in the outside world.

At year end, a high-level external committee conducted a comprehensive technical review of our waste-transmutation and energy-production concepts.[2] This committee strongly endorsed continued pursuit of these programs by Los Alamos National Laboratory in FY1991. The briefing book describing our ideas is available as Los Alamos National Laboratory document LA-UR-90-4432.

Other publications describing the ATW scheme, with the emphasis on the accelerator design and technology include references 3, 4, and 5.

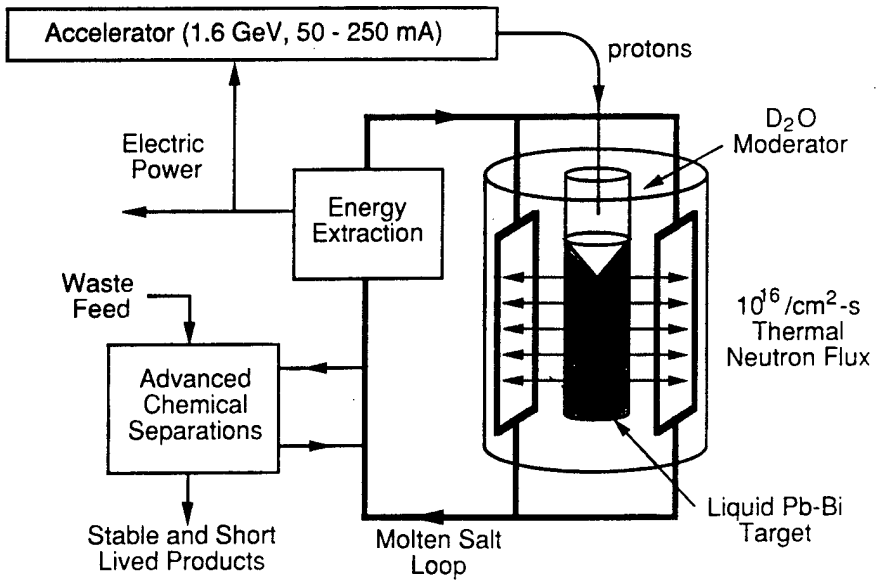

Figure 1.2. Los Alamos National Laboratory scheme for accelerator transmutation of waste.

References

1. "Accelerator Production of Tritium, a Presentation to the Energy Research Advisory Board," October 25, 1989, Los Alamos National Laboratory document LA-UR-90-3651.

2. "A Los Alamos Concept for Accelerator Transmutation of Waste and Energy Production (ATW), External Review," December 10-12, 1990, Los Alamos National Laboratory document 90-4432.

3. G. P. Lawrence, "New Applications of High-Power Proton Linacs," *Proc. 1990 Linear Accelerator Conference*, Albuquerque, NM, September 10-14, 1990, in press; Los Alamos National Laboratory document LA-UR-90-3309.

4. G. P. Lawrence, "High-Power Linear Accelerators for Tritium Production and Transmutation of Nuclear Waste," *Proc. Eleventh International Conference on Application of Accelerators in Research and Industry*, Denton, TX, November 5-8, 1990, Los Alamos National Laboratory document LA-UR-90-3315.

5. T. P. Wangler, G. P. Lawrence, T. S. Bhatia, J. H. Billen, K. C. D. Chan, R. W. Garnett, F. W. Guy, D. J. Liska, M. R. Shubaly, S. Nath, and G. H. Neuschaefer, "Linear Accelerator for Production of Tritium: Physics Design Challenges," *Proc. 1990 Linear Accelerator Conference*, Albuquerque, NM, September 10-14, 1990, in press; Los Alamos National Laboratory document LA-UR-90-3096.

Special Supporting Research Initiative (SSRI)

Introduction

The Special Supporting Research Initiative (SSRI) is funded to support high-quality basic and applied research in the field of free-electron lasers (FELs), and to demonstrate these advanced technologies. SSRI research will provide an understanding of the performance and engineering limits of FEL systems, thereby strengthening the science and technology base for existing and future laboratory and national FEL initiatives. The goal is to build a second-generation FEL system to research and develop advanced components. This system incorporates state-of-the-art components and is friendly and robust. Research and developmental areas include the various subsystems of the FEL: the electron source, accelerator, wiggler magnet array, optical system, diagnostics, and control system. State-of-the-art components include ultrabright, high-gradient, low-loss accelerators; electromagnetic microwigglers; emittance-preserving magnetic bunchers, and advanced optical resonators. This second generation of FELs, referred to as compact FELs because of their sizes, has many potential industrial, medical, and research applications.

Description

The present design of the compact FEL consists of a high-brightness accelerator and a microwiggler. The electron source is a laser-driven photoemitter which produces 5-nC and 10-ps-long micropulses at a rate of 108 MHz. The macropulse is 20 μs long and has a rate at 10 Hz. The electron beam is accelerated to 20 MeV by a 1.2 m on-axis coupled structure operating at 1300 MHz with a field gradient of 25 MV/m. The accelerated beam has excellent beam quality with a transverse emittance of 10 π-mm-mrad and an energy spread of 0.3%. The microwiggler is 10 cm long with a 3-mm period and has a double-helix design. It is driven by a pulsed dc current of 10 kA to generate a magnetic field up to 5 T on axis. The length of the optical resonator is 1.4 m. Including operation at higher harmonics, the laser wavelength extends from 7 μm down to 0.3 μm.

Present Status

The accelerator structure was reviewed by an external panel in July. We completed studies of the beam dynamics from the photoemitter to the end of the accelerator structure. We are currently working on the conceptual design for the beamline, including the diagnostics and computer control system, which transports the beam to the microwiggler.

We studied the techniques of microwiggler design and the advantages of operation at higher harmonics. We determined the optimum microwiggler design analytically, considering thermal heating and minimization of the magnetic field's quadrupole component. A working model has been built and is presently under testing.

The first beam is expected in the fall of 1991.

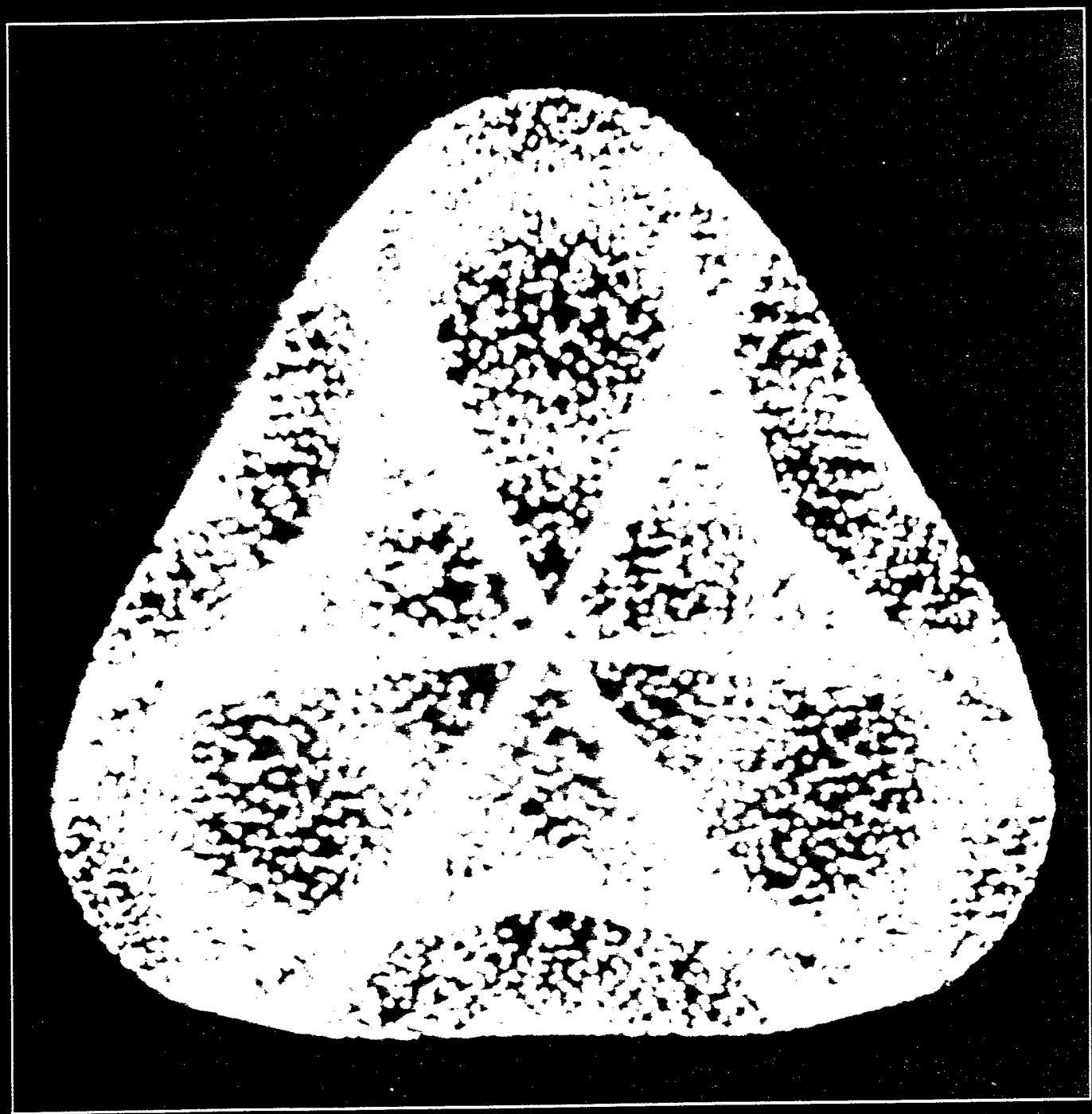

Phase space plot of a nonlinearly perturbed harmonic oscillator. Such plots are used in AT-6 to predict beam behavior in accelerators and storage rings.

Technical Highlights

AT-1
Accelerator Physics and Special Projects

James Stovall, Group Leader

Introduction

The Accelerator Physics and Special Projects Group, AT-1, provides accelerator design and physics for the division's varied projects. In addition, its members pursue advanced topics in accelerator physics and technology. The group also builds small accelerators for special applications. Following is a summary of these group activities for the 1990 fiscal year.

Projects Section

Ground Test Accelerator (GTA) Project Support

The following tasks were carried out in support of the GTA project:

■ Power Model Radio-Frequency Quadrupole (RFQ) Tuning: Lloyd Young wrote a software package to read the output of Jim Billen's radio-frequency (rf) field distribution data-acquisition program. Young also determined the slug tuner positions required to produce a flat quadrupole field at a specified frequency along with minimal dipole fields. An electro-mechanical system was designed and fabricated to allow us to measure rf field distributions while the RFQ is under vacuum at cryogenic temperatures.

■ DTL End Walls: The design of low-energy and high-energy end walls for the ten GTA drift-tube linac (DTL) tanks was completed. These end walls are cryogenically cooled, brazed copper units. The end walls for the first four tanks were fabricated and tested during FY 1990. The remaining end walls will be completed during FY 1991.

Low-power end walls with adjustable half-drift tubes were designed and fabricated for all ten tanks. These will be utilized during the tuning process.

We designed and fabricated a cryogenic bead-pull unit, modelled after the unit fabricated for the GTA RFQ.

■ IMS Cavities: A pair of buncher cavities for the intertank matching section (IMS) were designed and fabricated. These are large (0.6 m diameter), brazed copper cavities that are cooled by high-pressure liquid helium.

Continuous-Wave Deuterium Demonstrator RFQ Cold Model

A full-scale cold model of the Continuous-Wave Deuterium Demonstrator (CWDD) RFQ was designed and fabricated by AT-1 and AT-4 in FY 1989. This work was carried out under contract to Grumman Aerospace Systems, which is designing and fabricating the CWDD accelerator under funding from the Strategic Defense Initiative Organization. The 4-m-long, 352-MHz CWDD RFQ will be the electrically longest (4.62 wavelengths) device of this type thus far constructed. The power model RFQ will consist of four 1-m-long segments. Each segment will consist of four vane/cavity quadrants joined by electroforming, following the style of the Beam Experiment Aboard a Rocket (BEAR) RFQ.

During FY 1990, AT-1 staff carried out the rf tuning of the cold model RFQ structure, including:

■ determination of pre-electroforming alignment procedures.

■ determination of frequency compensation for:
- SUPERFISH errors.
- vacuum pumping ports.
- end effects.
- drive loops.
- azimuthal stabilizers.

■ testing and selection of stabilizers. Both azimuthal and end stabilizers were tested and found to provide nearly similar performance. End stabilizers were selected on the basis of significantly lower manufacturing costs.

■ determination of rf cavity performance:
- slug tuner sensitivity.
- stabilizer performance.

Photoinjector Linac for the Netherlands Center for Laser Research (NCLR)

Partway through the year, in conjunction with AT-5 and AT-7, we began design and fabrication of a 1300-MHz, 5-MeV photoinjector linac for the NCLR at the University of Twente, Enshedde, the Netherlands. This will be a near duplicate of the 6-MeV photoinjector linac which was completed for the Los Alamos National Laboratory High-Brightness Accelerator Free-Electron Laser (HIBAF) during the previous fiscal year. The new photoinjector linac is a compact, brazed-copper, on-axis coupled structure. The high vacuum requirement ($<1 \times 10^{-9}$ Torr) of the photocathode necessitates a high-vacuum conductance structure with an integral vacuum bakeout system. The assembly is shown in Fig. 2.1.

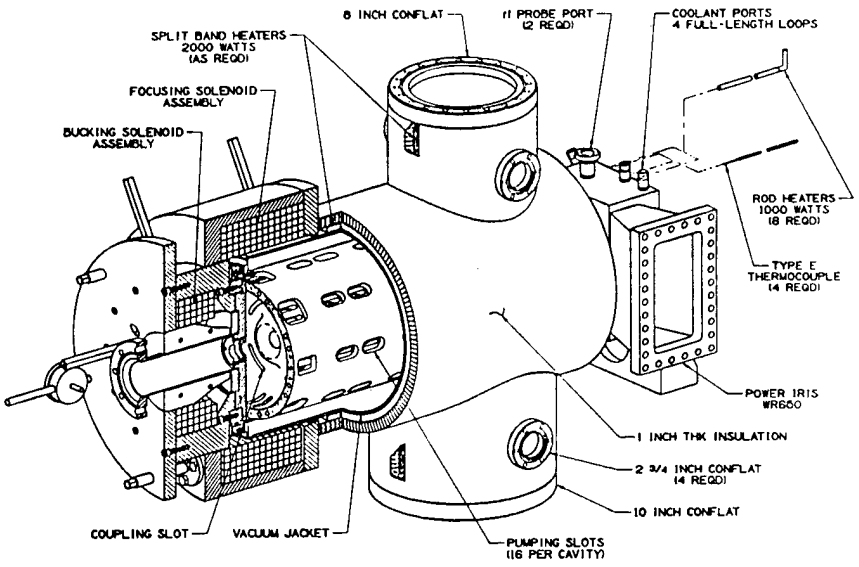

Figure 2.1. The 1300-MHz photoinjector linac for the University of Twente.

The NCLR linac incorporates some improvements which resulted from more than one year's operational experience with the HIBAF accelerator. These improvements include revised solenoid magnets and coupling slots to reduce the output emittance. The linac and photocathode preparation chamber (AT-7) is scheduled to be installed at the Univeristy of Twente in the summer of 1991.

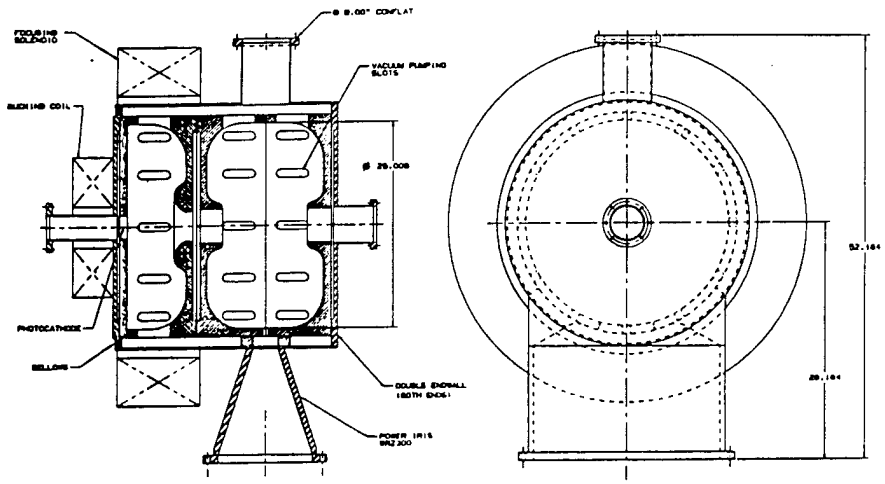

Figure 2.2. Preliminary concept of a 352-MHz ELFA injector for the INFN Electron Laser Facility for Acceleration.

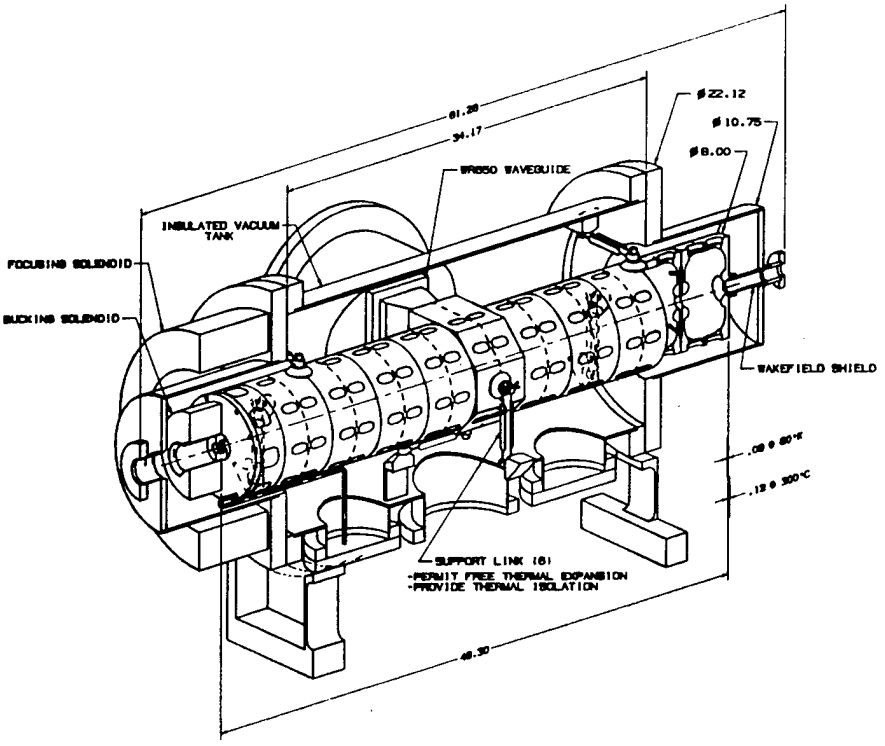

Figure 2.3. Advanced compact FEL injector general arrangement.

Photoinjector Linac for the National Institute of Nuclear Physics (INFN)

In conjunction with AT-5, AT-7, AT-8, and CLS-8, we completed a design study for a 10-MeV, 400-Amp peak-current photoinjector accelerator for the INFN Electron Linac for Acceleration (ELFA) project at the Laboratory for Accelerators and Applied Superconductivity in Milan, Italy. This system consists of a 352-MHz, 3-MeV, two-cavity, on-axis coupled photoinjector linac feeding a European Center for Nuclear Research large electron-positron collider (LEP_2) accelerator module (a 5-cell, niobium, superconducting accelerator, with 7-MeV gain). After focussing, the accelerator module feeds a wiggler, which produces 3-mm wavelength radiation. The injector linac is shown in Fig. 2.2. The system will initially be used for studies of superradiance.

Members of the participating groups traveled to Milan in the summer of 1990 to present the design study to INFN staff and management. Funding for the design and fabrication of the photocathode preparation chamber, two-cavity injector, photocathode laser, rf power system, and control system is planned to begin in FY 1991. The LEP_2 module, focussing quadrupoles, and wiggler will be procurred from Italian sources.

Advanced Compact FEL Linac

Under Special Supporting Research Initiative funding and in conjunction with AT-7, we began the design of a 20-MeV, 1300-MHz photoinjector linac which will be operated at liquid nitrogen temperature to take advantage of copper's lower resistivity at reduced temperature. The 11-cavity linac on-axis coupled structure, shown in Fig. 2.3, is an extension of the HIBAF design.

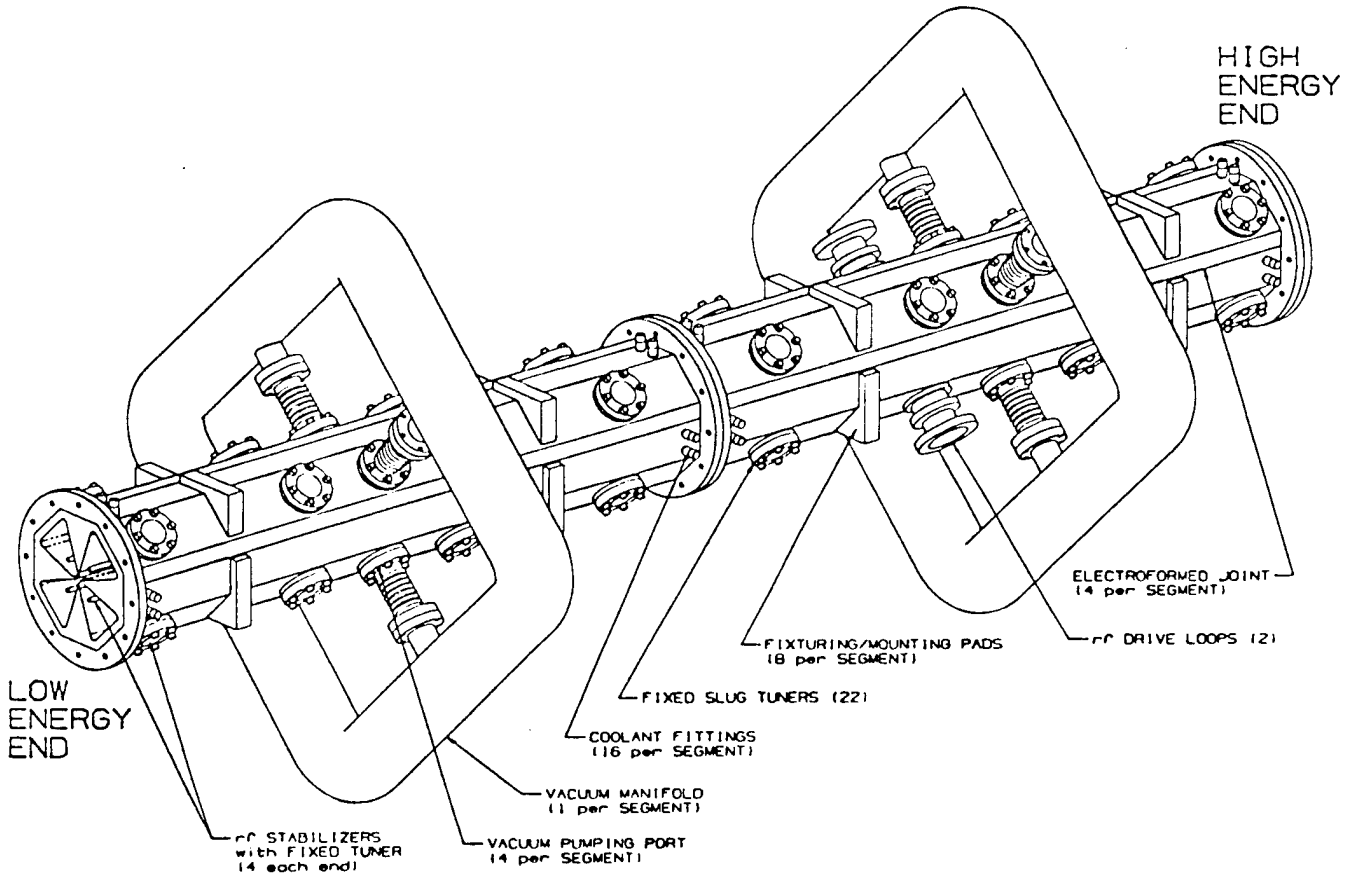

Figure 2.4. Preliminary concept for the SSC RFQ Linac 2.5 MeV, 428 MHz.

Superconducting Super Collider RFQ Linac

We completed a conceptual design study and a proposal for the design and fabrication of a 2.5-MeV, 428-MHz RFQ for the injector of the Superconducting Super Collider (SSC) facility. The RFQ, shown in Fig. 2.4, will be a two-segment, continuous cavity structure 2.2 meters in length. Each segment will consist of four vane/cavity quadrants joined by electroforming. This is the technique developed for the BEAR RFQ.

Detail physics and engineering design will be completed during FY 1991. Fabrication will carry into FY 1992.

Beam Dynamics

Ground Test Accelerator (GTA)

The transverse acceptances of the DTL tanks were modeled, and techniques were considered for correcting transverse misalignments by mapping the acceptance and centering the beam. This method produces minimum emittance growth through the DTL but requires mechanisms for moving the ends of the tanks.

We continued work on IMS beam-dynamics calculations, with an emphasis on below-optimum conditions such as mismatch, misalignment, and possible low magnetic fields in the variable-field quadrupoles. Simulations determined the range of steering available from the IMS for mapping the acceptance of the first DTL tank. We considered new GTA funnel configurations and estimated the length, emittance growth, etc., that would result from these configurations.

Beam dynamics in the GTA RFQ were calculated with a new version of PARMTEQ that includes 3-D space-charge and image-charge effects in the

vanes. The difference between the normal 2-D space-charge runs and the 3-D treatment without image charges was within statistics; however, including image charges reduced transmission by several percent. Emittance changes were negligible.

The least squares method of setting the rf power phase and amplitude was applied by simulation to the first and last DTL tank in GTA. (This method is explained later in this report.) The method seems to work quite satisfactorily on both the lowest- and highest-energy DTL tanks.

Calculations were completed that show that small fluctuations in output current from the ion source can lead to momentary mismatches at the RFQ input if the low-energy beam transport (LEBT) relies on beam-charge neutralization by a plasma and if the source fluctuations are more rapid than the plasma neutralization can accommodate. The mismatch amplitude depends upon the length of the LEBT. The results of such mismatches can be an amplification of the source current fluctuations, because a mismatch caused by a small source fluctuation can produce a much larger fluctuation in RFQ output current. Beam emittance can also be increased by this effect.

Single-Beam Funnel Experiment

Beam-dynamics support of the single-beam funnel experiment contributed significantly to the success of the effort and to our ability to obtain the most information from the experiment in the limited time permitted. There was continuous interaction between beam dynamicists and experimenters; simulations to predict or explain experimental data were performed as needed. In several instances, these simulations were instrumental in guiding the experiment, preventing misinterpretation of results, and correcting experimental errors. It proved very advantageous to have a beam dynamicist on the experimental team and to have computing facilities close to the control room so that simulations could be conducted simultaneously with the experiment. Considerable code work was done in support of the experiment; for instance the effect of steering quads movement on the beam centroid was displayed graphically, and phase and radial motion in linear accelerators (PARMILA) was modified to calculate beam-beam interaction. This experiment was primarily intended to test our simulation codes; the close correspondence between code predictions and final experimental results showed that the codes are correct and can be trusted.

Pegasus

We completed RFQ preliminary designs for two options: a high- and a low-current. These designs met all beam-dynamics and power criteria set for this program at this time. Considerable assistance was informally given to Grumman in their linac design effort.

Superconducting Super Collider (SSC)

A reference beam-dynamics design has been completed for the SSC Linac. The linac includes a 2.5-MeV RFQ, a DTL from 2.5 to 70 MeV, and a coupled-cavity linac (CCL) from 70 to 600 MeV. We completed extensive beam-dynamics studies including cavity characteristics and permanent-magnet quad requirements. Longitudinal and transverse matching sections were designed for transitions between tanks. Ramped fields were used in the CCL for longitudinal emittance control. Several options were considered, such as FODO vs. FOFODODO focussing in the DTL, and singlet vs doublet focussing in the CCL. Advantages and disadvantages of each of the options have been discussed at length with the SSC Laboratory to provide them the information to make a choice of design. We have established good working relationships with personnel in the SSC Laboratory Linac Group, and we expect these relationships to continue throughout the construction of the SSC Linac and beyond.

Superconducting Cavities

As a part of the program to establish the technology of niobium superconducting rf (SCRF) cavities at Los Alamos, we completed conceptual design studes of possible SCRF linacs.

Pion Linac (PILAC)

A joint study with MP Division was undertaken on the feasibility of a PILAC. Pions produced by the primary photon beam accelerated from 400 or 500 MeV to 920 MeV, opening up a new research area in η physics. Design and beam-dynamics studies were completed with various possible choices of accelerator parameters.

Electron Linac for Acceleration (ELFA)

We conducted feasibility and design studies on the design of an accelerator for the ELFA project, a FEL experiment in Milan, Italy. This project would be supported by the Italian Institute of Nuclear Physics; its focus is to test new regimes of interaction between electrons and radiation into a wiggler.

Code Development

The CCL design and dynamics codes were modified and enhanced as specific requirements arose. We modified the codes to include tank-to-tank ramps of synchronous phase and E_oT, a procedure that calculates quad gradients while holding the transverse phase-advance constant, more graphics, estimation of halo particle losses by extrapolation, cell-to-cell ramping, and independent cavities.

An end-to-end simulation of the Clinton P. Anderson Meson Physics Facility accelerator was completed, showing excellent agreement between the design and beam-dynamics codes and the measured beam parameters.

We developed a computer code to calculate the RFQ lens, which might be used as a LEBT. The advantages of such a LEBT would be that it can be accurately calculated, which is not the case with a plasma-neutralization LEBT, and that it does not change the

match into the RFQ significantly if the source output fluctuates by a small percentage. The disadvantages appear to be a low current-carrying capability and the necessity for a low-frequency source of rf power.

A new method of setting the phase and amplitude of the rf power in DTL tanks has been developed and tested in simulations. The method uses least squares fitting to determine constant errors, called "offsets," in data from phase and amplitude sensors on the beam and in the tanks. Relative phase differences in the output beam are correlated with changes in input beam phase and with changes in power amplitude settings as shown on the sensors. These phase differences are compared with beam-dynamics calculations from a code such as PARMILA. Sensor offsets are found by least squares fitting the differences between actual data and code expectations. We used artificially generated data produced by adding constant offsets and random errors to code expectations to develop and check the method. Results were very encouraging; the fitting code could reproduce offsets with good accuracy even when large offsets and large random errors were introduced into the artificially generated data. The method may provide a complementary method to Δ-t for setting rf phase and amplitude in accelerator tanks.

The RFQ beam-dynamics design code PARMTEQ has a 2-D space-charge treatment similar to that in PARMILA, in which a grid of axially symmetric rings of charge represents the bunches. There is no provision for calculating the effects of image charges in the vanes. We wrote a new version of PARMTEQ that uses a point-to-point 3-D space-charge treatment and includes a calculation of image charges in the vane tips. We ran several RFQ designs with this new code. For some of them, the image charges have little effect, and for others there is a large transmission loss. As might be expected, beam loss due to image charges seems to correlate fairly well with charge density very close to the vane tips. If the image charge calculation is bypassed, there is little difference between the 2-D and 3-D results.

Superconducting rf Structures Development Laboratory

Summary

During the past year this program has built nine 3-GHz high-β cavities. These cavities, as well as previously built 805-MHz cavities, have been chemically treated in ultraclean environments and tested at high fields. We have achieved accelerating fields of 11 and 9 MV/m in the 3-GHz and 805-MHz cavities, respectively. This represents performance comparable to the world state-of-the-art for chemically treated niobium cavities. We have also produced a mechanical design for a low-β superconducting cavity for neutral particle beam applications. In addition, using a low-power multicell, superconducting-accelerator model, we have developed the ability to tune individual cells to obtain equal field distributions throughout such structures.

A high-temperature vacuum oven has been modified for heat treating superconducting cavities to improve their field performance, but as yet no cavities have been so treated.

Method of Approach

In order to reach the high-accelerating gradients needed for such projects as PILAC niobium cavities have to be heat-treated or high-power conditioned. At the present time, heat treatment presents the best chance for obtaining such high gradients.

For heat treatment to be successful, state-of-the-art (chemical treatment) performance of cavities must be demonstrated. To this end, we have constructed thirteen 3-GHz cavities and concentrated on developing cleaning techniques for obtaining high-gradient operation. Repeated testing of cavities is necessary to obtain good, reproducible data statistics.

Our approach towards the heat treatment of niobium cavities is to first heat treat 3-GHz cavities, obtain reproducible high-gradient operation, and then extend the work to the larger surface area 805-MHz cavities.

When cavities are incorporated into coupled multicell structures, high-gradient operation can only be achieved if all cells have approximately the same fields. This field uniformity depends on how well the individual cells are tuned. To address this problem, we use low-power, normal-conducting multicell structures to develop tuning techniques.

To investigate the possibility of extending the use of thin-wall, niobium, superconducting cavities to the low-β region, we looked at the mechanical design of such a cavity.

The superconducting laboratory's clean room and ultrapure water system were made fully operational, and they are being used on a routine basis. Both facilities have met their specifications.

The mechanical design of the 3-GHz cavities was modified to maintain uniform niobium wall thickness during deep drawing. This redesign made the E-beam welding of the cavities easier, and the improved weld uniformity increased the number of times that the cavities can be chemically treated.

Variable-coupling power feeds have been built for the 3-GHz cavities. These feeds improve the accuracy of cavity Q and field-level measurements.

We have built nine 3-GHz niobium cavities and have repeatedly chemically treated and tested them at high fields. Two 805-MHz cavities have also been tested several times at high fields.

The cavity test cryostats have been magnetically shielded to improve the cavity Q's at 2 K operation. Operation at this low temperature is necessary to test the cavities for electric field limits without being limited by wall power dissipation (quenching).

We lowered the 805-MHz cavity test cryostat below floor level and installed radiation shielding over it to allow testing with high-field emission currents.

A fixture for tuning multicell structures has been constructed. We wrote computer programs for taking the measured field values in multicell structures and calculating the individual cell-frequency corrections needed to achieve uniform fields. We used a room-temperature copper structure to test the tuning procedures.

We modified an existing vacuum oven for high-vacuum, high-temperature operation and are beginning to run tests on it. A higher-quality oven has been obtained from the Stanford Linear Accelerator Center for future work.

Collaborative arrangements have been made with Cornell University for heat treatment of our 805-MHz cavities. Heat treatment of these larger cavities is not possible at LANL. Some of the fixtures needed for this work have been constructed.

Results

Ten high-field tests have been made on the 3-GHz cavities. On the average 9.5 MV/m accelerating field gradients have been obtained, with reasonable scatter around this average. The corresponding gradient average obtained in tests on the 805-MHz cavities is 8.2 MV/m. Figure 2.5 shows the LANL data converted to peak surface electric field plotted against the world's best results as a function of cavity surface area.

Laser Subsystems (LSS) for the Ground-Based Free-Electron Laser

We designed a new 433.33-MHz cavity shape for LSS having higher shunt impedance (8.98 MΩ) and yet retaining reasonably low coupling for higher-order modes.

Two low-power (800 MHz) models of the above cavity have been built and used to size the waveguide coupling slot, waveguide tapered section, and bar tuners needed to compensate for the frequency shifts caused by continuous-wave operation of the final full-power cavities. We used variable waveguide tapering near the cavity coupling slot to change the cavity to waveguide coupling factor without having to remachine the cavity coupling slot. We designed narrow bar tuners to vary the cavity frequency over approximately 200 kHz. The tuners were shaped so as to keep the cavity rf fields and beam-induced fields from penetrating to the tuner's rf contacts.

In addition, the low-power models were used to measure the cavity-cavity coupling for a center-to-center distance of 3/4 $\beta\lambda$. This coupling has to be less than 1×10^{-6} for the LSS case in order to allow operation of adjacent cavities at a relative phase of 90°. We used an analytical formula to estimate this coupling and verified this formula with the measurements.

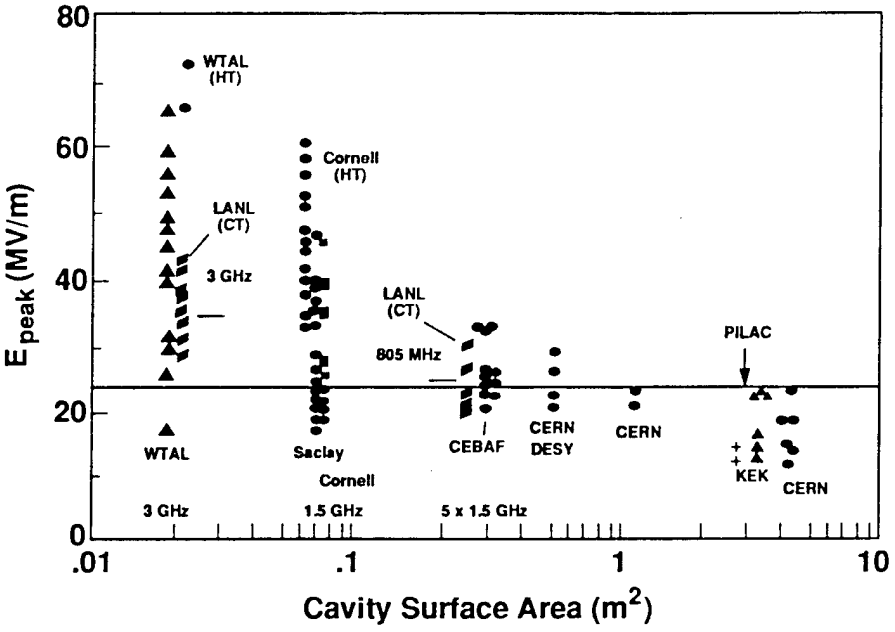

Figure 2.5. Peak field compared to cavity surface area.

Another analytical formula for estimating the electric fields in the waveguide coupling slot was tested on low-power models and found to agree with measurements to within ~10%.

We constructed a test fixture for measuring the field asymmetries introduced by the waveguide coupling slot and made preliminary measurements.

Coaxial-Line Azimuthal Stabilizer for RFQs

We performed azimuthal stabilization studies on a 1.75-m-long, low-power model of a 600-MHz RFQ. The model was modified to accept 7 coaxial

azimuthal stabilizers spaced at $\lambda/2$ intervals and alternating in orientation between two orthogonal planes (Fig. 2.6).

As shown in Fig. 2.6, the stabilizers consist of 41.6-Ω coaxial resonators (CRs) with shorted ends, inserted through a hole in an RFQ vane and walls. Their center conductors have a diameter of 0.64 cm. The CRs are nominally λ long at the RFQ operating frequency, with provision for tuning by approximately ±20 MHz by moving their shorted ends. They are arranged so that their electric field nodes are located at the vane centerline. The areas enclosed in adjacent quadrants by the resonator center conductor, the RFQ wall, and the vane should be approximately equal. For the orientation shown in Fig. 2.6, if no vertical dipole exists in the RFQ, the RFQ's magnetic field fluxes through the adjacent enclosed areas are equal. Voltages induced in the CR by these equal fluxes will cancel, leaving the CR unexcited. If, however, a vertical dipole is present, the fields in adjacent quadrants will be unequal. The CR will then be excited in such a way as to make the fields equal (zero dipole), acting just like the off-axis cavity in a side-coupled linac operating in $\pi/2$ mode.

Changing the position of the CR's electric field node by offsetting both shorted ends in the same direction has the same effect as changing the relative sizes of the enclosed areas. The CR then makes the fields unequal so as to make the fluxes equal. This offset can then be used to either introduce a dipole component into the RFQ or correct for unequal enclosed areas caused by mechancial asymmetries.

Measurements on the low-power RFQ model have shown that these stabilizers are easy to tune even on a very crudely constructed RFQ with large dipole field components. They are fairly insensitive to both asymmetries and tuning and can be used to adjust the dipole field components of the RFQ.

Figure 2.6. RFQ model with stabilizers.

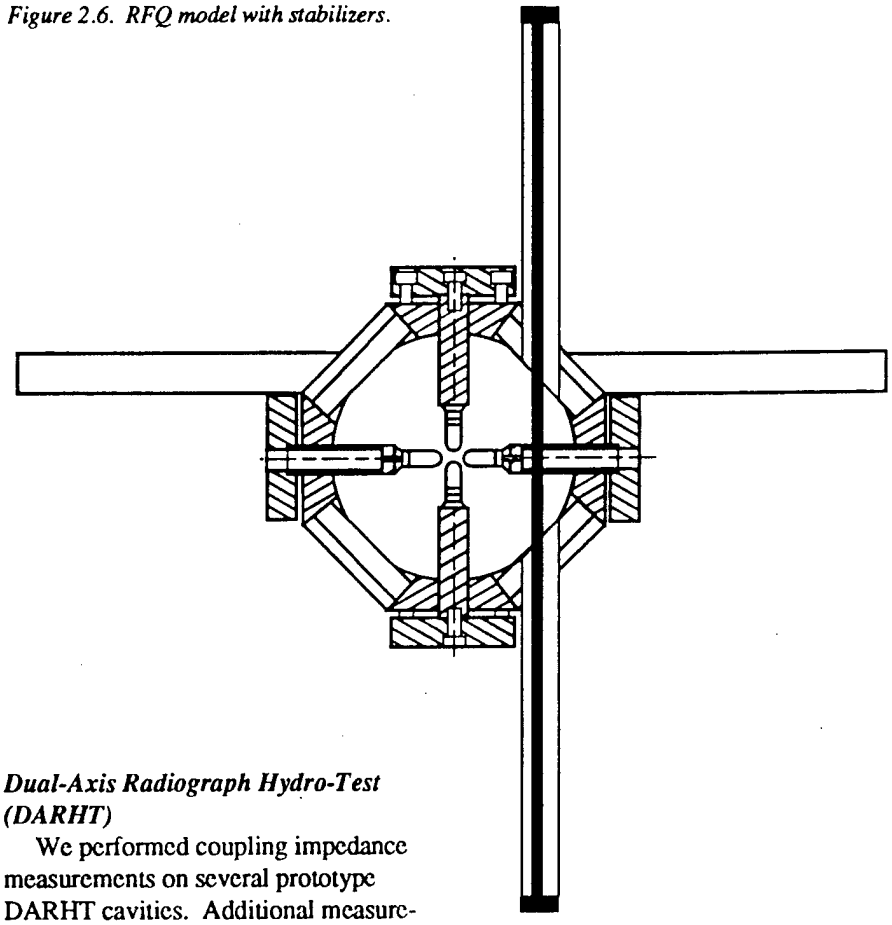

Dual-Axis Radiograph Hydro-Test (DARHT)

We performed coupling impedance measurements on several prototype DARHT cavities. Additional measurements were performed on components that attach to the DARHT cavities. We compared the results to calculations performed using the AMOS and URMEL-T codes. As a result of the measurements, improvements were made to the AMOS code. EMAS (a three-dimensional, or 3-D, infinite-element electromagnetics code that has material losses) was evaluated and found unsuitable for use in designing DARHT cavities.

Ground Test Accelerator/Accelerator Test Stand (GTA/ATS)

The ATS deflector cavity and the IMS buncher cavities were built, tuned, tested, and delivered to AT-10.

During tuning of the IMS buncher, we noted that the frequencies of the TM110 mode were close to harmonics of the drive frequency. Also, the noses had sagged a small amount during brazing, resulting in lowered cavity frequencies. A fixed paddle was installed in the cavity, 90° from the paddle tuner. This served to raise the fundamental frequency the desired amount and moved the TM110 modes sufficiently away from the harmonics of the drive.

RFQ Lens

An RFQ lens proposed by Science Application International Corporation (SAIC) was modelled using MAFIA code. The modelling yielded a frequency for the cavity that was 500 MHz (SAIC had predicted 300 MHz). Subsequent testing agreed with the MAFIA calculations. Field values were provided to the beam diagnostics group for a beam-dynamics study.

References

E. Gray, "BETA Measurements," Los Alamos National Laboratory Technical Note AT-1:89-28, January 26, 1989.

E. Gray, "Field Errors in Multicell Cavities," Los Alamos National Laboratory Technical Note AT-1:90-195, May 31, 1990.

E. Gray, "External Q and Emitted Power," Los Alamos National Laboratory Technical Note AT-1:90-305, September 12, 1989.

E. Gray, "Tuning Cavities for Field Uniformity," Los Alamos National Laboratory Technical Note AT-1:90-259, July 20, 1990.

E. Gray and J. McGill, "Helium Boiloff During Conditioning," Los Alamos National Laboratory Technical Note AT-1:90-192.

E. Gray, "Beam Tube Wall Loss," Los Alamos National Laboratory Technical Note AT-1:90-297.

E. Gray, "Comments on Coupled Resonator Model for Standing Wave Accelerator Tanks," Los Alamos National Laboratory Technical Note AT-1:90-180.

E. Gray, "Cavity Coupling," Los Alamos National Laboratory Technical Note AT-1:90-152.

AT-3
Magnetic Optics and Beam Diagnostics

Andrew Jason, Group Leader

Introduction

Group AT-3 is responsible for the magnetic optics and beam diagnostics portion of AT Division and Laboratory projects. Our charter is to apply beam-transport theory, state-of-the-art diagnostic instrumentation, and advanced magnet technology to the design, construction, and commissioning of accelerators and magnetic-optics systems. Toward this end, we have maintained expertise in high-order optics theory and codes with an emphasis on practical design. Sections of the group are concerned with innovative and conventional diagnostics for controlling the high-intensity beams associated with modern linacs. As well as developing a facility for magnet design, we have developed a magnet lab with equipment suitable for measuring a large variety of magnets—from small cryogenic devices to large-bore pulsed magnets.

Our main efforts during FY 1990 have been in support of the neutral particle beam (NPB) program. Activity has been in three areas:

■ The Pegasus program, an effort headed by Grumman Space Systems to launch a space test of a NPB device. AT-3 is responsible for the specification of the high-order aspects of the device output optics.

■ The Continuous-Wave Deuterium Demonstrator, being constructed by Grumman Space Systems. AT-3 has the task of qualifying the project linac magnets using the cryogenic mapping facility developed for ground test accelerator (GTA).

■ A strong focus of our effort has been design of the Ground-Based Free-Electron Laser (GBFEL) project post-wiggler transport system. We have been active in support of the Division accelerator transmutation of nuclear wastes (ATW) proposal and the MP Division pion linac (PILAC) proposal. AT-3 has also participated in several smaller projects.

GTA Program

Optics Design

The optics design effort has produced a configuration adequate for transforming the intense H^- beam produced by the GTA linac into an expanded ultra-low-divergence beam suitable for NPB applications. Several physics issues are involved in the device performance; experiment 3 of the GTA-24 program will test how well these issues have been addressed. In particular, we will test the concept of longitudinally expanding the beam in a matching section while maintaining tight transverse focusing to avoid emittance growth.

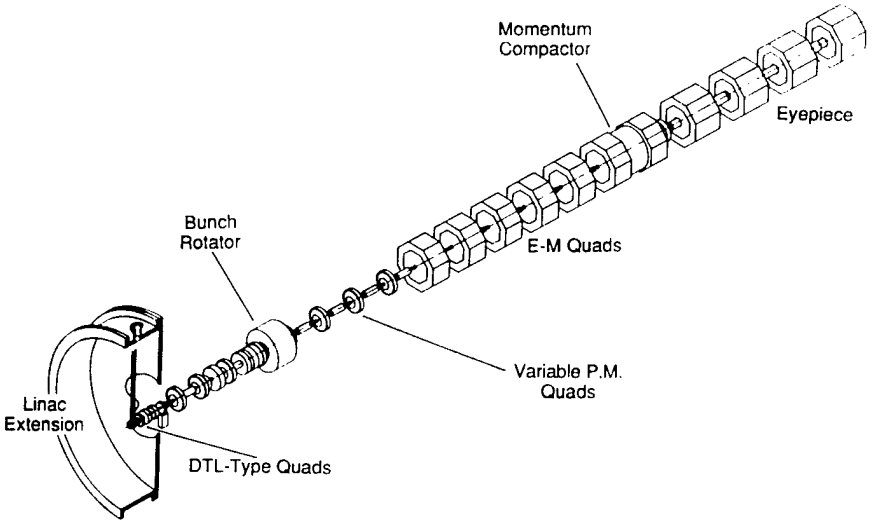

Figure 3.1. Isometric view of the GTA-24 matching section.

The optics design is a continuation of efforts from the previous year, when the basic concepts were developed. A final design review was held in December 1989. Reviewers' comments were addressed in a second iteration held in early February 1990. The reviews also included the optics design necessary to perform experiment 2D, measurement of the linac output parameters. Engineering design has proceeded from this basic design and should allow for completion of the equipment on the January 1992 schedule for the start of experiment 3.

The telescope design had been specified before the start of this reporting period. It consists of an approximately 40-m-long structure with a quadruplet lens configuration for focussing. A small modification of the magnet arrangement in the design was made to lower costs. Corrector magnets consisting of octupole, sextupole, and quadrupole elements aid in ensuring a high-quality beam. This year's efforts have completed the studies necessary to specify the corrector magnets and have provided a list of element sensitivities and tolerances to allow adequate engineering design of the device-support structure. Such engineering design has been accomplished, and the final engineering design review will be held early in FY 1991.

The matching section design is shown in Fig. 3.1. The linac extension vacuum chamber fits directly onto the linac end wall. There are three types of quadrupole lenses in the section: small, fixed-field, permanent-magnet quads; variable, permanent-magnet quads; and electromagnetic quads as appropriate for the application and cost. We have specified in detail the effect of the bunch-rotator momentum-compactor system shown in Fig. 3.1 on the beam. We have also developed specifications for the radio-frequency system and cavity design given. An engineering layout has been made, and detailed design of all components is well underway. The line contains a jitter correction system, flying-wire profile monitors, microstrip position probes, and steerer magnets. We expected to meet the January 1992 schedule.

Magnets

Magnets are a challenging aspect of the project and occupy a large fraction of the AT-3 effort. Progress and plans for the required optics magnets are:

■ Large-bore permanent-magnet quadrupoles. Field-Effects Corporation has been working throughout the year to complete these magnets. The first prototype delivered was mapped and

found to be within specifications. Four additional magnets are to be delivered on a schedule between January and April 1990. It seems clear that the schedule will be met.

■ Steerer magnet. The 0.5-m bore prototype fast steerer magnet has been constructed and is undergoing testing. Its construction proved more difficult than expected because of its intricate geometry; fabrication problems were solved with some iteration. Because of the high cost of constructing the full-bore steerer, GTA-24 will proceed with the prototype; a large-bore steerer will be constructed for higher-energy experiments. A four-quadrant power supply has been ordered from Danfysik Corporation. The proper functioning of this magnet and supply is a critical issue in the program because of the program specifications for speed and accuracy.

■ Corrector Magnets. These large-bore magnets perform first-, second-, and third-order corrections on beam in the telescope. They consist of a nested series of Lambertson-type panels with water cooling, as shown in Fig. 3.2. We completed the design of the magnets and contracted Allied Signal Corporation to construct them. The corrector magnets will be complete in approximately nine months. We must extend existing fabrication methods to produce the thick octupole layers required for trimming the telescope's geometric and space-charge-induced abberations.

■ Matching Section Magnets. Design of the electromagnetic quads shown in Fig. 3.1 is virtually complete, with a drawing package underway. We have established the variable-field quad design and qualification for the linac-RFQ matching section. We have also detailed the necessary modifications, which mainly involve simplification to a non-cryogenic configuration. The small quads in the first portion of the matching section, chosen for their high field strength of over 120 T/m, are identical to the linac quads with strength adjusted by boring out the device aperture.

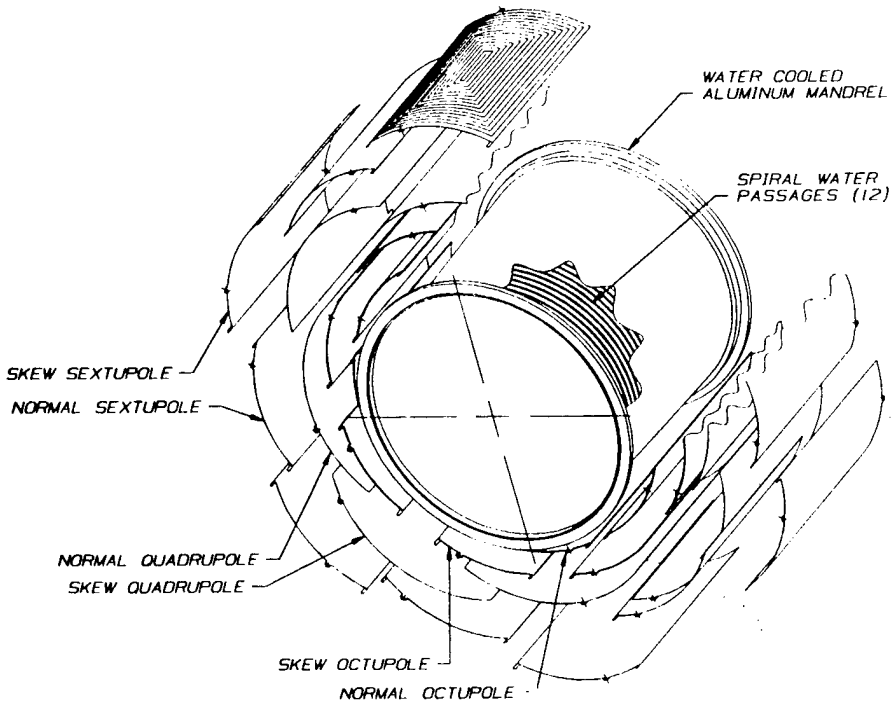

Figure 3.2. Exploded view of a corrector-magnet package.

■ Linac Quad Measurement. The linac quad strengths require 1% precision with low harmonic content at cryogenic temperatures. During FY 1989, we began construction on a cryogenic mapper to achieve this qualification. We completed and tested the mapper, consisting of a cryostat, a 1-cm rotating coil with 2-micron conductor width, and associated measurement instrumentation and software. Placing the device in operation required extensive iteration with Field-Effects Corporation, supplier of the quads, to achieve correlation between their measurements at high temperatures and our results at low temperatures. We believe that we have achieved a good absolute calibration for trimming the magnets' fields to the stringent requirements.

The magnet lab has also participated in measuring and qualifiying several other magnets for this project and others within the Laboratory. In particular, all magnets required for experiment 1 have been mapped.

Diagnostics

AT-3 is responsible for the diagnosis of beams during all stages of the radio-frequency quadrupole and linac testing. Group responsibilities are divided into two categories: permanent diagnostics and experimental diagnostics. Differing arrangements are required for the project's different experiments.

■ Radio-Frequency Quadrupole (RFQ) and Intertank Matching Section. The testing of these devices constitutes experiments 1B and 1C. For this purpose, we have constructed a device known as the D-plate. An assembly drawing of the D-plate is shown in Fig. 3.3. The beam is partially neutralized,

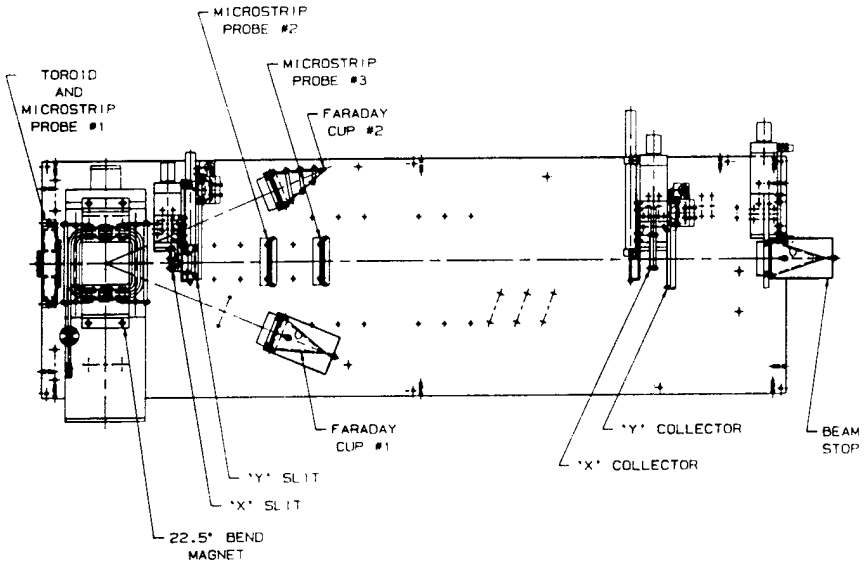

Figure 3.3. Top view of the GTA D-plate.

in either a transverse or longitudinal cut, by the laser-induced neutralization diagnostic approach (LINDA) laser located just upstream of the D-plate. After the charged remnants are swept out with the 22.5° bend magnet, the neutral beam passes through a set of defining slits positioned to sample a particular region of phase space. Measurement of the transmitted beam component, and hence the emittance, is accomplished by a sandwich collector. The microstrip probes and toroids respectively measure the beam position and intensity while the Faraday cups measure the charged contribution. Timing circuits measure the beam energy and phase. The D-plate is installed in the diagnostic tank and all electronics are complete. The LINDA laser-beam transport line is installed and the clean room which houses the laser has been delivered but not installed. The room installation will proceed as funding allows.

■ Linac. Diagnosis of the linac beam occurs for a single tank at an energy of 8 MeV in experiment 2A and upon assembly of 10 tanks at 24 MeV for experiment 2D. The D-plate is suitable for 2A, but an entirely new arrangement is required for 2D. We designed a 1-m-radius spectrometer system using a continuous-wave mode-locked laser for the LINDA system to measure the critical longitudinal-emittance parameters. An associated deflector magnet and beam stop dispose of the unneutralized beam. Because of the high cost of the new laser system and the possible adverse effect of the complex experiment on schedule, the spectrometer-laser combination will not be implemented. The beam dump and a transverse-emittance measurement system remain as part of the experiment. We accomplish longitudinal diagnosis in a less direct manner by using the planned pinhole diagnotics to observe the chromatic aberrations of the telescope in experiment 3.

The linac permanent diagnostics consist of a novel gas-fluorescence profile monitor, microstrip probes between tanks for timing and position monitoring, and a cryogenic-toroid current measurement system. The microstrip probes have been contracted to Allied Signal Corporation and will be complete early this year. We constructed, tested, and installed two toroids in the RFQ end walls for experiment 1B. Electronics design for all systems has been completed and is under construction.

Pegasus Program

Grumman Space Systems has contracted to design and implement a 24-MeV, medium-divergence space experiment for the NPB program. The output optics consists of a 180° bend matched to the linac and leading to a 9-m-long telescope. AT-3 has participated actively in the design of the output optics in cooperation with Science Applications International Corporation. We are uniquely qualified to contribute to the high-order aspects of the optics and have established the correction necessary to achieve the desired level of performance. We are also responsible for specification of the system diagnostics and jitter control. Design issues are similar to those involved in GTA, with the addition of issues regarding launch necessity and functioning in a space environment. In particular, magnet-temperature sensitivities and data-transmission rates provide interesting challenges. We will hold three design reviews in FY 1991.

The GTA accelerator will provide a test bed for the Pegasus optics. We plan to calibrate the wire-shadow diagnostic built for Pegasus using the GTA pinhole diagnostic. We will then attach the Pegasus optics to the GTA linac and test its performance using the calibrated wire-shadow equipment. An integrated test of the system in a large vacuum chamber is planned in the future.

Ground-Based Free-Electron Laser (GBFEL)

The GBFEL project will be constructed at White Sands, New Mexico, under the principal direction of Boeing Aerospace Electronics and with strong participation by Los Alamos. In particular, AT-3 has been responsible for conceptual design of the post-wiggler electron-beam transport system of the laser oscillator. A conceptual layout of the system is shown in Fig. 3.4.

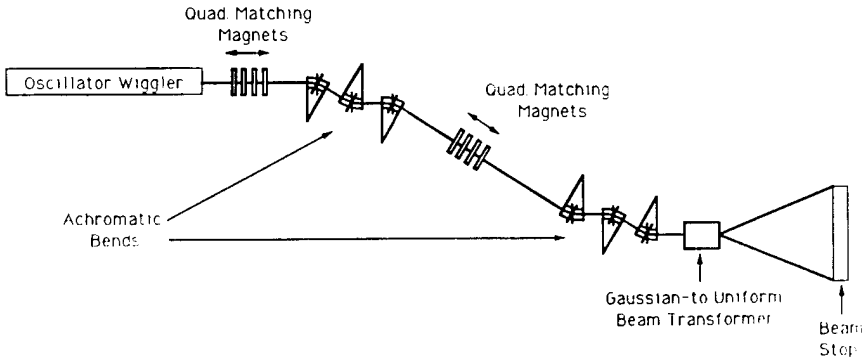

Figure 3.4. Conceptual layout of the GBFEL post-wiggler electron-beam transport system.

The system is required to transport a high-power electron beam, which is given a substantial energy spread in producing the laser radiation. The requirements have undergone extensive evolution in efforts to minimize architectural costs. In particular, the beam dump size was minimized and therefore requires a relatively high-quality beam to prevent disastrous spill and component damage.

We performed a trade study of several options for the transport system. The options selected ranged from a dual 270° bend system to a straightforward achromat. In general, second-order chromatic correction was needed. We have documented the selected designs in memos and a Linac Conference submission. Each design has various desirable attributes, and selection will be made on the basis of cost versus performance assessments.

The most attractive method of expanding the beam onto the dump utilizes a nonlinear expander to transform the Gaussian-distributed beam into a relatively uniform pattern. This method makes most efficient use of the dump, but requires a relatively long distance for beam preparation. The alternative, beam rastering, is somewhat more space-efficient but requires large magnets and is not as inherently safe as the nonlinear expander.

Superconducting Super Collider (SSC)

A fraction of a man year was devoted to work on the SSC diagnostic systems. In particular studies were made on design criteria, costs, and tradeoffs for the main ring beam-position monitoring and loss monitoring systems. AT-3 staff also participated in technical reviews of the ring designs. Information on a log-ratio processing circuit for project position-monitoring systems was transmitted. This concept, recently developed by AT-3 staff, represents a significant advance in system simplicity, cost, and performance.

Pion Linac (PILAC)

The PILAC system, a proposed MP Division project, injects 400-MeV pions from a target into a linac which then accelerates the pions to 920 MeV for experimental use. The design goal is an acceptance of 225 π-cm-mrad with a 4% momentum spread to achieve 10^9 pions on target. Additionally, the line must be short because of pion-decay loss, and the pions must be separated by a bend system from the proton beam which produced them. Correction of chromatic and geometric aberrations is required to match the beam both transversely and longitudinally into the linac.

The approach adopted was to first focus the beam appropriately with a four-quadrupole matching section. Next, a three-bend achromat separates the pions and protons. Four families of sextupoles correct chromatic aberrations and three octupoles correct both geometric and high-order chromatic terms. The code MARYLIE was invaluable in this design. The design transferred 75% of the target pions into the linac transverse acceptance. However, the longitudinal acceptance is inadequate, and further adjustment of the bend angles and linac period is necessary. We also investigated solenoid focussing, but this method produced large aberrations.

Work on this challenging problem continues into FY 1991.

Nonlinear Beam Expander

Work has continued on the concept of a nonlinear beam expander which transforms a nonuniform beam into a relatively uniform distribution. Such a device, which forms part of the ATW scheme, is particularly useful in safely dissipating the energy of a high-power beam. The use of dodecapoles as well as octupoles for the nonlinear focussing elements allows confinement to seven times the beam root-mean-square size. The expander is inherently safer than a raster system since magnet failure allows time for beam turn-off. Substantial jitter in the beam can be tolerated because of a diminished distribution motion.

We have received a patent on the nonlinear beam expander concept and will publish two existing papers on this topic in 1991.

Superconducting Quadrupole

We have constructed and tested an iron-core superconducting quadrupole for possible use in a superconducting linac. A photograph of the device is shown in Fig. 3.5. We put substantial effort into developing techniques for winding the coils to achieve high current density. The magnet produces a gradient of 320 T/m in a 1.8 cm aperture with a net gradient-length product of 16.4 T at 4.2 K. A 22% field boost is achieved at 1.8 K. The pole-tip field is more than twice that achievable with permanent magnet material and has the important advantage of having small residual field when deenergized.

In future work, the iron pole pieces will be replaced by the rare-earth metal holmium, which has a saturation field of over 6 T below 20 K. A field boost of about 30% is expected. With this material, the residual field disappears entirely as the magnet is warmed.

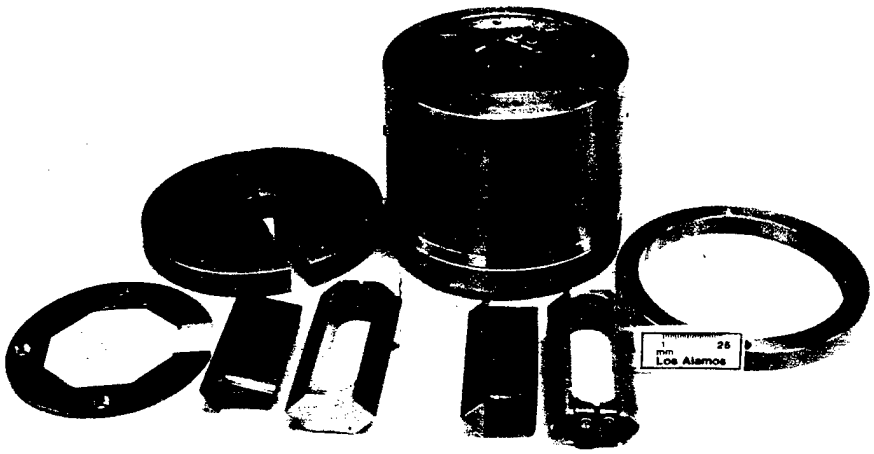

Figure 3.5. Photograph of the iron-core superconducting quadrupole.

References

D. Sandoval, R. Connolly, and V. Yuan, "GTA-24 Longitudinal Phase-Space Measurements," Los Alamos National Laboratory technical note AT-3:90-9, March, 1990.

J. D. Gilpatrick and J. Power, "RFQ and IMS Permanent Diagnostics," Los Alamos National Laboratory technical note AT-3:90-12, December, 1990.

R. Shafer, "Dispersion and Attentuation in Coaxial Cables," Los Alamos National Laboratory document LA-CP-90-70, January 1990.

R. H. Kraus and Pat Ruminer, "CWDD Prototype DTL Quadrupole Field Measurements," Los Alamos National Laboratory document, LA-CP-90-82.

Cliff Fortgang, "Experiment 2D Offset Beamline Diagnostics," Los Alamos National Laboratory document LA-CP-90-126, June 8, 1990.

Roger Connolly and Kenneth Johnson, "Longitudinal Emittance Measurements for GTA Experiments 1B &1C," Los Alamos National Laboratory document LA-CP-90-127.

Roger Connolly and Andrew Jason, "Spectrometer for 2D Longitudinal Emittance Measurements," Los Alamos National Laboratory document LA-CP-90-388, September 17, 1990.

P. L. Walstrom, "Fringe Fields From the GTA Sweep Magnet," Los Alamos National Laboratory document LA-CP-90-408.

AT-4
Accelerator Design and Engineering

W. E. Fox, Group Leader

Introduction

AT-4 is responsible for the mechanical design, fabrication, and assembly of accelerator structures and associated hardware for AT Division. During FY 1990, the group's primary objectives were the design, fabrication, and start-up installation of the ground test accelerator (GTA) and the design and development of continuous-wave (cw) laser subsystem (LSS) cavities for the ground-based free-electron laser (GBFEL).

Background

AT-4 was organized with its primary mission being the design, fabrication, and installation of the GTA structure and support system. The group was also set up to develop and exploit the mechanical engineering tools and expertise required to support AT Division. Whereas in previous years Group AT-4 was mostly involved in experimental development, conceptual designs, and preliminary designs, AT-4 devoted FY 1990 almost exclusively to the GTA detailed design, hardware fabrication and procurement, and initiation of assembly and installation.

A major milestone was reached with the completed final installation, cool down, and operation of the GTA front end; namely, the ion-source, low energy beam transport, and the 2.5-MeV radio-frequency quadrupole (RFQ) accelerator. The following describes in more detail the activities and goals achieved during the year.

Achievements

GTA RFQ

The first section of the GTA is a 2.5-MeV RFQ rated at 50 mA H^-, zero-emittance growth. This accelerator section operates at cryogenic temperatures to maximize electrical efficiency. This year saw the completion and initial successful operation of this GTA front end.

The RFQ is a 110-inch-long, 4-vane, transverse electric mode (H mode), radio-frequency (rf) cavity. It is

designed in two sections, each made up of four azimuthal segments. The vane segments are bolted together transversely with dowel pins to provide precision segment-to-segment alignment. A precision-machined mating interface socket assures transverse alignment between the upstream and downstream subassemblies. High-strength fasteners are used to hold the two sections together. Cooling passages are deep-drilled through each of the 55-inch-long sections and are closed at the ends with electron-beam welded plugs. The four vanes have a total of 16 coolant passages. Coolant is fed symmetrically through 16 ports into the center core and exits through 8 ports at each end. The quadrant region of each vane has a number of ports machined through the wall: some for vacuum pumping, others for tuning, and one for insertion of the rf drive loop. The resonant cavity is closed at the ends with actively cooled flat plates equipped with beam-current sensors.

This RFQ is the first machine designed to operate at cryogenic temperatures. As such, it presented a number of challenges and problems. These problems were solved successfully during the development program. The choice of copper-plated aluminum for the rf cavity, a first and a major technical risk, appears to be vindicated; high-power rf conditioning proceeded very quickly, and there is no evidence of unusual rf breakdown or degradation. Test results are very encouraging.

Figure 4.1 shows the assembled RFQ prior to its insertion in the cryostat. Note the field stabilization.

After field and frequency tuning, the RFQ is installed in the cryostat vessel shown in Fig. 4.2, which is also designed to house the intertank matching section (IMS) and drift-tube linac (DTL) modules.

The cryostat vessel was designed to meet the American Society of Mechanical Engineers section VIII design code. Deviations from the standard design approaches were analyzed using finite element models. The

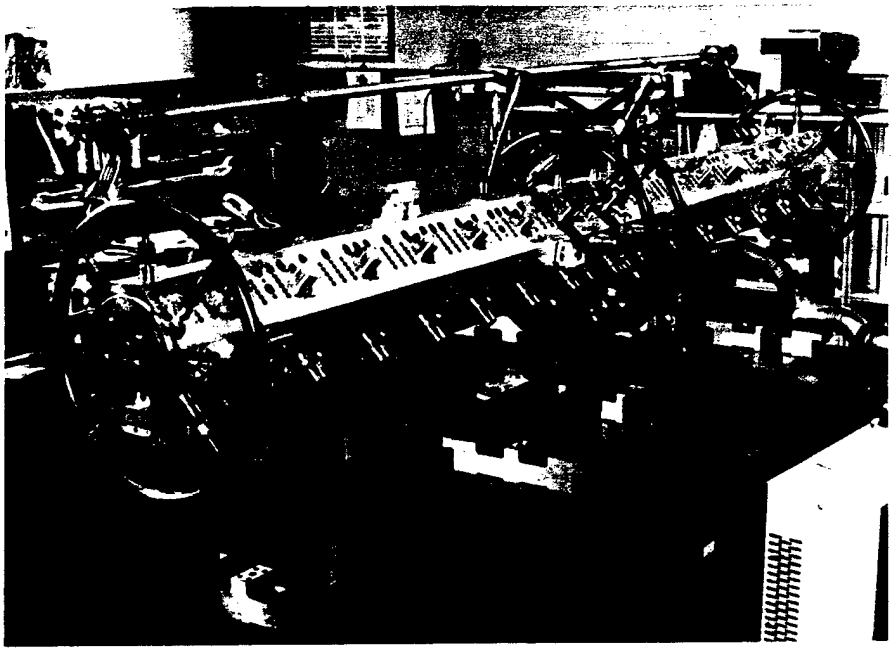

Figure 4.1. The assembled GTA RFQ.

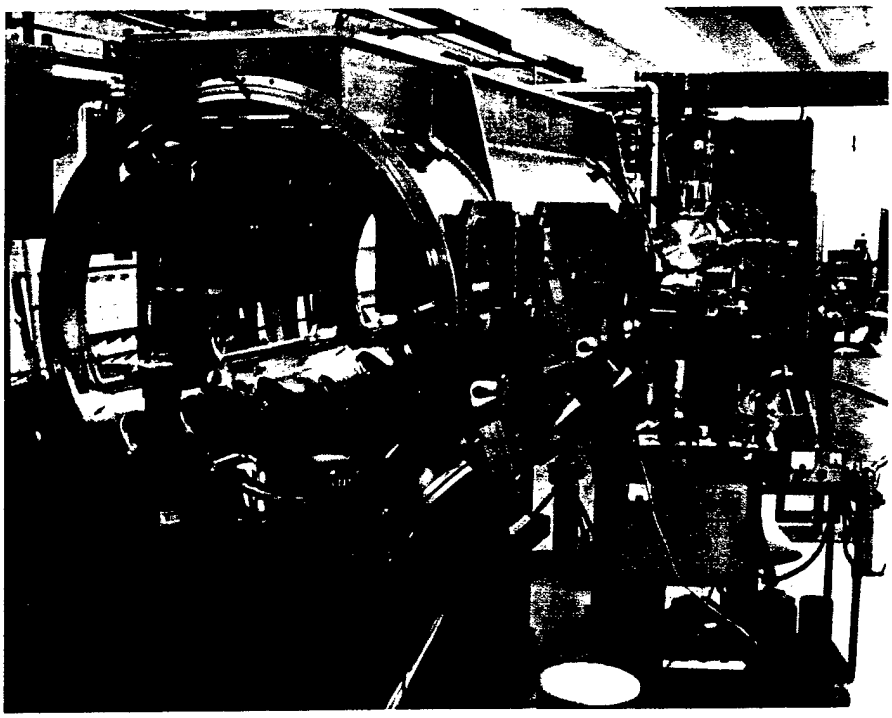

Figure 4.2. The RFQ cryostat.

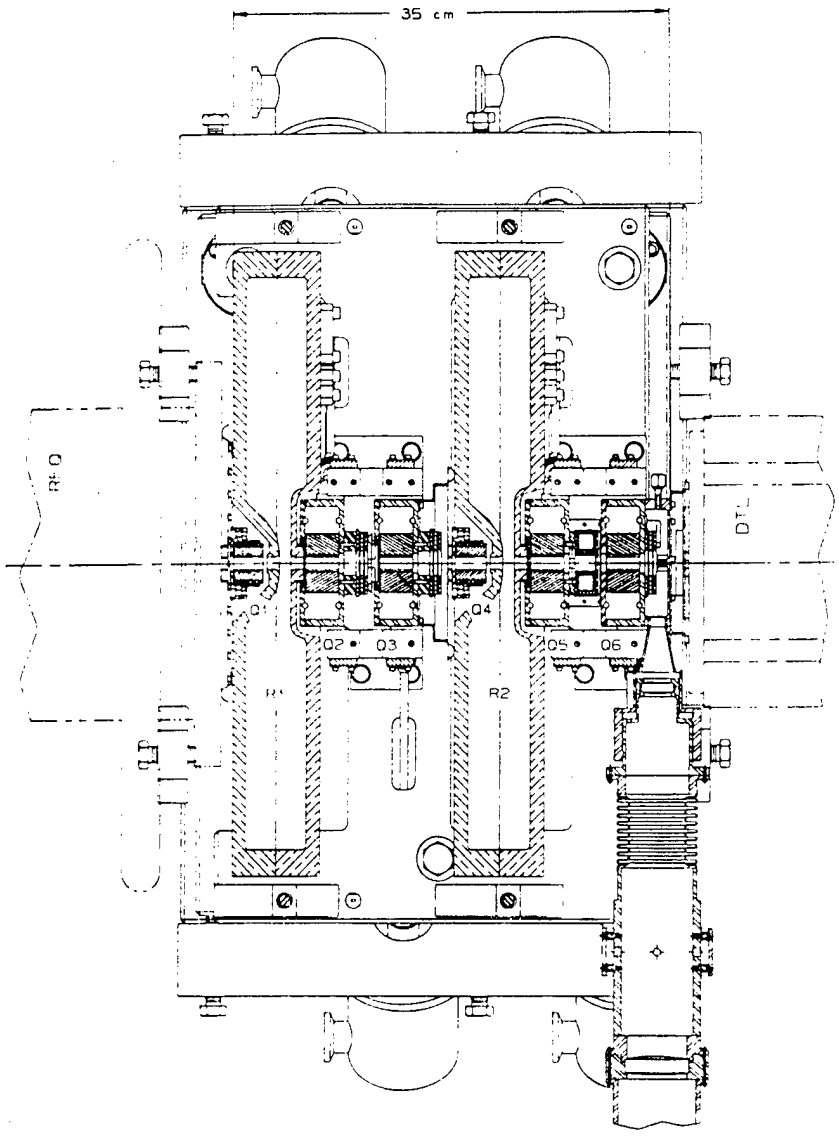

Figure 4.3. The assembled GTA IMS.

large, rectangular ports are needed for the use of optical alignment tooling to give the correct orientation between the injector, RFQ, IMS, and the first DTL module. The optical tooling requires three different positions with proper geometry to align to the required tolerances. The side ports also give the technicians availability for hands-on maintenance to change or repair malfunctioning devices. The top port had to be designed to allow for the installation and removal of the accelerator hardware. The port is designed to be open along the entire length of the vessel. Additionally, provisions were added to provide feedthroughs for the cryogenic lines, electrical and signal cables, air, gases, supports, remote location sensing devices, etc.

A substantial design effort was devoted to reach the best compromise in the ability to install the RFQ in the cryostat on a three-degree-of-freedom adjustable stable platform while minimizing the inevitable heat leaks to the outside world. This had to be accomplished while at the same time providing all the services required to operate the device, such as rf power, vacuum and cooling connections, etc.

GTA IMS

The IMS is a cavity assembly that resides between the RFQ and the DTL sections of the GTA. The function of the IMS is to match the nominal RFQ beam with a divergence error of up to 30 degrees and an emittance error of up to 50%. The transverse beam parameters are matched using six quadrupole magnets (Q), and the longitudinal parameters are matched using two buncher cavities (R). These elements are ordered as follows: Q1, R1, Q2, Q3, Q4, R2, Q5, Q6 (see Fig. 4.3). All the quadrupoles use permanent magnets, but since the RFQ beam parameters are only an estimation and may not be constant, the field strengths are adjustable on Q2, Q3, Q5, and Q6. The other quadrupoles, Q1 and Q4, are located at the entrance to the bunchers and can be repositioned with the accelerator control system to steer the beam. Gaps between the eight elements mentioned are filled with beam diagnostics: microstrip probes, current toroids, and a video-beam profile monitor.

During FY 1990, the IMS design was completed. Most of the fabricated and vendor hardware was completed and assembled to verify fits, alignments, and operation. In addition, off-line cryogenic testing was completed on the paddle tuners. The IMS is on schedule for January 1991 installation in the RFQ cryostat.

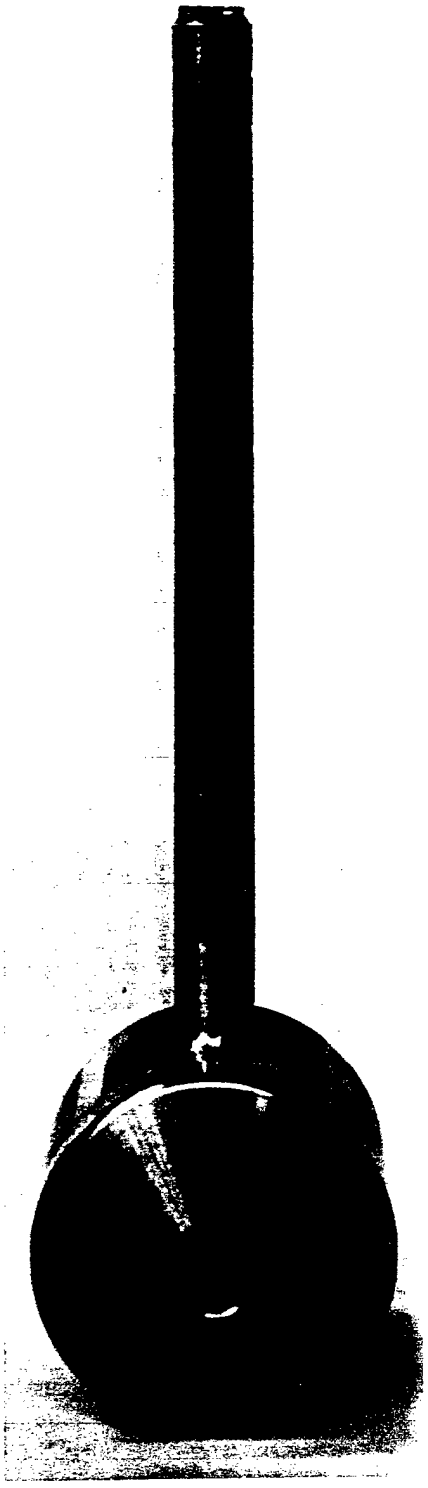

Figure 4.4. An assembled GTA drift tube.

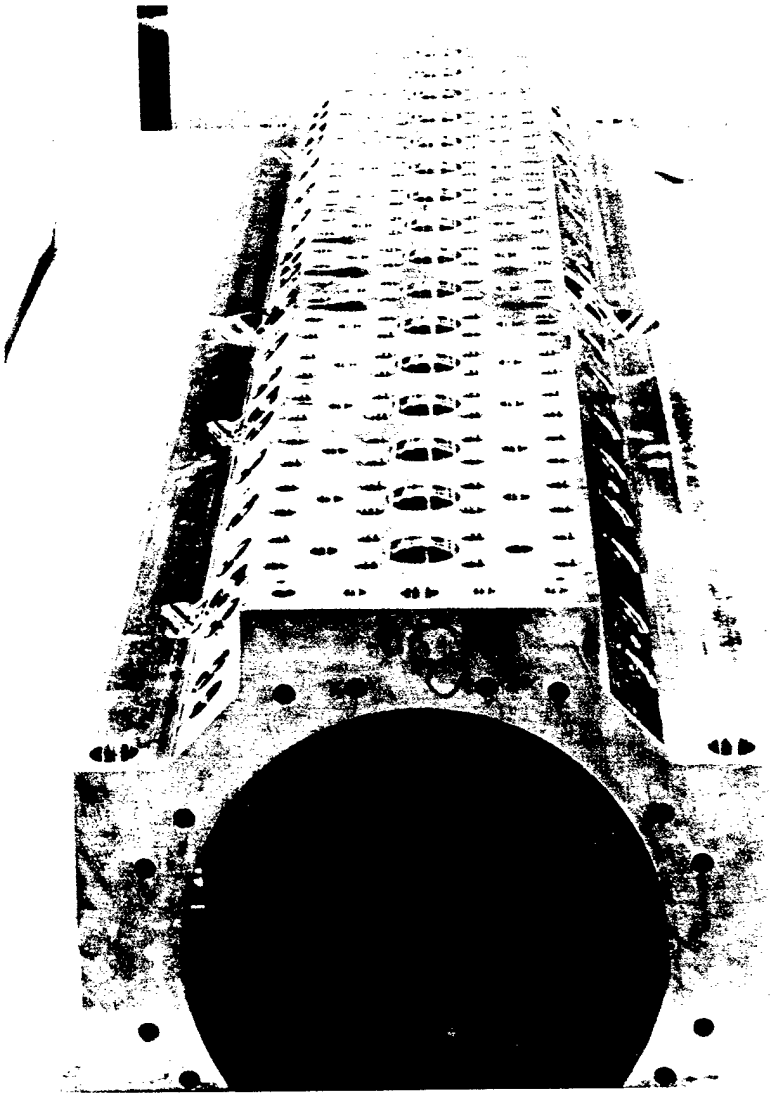

Figure 4.5. Deep-hole-drilled DTL tank forgings.

GTA Drift-Tube Linac (DTL)

The DTL comprises the major portion of the 24-MeV GTA. It consists of ten one-meter-long, 805-MHz cavities containing a total of 130 drift tubes. Each drift tube houses a permanent-magnet quadrupole lens for transverse beam focusing. Figure 4.4 shows a completed drift-tube assembly. The quadrupole lens is embedded and hermetically sealed in the drift-tube body. The drift tube is mounted in the DTL cavity center line by its support stem designed to provide adjustment and maintain drift-tube alignment accuracy to 25 μm. The support stem also provides cooling passages to maintain accurate drift-tube temperature.

During FY 1990, the DTL design effort transitioned from the final design phase to the full-scale hardware production phase. The first of the ten accelerating cavities was final-machined and brazed. Copper forgings for the remainder of the ten tanks were procured and rough-machined. After rough machining, the forgings were split longitudinally, the hydrogen furnace was annealed, and the coolant passages were deep-drilled around the bore. Figure 4.5 shows a DTL cavity after drilling and prior to final machining. Many of the ancillary components for the DTL have been delivered, including: post couplers, tuning bars, conditioning blocks, drift-tube positioners, and end walls. Designs for the production versions of the rotary tuner

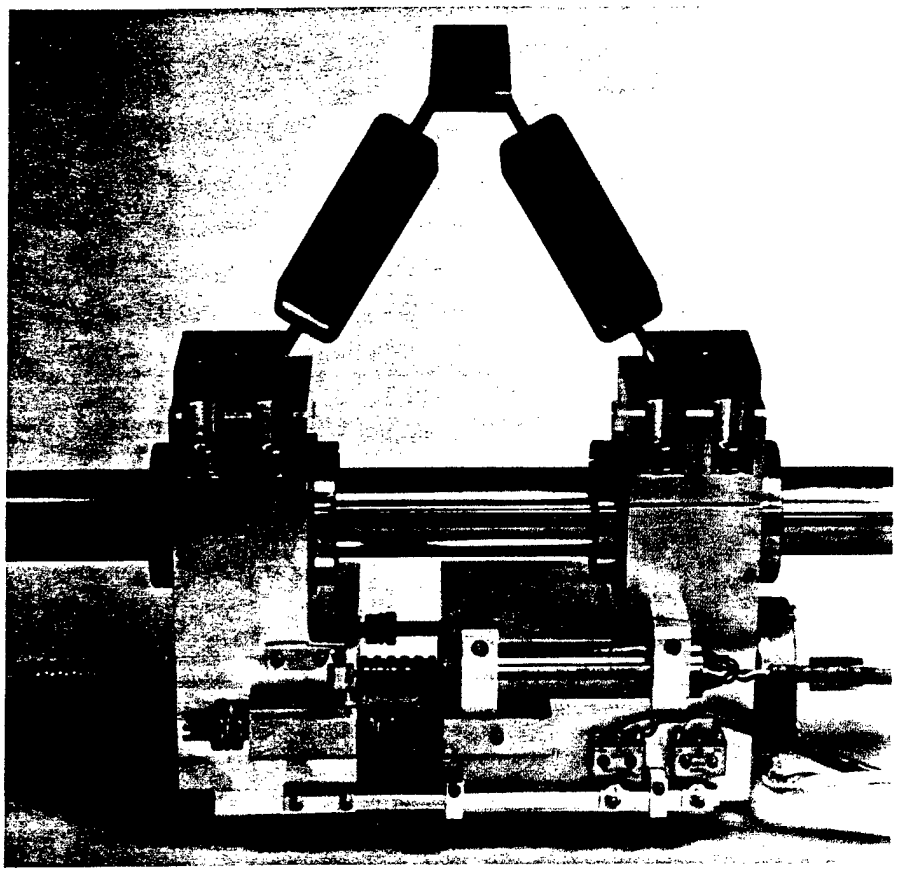

Figure 4.6. The DTL module positioning system.

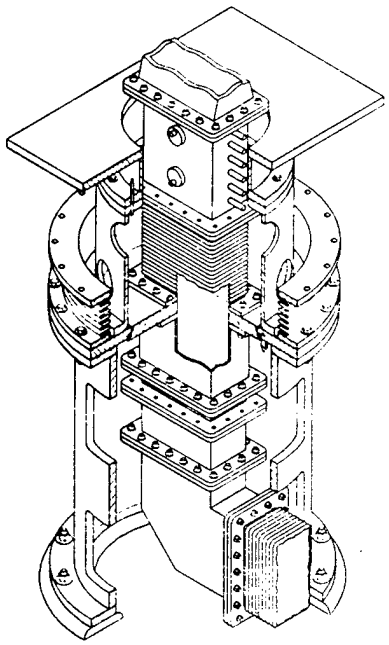

Figure 4.7. The DTL module rf waveguide support system.

and the steering magnet positioner were completed after extensive prototype testing. To avoid the complications arising from operating dynamic devices at cryogenic temperatures, Group AT-4 decided to design the mechanical portions of these devices to run at room temperature. The complete electron-beam welded drift tubes for the $2\beta\lambda$ portion of the accelerator have been fabricated to the point where they require insertion of the permanent-magnet quadrupoles (PMQ) before the final closure weld is made. Acquiring the assembled PMQs has proven exceedingly difficult because of our inability to obtain repeatable measurements calibrated to an absolute reference. Test programs were completed to assess the effects of various fabrication procedures on the rf properties and the cryogenic conductivity of the oxygen-free copper used for the DTL.

The design and development of the structural support providing remote positioning for the DTL has been completed. These devices allow positioning of the accelerator cavities to 25-μm accuracy. The positioners also keep thermal transfer to a minimum. Properly measuring the position of the DTL modules from outside the cryostat vacuum tank to ensure reliability was also incorporated in the design. Figure 4.6 shows the remotely controlled positioning device.

Additional support schemes have also been developed for all service connection to the DTL cavities. These schemes must support the hardware connected to the DTL without affecting the DTL's positional accuracy. They must provide rigidity to the system while minimizing the forces applied to the cavity. Figure 4.7 shows the design of the rf-waveguide support system. The support system provides a rotary vacuum joint for the waveguide, a high dynamic response to eliminate coupling with the rf structure while providing isolation from vibrations induced by the cryostat, and proper realignment when an rf module is removed and reinstalled.

GTA Beam-Transport System

AT-4 devoted FY 1990 to the system design and engineering analysis of the GTA telescope. We initiated detailed components design at midyear. This design is rather complex, in that extreme care must be taken to eliminate, avoid, or cancel all uncontrolled magnetic fields (e.g., earth field, induced fields in materials, etc.). The GTA output optics system, identified as the telescope, includes four "eyepiece" electromagnet quadrupole lenses. The lenses establish controlled expansion of the beam exiting the output matching section between the accelerator and the telescope. This controlled expansion is necessary for the beam's acceptance by the four permanent quadrupole magnets that form the "objective" lenses (see Fig. 4.8). Electromagnet "correctors" are provided for each of the four quadrupole objective lenses. The accelerated beam expansion is controlled by the objective lenses prior to

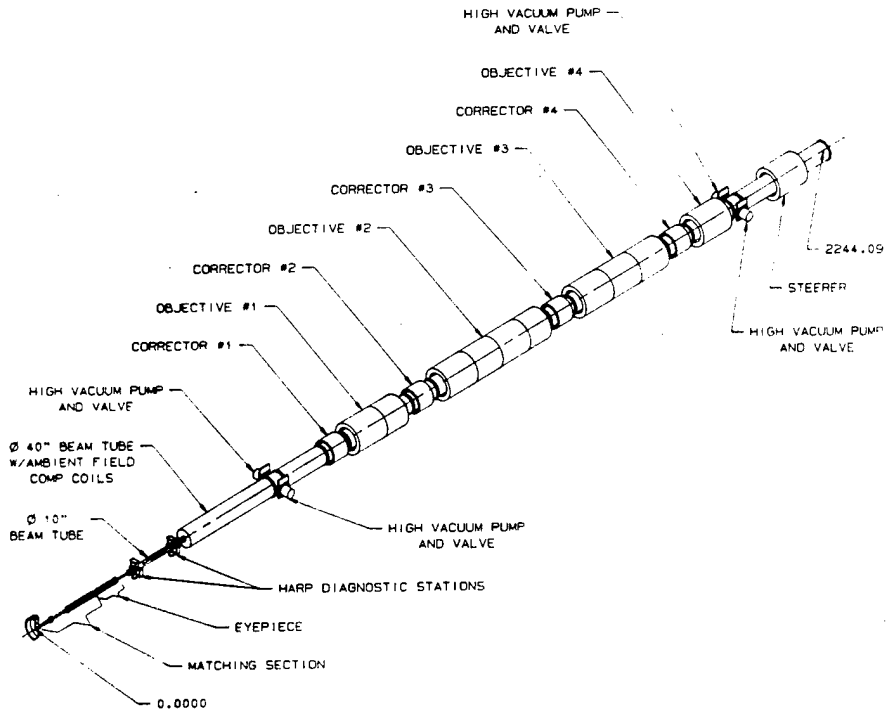

Figure 4.8. Layout of the GTA telescope.

the beam's entrance into a Lambertson-type steering electromagnet dipole. The telescope beam tube installation also includes quadrature ambient-field compensation electromagnet coils on all beam tube sections to trim the magnetic anomalies of the accelerator tunnel and the earth field.

The group responsible for the system design and analysis carried out this year paid particular attention to the problem of potential stray magnetic fields. In this respect, permeability of the beam tube material and of all hardware components near the beam path are of considerable importance. We also addressed other engineering issues such as stability of magnet support stands, vacuum system, services, etc.

GTA Components Testing

As part of the GTA developmental and construction effort, environmental test chambers have been constructed and used to validate component designs.

Three vacuum test chambers, have been built to provide GTA operating ambient condition for component test. The chambers incorporate 20 K helium gas cooling, vacuum levels of less than 1×10^{-5} torr, and a high-power rf environment. The high-power cryogenic test bed (HPCTB), with a volume of 17 m^3, can accommodate complete accelerator structures for off-line conditioning tests. The lower-power cryogenic test bed, with a volume of 9 m^3, can accommodate complete accelerator structures for tuning and testing subsystems in their operating configuration. The small cryogenic component test bed (CCTB), with a volume of 2 m^3, provides convenient, easily accessible testing for individual components. Each test bed is provided with computer data acquisition, temperature monitors, and pressure and position sensors. Computer control can be provided for long-term tests.

The RFQ system includes static and dynamic slug tuners, remote actuation RFQ positioners, proximity probes, temperature sensors, and related electromechanical devices. All RFQ system components have been characterized as individual components or subassemblies, depending upon their application.

Group AT-4 used the CCTB and the HPCTB at 20 K, high-vacuum, and high-power rf to characterize the components. Before installation of the RFQ into its beam-line vacuum vessel, Group AT-4 performed the following in the assembly laboratory: installation of the characterized components into the RFQ; pressurization and leak testing of gas-cooling channels; and tuning, alignment, and check-out of control systems, actuators, sensors, and rf pick-up loops.

Ground-Based Free-Electron Laser (GBFEL)

Los Alamos is teamed with Boeing Aerospace and Electronics for the design of the GBFEL accelerator, LSS, to be sited at White Sands Missile Range. The accelerator is a 100-MeV electron linac with a design average beam current of 0.27 A, operating in the cw mode. It consists of 92 individually driven rf cavities. The accelerator must come on-line and operate in either a pulsed or cw rf mode and remain matched to the fixed

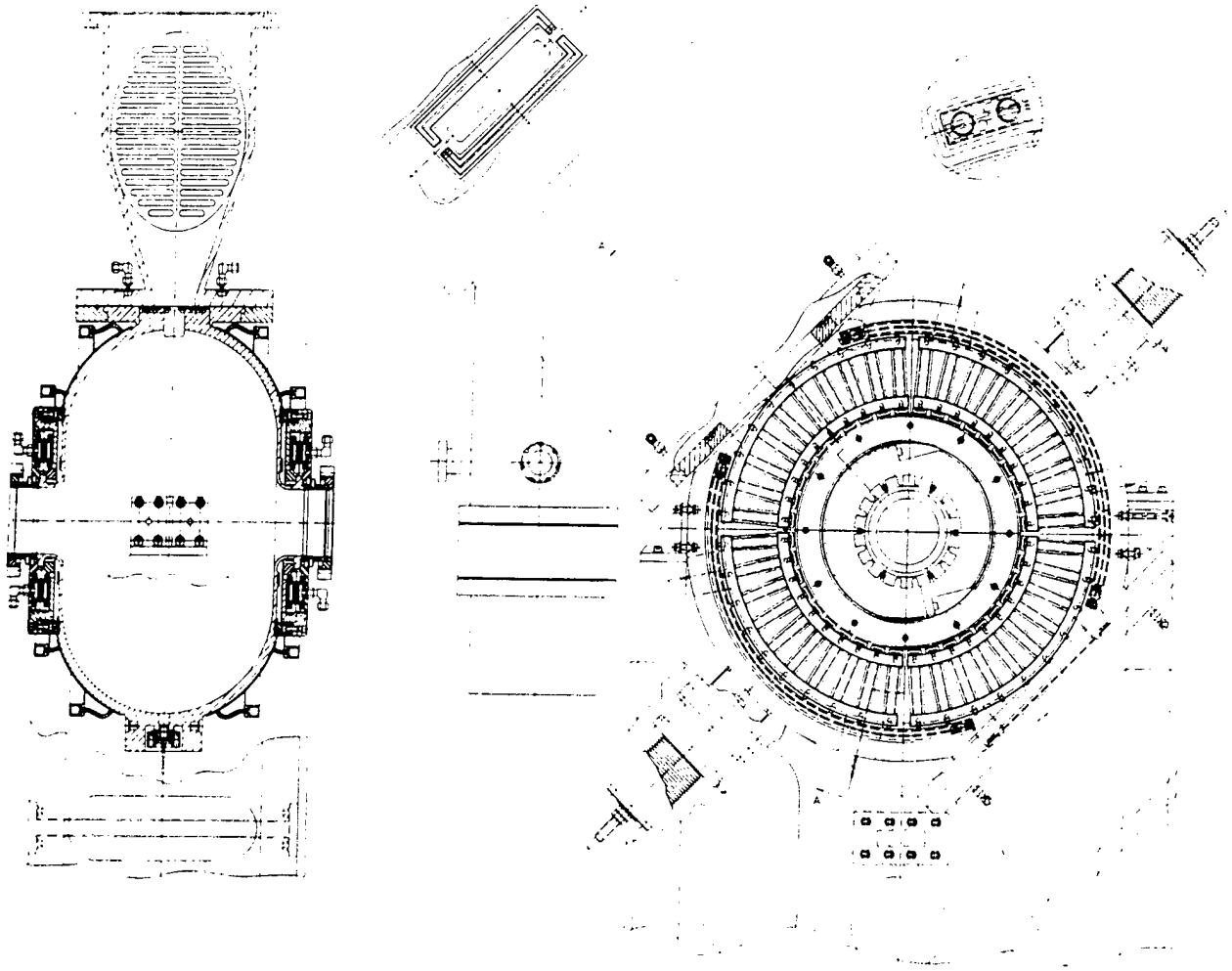

Figure 4.9. The LSS cavity.

drive frequency (433 MHz) within ±1.5 kHz at all times. The most challenging aspect of developing this design is determining the most effective way to maintain cavity resonance control over the range of rf duty factor from 0 to 100% while using the minimum amount of cooling water.

The first phase of the accelerator design effort is to design, build, and test a four-cell prototype on a test stand at the Boeing facility in Seattle. The tests will be done at a duty factor of 25% but at twice the nominal electric-field levels to simulate the thermal conditions for 100% duty factor. The mechanical design of the cavities combines extensive electron-beam welding on the cavity shells to incorporate cooling channels with high-temperature hydrogen furnace brazing to join the shell halves into rf cavities. Room-temperature tuning is accomplished through deformation of the cavity walls by stretching or compressing the walls axially. This provides a means of compensation for manufacturing errors in the cavity contour. Dynamic tuning is done through pairs of motor-driven movable bars inserted into the magnetic field at symmetric positions on the cavity equator, perpendicular to the coupling iris plane.

The LSS project was initiated in March 1990. After review of earlier test prototypes and conceptual designs, a decision was made to go forward with a four-cavity, individually powered prototype system. AT-4 took the responsibility for the cavity design.

By the end of FY 1990, a final cavity design was developed and detailed design was initiated. Figure 4.9 shows the LSS cavity design with its rf-feed waveguide and opposed matched termination.

AT-4 Engineering Development

In the course of providing mechanical engineering support and responsibility for the development and fabrication of hardware for AT Division, AT-4 faces particular challenges in engineering systems combining sometimes virtually exclusive requirements. Of particular interest are the problems of high-power rf combined with vacuum, cryogenic temperatures, and mechanical stability.

Cryogenic operation of rf accelerators offers the potential for higher rf efficiency and more stable operation in rf structures. The potential for lower rf power consumption motivated AT-4 to design cryogenic accelerators for the neutral particle beam (NPB) program. The increased electrical conductivity of accelerator structures at cryogenic temperatures promises to reduce copper losses, thereby reducing rf power consumption. Liquid oxygen and liquid hydrogen cryogens will be used on the NPB platform as an energy source to generate prime power. The availability of refrigeration capacity in the form of cryogens provided the premise upon which to evaluate the potential gains of operating an NPB accelerator at cryogenic temperatures. Substantial gains in thermal conductivity, in addition to increased electrical conductivity, are possible at cryogenic temperatures and should allow the use of much simpler cooling schemes in rf structures; in some cases, these cooling schemes provide the only viable means for handling the very high, local heat fluxes produced in these very compact high-power devices.

Defining cryogenic operation for these accelerators is important. The operating temperature range of the accelerator is between 20 and 35 K. The rf structures are not superconducting; however, rf conductivity in the structures can increase by factors up to six at these temperatures. Because the structures are not superconducting, they are not subject to the phenomena of quenching, which can produce dramatic changes in resistive heat loads in superconducting structures. However, a significant nonlinearity in the temperature-dependent electrical conductivity of these cryogenic structures does exist and must be considered in the design. The GTA is designed to be cooled by either gaseous helium at a pressure of 16 bars for a 2% duty cycle or by supercritical hydrogen at a pressure of 22 bars for cw operation.

Understanding how rf power loading and how cavity resonant frequency and stresses are affected by thermal losses inherent during accelerator operation is important. The ability to predict transient thermal-induced frequency shifts by combining SUPERFISH and FINITE ELEMENT ANALYSIS codes has been established. These outputs are being used to establish and predict the dynamic response of frequency tuner design for GTA. Also, cryogenic operation presents some large thermal strains during cool-down from room temperature to the 20–30 K required for operation. These strains have been analyzed with the same tools.

Another consideration of the cryogenic hardware is the thermodynamic properties and cooling characteristics of the high-pressure helium cooling fluid. Several temperature-dependent coolant programs were required for calculating the overall thermal response of components connected in series in the coolant system. For the GTA accelerator, transient responses were done for the RFQ, IMS, and the DTL systems for both low- and high-duty factor operation. These included thermally induced stresses in the drift tubes and tank walls of the GTA DTL and in the vanes of the GTA RFQ, pressure-induced stresses from pressurized cryogenic helium cool and natural frequencies of single stem drift tubes, and buckling and seismic response of large diameter beam tubes. These calculations often must consider nonlinear material properties because of the large temperature ranges the accelerating structures are subject to, in addition to anisotrophic material properties inherent in some of the materials used for fabrication.

Future Plans

AT-4 has at present but one goal and commitment: the successful completion of the GTA. In FY 1991, a concerted effort will be made to complete the task on schedule and within budget.

As the engineering support for GTA winds down, AT-4 will diversify its activities into new projects, such as accelerator transmutation of nuclear waste (ATW) and International Fusion Materials Irradiation Facility as well as support other AT programs such as the Dual-Axis Radiographic Hydrodynamic Testing Facility. As we diversify, it will be important to strengthen those engineering and design capabilities within the group that have led to the successful support of GTA. In particular, the areas of mechanical design, engineering analysis, and advanced accelerator engineering will be expanded to encompass a core engineering cadre from which to draw the engineering teams in new projects.

References

1. Don Liska, Mike Brown, and Bob Grieggs, "Cryogenic Operation of a Prototype Rotary Tuner," AT-4 Technical Note 89:519, November 1989.

2. Don Liska, "RF Window Locations for the GTA Tube Linac," AT-4 Technical Note 90:1, January 1990.

3. Don Liska, "Final Qualification of GTA DTL Drift Tube Adjusters," AT-4 Technical Note 90:2, January 1990.

AT-5
Radio-Frequency Technology

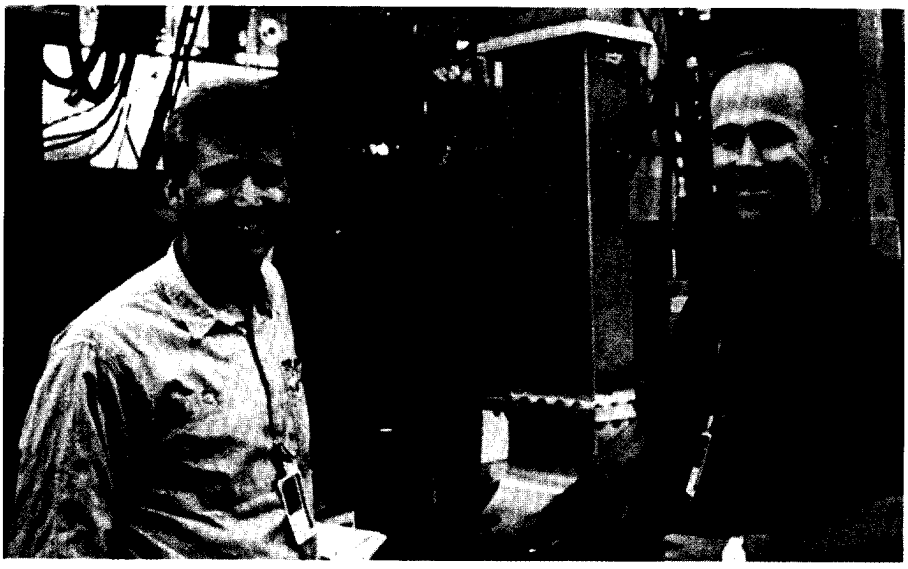

L. E. Eaton, Group Leader; Michael Lynch, Deputy Group Leader

Introduction

Group AT-5's charter is to design, develop, and build radio-frequency (rf) systems for accelerators. We have complete rf system capability, which consists of high-power amplifiers, low-level rf (LLRF) controls, and computer interface controls. These rf systems are for both linear accelerators and circular machines.

Group AT-5 delivered the rf systems for experiment 1B, IC for the ground test accelerator (GTA). We are presently building the 850-MHz system for experiment 2. We have also been involved in the Modular Concept Test Development (MCTD) project at Boeing Aerospace and Electronics, where we delivered a LLRF and resonance control for the Free-Electron Laser (FEL) project. We have negotiated and managed delivery on a $1.5 million klystron order from Thomson CSF in France. We modified a Clinton P. Anderson Meson Physics Facility (LAMPF) 805-MHz klystron to 850 MHz for the GTA program. We continue to be involved in the Superconducting Super Collider (SSC) ferrite tuned cavity design. We are also delivering a system for the University of Twente and are negotiating work with the University of Milan. We are proposing an rf system for the antisatellite (ASAT) program and FEL system.

In summary, AT-5 has developed an expertise and capability for rf system design, component building and installation for accelerators.

Ground Test Accelerator (GTA)

Overview and Goal

The GTA is a proton linear accelerator being developed in AT Division for the Strategic Defense Initiative. The accelerator is powered by rf sources, and AT-5 is responsible for delivering the total rf system for this accelerator. The goal of AT-5 is to build turn-key packages that are delivered to the GTA installation group.

Our emphasis is broken into two areas: rf power systems and rf controls.

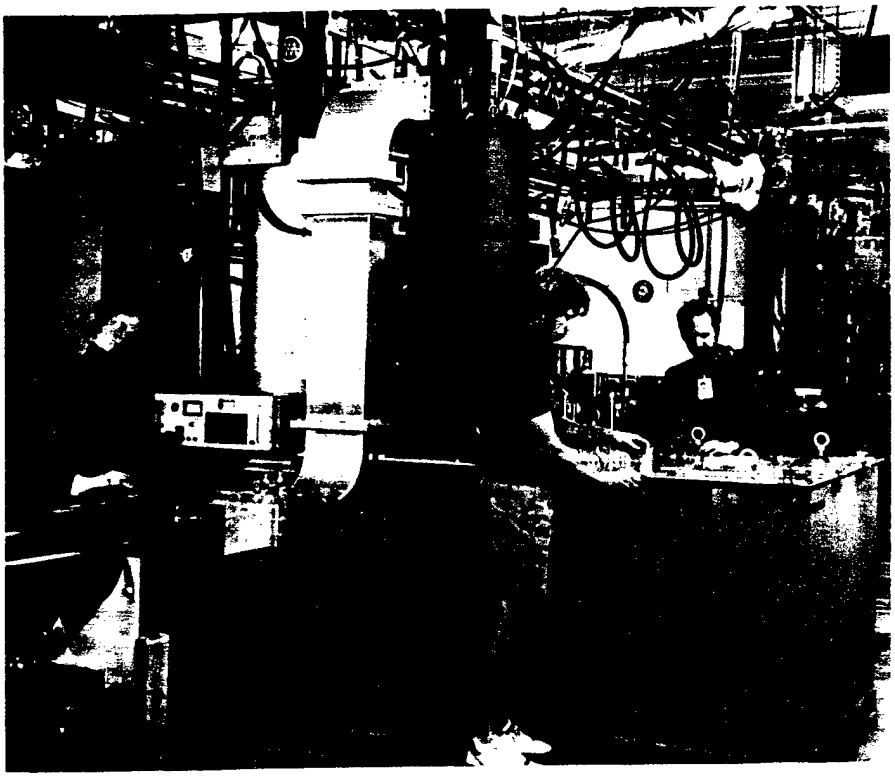

Figure 5.1. Dual-klystron, 850-MHz rf station during prototype testing.

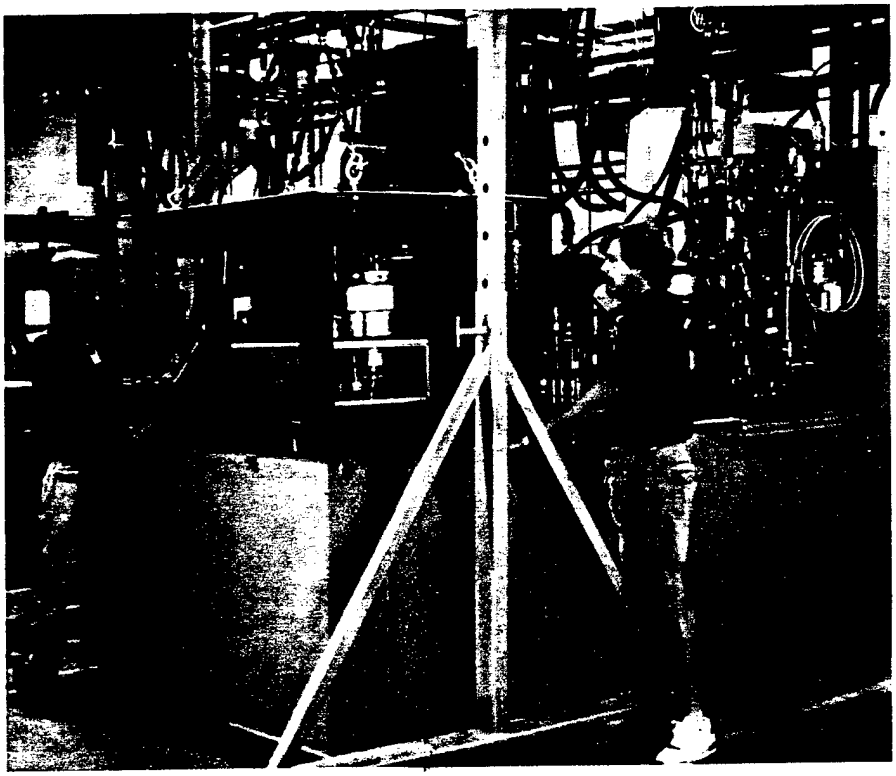

Figure 5.2. Dual-klystron, 850-MHz rf station with pulse modulator lifted.

GTA rf Power Systems

Introduction

The major progress for GTA in the high-power sector includes:

- redesigning of the single-klystron, 425-MHz modulator into a dual-klystron, 850-MHz modulator;
- completely controlling the new modulator and its associated power supply with a programmable logic controller;
- remanufacturing and converting an 805-MHz klystron to 850 MHz;
- testing and operating the 425-MHz tetrode system with cryogenic cavity and beam loading;
- producing and testing the first prototype and first three production 850-MHz klystrons;
- designing and beginning construction of the 850-MHz tetrode amplifier;
- operating the rf systems under closed-loop control for the funnel experiment.

Klystron rf Station 850-MHz

AT-5 developed a prototype dual-klystron, 850-MHz, high-power rf station, which has been in operation since August 1990. Figure 5.1 shows the waveguide-output side of the station, with two Varian 850-MHz klystrons installed. The klystron to the right is the specially developed Varian VKP-8362, based on the highly successful 805-MHz klystron used at LAMPF. The klystron on the left is a rebuilt LAMPF klystron, using reduced-volume rf cavities to tune to the higher frequency. This klystron was designed and executed by the Electron Tube Lab of Los Alamos National Laboratory (LANL).

Both tubes are operated from the same high-voltage cathode bus and pulse modulator. Figure 5.2 shows the other side of the rf station, with the pulse modulator raised from the oil tank by means of a portable gantry and electric hoist. The water-cooling manifold, also common to the two tubes, is to the right of the technician in the foreground.

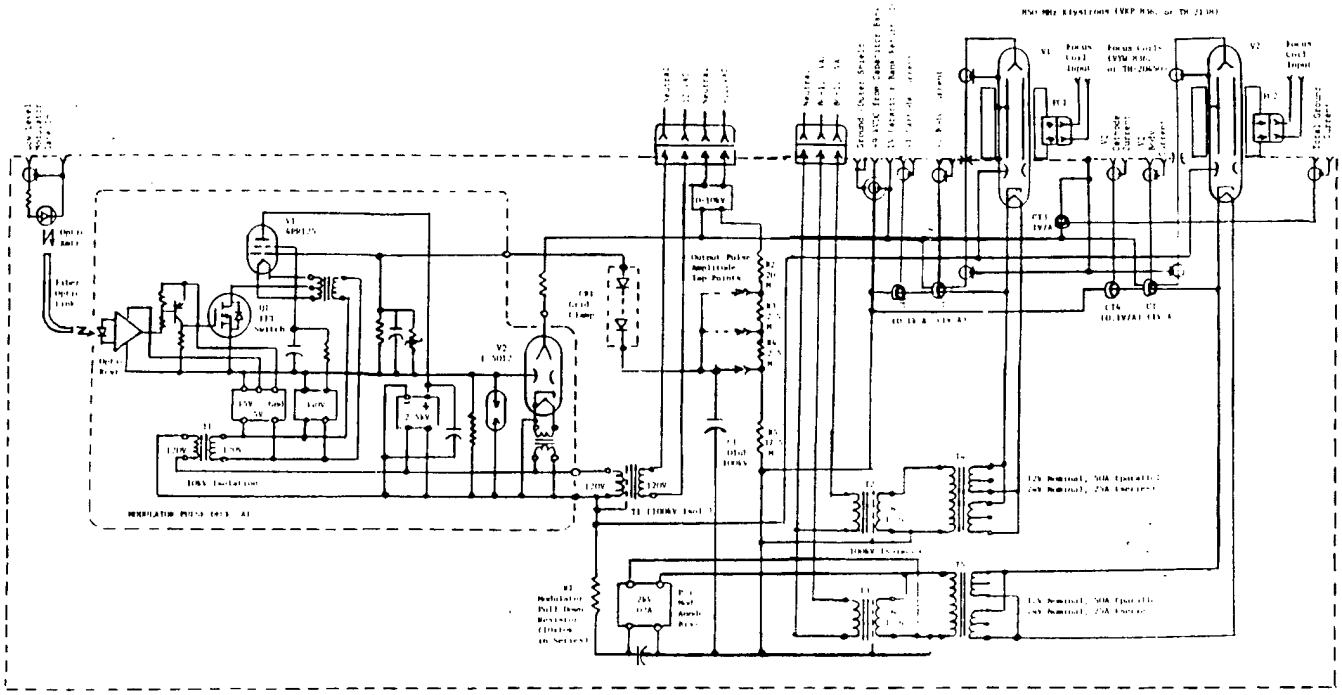

Figure 5.3. Simplified schematic diagram of dual-klystron, 850-MHz rf station oil tank.

The oil-filled tank, the water manifold, and many of the components used in the pulse modulator were reclaimed from the GTA-1 single-klystron, 450-MHz rf station (one of which can just be seen in the background of Fig. 5.1). Figure 5.3 is a simplified schematic diagram of the rf station oil tank. The pulse modulator (subassembly A1) uses a single Litton L-5012 "Injectron" beam switch tube as the high-voltage electronic switch. Two such tubes are used in the GTA-1 rf stations. The modulator is connected as an "active pull-up, passive pull-down" floating-deck modulator. Its output directly drives the modulating anodes of the two klystrons.

The 850-MHz klystrons operate at a current of approximately 30 A and a voltage of approximately 85 kV, with a modulating anode swing of 60–75% of the nominal cathode voltage. This results in an intrapulse modulating-anode voltage of 30 kV negative with respect to ground. The grid of V1 in section A1 is connected, by means of high-voltage diode CR1, to a tap on the voltage divider comprising resistors R2-R5. The voltage divider is connected across the high-voltage dc klystron beam supply. When the modulator output pulse attempts to become more positive than the tap-point voltage, the current flow through CR1 and the A1-V1 grid resistor shuts off A1-V1, clamping the modulator output voltage near the tap voltage. The modulator, in this mode, acts as an amplified cathode follower, regulating the output voltage regardless of klystron modulating-anode interception current. Moreover, because of coupling capacitor C1, connected across the low end of the divider, the output voltage of the modulator tends to track the intrapulse variation of the klystron cathode voltage. The cathode voltage

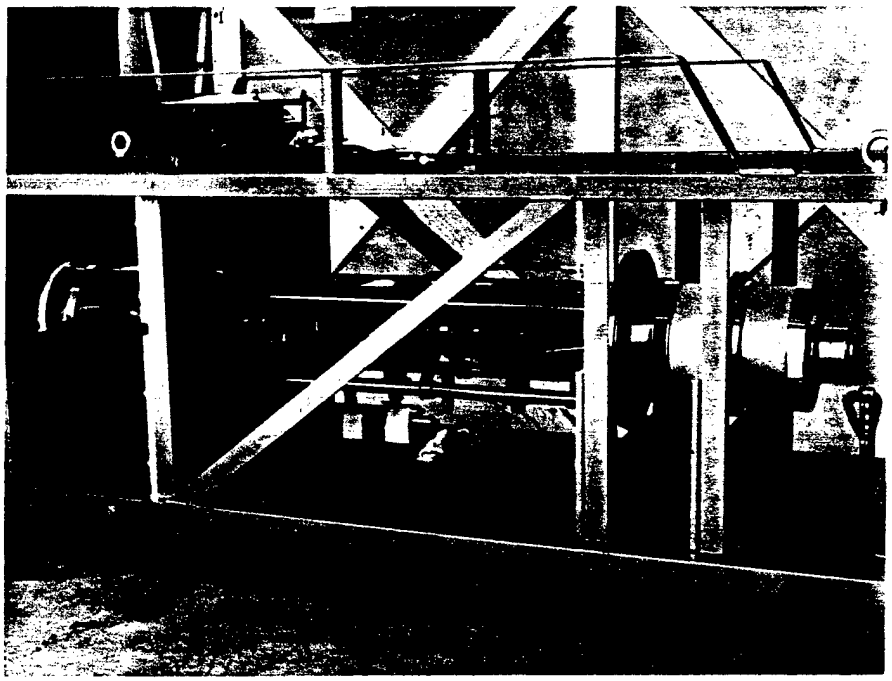

Figure 5.4. First Thomson TH-2138 850-MHz klystron at LANL.

normally has linear droop due to the discharge of the energy storage capacitor bank by the klystron cathode current. This results in nearly constant intrapulse voltage from the klystron cathode to the modulating anode. The beam current is therefore nearly constant, despite the cathode voltage droop.

At the end of a pulse, which has a nominal maximum duration of 2 milliseconds, A1-V2 shuts off and the load capacitance discharges through R1.

The first production Thomson TH-2138 klystron successfully completed acceptance testing at the Thomson plant in early October and has since arrived at LANL, as shown in Fig. 5.4. We cannot install the klystron in the prototype rf station until (1) we receive the international-type water fittings and (2) complete testing of the LANL-designed blind-mating socket for the klystron. The socket, which is not offered by Thomson, consists of a modified LAMPF-type klystron socket, as shown in Fig. 5.5. This socket mates with an adapter mounted to the heater-cathode end of the klystron.

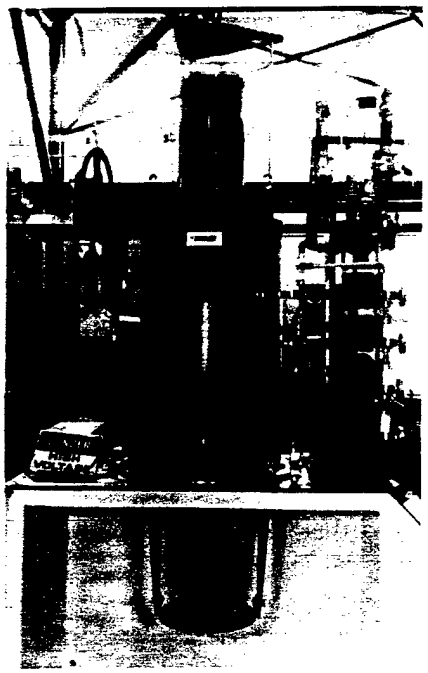

Figure 5.5. Thomson klystron mounted in LANL-designed blind-mating socket.

The support racks for the rf station, shown in Fig. 5.6, house the ion-pump supplies; a local pulse generator; high-speed fault-reaction circuits, that respond to klystron pulse-current indications; a remote controller for the pad-mounted high-voltage direct current (HVDC) power supply; focus-coil power supplies (four in parallel for each klystron focus coil); a power-distribution unit; and an Allen Bradley programmable industrial controller and plant-floor display terminal, through which the rf station interlocks and controls are coordinated and processed for operator interaction. A closeup of the Allen Bradley input/output (I/O) crate, with processor and I/O modules, and the T30 display is shown in Fig. 5.7.

The rf station operated with an 11.2 μF capacitor bank, and a 120-kV dc, 1A high-voltage power supply. The capacitor bank, housed in a shielded room, has current-limiting and energy-absorbing series resistance and a pneumatically operated HV dump relay. The pad-mounted power supply has a primary silicon-controlled rectifier controller. The capacitor bank is being equipped with an electronic crowbar, similar to the infinite-voltage range types used in the LAMPF rf system, in order to provide the klystron fault protection specified by Thomson for their klystrons.

Operation of the rf station, especially with the Varian VKP-8362, has revealed much new experimental data concerning running the klystron at less than the 1.25-MW full-rated power output and reduced beam current, and regaining lost efficiency by deliberately mismatching the rf output line. The Thomson klystron, in its acceptance testing, exhibited possibly improved performance in such a mode, reaching rf saturation with nearly the same rf input regardless of beam current.

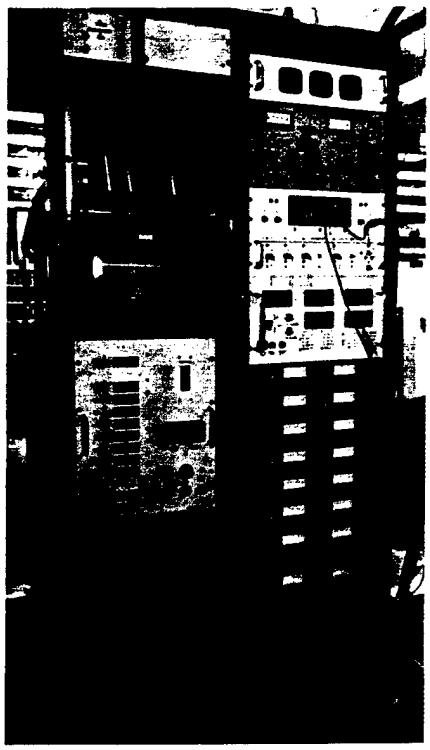

Figure 5.6. Support racks for dual-klystron, 850-MHz rf station.

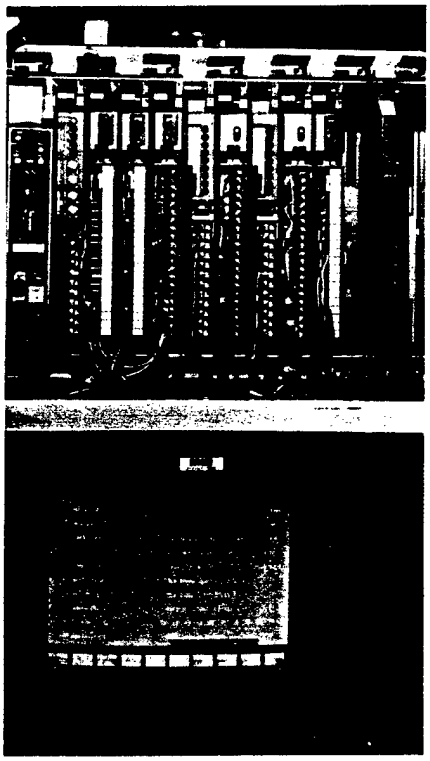

Figure 5.7. Closeup view of Allen Bradley industrial controller interfaces.

Screen Room

We finished the MPF-365 screen room for for the GTA experiment. We built and tested the cap bank configuration shown in Fig. 5.8. Two cap banks are being configured; one for the rf conditioning stand at 850 MHz and the other to drive the ten klystrons for the drift-tube linac (DTL) section of the accelerator. Both cap banks are fed by 100-kV power supplies. The conditioning cap bank is 8.4 μF and holds 30 kJ at 85 kV. The main cap bank is 70 μF and holds 253 kJ at 84 kV.

LAMPF Rebuild 805 MHz to 850 MHz

The impressive *tour de force* was the rebuilding of a broken 805-MHz LAMPF klystron for GTA operation at 1.25-MW peak power at 850-MHz. We cut the klystron into over two dozen pieces (see Fig. 5.9) that included the electron gun, the five rf cavities, the window, the collector, and the output waveguide. We performed calculations performed on the cavities to determine the volume of metal that had to be added to raise the resonant frequency of each cavity by 45 MHz. Cold models of several cavities were made of aluminum, and the calculated changes were verified by experiments with the cold models.

We considered five unique methods for adding metal to reduce cavity volume, and in the end we chose to weld new pieces inside each cavity. Three of the cavities have frequency tuners with ranges of a few MHz, and the perturbing volume had to be fashioned so as to not interfere with these tuners. The input cavity has an input loop as well as the tuner, so its perturbing volume had to be broken up into two pieces to fit into the available space. The output cavity is copper and copper plated, so welding was not used. We calculated the sensitivity of the output cavity frequency to the length of the output gap. Based on these calculations, we machined the noses of the output gap to raise the resonant frequency by 45 MHz.

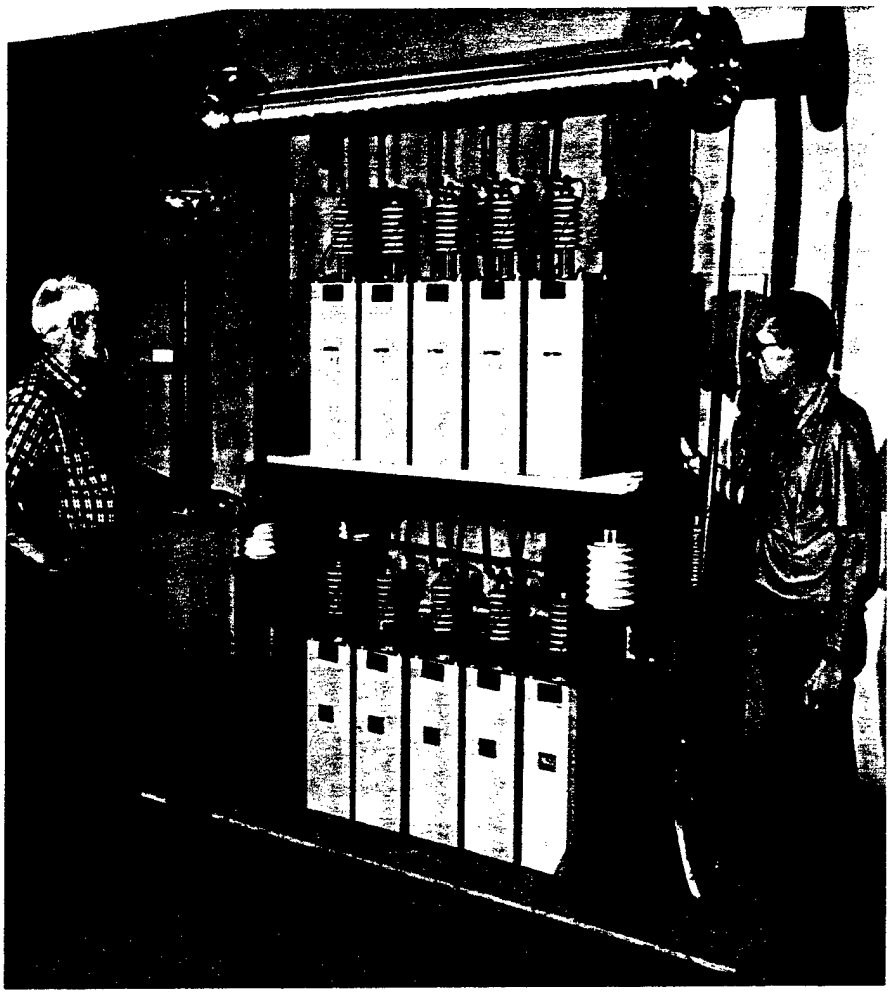

Figure 5.8. GTA conditioning stand cap bank.

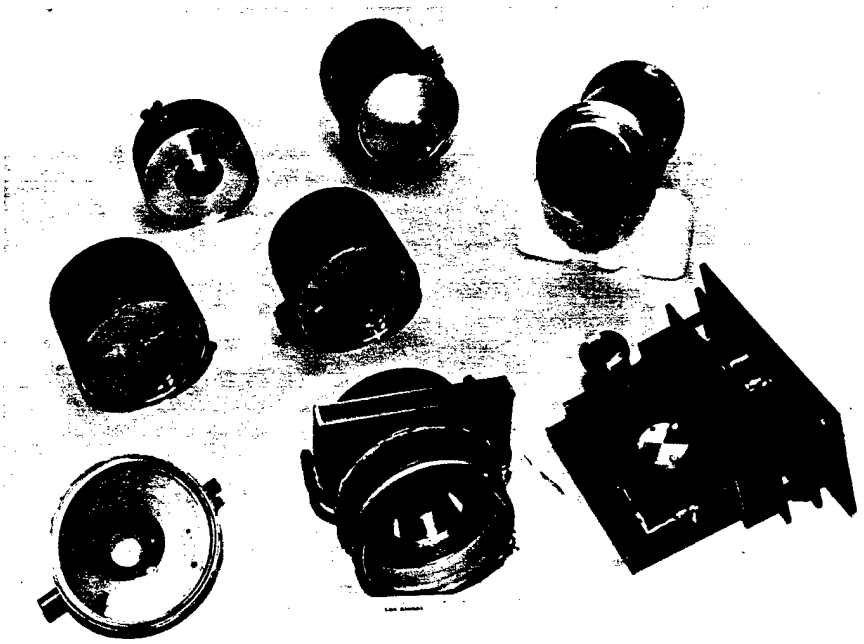

Figure 5.9. Cavity parts from disassembled LAMPF klystron.

Due to the large number of saw cuts required to take the klystron apart, we had to make spacer rings to restore the lost length. We machined the cavities to create ends perpendicular to the klystron axis after the welding of the frequency-control blocks. We then cold-tested the cavities before final assembly. The electron gun was cleaned, hydrogen fired, and recoated with an oxide-cathode mixture. Several jigs and fixtures were used for the final assembly process. These fixtures and a large oven had been built years ago to repair the 805-MHz LAMPF klystrons. After leak checking the klystron, we baked it in the large oven; then we activated the cathode. The emission capability of the cathode was good on a low-voltage test; we made the final pinch-off to separate the klystron from the oven's vacuum system. The external parts of the klystron were then replaced, and the klystron was tested in a LAMPF modulator and tuned to produce over 1 MW at 850 MHz. The klystron was then sent to MPF-18, a GTA test lab, where it was installed in the prototype GTA two-klystron modulator. This klystron has operated both alone and with the commercial prototype klystron in the GTA modulator, and both klystrons exceed the requirements for the GTA.

Tetrode 425-MHz

During FY 1990, the prototype 425-MHz tetrode amplifier delivered power to the GTA radio-frequency quadrupole (RFQ) under the control of the low-level rf subsystem, and work is nearing completion on the three production amplifiers. The tetrode amplifiers are capable of delivering 50 kW to 250 kW of rf power in a linear mode and are controlled by Allen Bradley industrial controllers that interface to the GTA control system (see Fig. 5.10).

We have also begun prototype development on an 850-MHz gridded tube amplifier. The amplifier consists of a solid state driver and three gridded tube stages under Allen Bradley control. This amplifier will deliver up to 60 kW of rf power in a linear mode. The cavity design and fabrication is complete for the first two gridded tune stages and the solid state driver. The fabrication of the last stage and testing of the integrated package will be completed in FY 1991.

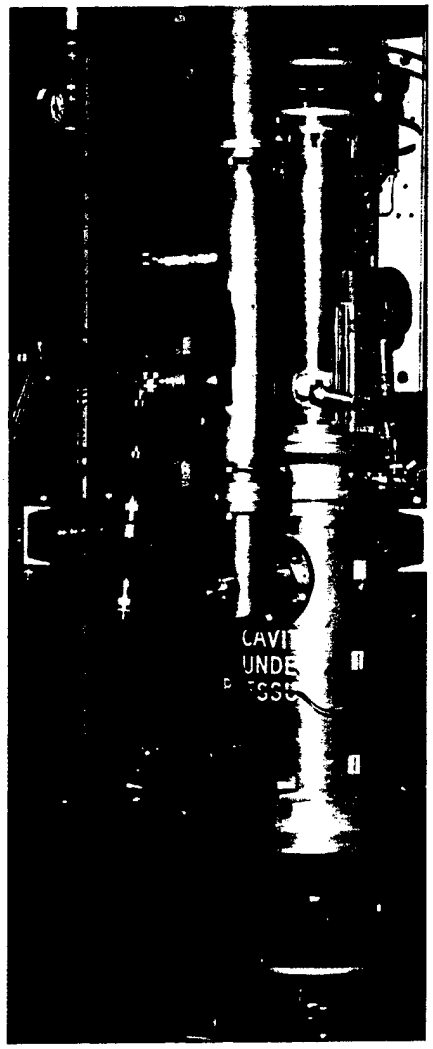

Figure 5.10. Output stage of GTA 425-MHz tetrode amplifier.

GTA rf Controls

Phase-Stabilized rf Transport for GTA

The low-level rf transport system requires a phase-stable means of delivering rf signals to their appropriate points of use. Each cavity requires both an rf reference transport and a cavity-field sense transport. Both transports use long cable runs up to 250 feet in length. Any phase errors that occur in transport can contribute directly to the phase errors in the cavity-to-cavity phase of the accelerator. Because this is a fixed-frequency system, a change in ambient temperature is the primary condition that can lead to a significant change in the insertion phase of any transported signal. Fluctuations over the anticipated ambient temperature range can introduce as much as a 27° electrical phase change at 1700 MHz.

A successful solution to this problem is shown in Fig. 5.11, wherein a signal from a reference oscillator is transported to a remote load. The circuit shown in Fig. 5.11 operates as follows: an rf calibration signal at a frequency equal to 1.5 times the frequency of the signal being delivered to the load is split and applied to both a

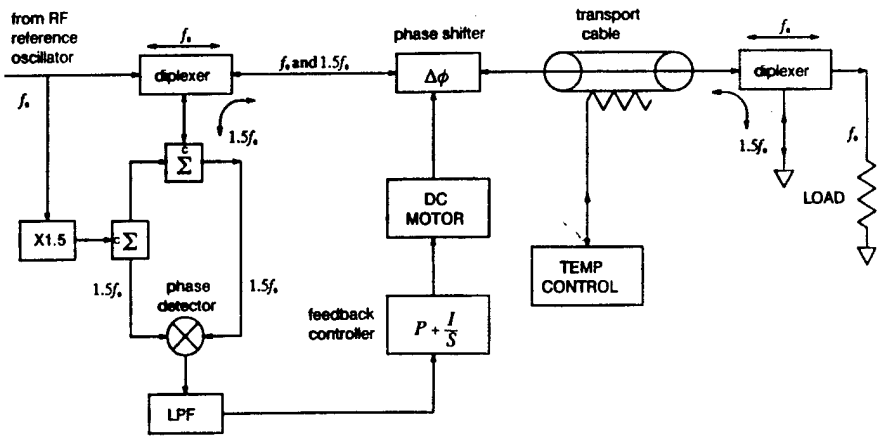

Figure 5.11. Cable phase stabilization technique for GTA.

phase detector and another splitter/combiner where it is then transmitted through a diplexer (described below) onto a single coaxial line. Upon arrival at a second diplexer, this calibration signal is reflected, via a short-circuit termination, back toward the first diplexer where it is extracted from the coaxial line and applied to the phase detector. The output of the phase detector is filtered and proportional and integral control actions are developed from this information. The output of the feedback controller is used to drive the phase shifter via the dc motor in such a way as to hold the electrical length of the transport path constant. The rf reference signal is superimposed and transported on the same stabilized path.

A diplexer is a passive device used to combine or separate two signals of different frequencies. Space does not allow a full description of the diplexer that was used, but it exhibited the required degree of phase stability. The results of a 68-hour test of the above scheme with a 150-foot coaxial transport cable yielded an output phase that was held constant to within ± 0.036° at the fundamental frequency over an ambient temperature range of 17°–22° C. Not only is this well within the ± 0.15° tolerable variation, but it also provides much better performance than our previous phase-stabilization plan. The earlier plan required at least twice as much hardware and was not as universally applicable as the diplexer scheme.

GTA rf Field Control System (In-Phase and Quadrature Control)

Due to the time-varying nature of the rf accelerator, rf field amplitude and phase parameters must be precisely controlled in order to confine and accelerate the charged partible beam. Typically, a feedback control system regulates the rf field, rejects noise and disturbances, and maintains operational stability over changes in the electrical structure of the accelerator. For GTA, a multivariable control system compensates the electrical structure of the rf amplifier and cavity to provide the desired performance characteristics. The design theory, based on gain shaping in the frequency domain, designs mathematical transfer functions into a compensator. Due to the mathematical relationships of the rf field, the amplitude and phase quantities have been resolved into in-phase and quadrature (I&Q) components. These orthogonal variables have simple mathematical relationships and can be analyzed using linear transfer-function matrices. We have applied the transfer matrix theory to the design of a multivariable control system that regulates the I&Q components of the rf field. I&Q controllers compensate the two signals to provide the desired frequency response characteristics. Since an accelerator contains many rf systems, the instrumentation must include sophisticated computer controls and diagnostics to support remote, autonomous operation. Consequently, computer interface circuitry allows the adaptive optimization of the mathematical transfer functions of the compensators.

This system controls the I&Q components of the accelerating field, creating a system with two inputs and two outputs. Multiple input and multiple output systems complicate the intuitive understanding of the dynamics to a degree that a matrix or state variable design approach is required. Although this is a true multivariable system with cross-coupling between the two variables, a modal transformation is performed on the variables by a predistorter stage (see Fig. 5.12). This control predistorter performs an inverse cross-coupling function on the two signals so that they are effectively decoupled by the amplifier and cavity systems. Consequently, the two variables (I and Q) can be controlled separately as single input, single output systems as shown in Fig. 5.13. The frequency-domain gain-shaping theory can be applied to each variable independently to adjust the total system performance characteristics.

GTA Reference System

Coherent phase-stable signals from the rf reference-generating system are required by each cavity field-control system to regulate the driving signals for each high-power amplifier exciting the rf field in the accelerator cavities. The rf reference-generating system is configured in a star distribution format originating at a master oscillator. The master oscillator supplies three phase-coherent frequencies that are

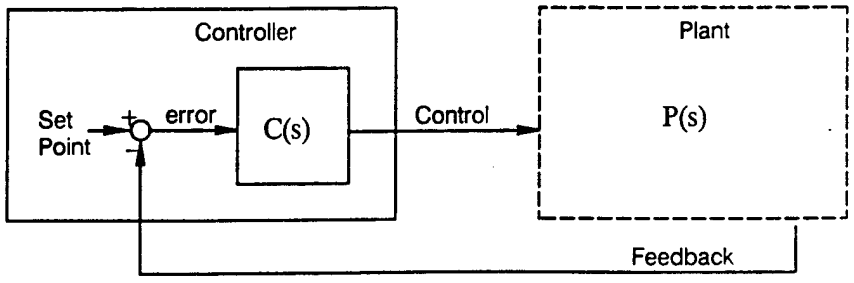

Figure 5.12. Simplified block diagram of the system seen by the I/Q controllers.

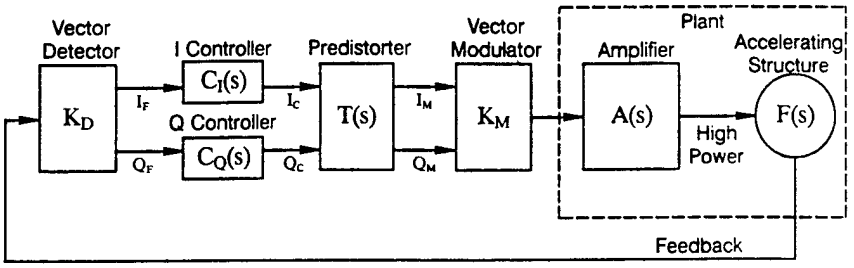

Figure 5.13. Simplified block diagram of I/Q control system.

harmonically related to a fixed fundamental. Phase-locked loops and Wilkinson splitters distribute these signals to many different output ports in a phase-stable manner, and a monitoring module assures the stability of the distributed signals. A block diagram of the rf reference generation system is shown in Fig. 5.14. One of these systems is required for the entire accelerator.

The system design is modular such that by simply changing a few components the higher frequencies' architecture will be the same as the fundamental's. The distribution requirements for the three frequencies differ in that only a few cavities are driven at f_0 and at $4f_0$ while more are driven at $2f_0$. To maintain modularity of the entire subsystem, however, each frequency leg was designed to accommodate the highest number of cavities driven at a single frequency.

The design relies on the phase stability of eight-way Wilkinson splitters. Temperature chamber data have been measured on the splitters, and the phase change of a signal through the splitters over a 20° to 50° C range appears negligible. However, to safeguard against any potential phase change due to temperature differential, the splitters are housed in temperature-controlled compartments. A phase-locked loop maintains a stable signal through the first eight-way splitter. This splitter fans out to a second set of eight-way splitters. Each eight-way splitter is formed by three stages of Wilkinson splitters in strip line. Because of the mechanical symmetry of the Wilkinson, the phase of the signals out of each leg of the splitters is either the same or different by a constant delta. Therefore, the phase-locked loop is necessary only to control the input signal to the first eight-way splitter. After that, the phases of distributed signals are all related by constants.

The initial design of the reference distribution system used several stages of amplification and phase control. By relying on the inherent consistency of the Wilkinsons, a single 4-watt amplifier and phase-locked loop per frequency is all that is required to achieve the desired output level. The inherent phase degradation of a signal through this amplifier is the driving force behind the requirement for the phase-locked loop. Although the amplifier runs class A and is operated in its linear region, time and temperature change its output phase beyond the allowable ± 0.15 degrees.

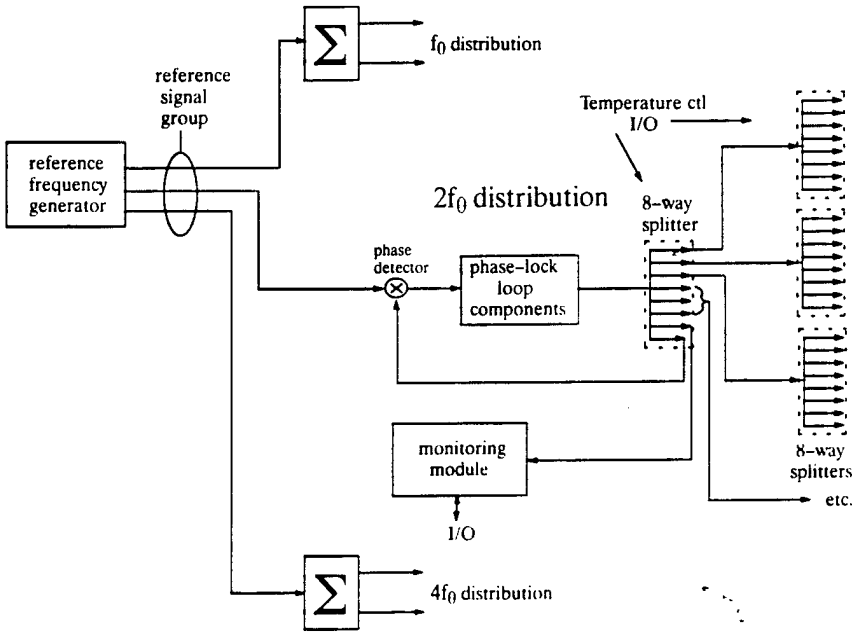

Figure 5.14. Block diagram of the rf reference-generating system.

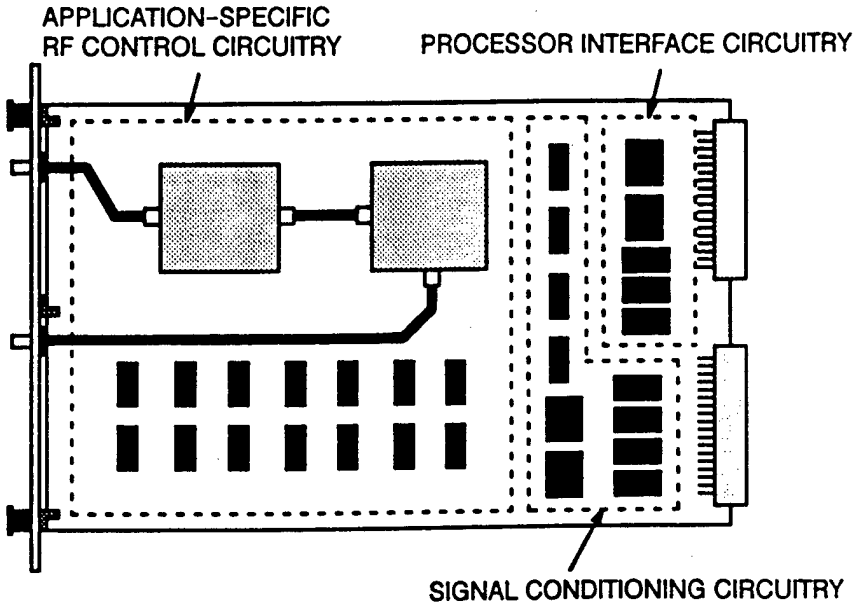

Figure 5.15. Conceptual view of a typical LANL VXIbus module.

Computer Interface for GTA

The design approach which combines the rf, signal conditioning, and computer interface electronics into VXIbus modules provides a flexible, high-performance, tightly packaged, rf control system. Figure 5.15 provides a conceptual view of a typical LANL VXIbus module, showing the combination of interface, signal conditioning, and rf circuitry.

The backplane processor interface circuit enables the VXIbus device communication, which allows the application-specific rf circuitry to operate under local processor control. This interface circuit provides the standard VMEbus processor interface functions, including the backplane buffers, the data transfer cycle handshaking, and the interrupt cycle handshaking. In addition, this interface takes advantage of some VXIbus features that were not offered in the VMEbus environment, including the VXIbus configuration functions, the dynamic configuration of a module's base address, module self-test functions, module slot identification, and failed-module inhibit capability. Furthermore, a timing signal generator is included in the processor interface to accommodate the LANL applications. The LANL VXIbus processor interface circuit resides upon a daughter board that can be removed from the application-specific mother board. This allows the processor interface to be replaced or checked out as a separate unit.

For the LANL accelerator applications, VXIbus modules perform the various rf control functions. The structure, address, map, and software driver are consistent for all devices since the identical VXIbus interface circuit is used on all LANL modules. A block diagram of the custom LANL processor interface circuit is shown in Fig. 5.16. The custom LANL VXIbus modules contain rf and analog circuitry that require some simple register-based I/O. Binary, analog, and timing signals required by the LANL modules are represented as 16-bit data registers. The division of the registers is consistent for all custom LANL VXIbus modules and, consequently, allows the use of a single software driver. Database software has been designed to address map the I/O channels directly to these registers. With the direct accessibility of the LANL register-based VXIbus system, average data transfer rates achieve 4 megabytes/second.

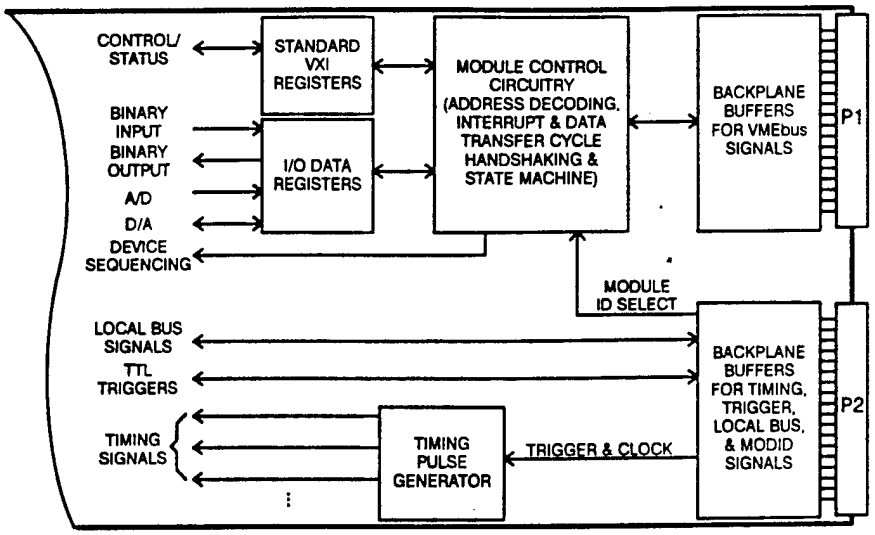

Figure 5.16. Block diagram of the VXIbus processor interface circuitry.

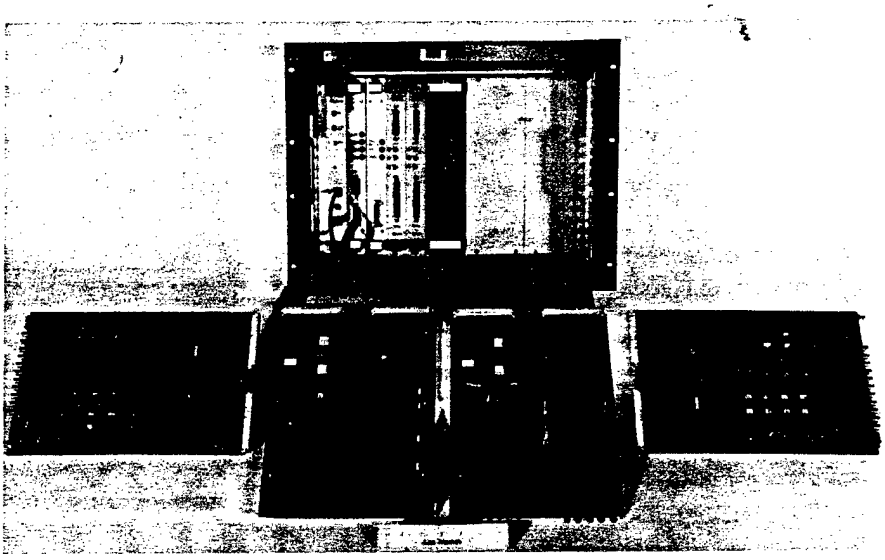

Figure 5.17. AT-5 custom-designed VXI modules for GTA LLRF system.

VXI Packaging

Group AT-5 has been instrumental in designing and using the VXI system for packaging both rf and digital electronics in the same modules. The VXI system is an industrial standard that AT-5 has adopted. Figure 5.17 shows a collage of the LLRF system.

Results of GTA Experiment 1B

AT-5 was instrumental in the success of experiment 1B for the GTA program. The rf system held the fields to the required tolerances. Figure 5.18 shows the rf system during the running of experiment 1B.

The early results of feedback control on the GTA RFQ are shown below. Figure 5.19 shows the forward and reflected rf waveforms and the detected in-phase (I) and quadrature-phase (Q) components, of the cavity field under closed-loop control with beam. The loop setpoints are 4.665 V for the I rail and 0 V for the Q rail.

Figure 5.20 shows the detected loop I&Q errors relative to their setpoints and the I&Q integral errors. Each error signal has been amplified by a factor of 20 from its actual value. Thus, in both cases, the peak error is:

$\varepsilon_{pk} \approx \pm (0.5V/20) = 50\ mV.$

Therefore, the peak field amplitude error is:

$\Delta_{amp} \approx \pm (25\ mV/4.665\ V)*100\% = \pm 0.54\%$,

and the peak phase error is:

$\Delta_{phase} \approx \pm (25\ mV/4.665\ V)*(360°/2\pi) = \pm 0.31°$.

Much of the residual error in these photographs is due to a low-frequency interference tone in the control system. The source of this tone is under investigation. When it is eliminated, the residual loop errors should be reduced. Also, since these photographs were taken, the control loop integral gains were increased, resulting in improved dynamic performance.

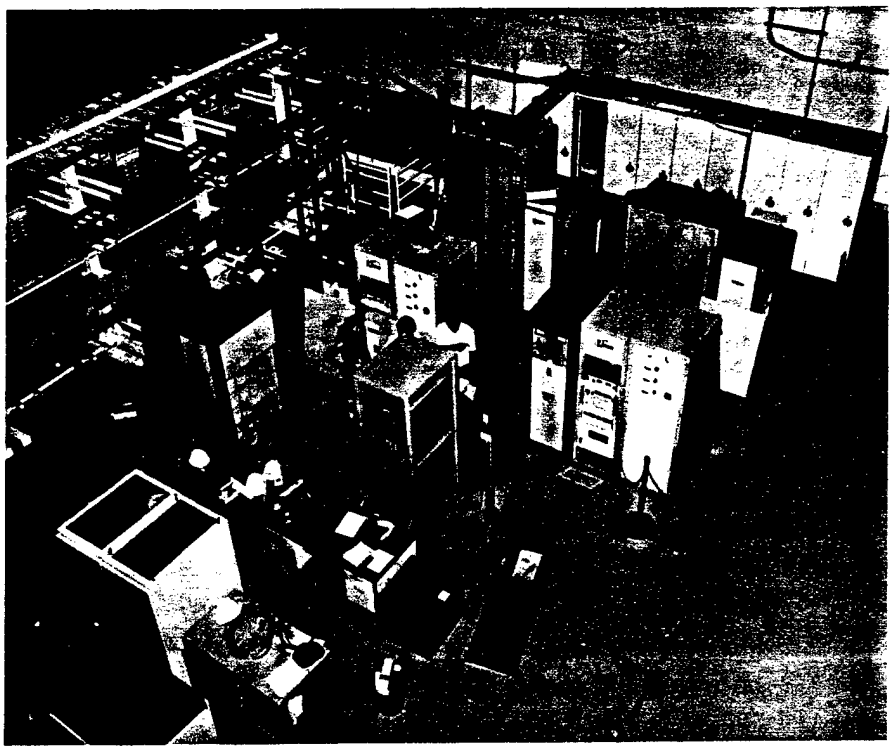

Figure 5.18. View of initial installation of tetrode amplifiers for GTA.

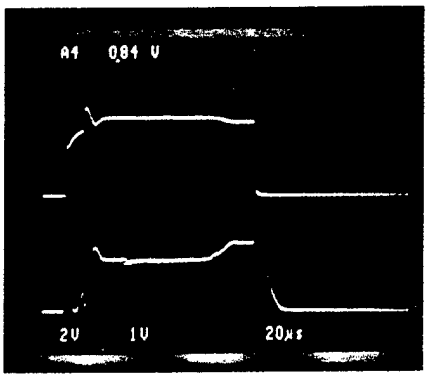

Figure 5.19a. Detected forward and reflected rf waveforms, under closed-loop control with beam.

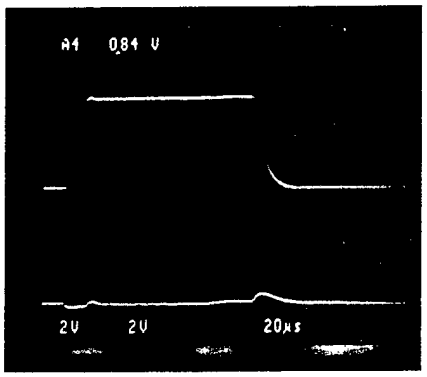

Figure 5.19b. Detected in-phase (I) and quadrature-phase (Q) components of cavity field.

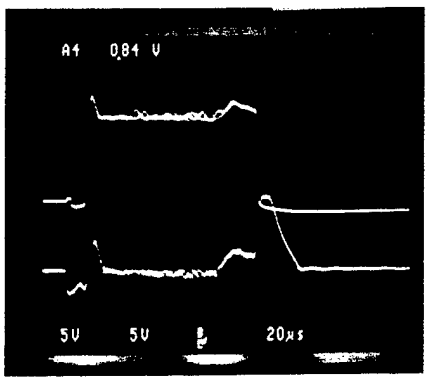

Figure 5.20a. Detected loop I&Q error signals.

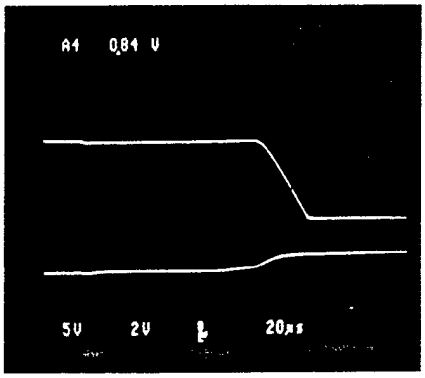

Figure 5.20b. I&Q integral error signals.

Ferrite Tuned Cavities for SSC

AT-5 has been pursuing a design for the low-energy booster (LEB) accelerating cavity, rf amplifier package. The LEB must be capable of rapid tuning over the range from 47.5 MHz to 60 MHz.

The specific design, which includes direct liquid cooling of the ferrites, will be capable of operation at gap voltages of 120 kV. There are two other candidate designs, but neither will be capable of operation much above 50 kV per cavity. The direct liquid-cooled design is the leading candidate, both because it has the potential of offering the most advantages and because its design is in a more advanced stage.

The gap voltage limitation is a ferrite tuner limitation. The tuner, and thus the ferrites, must experience an rf voltage which is approximately 45% of the gap voltage for the LEB tuning range. The cooling liquid is also used as a dielectric medium to preclude breakdown in the ferrite region. This feature is the reason for the higher proposed gap voltage in the liquid-cooled design. The liquid-cooled design is very compact, and this results in a very efficient tuner. The required tuning power is less than 30% of the other designs.

There are two liquids currently being considered: pure water and Fluorinert (3M). We are currently designing and fabricating a two-disk, liquid-cooled test tuner. This tuner will replace the tuner on the Advanced Hadron Facility Main Ring Cavity, which was recently shipped from Los Alamos to SSC. Favorable results from this test tuner will result in the design and construction of a liquid-cooled prototype.

A conceptal drawing of a water-cooled LEB cavity is shown in Fig. 5.21.

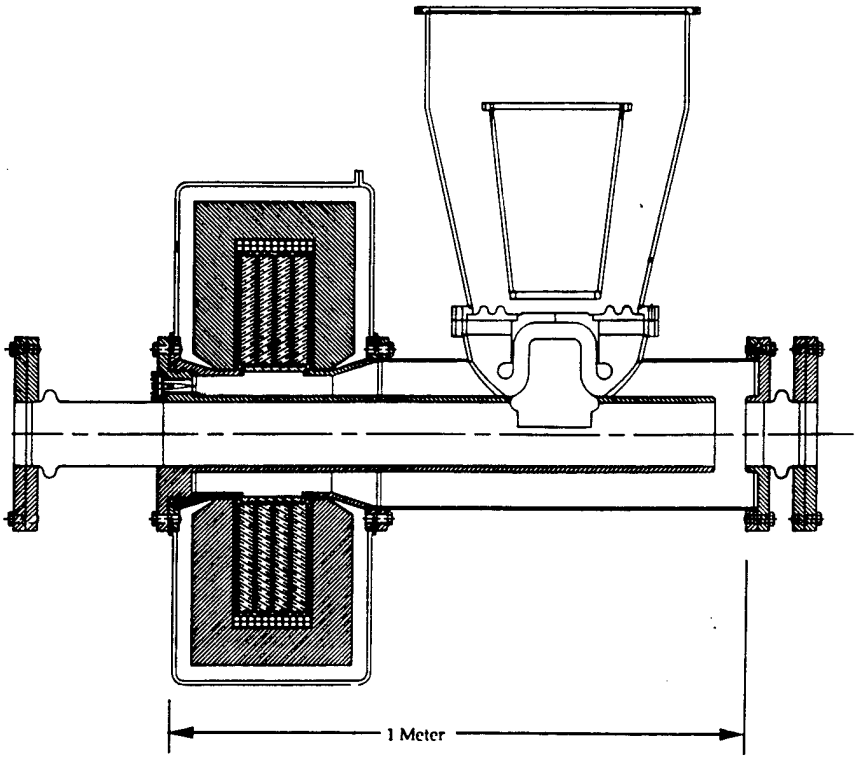

Figure 5.21. Conceptual drawing of a water-cooled LEB cavity.

Antisatellite (ASAT) Program for FEL

Scope

Group AT-5 has contributed to the system design and conceptual design of the antisatellite program at Los Alamos. ASAT uses an FEL for studying effects on satellite weaponry. AT-5 provided a conceptal design for the rf modulators and control systems shown in Fig. 5.22.

The following describes the 4-klystron UHF (425 MHz) rf station capable of producing a total peak output power of 5 MW at a maximum duty factor of 0.06, for an average power of 300 kW. The intended mode of operation is with pulses of 4-millisecond-duration at a repetition rate of 15 pulses/second. The klystrons used are the Litton L-5773, which are higher-efficiency, lower-voltage modifications of the Litton L-3403, the ballistic missile early warning system's transmitter tube.

Physical Description

The physical arrangement of the 4-hole rf station is shown in Fig. 5.22. It is based on the use of an oil-filled tank, into which the sockets for the four klystrons and the floating-deck pulse modulator are immersed. The tank lid comprises five bays, one for each klystron and one for the removable modulator assembly. The design is an extension of the existing 2-hole, 850-MHz klystron rf station designed for use with the neutral particle beam GTA. In Fig. 5.22, a portable gantry with electric hoist is shown having lifted the modulator assembly from the oil tank, permitting either modulator maintenance and repair or access to the remainder of the tank.

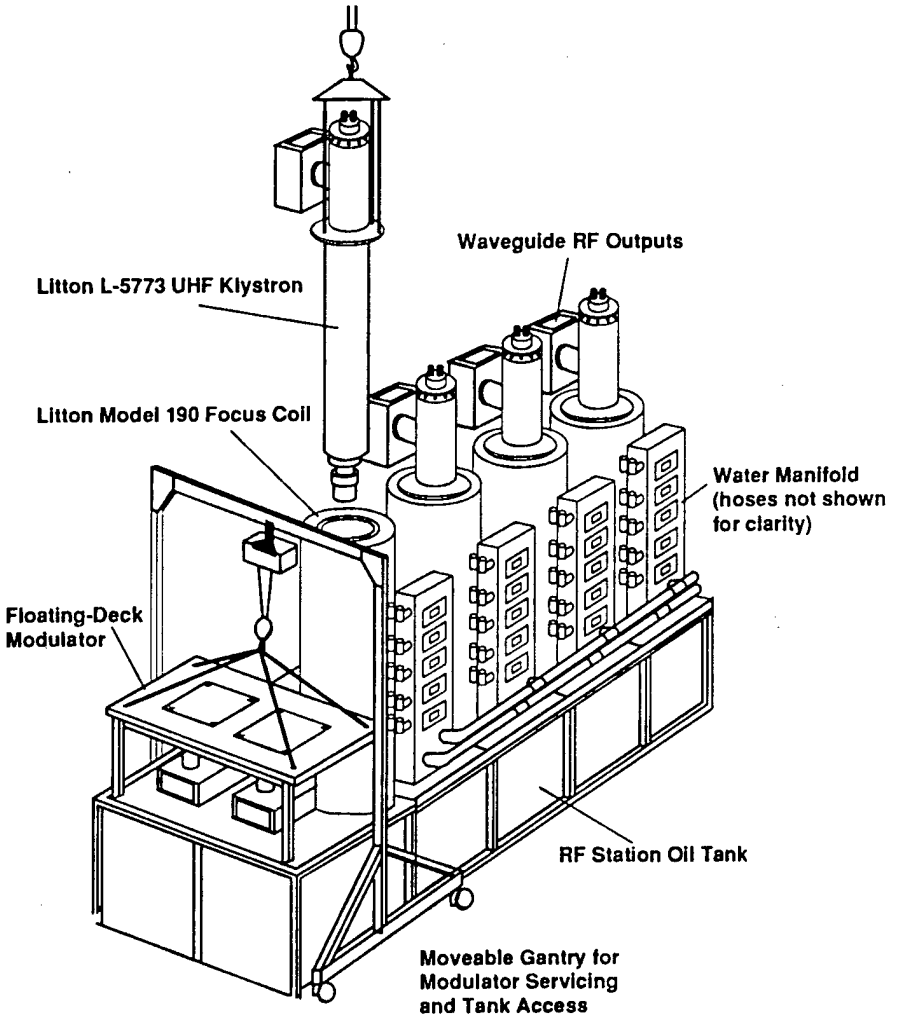

Figure 5.22. Physical arrangement of 4-hole UHF klystron rf station.

The seated weight of the four klystrons and magnets is 9600 pounds. The water manifolds for each klystron, which contain the flow meters and interlock switches, temperature indicators and switches, valves, tees, etc., are located beside each klystron on the right side of the tank lid segments. In the interest of clarity, we have not shown the flexible hoses that connect to the klystron and magnet water fittings.

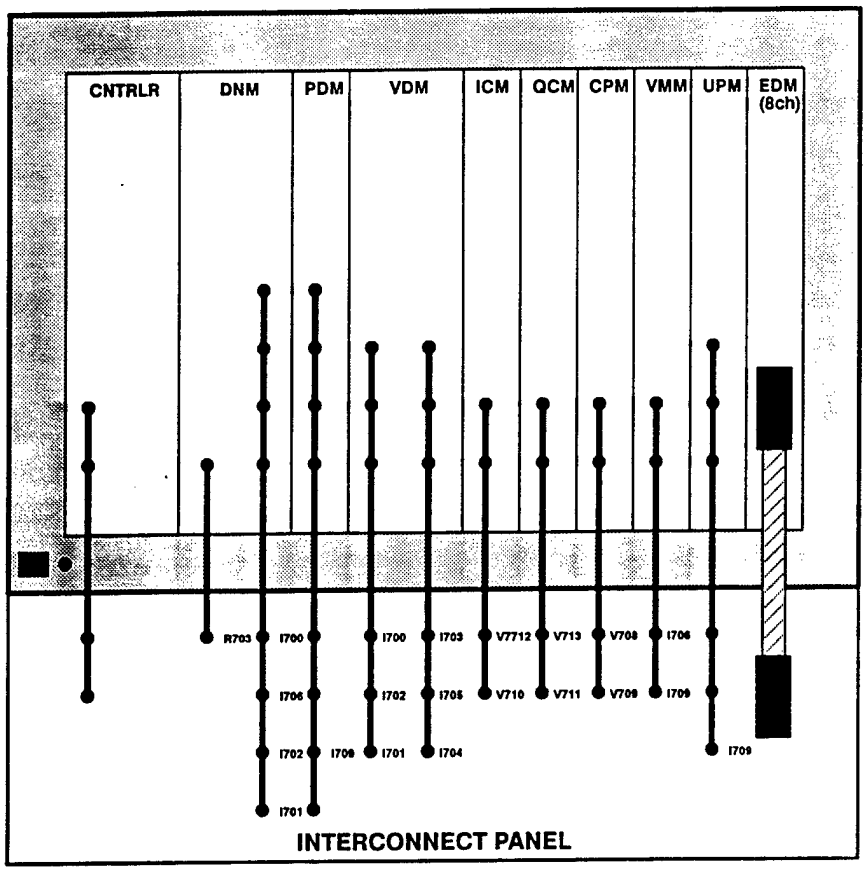

EDM - Envelope Detector Module
UPM - Upconverter Module
VMM - Vector Modulator Module
CPM - Contrpl Predistorter Module
QCM - Q Controller Module
ICM - I Controller Module
VDM - Vector Detector Module
PDM - Polart Vetector Module
DNM - Downconverter Module
CNTRLR - Imbedded Controlle

Figure 5.23. Block diagram of a proposed VXI-based LLRF system for the University of Twente.

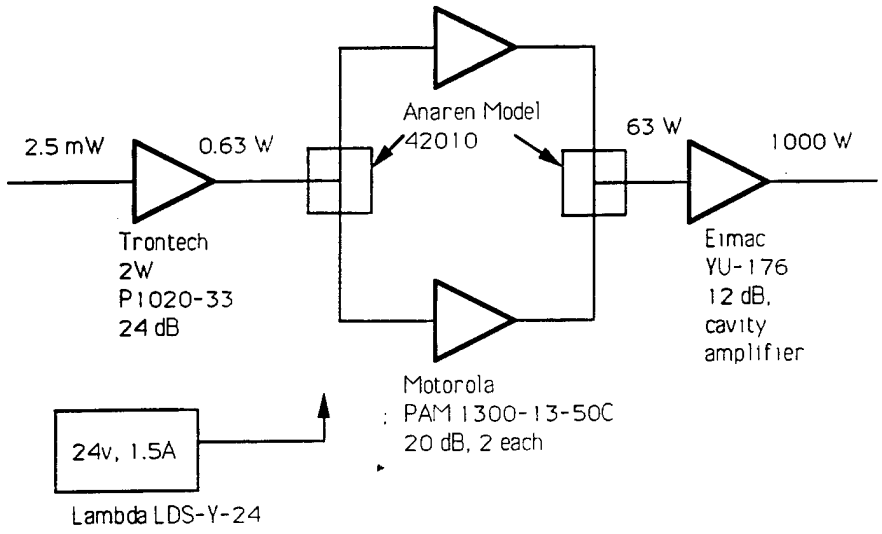

Figure 5.24. Amplifier architecture of the University of Twente klystron driver.

University of Twente FEL Accelerator rf System

AT-5 is providing rf system design and hardware development for the University of Twente FEL. Work in FY 1990 included a preliminary system design, initial design of the LLRF control system, electrical design of the klystron driver, and initial system modeling.

The preliminary design for the LLRF control system uses one VXI crate, and it will incorporate a stand-alone controller. Figure 5.23 shows a block diagram of the crate and the modules that will be used in it. The stand-alone controller will consist of National Instruments' Macintosh-compatible controller imbedded in a VXI module. We will use the software package Labview, which is also available from National Instruments.

The klystron driver will be an amplifier based on the Eimac YU-176 planar triode and a Motorola solid state preamp. See the attached amplifier diagram (Fig. 5.24).

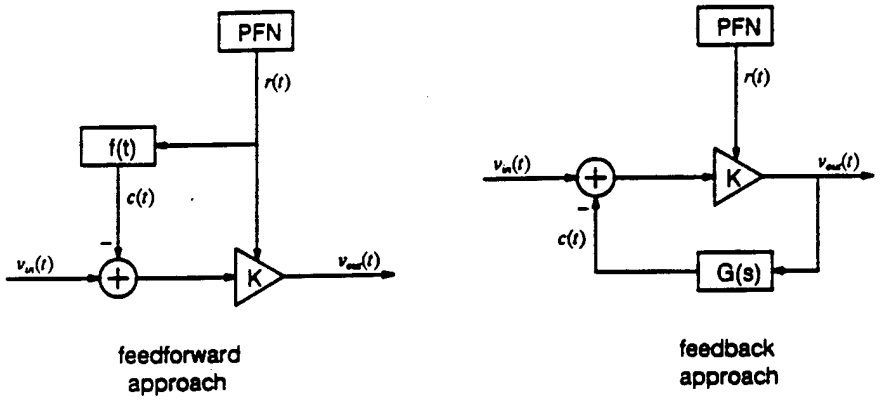

Figure 5.25. Two methods under investigation to correct problem arising from PFN ripple.

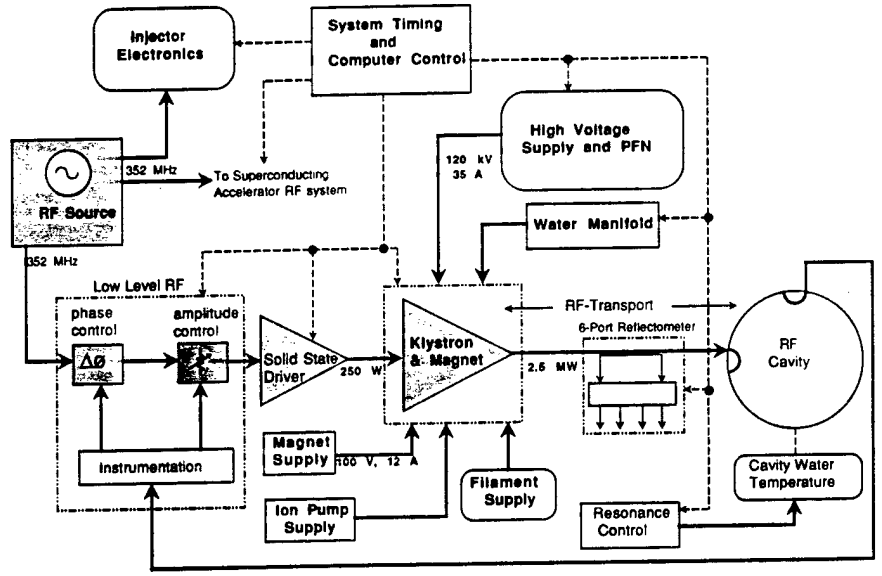

Figure 5.26. Conceptual design of the ELFA rf system.

The initial modelling efforts have pointed toward finding a solution to the detrimental effects of pulse-forming network (PFN) ripple on the operation of the rf system. The PFN is expected to have output ripple of approximately ±1%, which will create a variation in output phase of ±5°. The output amplitude will also vary due to the ripple by as much as ±1.5%. In addition, the ripple will have high enough frequency (500 KHz to 1000 kHz) that it will be impossible for the standard rf feedback control system to correct the variations. Two methods are currently under investigation as possible solutions for this problem (Fig. 5.25).

University of Milan ELFA rf System

During FY 1990, AT-5 performed a feasibility and cost study of the rf system as part of the overall proposal by several AT Division groups to provide a photocathode injector for the Electron Linac for Acceleration (ELFA) project at the Laboratory for Accelerators and Applied Superconductivity in Milan. The proposal was very favorably received, and funding information is expected in early FY 1991. A block diagram of the conceptual design for the rf system is shown in Fig. 5.26.

Boeing Modular Concept Test Development (MCTD) rf Control System

AT-5 provided a LLRF control system which included an I&Q field control system and four complete resonance control systems for the the Boeing MCTD project. The hardware design was based on the GTA technology but had to be modified for a different operating frequency. The hardware was installed and has operated successfully. Operation of the MCTD system at high average power was possible only because of the successful implementation of the resonance controllers.

AT-6
Accelerator Theory and Simulation

Richard K. Cooper, Group Leader

Introduction

The Accelerator Theory and Simulation Group, AT-6, provides theoretical and computational support for the programs of AT Division. In addition, AT-6 contains the Los Alamos Accelerator Code Group (LAACG), which provides source codes, documentation, and assistance for users of accelerator codes. The following is a summary of our activities for the 1990 fiscal year.

Free-Electron Laser Work

AT-6 provided support for the various free-electron laser (FEL) projects at the Lab, namely the Ground-Based FEL (GBFEL), the Space-Based FEL, and the Special Supporting Research Initiative. The GBFEL effort included work at Los Alamos on the High-Brightness Accelerator FEL (HIBAF) and work at Boeing. As usual, this work was documented in a timely manner and presented at conferences and reviews (see the bibliography). Highlights of this effort are presented here.

HIBAF Studies

The HIBAF accelerator employs a newly designed photoinjector with an on-axis accelerator structure. Initial observation of the beam indicated that there were nonaxisymmetric fields acting on the beam, preventing the expected cylindrical symmetry of the beam. Analytic and numerical simulations demonstrated that these fields arise from the coupling slots between the accelerating cavities and the coupling cavities. The slots on the opposite faces of the accelerating cells were displaced 90 degrees azimuthally with respect to one another; zero azimuthal displacement would have practically, but not entirely, eliminated the effect. The analytic studies are documented in Accelerator Theory Note AT-6:ATN-90-6. The numerical studies of the fields arising from the slots were carried out using the three-dimensional code MAFIA, which was a joint development of the Los Alamos National

Laboratory, the Deutsches Elektronen Synchrotron, and the Kernforschungs Anlage Jülich (KFA-Jülich). As noted in "Code Development and the LAACG," two new postprocessors were developed to assist in this study. These efforts are documented in memos AT-6:TM-90-13, AT-6:TM-90-15, and AT-6:TM-90-11.

GBFEL Studies

For the Boeing Modular Concept Test Development, we studied the performance of various portions of the GBFEL accelerator. Through a number of numerical investigations, we studied: the effect of the cavity radio-frequency (rf) feeds on the emittance of the beam (see AT-6:TM-89-22), the beam-bunching process in a wiggler, the effects of magnet fringe fields on the beam motion in the transport line, and the quantitative effects of magnetic flux linking the cathode. Some of the results of these studies were incorporated into the FEL physical process code (FELPPC) described in Section 6, "Code Development and the LAACG."

We reviewed the cavity shape for the laser subsystem GBFEL to optimize it for ease of tuning and machining. Because of the large number of cavities and the length of the GBFEL accelerator, the possible instability due to cumulative beam breakup (BBU) was an important issue. We performed a series of cumulative BBU simulations to assist the work on the cavity engineering design. Technical memo AT-6:TM-90-238 was written to summarize the results of these simulations.

Space-Based FEL Work

We examined conceptual designs for a 180° bend for use between the FEL and the energy recovery unit and found one design to be feasible. The bend is challenging because of the beam's wide energy spread after its interaction with the FEL and because of the beam characteristics required by the energy recovery unit. We surveyed and documented rf power sources from the leading vendors.

Antisatellite FEL Work

AT-6 performed simulations in support of Beacon-Illuminator design. Using FELPPC, we identified parameter spaces giving adequate output optical power and short enough resonator length for electron beam currents of 30 and 50 mA. See the list of technical memoranda at the end of this report for references and documentation titles for these and other items.

Ground Test Accelerator (GTA) Work

Although the GTA theory is principally carried out within the project structure, the specialized knowledge and capabilities possessed by the staff of AT-6 is often brought to bear on GTA problems. A sampling of these efforts follows.

Wakefield Effects in Experiment 3

At the matching section of the GTA Experiment 3, the beamline is quite complex, with many components and steps along the vacuum pipe. A proposal has been made to enclose all the beamline elements in a vacuum vessel of 20-cm radius and to remove the beam pipe connecting the beamline elements. The removal of the beam pipe will expose the beam to the discontinuities between the beamline elements. Before this proposal can be adopted, some understanding of the wakefield problems when the beam traverses these discontinuities is required.

We performed simulations using the computer code TBCI to investigate the wakefield effects. The typical beam parameters used were: beam energy of 24 MeV, beam current of 50 mA, bunch frequency of 425 MHz, and a bunch gaussian in shape with a σ_{rms} of 6 mm. Results show that the longitudinal wake force has a profile similar to the longitudinal space-charge force and modifies the longitudinal energy of the beam on the order of 1 keV for a typical discontinuity. The radial wake force is insignificant. These results have been summarized in memo AT-6:TM-90-223.

Momentum Compactor Cavity

We provided a SUPERFISH design for an 850-MHz momentum compactor to AT-3. This design is detailed in AT-6 technical memorandum AT-6:TM-90-14.

Ion Source Instability

We explored a theory for the low-frequency instability now observed on the negative ion sources. The hypothesis is that the instability is a Harris-type electrostatic instability driven by a nonmonotone ion velocity distribution along the magnetic field lines. It is possible that the nonmonotone ion distribution is a result of the higher frequency ion-acoustic instability previously observed and treated theoretically. Experimental evidence is consistent with this scenario. A possible cure might consist of using cylindrically symmetric anode shapes to confine electrons better.

Research Items

With the diverse interests possessed by theorists, the following selection of items represents only a portion of the broad spectrum of topics investigated by AT-6 staff members.

Stable Maps

A class of rigorously stable symplectic maps in arbitrary dimensions was found. (This discovery extends to higher dimensions results found originally by Edwin McMillan, but uses a completely different technique from McMillan's.) The practical importance lies in the fact that the class of maps is very large and is sufficiently realistic that one might design machines, by including appropriate nonlinear magnets, that come very close to one of this class of maps, thus insuring nonlinear stability for infinite time.

Beam Stability

We have previously investigated, in the frequency domain, the longitudinal and transverse stabilities of counter-rotating, bunched beams in a storage ring or a synchrotron. Our investigations were based on a rigid body model. We found cancellation of the wakefield effect for certain arrangements of the rf cavity locations in a ring. The complex mathematical derivations in the references make this kind of cancellation effect difficult to understand intuitively in the time domain. A continuation of previous authors' study was initiated, and a check on the mathematical formalism used by these authors has been carried out. More detailed study for understanding the cancellation effect has been undertaken. We derived an eigenvalue equation for the stability condition by considering the wakefield effect in short rf cavities and by using the Vlasov equation. Simultaneously, we began a kinetic theory analysis to study the stabilities of the modes of higher synchrotron oscillation harmonics and the synchrotron-betatron mode for counter-rotating beams.

Beam-Beam Interaction

It was discovered that the beam-beam interaction for relativistic beams in storage rings is a Lie-Poisson dynamical system if radiation effects are ignored. Using the experience gained with BEDLAM, we quickly wrote a strong-strong beam-beam interaction code. The code includes higher-order forces than any other beam-beam code and is fairly fast. Preliminary results are already surprising; for example, in some cases the strong-strong case is more stable than the weak-strong case. This work was discussed at the recent B-factory workshop at Lawrence Berkeley Laboratory. There was great interest in the topic. More work remains to be done.

Heavy Ion Fusion (HIF)

We explored the possibility of using GTA, the world's largest forefront optics device, to simulate the final focusing optics problem for HIF. The scaling of parameters in all three dimensions has proven correct, with even the required emittance agreeing. To simulate all the HIF optics scenarios being considered, we must modify the GTA output optics to increase the dynamic range.

Wakefields

Wakefield calculations of various components in FEL systems continue. Components studied include pump covers, beam pipe discontinuities, and the microwiggler. A design for a wakefield-free junction between a circular and an elliptical beam pipe was presented at the Impedance and Bunch Instability Workshop at Argonne Photon Source (APS), Argonne National Laboratory. We also helped APS identify problems that cause slow convergence in transverse beam-cavity interaction calculations for taper junctions with small taper angles.

Energy Recovery

In collaboration with AT-1, we have investigated methods of replacing the mechanical tuners used in changing the relative coupling between the accelerator and decelerator of energy recovery schemes. Such mechanical tuners have high peak surface fields and arcing problems, and we studied two schemes to control the energy recovery electrically using ferrite tuners. Unfortunately both methods had problems which made them not feasible.

Vaguine Structure

In collaboration with AT-1, we have been performing calculations on a method of increasing the achievable gradient in an accelerating cavity. Normal accelerating structures operate in either the zero or π mode on axis. Therefore, they can be made as resonantly coupled structures. There are indications that, if the structures could be operated with a 90° phase shift per cell, the achievable gradients could increase. Such a structure is referred to as a Vaguine structure.

We have been studying pillboxes to get a feel for how the Vaguine structure should behave compared to a $\pi/2$ structure. We first looked at pillboxes without holes and looked at the shunt impedance as a function of wall thickness for both $\pi/2$ and $\pi/4$ structures. We found that the shunt impedance was about 40% higher for the $\pi/4$ structure for zero wall thickness. The advantage decreased as the wall thickness increased, and the shunt impedances were comparable for a wall thickness of one-fifth the cavity length.

We then looked at pillboxes with apertures to see if the peak surface field is lower in the $\pi/4$ structure for the same accelerating gradient. We found that the peak surface field is indeed about 20% lower.

Operation at a 90° electrical phase shift is currently possible only if the cell-to-cell coupling is very small, that is, for small beam apertures. We have begun studying the feasibility of retaining a 90° phase shift with larger beam apertures by compensating for the capacitive cell-to-cell coupling with appropriately shaped magnetic slots. MAFIA runs indicate that such decoupling is possible; the next step is to verify the results experimentally.

Accelerator Community Activities

The staff of the Los Alamos Accelerator Theory and Simulation Group are involved in the accelerator community both nationally and internationally. During the report period, Tai-Sen Wang spent a sabbatical leave at the European Center of Nuclear Research (CERN), working with Bruno Zotter and participating in the commissioning of the large electron-positron collider ring. He attended the Fourth Advanced International Committee on Future Accelerators Beam Dynamics Workshop at KEK in Japan and the 12th USSR National Particle Accelerator Conference in Moscow.

Tai-Sen Wang and David Neuffer participated in the Kaon Factory Workshop held in Vancouver July 30 to August 3, 1990, and David Neuffer attended the Fermilab II Instability Workshop. Earlier, Neuffer visited CERN for discussions of chromatic correction schemes; he then accepted an invitation to Serpukhov in the Soviet Union, where he visited nuclear research facilities and the Institute for High-Energy Physics. At Novosibirsk he held discussions on nonlinear instabilities (e-p) and light sources. Neuffer also participated in chromatic correction studies at the Superconducting Super Collider (SSC). He participated in the site-specific conceptual design at SSC. During the report period, the adoption of the so-called Neuffer Correction by the CERN Large Hadron Collider design was announced by G. Brianti at Tsukuba.

David Neuffer and Paul Channell participated in the Lawrence Berkeley Laboratory B-Factory Workshop; Channell presented his calculations on the beam-beam interaction using Lie-Poisson methods.

Richard Cooper and Dominic Chan participated in the Impedance and Bunch Instability Workshop held at Argonne National Laboratory, October 31 to November 1, 1989. Cooper chaired one session of the workshop and Chan presented a paper on beam-induced energy spreads at beam-pipe transitions.

Richard Cooper chaired a session of the Third Charged Particle Optics Workshop in Toulouse, France.

Dominic Chan presented a paper at the 12th International Free-Electron Laser Conference in Paris, France, September 17 to September 21, 1990.

Code Development and the Los Alamos Accelerator Code Group (LAACG)

The 1990 fiscal year was quite a productive year for the LAACG. In January 1990, we hosted the Conference on Codes and the Linear Accelerator Community. The proceedings of that conference were published later in the year. The second edition of the popular compendium "Computer Codes for Particle Accelerator Design and Analysis" was published. And in August we held a quite successful review of the Code Group activities and its plans for extensions. The report of the review panel was very favorable and supportive of the proposals for continued activities in this area. Following are some highlights of code development and distribution activities carried out in AT-6.

Computer Simulation Program HERSIM2

HERSIM is a computer simulation program for studying the longitudinal and transverse wakefield effects due to beam-cavity interactions in circular accelerators or storage rings. The program uses a Hermite polynomial expansion method for wake potential calculation and look-up tables to reduce the computation time. HERSIM works correctly only for a single rf station and has no nonlinear elements in the ring. While on sabbatical leave to CERN, Tai-Sen Wang contributed to this useful simulation program, removing these limitations by including multiple rf stations and the effects of sextupoles, dispersion, and chromaticity. He also made modifications to HERSIM so that, when sextupoles are considered, the transverse motion studied can be either in the vertical plane or in the horizontal plane. This new version of HERSIM is called HERSIM2.

The Moment Code BEDLAM

The acronym BEDLAM stands for the description of beam dynamics through the linear application of moments. During the report period, significant improvements were made to the code. Many of these improvements, most notably an improved integration scheme, were reported at the Conference on Computer Codes and the Linear Accelerator Community, held in Los Alamos in January, 1990. Additional work on the code follows:

- We discovered the general setting for the expansion about the center of mass in BEDLAM. Higher-order terms in the motion of the center of mass, including effects due to collective fields, can now be included systematically.

- We wrote a rudimentary "shell" to generate input force files for BEDLAM. The shell allows the inclusion of an arbitrary number of Halbach quads of arbitrary strengths in a straight line for on-axis beams.

- As suggested by Lysenko, we are developing a better space-charge model based on the work of Sacherer. We have successfully demonstrated the ability to include off-axis effects in a way fully consistent with the space-charge forces. Modifying BEDLAM to include these effects will leave almost all of the code (the integrator) unchanged.

The Wakefield Code AMOS

Members of the Code Group met with G. Craig and J. DeFord, the authors of the azimuthally symmetric mode simulator (AMOS). Together, they agreed upon a series of calculations to be performed using both TBCI and AMOS. These calculations served as a benchmark for AMOS and an extension of our capability to handle lossy materials and impedance boundary conditions. This work was essential in establishing confidence in the ultimate dual-axis radiograph hydrotest cell design. We found the agreement between the AMOS code and the TBCI code to be excellent.

Work is continuing on a postprocessor that will not only give quick summary of the field solutions from

AMOS, but is structured generally enough to permit viewing solutions from a variety of two- and three-dimensional electromagnetic solvers. Currently, subroutines exist for:

- plotting functions of two independent variables, with and without hidden lines. (A completely different approach was taken from that used in MAFIA, to avoid any copyright problems.) The subroutines are written such that they will be used for real three-dimensional (3-D) problems, that is, functions of three independent variables.

- plotting "histograms" of two independent variables.

- the next step is to write an arrow plot routine. This routine will also initially be written for two independent variables so that it can be fairly easily modified to three independent variables.

We have an agreement with DeFord on how AMOS will format its output (AMOS is a two independent-variable problem.) After DeFord makes his changes, we can write an appropriate input routine so that the postprocessor can be used with AMOS.

PSR ARCHSIM Code Development

The cyclic accelerator code ARCHSIM was upgraded into a program with much better graphics (using the DISSPLA package) and a faster executing program running on the CRAY computer. The current version, PSR ARCHISM, runs approximately 10 times faster than the program on the MPVax computer.

Transverse space charge was implemented using the particle in the cell approach. The transverse force of space charge is approximated by an area-weighted smooth distribution. This technique properly represents the global charge/field profile without the close interactions with neighboring particles. The beam bunch is divided along the bunch at each time step, and the particles in each segment are represented as charged rods. In this algorithm, an arbitrarily-shaped vacuum wall with image charge interacting with the particles can be included in the program in a straightforward manner.

PARMILA

Several things were accomplished to make the computer program PARMILA (phase and radial motion in linear accelerators) more available to users. A user's and reference manual was published. The characteristics of this documentation were described at the Los Alamos Conference on Computer Codes and Linear Accelerators. The manual is being distributed by the LAACG. The code and copies of the manual were sent to the National Energy Software Center for distribution through that channel. The program has also been modified to run on the CRAY-2s at the National Energy Research Supercomputer Center (NERSC) and is now available to NERSC users.

MAFIA Postprocessors

While studying the effect of coupling slots on the fields in HIBAF cavities, we felt the need for a program to interpolate the MAFIA-generated electric and magnetic field components to a given point. (MAFIA calculates the magnetic field components at the center of each mesh cell face and calculates the electric field components at the center of each cell edge.) This interpolation was never added to the standard MAFIA postprocessor P3 because the problem of handling boundaries with metal and with the ends of the mesh was considered too difficult. Such a program has now been written and compared with analytical solutions for a rectangular pillbox, a cylindrical pillbox, and a coaxial cable. In general, there is excellent agreement between the interpolated and analytical results.

A number of other special purpose postprocessors for the MAFIA codes were also written. See references for titles.

MAFIA Codes

Version 3.0b of the MAFIA codes was installed here at Los Alamos National Laboratory for the CRAYs running with the CRAY time-sharing system (CTSS) operating system. All controllees (executable codes) are available in a cftlib library in the following Central File System (CFS) nodes:

/mafia3.0b/libs/libmafia
/mafia3.0b/libs/libmafra

The difference between the two libraries is that the libmafia library has controllees making FORTRAN 77 direct access files for intracode communication, and the libmafra library has controllees making cftlib random access files for intracode communication. It is recommended that the libmafra library be used. Both libraries contain a README file and test examples, but it is strongly recommended that prospective users also have a user's manual before attempting to use these codes. Codes available in version 3.0b are M, R, E, P, and S, where M, R, and P are comparable to the version 2.+ codes M3, R3, and P3; E is comparable to version 2.+ code E31; and S is the new Statics Solver.

Version 2.+ codes continue to be supported both here at LANL for the CRAY-XMPs running CTSS and at NERSC for the CRAY-XMPs and CRAY-2s.

POISSON/SUPERFISH Codes

Version 3.0 of the POISSON/SUPERFISH codes is in the final testing phase. These codes are supported by the CTSS, VMS, UNIX and UNICOS operating systems. The codes

are installed on CFS both here and at NERSC in the following file:

/laacg/psv3

Changes to these codes include corrections, modifications and restructuring. Most corrections were necessary due to the new stored-energy calculation introduced in version 2.003. The code now runs properly for the many options available.

Modifications to POISSON/PANDIRA/MIRT include implementation of the R. Early 1010 steel permeability table as the default for material 2 and calculation of the harmonic analysis around points other than the origin. Additional POISSON modifications include implementation of an expansion algorithm for an entire range of values of B and linear interpolation on values of B rather than on B^2.

Restructuring changes include placing all coding in upper case while providing for input in either upper or lower case independent of the operating system. All machine, system library, and operating system code is now contained, as far as possible, in the library in a subroutine called SETMIL. CTSS is the only operating system which will require dependent changes outside SETMIL. The graphics module now includes code for the GKS, DISSPLA, and PLOT10 graphics packages, as well as coding for a PostScript file conforming to the PostScript file structure conventions. Changes can be made with an editor to adapt the POISSON/SUPERFISH group of codes for a supported or unsupported operating system and for a chosen supported graphics package and/or a PostScript file.

Distribution Activities

Table 6.1 lists the number of copies of source codes that we sent to users in FY 1990.

Table 6.2 shows the code documentation that was sent during FY 1990.

Code Name	Number of Copies
POISSON/SUPERFISH	65
POISSON/SUPERFISH UNIX version	9
TRACE3D	4
DISPERSION	2
PARMTEQ	4
PARMILA[AT1]	7
PARMILA[AT6]	3
RMKT	3
LOOPER	1
SHRIMP	2
GYROCON	1
PARMELA	8
TRACE2D	3
TRANSPORT LBL	2
SNOW2D	1
RAYTRACE	1
CHARGE2D	1
CHARGE3D	1

Table 6.1. Distribution of source codes.

Code Name	Number of Copies
POISSON/SUPERFISH USER'S GUIDE	123
POISSON/SUPERFISH REFERENCE MANUAL	123
POISSON GROUP PROGRAMS USER'S GUIDE	83
FORCE - INFINITE WIRE	9
MAFIA USER GUIDE	41
RAYTRACE	
GYROCON RADIO-FREQUENCY GENERATOR	1
LIE ALGEBRAIC EQUIPMENT....	11
MANUAL FOR GIOS	4
PARMELA-A PARTICLE....	16
PARMILA USER'S GUIDE	34
A SELF CONSISTENT...KLYSTRON....	2
SNOW...SIMULATION....	1
TBCI SHORT USER GUIDE	9
TOSCA REFERENCE MANUAL	3
TRACE3D (rough draft)	27
TRACE2D	3
TRANSPORT...LBL VERSION	4
URMEL and URMEL -T USER GUIDE	10
PROCEEDINGS CONFERENCE on CODES	30
New COMPENDIUM	108
Old COMPENDIUM	6

Table 6.2. Distribution of code documentation.

References

Accelerator Theory Notes

The following AT-6 Accelerator Theory Notes were distributed during the report period:

1. Robert L. Gluckstern, "Orbit Dynamics in the Field of a Bifilar Helix," Los Alamos National Laboratory technical note AT-6:ATN-89-20, November 20, 1989.

2. Robert L. Gluckstern, "Effects of Fringe Fields and Errors in a Bifilar Helical Wiggler," Los Alamos National Laboratory technical note AT-6:ATN-89-21, September, 1989.

3. M. Jean Browman and Maria Rivera-Dirks, "Programmer's Guide to the New MAFIA Power Loss Routines," Los Alamos National Laboratory technical note AT-6:ATN-89-22, September, 1989.

4. Linda Walling and M. Jean Browman, "Using the MAFIA Codes in the Analysis and Design of an RF Deflector," Los Alamos National Laboratory technical note AT-6:ATN-89-23, October 4, 1989.

5. R. K. Cooper, P. L. Morton, and L. E. Thode, "Electron Beam Energy Spread Induced by Charge Fluctuations," Los Alamos National Laboratory technical note AT-6:ATN-89-24, October 13, 1989.

6. Robert L. Gluckstern, "Wakefields in a Dielectric Waveguide," Los Alamos National Laboratory technical note AT-6:ATN-90-1.

7. R. L. Gluckstern, "Analysis of Slotted Cylindrical Shell for use as a Compact Wiggler," Los Alamos National Laboratory technical note AT-6:ATN-90-2.

8. M. Jean Browman and Lloyd M. Young, "A Study of Radio-Frequency Quadrupoles Using the MAFIA Codes," Los Alamos National Laboratory technical note AT-6:ATN-90-3.

Technical Memoranda

The following AT-6 Technical Memos were written during the report period:

1. P. Morton and R. Cooper, "Efficient Energy Recovery," Los Alamos National Laboratory technical memorandum, AT-6:TM-89-46, October 30, 1989.

2. J. Merson and R. Cooper, "180° Bend for SBFEL," Los Alamos National Laboratory technical memorandum, AT-6:TM-89-47, October 18, 1989.

3. H. Takeda, "The Emittance Growth by the Space Charge in a Chicane Bunch Compressor," Los Alamos National Laboratory technical memorandum, AT-6:TM-89-48, October 1989.

4. M. J. Browman, "Program to Calculate the Difference Between the MAFIA-Calculated Electromagnetic Fields for a Perturbed and Unperturbed Structure," Los Alamos National Laboratory technical memorandum, AT-6:TM-89-50, November 22, 1989.

5. M. J. Browman, "Program to Calculate the Difference Between Two Modes of the MAFIA-Calculated Electromagnetic Fields for a Resonant Structure," Los Alamos National Laboratory technical memorandum, AT-6:TM-89-51, November 22, 1989.

6. H. Takeda, "Analytical Calculation of Large Hole Coupling by a Rectangular Hole, and Comparisons with 3-D Simulation Codes and with Boeing Experiment," Los Alamos National Laboratory technical memorandum, AT-6:TM-89-52, November 22, 1989.

7. G. Boicourt, "Simulation Particle Sets at Output of the ATS 5 MeV Linac," Los Alamos National Laboratory technical memorandum, AT-6:TM-89-53, December 11, 1989.

8. M. J. Browman, "Program to Generate a MAPPER File to Plot Two-Dimensional Cross Sections of the Structure Specified in a MAFIA M3IN File," Los Alamos National Laboratory technical memorandum, AT-6:TM-89-54, December 11, 1989.

9. M. J. Browman, "Testing the Power Loss Due to the Finite Conductivity of Metal for the New Postprocessor POWER," Los Alamos National Laboratory technical memorandum, AT-6:TM-90-1, January 1, 1990.

10. M. J. Browman, "Programs to Calculate the Lowest TM and TE Modes of a Cylindrical Cavity," Los Alamos National Laboratory technical memorandum, AT-6:TM-90-2, January 5, 1990.

11. M. J. Browman, "Program to Calculate the Lowest Modes of a Right Circular Cylindrical Cavity," Los Alamos National Laboratory technical memorandum, AT-6:TM-90-3, January 8, 1990.

12. M. J. Browman, "Comparison of Two Programs to Print the Frame of a Flow Chart," Los Alamos National Laboratory technical memorandum, AT-6:TM-90-4, January 19, 1990.

13. P. Morton, "Summary of FY89 Work on SBFEL," Los Alamos National Laboratory technical memorandum, AT-6:TM-90-5, February 1, 1990.

14. M. J. Browman, "Amendment to Memo TM-89-44," Los Alamos National Laboratory technical memorandum, AT-6:TM-90-6, February 22, 1990.

15. G. P. Boicourt, "Documentation for the PARMRMF version of PARMILA," Los Alamos National Laboratory technical memorandum, AT-6:TM-90-7.

16. J. L. Merson, "Modification of BEACONQ3 to Avoid Postprocessor," Los Alamos National Laboratory technical memorandum, AT-6:TM-90-8, April 30, 1990.

17. J. L. Merson, "Pulsed Power Tubes with Average Output of at least 150 KW and Operating Frequency Approximately 1300 MHz," Los Alamos National Laboratory technical memorandum, AT-6:TM-90-9, May 1, 1990.

18. J. L. Merson, "Parameter Space with Adequate Optical Power and Resonator Length Values for Illuminator Using a 30 mA Average Current Beam," Los Alamos National Laboratory technical memorandum, AT-6:TM-90-10, May 9, 1990.

19. M. J. Browman, "Program to Normalize the Fields in a MAFIA Direct Access File," Los Alamos National Laboratory technical memorandum, AT-6-TM-90-11, May 11, 1990.

20. J. L. Merson, "50 mA Average Current Beam - Parameter Space with Adequate Optical Power and Resonator Length Values for Illuminator," Los Alamos National Laboratory technical memorandum, AT-6:TM-90-12, May 14, 1990.

21. M. J. Browman, "Effect of the Coupling Slots on the Fields of an On-Axis Coupled-Cavity Linac," Los Alamos National Laboratory technical memorandum, AT-6-TM-90-13, May 16, 1990.

22. J. L. Merson "850 MHz Momentum Compaction Cavity-SUPERFISH Design for 2 cm gap and 1 cm bore radius," Los Alamos National Laboratory technical memorandum, AT-6-TM-90-14, May 17, 1990.

23. M. Jean Browman and Alessandra Lombardi, "Program to Interpolate MAFIA Electromagnetic-Field Components to the Same Point," Los Alamos National Laboratory technical memorandum, AT-6-TM-90-15, June 4, 1990.

24. Alessandra Lombardi and M. Jean Browman, "Testing Program FIELDS," Los Alamos National Laboratory technical memorandum, AT-6:TM-90-16, August 1, 1990.

25. M. Jean Browman and Alessandra Lombardi, "Notes on Program FIELDS," Los Alamos National Laboratory technical memorandum, AT-6-TM-90-17, July 26, 1990.

26. M. Jean Browman and Alessandra Lombardi, "Program to Generate a Mapper File of a Specified Cross Section of a MAFIA Model," AT-6-TM-90-19, August 20, 1990.

27. M. J. Browman, "New Program to Normalize the Fields in a MAFIA Direct Access File," Los Alamos National Laboratory technical memorandum, AT-6-TM-90-22, August 31, 1990.

28. M. Jean Browman and Alessandra Lombardi, "Addition of Subroutine CHKIO to Program Fields," Los Alamos National Laboratory technical memorandum, AT-6-TM-90-23, September 5, 1990.

29. M. Jean Browman, "Modification of Program DIFF to Handle Long Files," Los Alamos National Laboratory technical memorandum, AT-6-TM-90-24, September 20, 1990.

30. M. Jean Browman, "PARMELA INPUT-HIBAF CAVITY" Los Alamos National Laboratory technical memorandum, AT-6-TM-90-25, September 27, 1990.

AT-7
Free-Electron Laser Technology

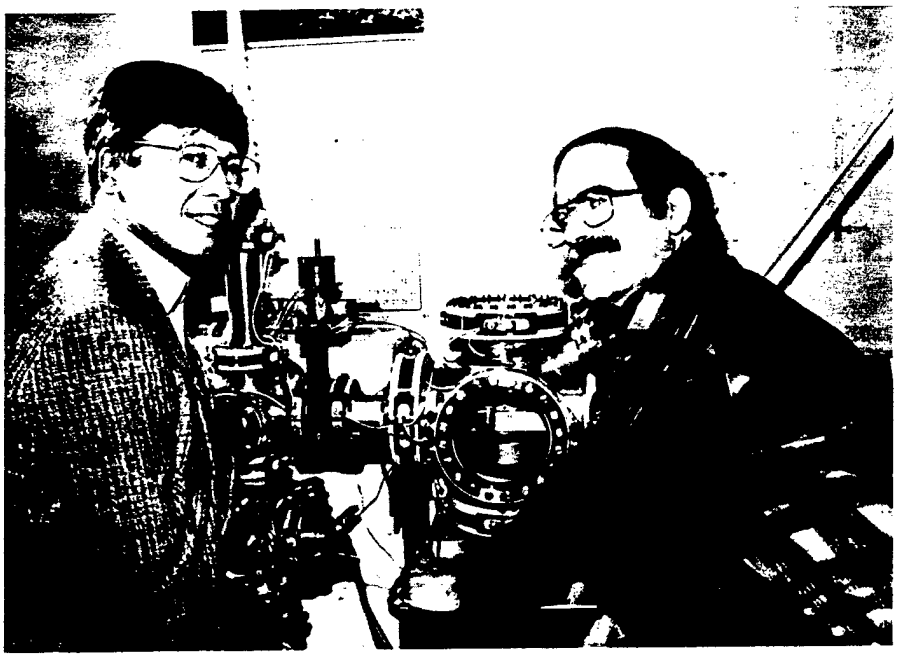

K. Dominic Chan, Deputy Group Leader; Richard Sheffield, Group Leader

Introduction

With primary responsibility for free-electron laser (FEL) program activities within AT Division, Group AT-7 manages accelerator-based experiments, coordinates the work of other contributing groups, and provides technical guidance to the FEL Program Office for proposals, program direction, and external collaborative arrangements.

The Los Alamos FEL program began in the late 1970s to investigate the practicality of FELs. Since then, AT-7 has operated both FEL amplifiers and oscillators. An energy-recovery experiment was performed that demonstrated a technique for improving the overall efficiency of an FEL. A new electron source, the photoinjector, was developed. This type of source produces an extremely bright high-current electron beam, necessary for successful operation of high- and low-power FELs. The successes of these programs eventually resulted in our involvement in the design of very powerful FELs for the Strategic Defense Initiative (SDI) program, funded through the US Army Strategic Defense Command at Huntsville, Alabama, and White Sands Missile Range, New Mexico. Our SDI mission has been to develop the potential of FELs as ground-based directed-energy weapons. Group AT-7's development of a photoinjector for improved FEL operation has led to a program aimed at making FELs more compact and simpler to operate. Group AT-7 is also investigating an extension of the FEL wavelength range into the ultraviolet region, where there are many potential chemical and solid-state applications as well as semiconductor-processing applications.

Group AT-7 addresses many important technical issues concerning FELs: power, efficiency, optical quality, bandwidth, reliability, optics, and high-current, high-brightness accelerators. Important advances have been made in nearly all these areas.

High-Brightness Accelerator FEL (HIBAF)

HIBAF is an upgraded experimental facility at TA-46. By adding two accelerator tanks and another wiggler, a master-oscillator power-amplifier (MOPA) experiment can be performed at wavelengths as short as 3 μm. A completed upgrade allows HIBAF to produce a beam that is significantly brighter and of higher quality throughout the entire laser spectrum, thus bringing us closer to meeting the needs of SDI for high-power ground-based FELs. The upgraded design of HIBAF is based on information provided by the integrated numerical experiment (INEX) group of codes, which have gradually become the cornerstone of all the FEL designs in the Los Alamos National Laboratory (LANL). A completed HIBAF allows us to validate the use of these codes.

In FY 1989, the original facility at TA-46 was dismantled and rebuilt, with the addition of a photoinjector. A micropulse electron charge of 5 nC was accelerated to 17 MeV in the first two accelerator sections.

During the first half of FY 1990, beams with micropulse charges up to 12 nC have been accelerated. The facility continued operations until May, and the beam quality was carefully analyzed.[1] At a micropulse charge of 5 nC, an energy spread of 0.3% and a normalized transverse emittance of 35 π-mm-mrad were measured (Fig. 7.1).

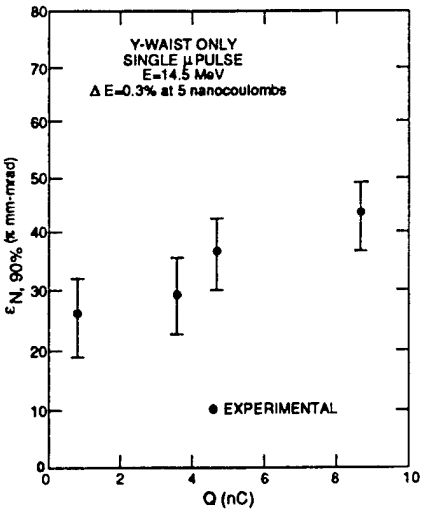

Figure 7.1. Emittance as a function of micropulse charge measured in HIBAF.

These results were found to be in agreement with INEX calculations. Other achievements during this period of operation were: the preparation and operation of photocathodes became routine procedures with quantum efficiencies between 5 and 10% and operation lifetimes of 1 to 3 days between cathode fabrications; the radio-freqency (rf) feedback circuits were improved; and the E-beam diagnostic technique using Optical Transition Radiation interferometer was validated. Problems encountered included the observed field-emission electrons from the photocathode and the multipactoring in the coupling cells of the on-axis coupled accelerator structure. The multipactoring problem was circumvented by detuning the first cell to raise the fields in the coupling cells.

In June, experiments were stopped to permit installations of two additional accelerator structures and associated klystrons and a FEL oscillator section. The added accelerator structures will bring the beam energy up to 40 MeV. Lasing is expected in early FY 1991.

Advanced FEL Technology Development

Group AT-7 is responsible for developing advanced FEL technology in key technical areas. These areas include: high-brightness beam, wiggler and harmonic operation, optical systems, control and diagnostics, rf system, and user facility. During FY 1990, development activities in these areas have been organized as a Special Supporting Research Initiative with funding provided by LANL.[2] This funding will last for five years at a level of 2 million dollars per year. An advanced FEL (AFEL) will be built to achieve the following goals: (1) to develop advanced components and incorporate the present state-of-the-art components in a FEL design, and (2) to demonstrate the feasibility of a FEL system that can be described as user friendly and robust.

The AFEL facility will be built at Meson Physics technical area 53, building 14. The accelerator and FEL will be so compact that they can be housed in a 12' x 25' vault. An electron

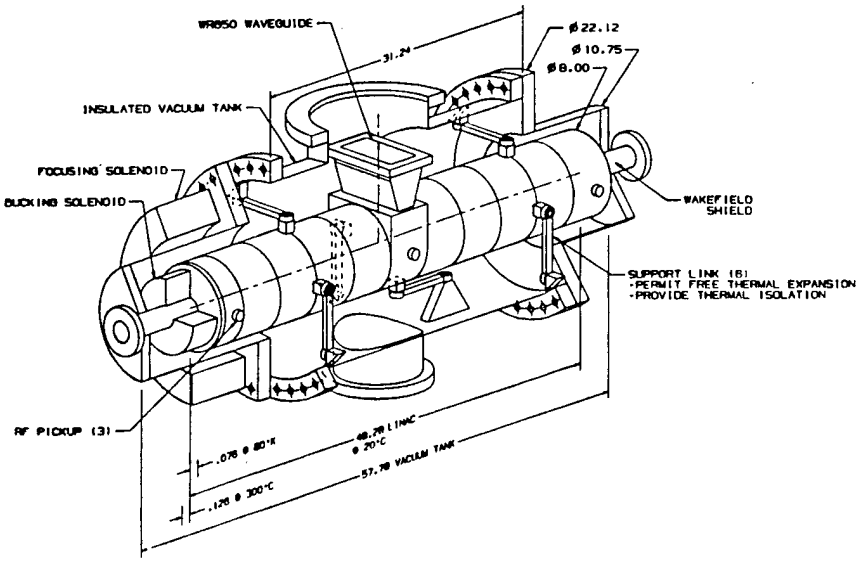

Figure 7.2. Accelerator structures designed for AFEL.

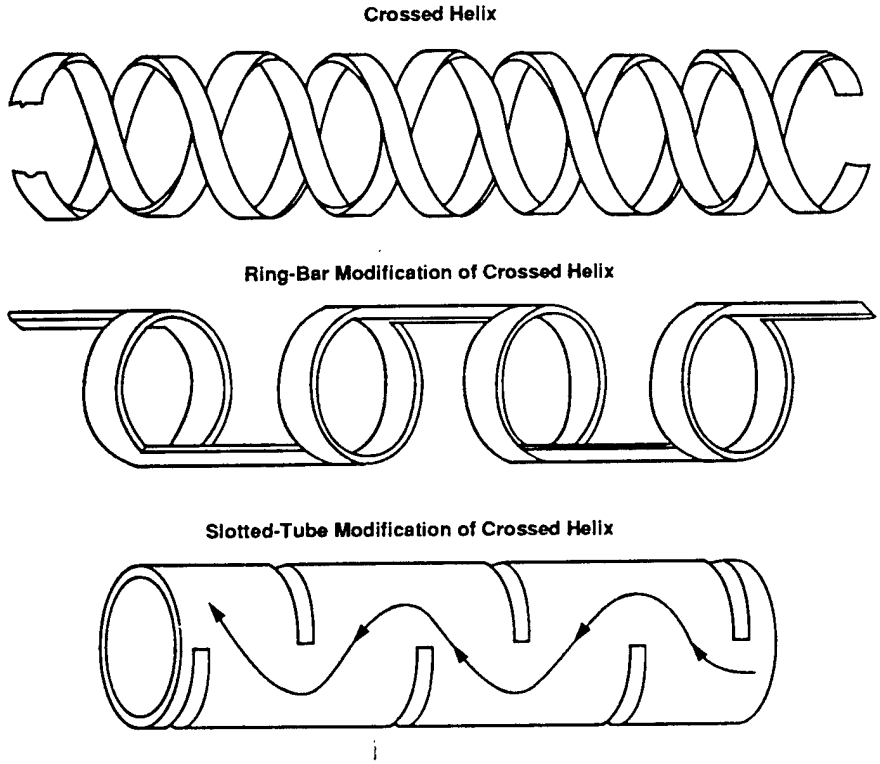

Figure 7.3. Realization of cross-helix configuration in a slotted tube for microwiggler development.

beam with a normalized 90% transverse emittance of 10 π-mm-mrad will be generated by a photoinjector and accelerated to 20 MeV in a 1.2-m on-axis-coupled accelerator structure. The 1300-MHz accelerator structure will operate at a cryogenic temperature of 77 K and a high field gradient up to 25 MV/m. This electron beam will be used in an FEL which consists of a 1.4-m oscillator and a 10-cm microwiggler to produce laser light at wavelengths between 0.3 and 7 μm.

The accelerator design (Fig. 7.2) was reviewed in July by an external panel. Designs of other parts of the facility are presently in progress, and the first beam is expected in the fall of 1991.

Wigglers

Development of wigglers continues. Efforts have concentrated in the area of pulsed electromagnetic microwigglers because of their potential to greatly reduce the E-beam energy required to reach short wavelengths. These wigglers are iron-free and have high-undulating field driven by high-pulsed current to achieve high-FEL gain.

In FY 1990, techniques of wiggler design and advantages of operating these wigglers on high harmonics were studied (Ref. 3 and 4). The crossed-helix configuration (Fig. 7.3) realizable in a slotted tube has been chosen among other configurations. Analytic results were obtained for the undulator magnetic field. The optimum length of a slot was found to be 0.62 times the tube circumference, independent of its wiggler period. At this slot length, the undesirable quadrupole component of the undulator field is zero. The heating at the ends of the slots was also studied. A working model with a 3-mm period has been built (Fig. 7.4). It will be tested using a recently upgraded field-measuring system. In this system, a laser light source replaces the LED used before, improving the signal-to-noise ratio by a factor of 100.

A microwiggler will be incorporated in the AFEL.

Figure 7.4. Working model of a microwiggler using a slotted tube with 3-mm period.

Numerical Simulations

Numerical simulation is an important tool for FEL development and the understanding of high-brightness E-beams. The INEX package of computer codes has been used extensively to model FEL experiments in Group AT-7. It facilitates designs of FEL and provides guidance to experiments.

Simulations of the HIBAF experiment have shown agreement with measurements for the parameterization studies at 17 MeV (Ref. 5). These simulations required the inclusion of focusing effects due to the three-dimensional (3-D) fields of the coupling slot and the power flow between the accelerating cavities. Also, a less noisy 3-D space-charge routine was added to the INEX model. The transverse emittances of 45 and less than 40 π-mm-mrad predicted, respectively, for 5-nC and 3-nC micropulses, were achieved experimentally. Simulations indicate that an emittance of 40 π-mm-mrad for 5-nC pulses at 40 MeV should be achievable in the HIBAF MOPA configuration. In this configuration, the 150° bend can operate as a magnetic buncher to achieve a peak current of up to 1 kA. Simulations using computer code PARMELA have been used to study and understand the physics in magnetic bunchers to achieve high-peak current while preserving good beam quality.[6]

References

1. D. W. Feldman, B. E. Carlsten, P. G. O'Shea, A. H. Lumpkin, W. J. D. Johnson, S. C. Bender, W. E. Stein, R. B. Feldman, R. L. Sheffield, K. McKenna, "Performance of the Los Alamos HIBAF Accelerator at 17 MeV," 12th International Free-Electron Laser Conference, Paris, France, September 17-21, 1990, Los Alamos National Laboratory document LA-UR-90-3189.

2. R. L. Sheffield, B. E. Carlsten, J. C. Goldstein, and R. W. Warren, "Advanced FEL Technology Program at Los Alamos National Laboratory," 12th International Free-Electron Laser Conference, Paris, France, September 17-21, 1990, Los Alamos National document LA-UR-90-1798.

3. R. W. Warren, "Lasing on Higher Harmonics," 12th International Free-Electron Laser Conference, Paris, France, September 17-21, 1990, Los Alamos National Laboratory document LA-UR-90-1915.

4. R. W. Warren, "Design consideration for pulsed microwigglers," 12th International Free-Electron Laser Conference, Paris, France, September 17-21, 1990, Los Alamos National Laboratory document LA-UR-90-3104.

5. B. E. Carlsten, L. M. Young, M. J. Browman, H. Takeda, D. M. Feldman, P. G. O'Shea, and A. H. Lumpkin, "INEX Simulations of Experimentally Measured Accelerator Performance at the Los Alamos HIBAF Facility," 12th International Free-Electron Laser Conference, Paris, France, September 17-21, 1990, Los Alamos National Laboratory document LA-UR-90-3897.

6. B. E. Carlsten, B. D. McVey, E. M. Svaton, and L. M. Young, "Magnetic Bunchers for the Generation of High-Peak Current, Low-Emittance Electron Pulse at Medium Energy," 1990 Linear Accelerator Conference, Albuquerque, NM, September 10-14; Los Alamos National Laboratory document LA-UR-90-1699.

AT-8
Accelerator Controls and Automation

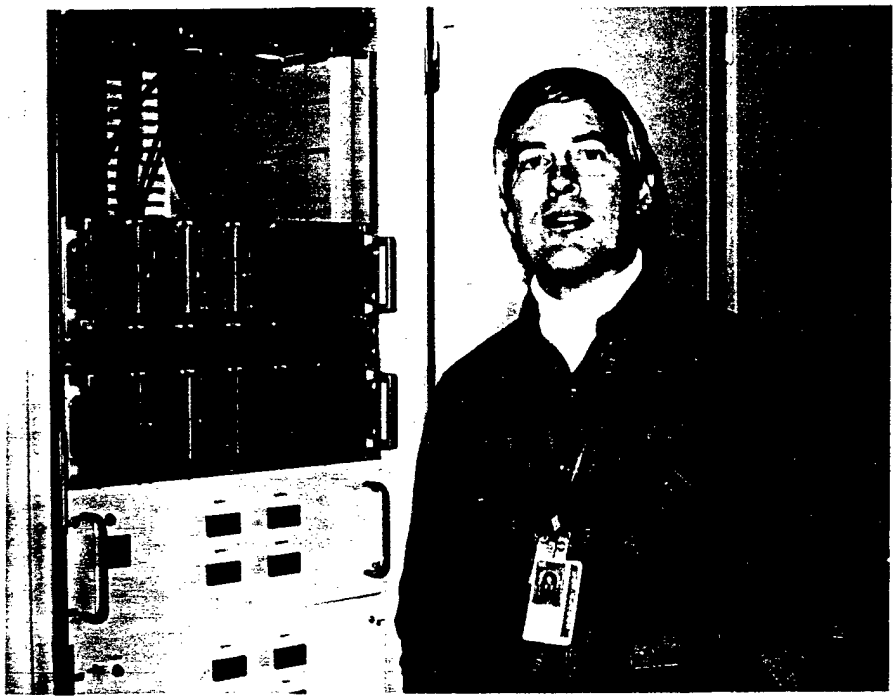

Michael Thuot, Group Leader

Accelerator Controls

Injector Controls

The ground test accelerator (GTA) injector has been operating all year. Group AT-8 completed controls for the source and low-energy beam transport (LEBT) including vacuum, emittance measurement diagnostics, steering, and focusing magnets. The injector was moved to building 365 during the year and operations resumed. We moved the control system to the classified network to protect emittance measurement data. Controls continue to be refined and enhanced to integrate better with the radio-frequency quadrupole (RFQ) and safety interlock subsystems.

The reliability of the injector controls was improved greatly during the year. The injector produces an extremely harsh electromagnetic interference environment for electronics and instrumentation. Improvement in electrical shielding and isolation has resulted in increased operational reliability.

The input/output controller (IOC) and control software provide many, behind-the-scenes capabilities useful for the injector, such as automatic rate-of-change control for magnet power supply currents and feedback-loop control to automatically maintain temperatures and power supply currents. An algorithm to steer the beam through the LEBT to predictable coordinates at the RFQ match point was implemented in the injector IOC. We used this algorithm during experiment 1B measurements.

Radio-Frequency Quadrupole (RFQ) Controls

The RFQ became operational during the year. Several RFQ devices requiring computer control and measurement have been tested extensively off-line but, for various reasons, have not been commissioned during RFQ operation. We also tested extensively a system of mechanical positioners which make minute adjustments of the RFQ alignment. Algorithms translate an operator's desired movement in an x-y coordinate space to simultaneous

movements of five stepper motors which drive the positioner actuators. Proper movement and position are checked by proximity probe measurements and are indicated by positive readback of the motor positions.

We produced software to support high-power conditioning of the RFQ. This software provides control of the radio-frequency (rf) power into the cavity and can automatically step the power through a programmed sequence. The software displays plots the cavity temperature, vacuum, and rf power. We also produced higher-level software to analyze transmission of a beam through the RFQ. This analysis can be based on either the mechanical position of the RFQ or the beam position as steered into the RFQ from the LEBT. This software adjusts either the mechanical position of the RFQ or the beam steering into the RFQ through a preprogrammed sequence. For each programmed position, a transmission measurement is made. This data is then represented on a surface plot for easy inspection.

Heating elements and temperature diodes are mounted on the RFQ strongback to provide a method of stabilizing the strongback temperature. This is intended to prevent minute misalignments due to temperature differentials. Control system software is available to implement feedback loops for driving this equipment. In response to this and other cryogenic temperature measurement requirements, we have added a Scientific Instruments temperature silicon diode controller to our control system hardware. This controller is a general purpose interface bus (GPIB) device which collects readings from up to eight diodes and supplies calibrated readings to the IOC.

Dynamic frequency tuners serve to maintain the desired resonant frequency in the RFQ cavity. Each of eight tuners is driven by a stepper motor. Typically, all eight motors are driven together by the same amount. An algorithm in the system IOC calculates the amount of movement required of the motors based on resonance measurements. The movement value is communicated over the computer network to the RFQ system IOC which commands the movement. This closed loop can correct resonance tuning between each beam pulse at 10 Hz.

Radio-Frequency (rf) Power Control

This control subsystem was developed and tested using a test cavity. We commissioned controls for automatic frequency tuning, tetrode control, and RFQ field control. The control system was enhanced to communicate with an Allen-Bradley programmable logic controller (PLC), which serves as an embedded controller in the tetrode instrumentation. A rf network analyzer was also added to the repertoire of devices operable by the control system.

Extensive use of AT-8's Sequencer tool has been made to automate parts of the rf system. The most fully developed application is automatic resonance control, which automatically adjusts frequency tuners in the rf cavity based on resonance feedback. Work continues to automate field control and fault detection. As more rf equipment is added in support of intertank matching section and drift-tube linac (DTL) components, this year's development investment will allow us to "add on" with little effort.

Vacuum Controls

A test station was built and used for testing prototype vacuum equipment and instrumentation prior to installation of beam-line components. The test station provided an opportunity to test controls, interlocks, and operator screens before they were needed on the beam line. Once the instrumentation was finalized, a duplicate system was built and installed in the equipment area. We designed the RFQ vacuum system so that subsequent vacuum systems for the DTLs would be identical. Therefore, implementation of these downstream systems will be duplication, involving much less effort. We are pursuing automatic start-up and shutdown sequences using AT-8's Sequencer tool which would simplify vacuum system operation.

Magnet Mapping

Support for the magnet mapping lab has continued through the year. We added software enhancements and new hardware to improve the system's capability and usability. The magnet mapper makes use of an 18-bit resolution digital multimeter which is controlled by the IOC using a GPIB interface. A specialized tachometer was installed in the IOC to measure fluctuations in motor speed. The mapper software also exploits the IOC's capability to write files on network host computers. Data acquired from the mapper is written to a VAX host on the network for subsequent analysis.

Control System Software Development

A single set of control system tools and run-time software for accelerator monitoring and control through data entry has been successfully fielded on several subsystems across a number of programs. The control system has been used to monitor and control the rf power, the injector, the diagnostics, and the RFQ for GTA. The control system also controls the discharge test stand, the magnet mapping laboratory, the vacuum test stand, and the control system test and staging areas at Los Alamos. The control system has also been applied to a rf test station and the controls test station at Argonne National Laboratory.

This year, the control system has been improved and extended in several areas. The most noticeable change is the development of a new operator interface (OPI). The new interface features much higher performance, and extended capabilities in both the editor and at run-time. It is based on X-windows, allowing any X-server to act as an operator station. The X-windows OPI is in a test at this time.

The most significant new system function is data archiving and retrieval. This package provides the user a variety of methods for archiving data from a user-created archive file. The IOC has been extended to support the

VXI bus, digitized waveforms, 6-axis motor controllers, and time stamping for data synchronization. The channel access software bus has been extended to provide connection management. This notifies the subsystems and any user programs when a connection is broken or reestablished.

Control System Hardware Development

The primary development in the hardware area this year is the production of eight IOCs for the RFQ experiment on GTA. These include the two Diagnostics IOCs, the RFQ IOC, the Vacuum System IOC, the timing subsystem IOC, the microstrip measurement system IOC, a mapper IOC, and a mechanical test IOC.

RFQ Control Hardware

The RFQ IOC Device Document now includes 17 different RFQ device types (75 individual devices) interfaced to the GTA control system. Templates are complete for the 17 devices. Device responsibility assignments in AT-8 have been made for all 17 devices. We designed and fabricated an end-to-end model (including trunk wiring) for each device. End-to-end documentation is included for 5 core tank positioners, 8 dynamic frequency tuners (slug tuners), 18 silicon diodes (2-wire and 4-wire), 6 core tank proximity probes, and 6 strongback heaters. A total of 501 individual trunk wiring paths (167 shielded twisted pairs) are required for the specified devices. Wireflex path numbers and the current status of each device are included in the RFQ IOC Device Document.

We moved the RFQ assembly into an alignment lab to check the core tank positioning hardware and software. The RFQ IOC and its associated electronics were assembled into a portable rack and rolled into the alignment lab to support these tests. All devices on the RFQ and the associated wiring on the RFQ were verified for proper operation.

End-to-end continuity testing of the wiring from the RFQ racks to the core tank devices was completed. While the devices were disconnected at the core tank end and the signal conditioning was disconnected at the rack end, we used a 200-V megohm cable tester to check for shorts on each cable. Next, we attached test devices to each connector on the core tank wire harness and verified proper operation of the device from the equipment rack area. Problems were corrected as they were found. We fabricated and connected ac power cables and instrumentation cables for the IOC and each of the RFQ equipment racks. We calibrated the proximity probes and recalibrated the slug tuners for operation over the long trunk wiring. Work is beginning on termination of the cables which run from the RFQ vacuum rack to the junction box.

GTA Stepper Motor Standardization

Work continues on the development of standard motion-control components for use on the GTA. Two commercial phase drivers were selected during the evaluation period. The phase drivers were designed into standard DIN form factor packages for use with variable reluctance and permanent magnet-hybrid stepper motors on the GTA. We evaluated design modifications for driving motors over the long cables needed on the GTA. We used the new GTA standard IOC motor-driver hardware initially on the core tank positioner and frequency tuners.

A prototype of the 2-Phase Motor Driver card was successfully tested. The 2-phase driver is a standard component on the RFQ core tank positioner device. The prototype version of the new variable reluctance (4-phase) DIN-packaged phase driver for the GTA motion control system is complete. The 4-phase driver will be a standard component on the RFQ slug tuner device. We will also use this driver on other GTA beam-line devices using the Princeton Research, Inc., stepper motors. In the standard IOC configuration, six of the DIN phase drivers are interfaced to a single Versa Module European (VME) bus stepper indexer module. In addition, each driver module includes local front panel controls and monitors for manual operation. Schematics for the 4-phase driver are located in Tech Note # IOC:90:003.

Several minor improvements were made to the new GTA 4-phase driver to permit a ramped "soft start" of the motor during manual operation of the hardware. The motion control hardware and software have been successfully tested using the linear variable differential transformer output in the feedback loop; this permits the motor to recover from missed steps during movement and to correctly move to a specified absolute position. We successfully operated a prototype to specification through the trunk wire test spool model. The current testing effort is to guarantee operation of the slug tuner to the 1 mil accuracy requirement (positioning accuracy of 1 mil permits a tuning resolution of 200 Hz).

Magnet Mapping Lab

We revised the IOC hardware to handle solenoid mapping as well as quadrupole mapping. We are presently testing hardware for a second quadrupole mapper, IOC 35. A VME bus tachometer module was implemented to verify rotational velocity of the quadrupole mapping system. The tachometer permits a rotational velocity data point to be obtained with each field mapping data point. Documentation covering both mapper IOCs, and the associated hardware changes was completed. The large bore mapper IOC interface prototype was successfully tested. The interface supports gain selection and coil multiplexing on the rotating mapper coil assembly.

Mechanical Test IOC

An IOC to support the mechanical testing of motors in the motor assembly lab has been fabricated, tested, and delivered. This IOC employs GTA-standard hardware and software and therefore can be easily expanded as future testing requires.

Timing System Hardware

We have completed, prototyped, and

tested the designs of all timing modules required for experiment 1C. The time-stamping/beam-synchronization mechanism appears to work well. The production version of the last module, the clock/trigger generator was delivered. We have fabricated and tested a sufficient number of timing modules and motor driver hardware to support the requirements of experiment 1B. A minimal number of spare modules has been added to our inventory.

Diagnostics Interface Hardware

Test and evaluation was completed on the VME/VXI bus simultaneous sample-and-hold module. We will use this module on GTA permanent diagnostic devices such as the micro-strip beam probe and the beam toroids. The use of this module offers a significant reduction in the cost and time required to implement the permanent diagnostic IOC. The 3-dB point of the new sample-and-hold is 750 kHz. The software driver for the analogic sample-and-hold modules is working reliably. Use of the DMA controller available on these cards has been integrated into the driver, resulting in a significant decrease in the amount of processor time required on each beam pulse to gather the data from these modules.

Commissioning Support

In early December, a Controls Specification and Priorities Panel for GTA formed to ensure that (1) all sectors provide documented requirements for the controls sector and (2) the requirements are consistent and of sufficient detail to prioritize. This panel resolved questions and issues concerning a number of topics including: temperature measuring devices, the new OPI, plotting the use of PLCs, and the VXI module support required by AT-5.

We converted two application programs from the VMS systems ESCAN and EMITS into the control system environment. The two programs measure beam emittance. They are now part of the GTA control system. Other applications were completed include the implementation of a control system on the Discharge Test Stand, the building of a GTA software tool, IMAGETOOL, that handles video images, and the development of a tool that allows steering of the beam at the RFQ entrance.

In a continuing effort to understand the noise found on the beam current emanating from an ion source, we decided to modulate the source arc current to disrupt any resonances that might naturally build up. A high-power modulator was built for the arc current. The data that was collected indicated that, at certain frequencies, the injection of a modulation on the arc current decreased the standard deviation of the noise by as much as 15 percent. This work formed the core of a master's degree thesis.

In an attempt to build a user friendly tool to expedite accelerator component design, we built a spreadsheet that solves a set of self-consistent equations describing the properties of an RFQ. Given a set of properties to which the RFQ adheres, such as a certain frequency and beam current, this spreadsheet provides a good starting place for the design. We presented a poster on this tool at the 1990 Linear Accelerator Conference in Albuquerque.

Free-Electron Laser Controls

Los Alamos has worked very closely with Boeing Aerospace and Electronics during the past year to develop a laser subsystem (LSS) control system for the ground-based free-electron laser technology integration experiment. Boeing has principal responsibility for the control system and Los Alamos is to provide (1) system software, (2) controls for the photoelectric injector (PEI), and (3) controls technology support. The system software, which was originally developed for the GTA, is being enhanced for the LSS. The major components of the system software are the common run-time environment (CORE) and the applications Toolkit. The CORE includes all run-time capabilities (data acquisition, operator interface, archiving, etc.), and the Toolkit includes the graphical editors and other tools to build applications with minimal programming. PEI controls will include automation of PEI operation and integration into the LSS central controls. Controls technology support includes VME and VXI hardware technology, operator console concepts, and computer network architecture support.

The year was marked by extensive interaction with Boeing and the major subcontractors. This interaction included weekly technical information meetings by telephone conferences, training sessions on the system software, and Los Alamos participation in the project Preliminary Design Review and In-Process Review.

The CORE and Toolkit software are being developed to DOD-STD-2167A, which is the military standard for imbedded software. A software development plan was prepared for the Los Alamos software, and a software requirements specification was written for the CORE software. A computer-aided software engineering tool was purchased to assist in developing software to the military standard.

Performance of the control system hardware and software was a major issue we faced this year. A major trade study was conducted by Boeing and Los Alamos to determine which of two competing architectures best satisfied all the performance requirements. This study led to a third architecture, which was ultimately adopted. This architecture uses a dual ethernet concept that isolates the critical control loops from the acquisition and display data.

To familiarize Boeing people with the Los Alamos hardware and software, controls were installed on the Modular Concept Test Development (MCTD) at Boeing in Seattle. These controls perform rf amplitude, phase, and resonance control on four cavities. This work was performed in conjunction with the rf power group, AT-5. Control algorithms developed for the GTA were modified for the MCTD.

AT-9
Very High-Power Microwave Sources and Effects

Robert Hoeberling, Group Leader; Michael Fazio, Deputy Group Leader

Introduction

AT-9, the Very High-Power Microwave Sources and Effects Group, was formed in August 1988 to perform research, development, and testing of very high-power microwave sources, advanced pulsed power development, and microwave effects testing. This charter has expanded to include the development of new high-power, ultra-wideband, subnanosecond rise time video pulsers. We are also investigating the effects of these pulses on electronic systems.

Our long-term intention is to provide powerful radio-frequency (rf) systems able to drive advanced accelerators for a variety of uses. These rf systems can power improved, compact medical linacs; compact accelerators for free-electron lasers; and ion accelerators for particle physics research and defense applications. The potential compactness and unprecedented power of these new rf systems will make such accomplishments more cost-effective and, hence, more feasible than they are with existing technology. In addition, such technology can be applied to both new weapons systems and to defensive tactics against foreign assault. The Department of Defense (DoD) is concerned with the presence of microwave weaponry on the tactical battlefield of the future. The issues to be considered here are the vulnerability to microwave radiation, of both our weapons as well as those of the enemy, and the ability of the US to field a microwave weapon. In this age of microelectronics, conventional weapons have become much smarter and more accurate due to the ability to place progressively greater computing power on the weapons platforms. The consequence is that the electronics in these weapons are much more sensitive to upset and burnout when irradiated with microwave energy. AT-9 is chartered with building the high-power microwave systems and working on advanced microwave weapon concepts.

Over the last several years, AT-9 has become the focus of the high-power microwave source development effort at Los Alamos. This move coincided with an appreciation of the need to incorporate pragmatic engineering aspects needed to develop practical high-power rf source systems into rf source designs—even as they are being researched. From this perspective, AT-9 is focused upon developing high-power microwave sources which, from their inception, are designed for eventual incorporation into an integrated system comprised of prime power, pulsed power, an electron-beam diode or thermionic electron gun, a high-power microwave source, and rf extraction into a waveguide or an antenna. Issues of size, weight, shape, etc., are ever-present considerations in this process.

Other divisions at the Laboratory which interact synergistically with AT-9 include the Dynamic Testing (M) Division, which provides experimental pulse power support; the Applied Theoretical (X) Division, providing advanced computer modeling; Chemical and Laser Sciences (CLS) Division which provides pulsed power support; and the Space Science and Technology (SST) Division, which addresses problems associated with rf propagation through the atmosphere, such as rf induced atmospheric breakdown.

High-Power Microwave Source Research and Development

The ongoing high-power microwave (HPM) program includes several rf source projects, including the high-current relativistic klystron amplifier (RKA), the resonant cavity virtual cathode oscillator, and the large orbit gyrotron (LOG). The RKA is funded jointly by the DOE and the DoD as part of a broad investigation of technology potentially important for the DoD. The LOG effort is presently funded with internal Los Alamos support because of its potential merit in a wide range of defense, particle physics accelerator, and commercial applications. The virtual cathode oscillator research is funded by the Air Force's Wright Research and Development Center because of its attractiveness as the rf source for a first generation rf weapon. We believe that each of these rf sources has unique merit and is suitable for different systems applications.

High-Current Relativistic Klystron Amplifier (RKA)

Summary

This project, which began in October 1989, is an interdivisional effort with AT-9, M-6 (Shock Wave Physics), and X-10 (Pulsed Energy Applications). The experimental work is a collaborative effort between AT-9 and M-6, with X-10 performing the computer code simulations in support of the experiment. AT-9 has the project leader responsibility for the overall effort. The work has been supported by the Joint DoD/DOE Munitions Technology Program.

Our interest in high-power microwaves and intense bunched electron beams is stimulated by (1) the need for advanced rf sources for future accelerators and (2) the demand for very high-power microwave amplifiers that can in addition be phase-locked for some high-power microwave weapons applications. The RKA is a suitable microwave source for a single- or modest multiple-shot deliverable weapon powered by an explosive magnetic flux compression generator. The RKA is also suitable as a continuously pulsed microwave source driven by a conventional pulsed power system.

The goal of this research effort during the past year was to design, build, and begin the experimental testing of a long-pulse RKA at 1.3 GHz in an attempt to extend the pulse length of this gigawatt-class device by an order of magnitude beyond the current state-of-the-art (100 ns). So far, we have produced a modulated electron beam for one microsecond with a peak rf current of 0.9 kA and a voltage of 350–400 kV. In some cases we have observed beam modulation in excess of 2 μs. The component of beam power at the microwave drive frequency (1.3 GHz) is approximately 350 MW. Although only a small effort was put forth to address the output coupling problem this year, approximately 50–70 MW was coupled into a dominant mode rectangular waveguide.

Background

This year we began a program to develop the RKA, based upon the encouraging results reported by Moshe Friedman[1] and his collaborators at the Naval Research Laboratory (NRL). (The RKA is a high-current [>2 kA] relativistic klystron, in contrast to what some other researchers call a relativistic klystron, which is a classical klystron [<1 kA] operating at relativistic voltages.) The RKA, as tested by Friedman, has produced several gigawatts of power with 40% beam-to-microwave power efficiency at 1.3 GHz in a 100-ns-long pulse on a single-shot basis. We have identified the high-current relativistic klystron as a very promising source that has exhibited very good performance in a very limited parameter space. During this past year, we have undertaken an effort to extend the pulse length of the RKA by an order of magnitude, from 100 ns to 1 μs, while maintaining very high power levels. We have embarked upon a program having a somewhat different approach than that of NRL; from the outset, we have addressed the engineering problems associated with designing a device capable of microsecond operation, direct coupling of the rf energy into a rectangular waveguide, and ultimate repetitive operation at several hertz. This program is well underway, and results to date are encouraging. With a sustained development effort, repeatable, high-energy, single-shot and repetitively pulsed operation at these very high power levels will eventually become feasible.

The operation of this device, while not fully understood, can be compared to a classical high-power klystron. A classical klystron consists of a series of two to five resonant cavities and an electron gun that supplies a pulsed electron beam 5–10 mm in diameter. This electron beam is nominally at 200–300 keV with a current of 200–400 A in a typical high-power device (20–70 MW of rf output). The electron beam is repetitively pulsed anywhere from 1 to 200 Hz, at pulse lengths of 1–200 μs. This electron beam is injected into the first cavity, which is driven by a low-power microwave source. The low-power source excites an oscillatory electric field across the gap which the electron beam must traverse in the first cavity. The electrons experience an electric force as they cross the gap. This force and hence the electron's velocity after leaving the gap, depends on the phase of the electric field as the electron crosses the gap. The electron beam is therefore velocity modulated as it leaves the cavity. After drifting some distance, the fast electrons catch up with the slower ones, producing a spatial modulation of the electron beam. The electron beam then consists of a series of charge bunches at the rf drive frequency. The succeeding (undriven) idler cavities interact with the beam to further spatially compress the electrons into even tighter bunches. The final cavity then extracts the microwave energy from the bunched beam by decelerating the bunches. This current klystron technology is the culmination of almost 50 years of effort which began during the World War II development of radar. The Stanford Linear Accelerator Center and several commercial companies have attempted to scale the output power levels into the 50–100 MW and higher regime but have met with limited success. These results have led us to seriously consider other alternatives, in particular the high-current relativistic klystron, for the next generation of very high-power microwave sources.

The high-current relativistic klystron differs from a classical klystron in several significant ways. Most importantly, the current of the high-current relativistic klystron, at 2–10 kA, is higher by 1–2 orders of magnitude. The electron beam is relativistic, with an energy of 300–1000 keV. An important distinction is the potential energy associated with the beam's space charge. In the classical klystron the potential energy of the beam is small compared to the kinetic energy. In the high-current relativistic klystron, the potential energy is comparable to the kinetic energy due to the much higher space charge. The practical implication of this phenomenon is that a small velocity modulation on the beam, produced in the first cavity, causes a dramatic increase in the space-charge potential energy. This potential causes the beam to slow down and strongly bunch. This bunching effect is much more dramatic than in a classical klystron and is due primarily to the fact that the beam current is much more intense. The high-current relativistic klystron is therefore inherently a high-power device because it relies on the effect of high space charge for efficient operation. The device is more suitable for high-power operation because the electron beam is annular and several inches in diameter. This enables a more intense beam to propagate through the device without exceeding the space-charge-limiting current. Also, the larger surrounding cavity structures are less likely to be plagued by high-voltage rf breakdown.

In AT-9, we possess a pulsed power capability that is well suited for driving either a single-pulse or a repetitively-pulsed high-current RKA. The BANSHEE modulator, located in MPF-18, is designed to produce 1-MV, 10-kA pulses with a 1-μs flat top at a rate of 5 Hz. The performance specifications of this pulser represents a unique capability that does not exist elsewhere in the US. BANSHEE is well on its way to achieving its design specifications, with improvements being made continuously. The RKA is the first experiment to be fielded on the BANSHEE modulator.

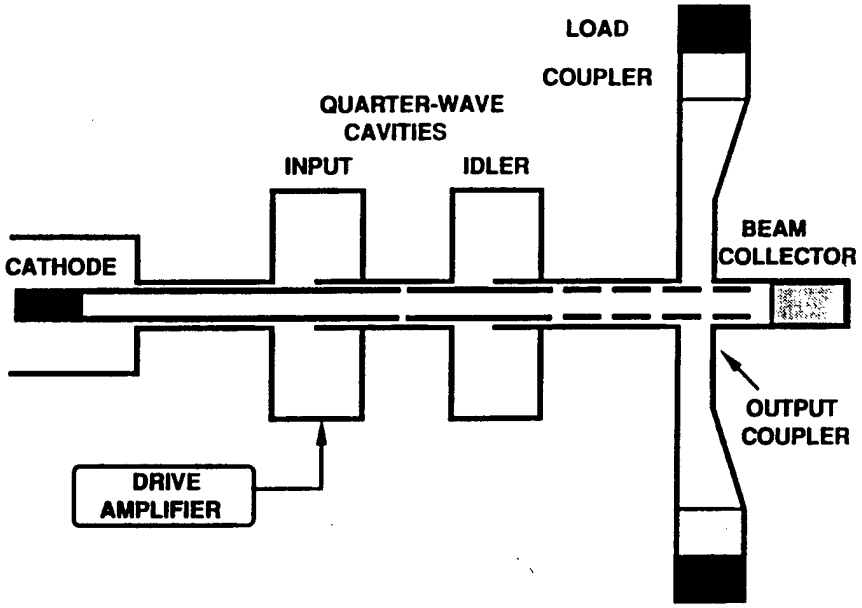

Figure 9.1. Los Alamos RKA.

Current Experimental Work

The current work has progressed well and has been described in detail in several publications.[2-4] The RKA, shown schematically in Fig. 9.1, has been constructed and operated on the BANSHEE pulsed-power modulator. This RKA contains a field-emission diode. This diode produces a hollow beam that passes through the coaxial quarter-wave input and idler cavities to the rectangular-waveguide output coupler. For rf beam modulation measurements, a beam pipe containing a linear array of B-dot loops is placed on the beam line. The experiment and the experimental team are shown in the photograph in Fig. 9.2. The copper-plated stainless steel cavities were designed using SUPERFISH. The cavities are shown in Fig. 9.3. The annular electron beam is supplied by a 2.5-in.-diameter circular ("cookie cutter") stainless steel field-emission cathode. The axial guiding magnetic field (~5 kG) required by the RKA to control the electron-beam trajectory is supplied by a set of 11 coils arranged one after another along the beam line with a several inch spacing between each pair of coils. A 20-kJ capacitor bank was constructed and used to provide the current pulse needed to energize the magnet. The spacing between magnet coils allowed room for attaching input and output waveguides to the RKA cavities. The magnetic field has been mapped and determined to be sufficiently uniform for proper operation of the RKA.

In the RKA, the beam bunching (rf current) peaks at some point downstream from the gap of the input cavity. This point is the desired location for the gap of the idler cavity. Likewise, the beam bunching also peaks at a point downstream of the idler cavity, and this is where the output gap should be located. These positions of maximum beam bunching were determined with a linear array of B-dot loops along the beam drift pipe, and the cavity gaps were located accordingly.

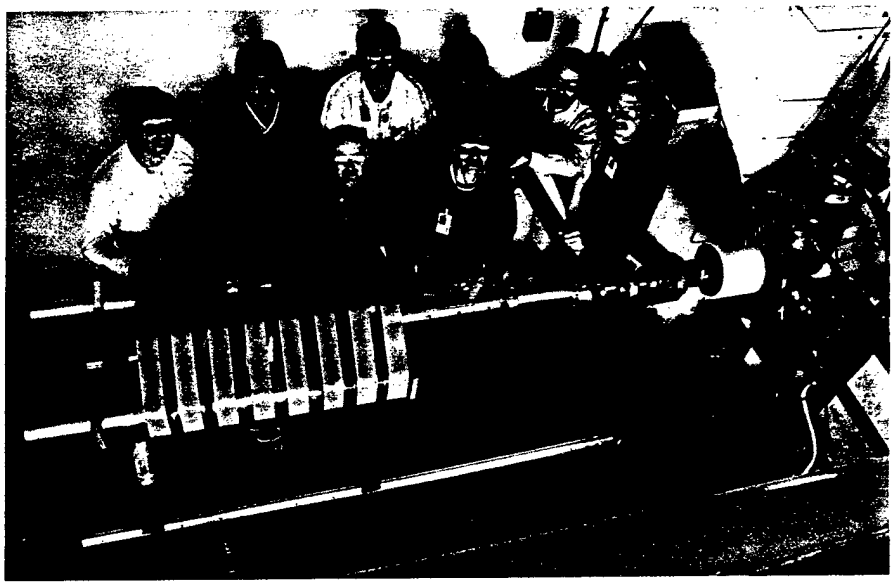

Figure 9.2. The RKA experiment shown with the experimental team. The magnet assembly with eight coils is shown on the left and has been retracted to expose the relativistic klystron on the right.

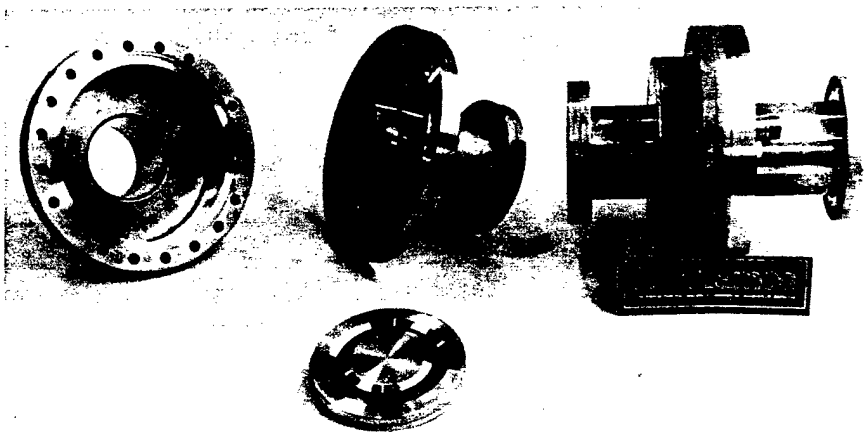

Figure 9.3. Copper-plated stainless steel RKA cavities.

The nominal injection-beam parameters are 350–400 kV and 3 kA. The rf current downstream of the input cavity was ~ 25 A with 5 kW of rf input power. The second (idler) cavity was added to enhance the beam bunching. We made measurements of the rf current downstream of the second cavity. Electron-beam bunching has been observed downstream of the second cavity for 900 ns at an rf current of 900 A. A bunched beam of this pulse length and intensity is a significant accomplishment in the high-power

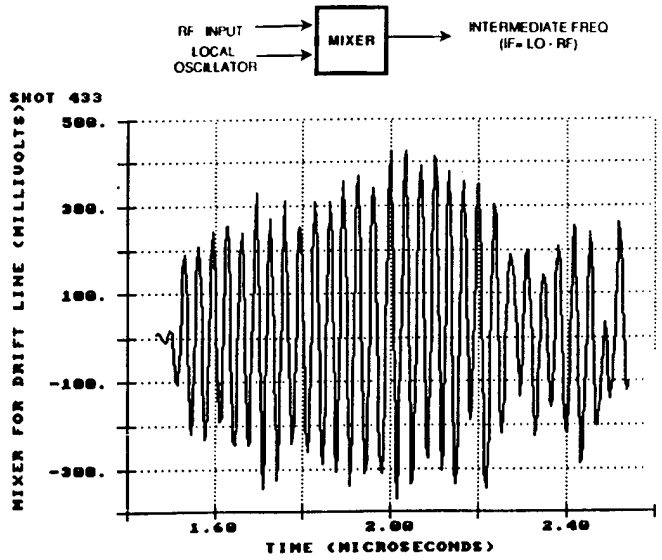

Figure 9.4. Frequency down-converted (IF) signal from a B-dot probe downstream of the idler cavity that shows the rf current on the bunched beam for 900 ns.

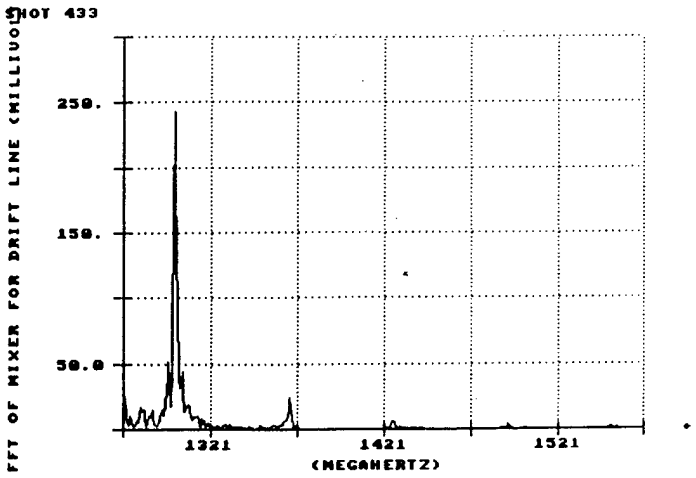

Figure 9.5. Fast Fourier Transform of the signal in Fig. 9.4 which shows the spectral content of the microwave pulse.

microwave community. Figure 9.4 shows the frequency down-converted signal from a B-dot loop located downstream of the idler cavity. The signal shows the rf current on the bunched beam for 900 ns. The spectral content of this pulse is shown in Fig. 9.5.

The RKA output power at 1.3 GHz was initially measured at the 50–100 MW level in 100–150 ns pulses. This pulse length was much shorter than expected, since the electron beam pulse was over 1 μs long. Careful observation indicated that this pulse shortening was caused by the heavy beam loading in the input cavity. This heavy beam loading resulted in a large impedance mismatch between the low-power driver amplifier and the input cavity, causing most of the rf-input drive power to be reflected from the cavity during the beam pulse. This effect is very small in conventional klystrons because of their relatively light beam loading, and this problem has not been encountered in other short-pulse (100–150 ns) RKAs experiments. The impedance mismatch is not a problem with RKA in the short-pulse regime because, on the few hundred nanosecond time scale, one is simply using the stored energy in the input cavity to bunch the beam; therefore, input power reflected during the 100-ns electron-beam pulse is unimportant. Since we are trying to produce a 1-μs pulse, the cavity fields must be maintained throughout the pulse so we needed to resolve the impedance mismatch problem. We solved this problem by matching the driver impedance to the cavity impedance under the condition of heavy beam loading. The solution required that the driver amplifier be very strongly overcoupled to the input cavity without the beam present (VSWR ~ 30). The cavity shunt impedance and Q drop dramatically when the beam is injected, resulting in a good impedance match (VSWR ~ 1) between the beam-loaded cavity and the driver amplifier.

The output coupler consists of a 27 in. section of a reduced-height, rectangular waveguide (1.5 x 6.5 in. cross section) that tapers at both ends to a full height (3.25 x 6.50 in.) WR-650 waveguide over a 10 in. length. The approximately 2.5-in.-diameter electron beam passes through 2.9-in.-diameter apertures in the opposing broad walls located in the center of the reduced-height waveguide section. The beam interacts with the electric field across the waveguide gap in order to couple microwave energy from the beam to the waveguide fields. Because the beam impedance is relatively low, on the order of 100–200 Ω, this output-coupling scheme was chosen over the more conventional approach of using a high-Q cavity that is employed in a classical klystron. For optimal coupling, the beam impedance must equal the impedance of the output gap. A high-Q cavity has a much higher gap impedance than is desired. A full-height waveguide also has a higher impedance than desired, which is why we reduced the height. This approach to output coupling has the advantages of being relatively simple to build and of putting the energy into rectangular waveguide in the dominant mode. This allows us to make unambiguous power measurements with commercially available directional couplers. It also allows us to either (1) radiate the power with readily available antennas with good, high-gain radiation patterns or (2) drive an accelerator load directly. Although we did incorporate into the design a provision for tuning the gap impedance, the provision proved unusable because of problems with beam interception and consequent plasma production. More effective means to tune the gap impedance for optimum coupling to the beam will be a future improvement to the output coupler.

To date, we have produced a modulated electron beam for 1 μs with a peak rf current of 0.9 kA and a voltage of 350–400 kV. In some cases we have observed beam modulation in excess of 2 μs (the full base-width of the electrical power pulse). The dc beam current is about 3 kA, giving approximately a 30% beam modulation. Greater than 100% modulation should be possible and has been demonstrated by Friedman at the 100-ns pulse lengths. The component of beam power at the microwave drive frequency (1.3 GHz) is approximately 350 MW (beam voltage times rf-modulated beam current). The rf drive level is 5 kW, which will result in a power gain of 42 dB if one can extract this power with an (conservative) efficiency of 25%. Although only a small effort was put forth to address the output coupling problem this year, approximately 50–70 MW was coupled into a dominant mode rectangular waveguide. The gain was observed to be a sensitive function of the axial magnetic profile which was adjusted by moving the entire magnet assembly along the longitudinal axis of the RKA. This movement places the electrons leaving the cathode in a region of converging magnetic field lines as they accelerate toward the anode and enter the beam drift pipe. One effect of this converging field is a beam of smaller diameter than one that is born in a uniform axial magnetic field. We do not yet fully understand the effects of beam diameter, magnetic field shape, and cavity gap diameter on RKA performance.

Computational Modeling

Modeling was done by X-10 to complement the experimental effort. The two-dimensional, fully electromagnetic, relativistic particle in the cell (PIC) code MERLIN was used to investigate several aspects of the RKA experiment, including the power flow characteristics, diode performance, and the beam-cavity interaction. The details are included in Ref. 4. and are briefly summarized here.

A series of numerical simulations were done on the diode to determine the optimal geometry that would permit maximal beam transmission at the desired beam radius. Because the axial electric fields in the cavity gaps are highest at the radius corresponding to the beam-pipe wall, the highest gain is obtained with the beam operating as close to the wall as possible, consistent with the constraint that the beam-current density be large enough to approach the space-charge limit. The disadvantage of operating the beam close to the wall is that a few stray electrons can strike surfaces, creating plasma and inducing high-voltage breakdown.

The effect of the anode-cathode (AK) gap on the diode current was studied in detail by computer simulation. In Fig. 9.6, we show the electron-beam current as a function of the spacing between the cathode and the anode (AK gap), as obtained from a series of simulations. The behavior of the beam current can be explained in the following way: the anode starts out with a radius of 10.43 cm, which is stepped down to 3.63 cm as the beam enters the drift pipe. The electron-beam radius is approximated by the cathode radius. At equilibrium, the space-charge limiting current of the hollow electron beam is approximately given by $I_{SCL} = 8.5\,(\gamma^{2/3} - 1)^{3/2}/(\ln(r_a/r_c))$ in kA, where γ is the relativistic factor of the electron beam and r_a and r_c are the radii of the anode and cathode respectively. In the section where the anode radius is 10.43 cm, the space-charge limiting current is $I_1 = 2.7$ kA, with $\gamma = 1.88$ corresponding to beam energy of 450 kV. However, the space-charge limiting current for the electron beam in the section with the reduced radius of 3.63 cm is $I_2 = 25.5$ kA. The electron-beam current generated by the diode will be between these two limiting currents, depending on where the beam achieves its equilibrium state. For large AK gap spacings, the electron beam can evolve into an equilibrium before it enters the drift tube with the small radius. Consequently, the diode current is approximately given by the I_1. For small AK gap spacings the beam equilibrium occurs near or inside the drift tube, so the diode current would approach the limiting value given by I_2. The dependence of the diode current on the AK gap spacing in Fig. 9.6 clearly demonstrates the behavior.

To produce a high-current electron beam in the present configuration, the AK gap must be small. However, small AK gap spacings tend to contribute to diode closure (shorting) resulting from plasma formation around the cathode and the anode. Especially in long pulse regimes (>1 μs), large AK

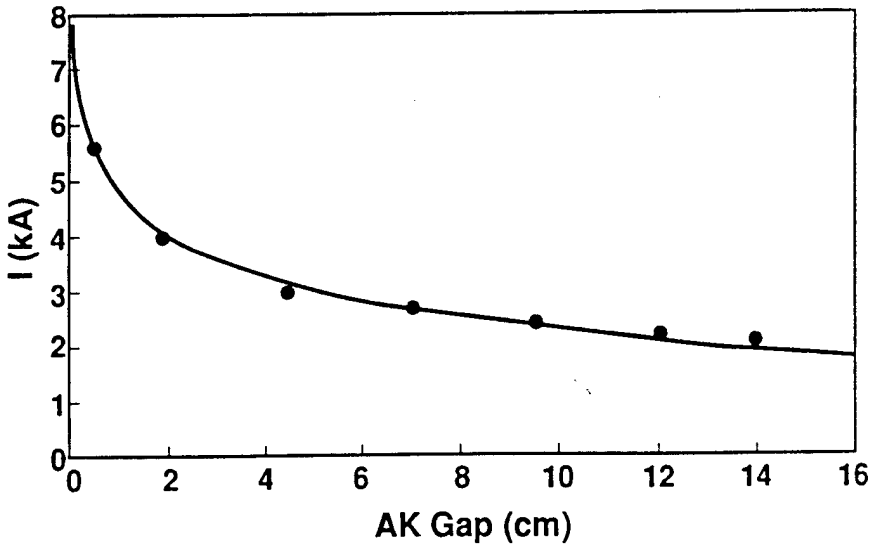

Figure 9.6. Electron-beam current from the foilless diode with different AK gap spacings showing the asymptotic behavior. The data points are from computer simulations, and the curve joining them shows the characteristic dependence.

gap spacings are much more desirable even though the diode current is reduced. The computer simulations of the experimental configurations indicate that the electron-beam current only increases from 2.5 kA to 5.5 kA for an AK gap of 9.53 cm to 0.64 cm. We conclude that a change in diode geometry will be required to achieve currents greater than 3 kA for 1 μs. To facilitate the understanding of the physics in the RKA interaction, a cold, 450-kV, 3-kA cylindrical beam was injected into the RKA. The first cavity was located at 28.6 cm. For simplicity, a uniform axial magnetic field of 5 kG was applied over the simulation region. The rf channel from an external source supplies rf drive power to the buncher cavity.

The rf signal across the input cavity gap produces electron bunching which peaks at some point downstream of the gap. The simulations explored the effect of six different gap voltages, from 4 kV to 175 kV (corresponding to experimental rf-input powers of 5 kW to 10 MW), on the electron bunching. Figure 9.7 illustrates the beam current for the different gap voltages. These currents were measured by a single probe at a position 45 cm downstream of the input cavity gap, and each curve measures the temporal history for a beam with a 3-ns rise time. Time averaging the current waveforms shows the beam current to be 3 kA. The waveform for the 175-kV voltage case shows strong nonlinearity with a frequency spectrum depicting a series of hamonics of the fundamental 1.3-GHz resonator mode. The waveform saturation is also apparent in Fig. 9.8, which shows the peak degree of modulation

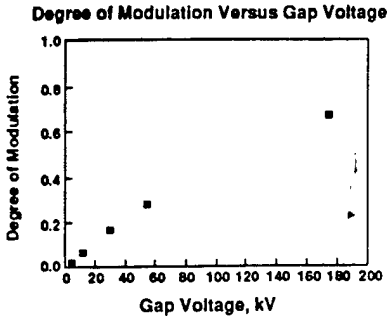

Figure 9.8. Degree of beam modulation versus gap voltage.

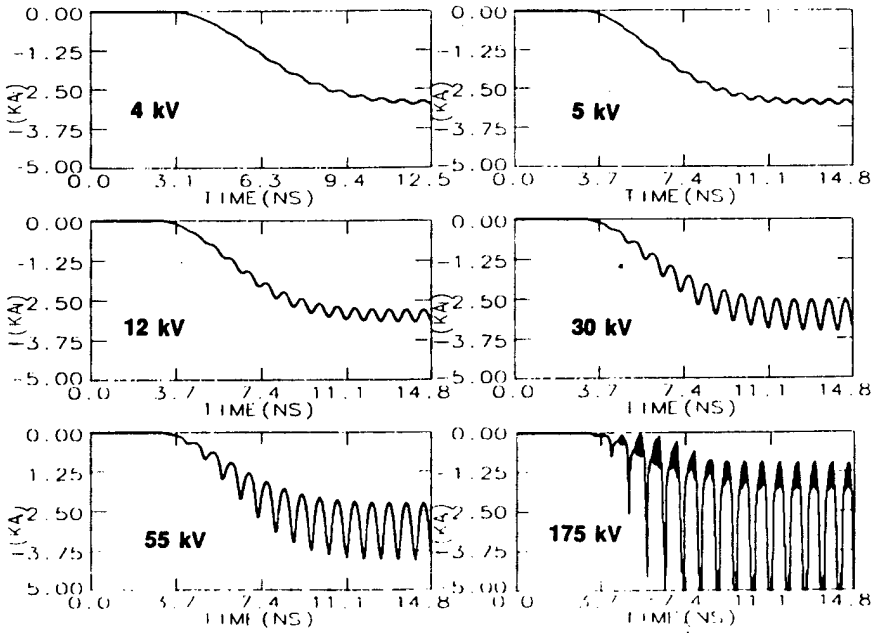

Figure 9.7. Current waveforms at z = 74 cm (downstream of buncher cavity) versus time for 4–175 kV gap voltages.

versus gap voltage. The current modulation is very nearly linear up to about 30 kV.

A more complete RKA simulation was accomplished by placing an idler cavity, identical to the first but with no rf injection, 50 cm downstream of the input gap. The axial momentum p_z is identical to the single-cavity momentum up to the second cavity. This cavity, the "idler," is strongly excited at 1.3 GHz. This excitation results in a 45-kV peak signal induced at the gap with the subsequent large-signal momentum oscillations at 1.3 GHz. The corresponding current waveform beyond the second cavity showed an increase in percentage modulation from 3% to 17%.

Future Plans

The performance of the RKA can be enhanced significantly with several experimental modifications. The RKA operates as an amplifier, and hence the output power is determined by the amplifier gain and the magnitude of the input power. During these initial experiments, our input rf power has been limited to 3–5 kW by the availability of conveniently accessible sources. This power level is not enough to lead to full modulation of the klystron electron beam. Steps will be taken to provide more input rf drive power, which should result in greater output power. Also, the diode configuration must be adjusted for optimal beam diameter and a current approaching 5 kA. Finally, the output coupler needs to be redesigned for a much higher efficiency for the conversion of modulated beam power to microwave power in the output waveguide.

Very careful design is needed for a 1-μs device, because a number of phenomena that can be ignored on a 100-ns time scale cannot be ignored when the longer, microsecond pulse length is required. For example, the formation of a plasma can have a deleterious effect on beam quality and microwave energy production. A very small amount of the electron beam striking a surface inside the device can heat the device, evolving a plasma which can migrate several centimeters in a microsecond to interfere with the electron beam dynamics and microwave production. Therefore, carefully understanding and controlling the factors that affect beam quality is essential for successful operation of the RKA. A relatively thin annular beam is needed, streaming at a controllable radius in the beam pipe, with minimal

oscillation in the radial dimension. Because the axial electric fields in the cavity gaps are highest at the radius corresponding to the beam-pipe wall, the highest gain is obtained with the beam operating close to the wall. We must investigate the tradeoffs among beam radius, gain, output power, and the pulse stability on the microsecond time scale. The ultimate goal is to optimize the output power at the microsecond pulse length.

The Large Orbit Gyrotron (LOG) Amplifier

Summary

The development of the LOG amplifier could have a major impact upon both the accelerator community and DoD requirements for testing and weaponry. The device is well suited for operation in the 10–20 GHz range that is required by the proposed TeV electron-positron collider. By virtue of its design, the LOG amplifier uses small magnetic fields of a few hundred gauss, regardless of operating frequency. This is a big advantage over alternative sources. In addition, the operating frequency can be changed merely by replacing the original cylindrical rf structure with another azimuthally periodic vane structure designed for the appropriate frequency. The electron beam and magnetic field requirements can remain fixed. Since it is an amplifier, many sources can be combined effectively to drive large accelerators or phased-array antennas. Hence, the LOG amplifier can add unprecedented flexibility to rf applications.

An independent research project (IRP) was begun in FY90 to develop an amplifier based upon the concept of the LOG. The goals of the three-year program are to design, build, and characterize such a device. These goals, rescaled to reflect a smaller allocation of funds than were requested, include the following: (1) develop an enhanced ability to control the electron-beam optics in the beam-forming diode and magnetic cusp regions; (2) develop the techniques needed to accurately guide the annular, rotating, and drifting electron beam in the rf structure to vary the degree of interaction of the beam with the rf fields; (3) develop an rf coupler to extract the microwaves from the device into waveguide; and (4) configure a prototype LOG amplifier and provide initial characterization of its performance.

During this first year of the effort, we carried out preparatory studies leading to the design of the amplifier hardware. Our effort began with a computational study of electron beam injection from a diode region, through a magnetic cusp, into the rf structure. It has resulted in the construction of electron-beam diode hardware for testing during November through February, FY 1991. Following the diode- and electron-beam optimization effort, hardware for the amplifier circuit will be designed and built for full-device testing in FY 1992. Additional effort to date has included an examination of the systems issues of amplifier design and alternatives for rf extraction into waveguide. Two well-known rf-extraction geometries have been chosen for experimental examination in our application. Computational work with the 3-D electromagnetic code, MAFIA, also was begun to acquire the ability to design amplifier and rf output structures in FY 1991.

Background

During the past four years we have investigated the LOG experimentally as an oscillator operated at a frequency of 2 GHz.[5,6] These results were the basis for the initiation during FY90 of the first year of an IRP to demonstrate an amplifier based upon the LOG's basic operating principles. The LOG amplifier is attractive for linear collider applications, since it requires a relatively modest applied magnetic field of only a few hundred gauss. This benefit is due to the ability of the device to operate at a harmonic of the cyclotron frequency. It can operate at frequencies of 15 GHz or more with these small magnetic fields. The rf breakdown problems should be relatively small, as well, since the electrons move to smaller orbits, away from the walls of the device, as they convert their energy into microwaves. Hence electron bombardment of the walls, which can lead to breakdown, is relatively modest. Other groups have investigated the LOG amplifier either theoretically[6] or as an experimental[7] device. However, our focus on operation at high power (10–100 MW) has not been undertaken elsewhere.

The Institutional Supported Research and Development LOG Amplifier Program

Developing a LOG amplifier has many similarities to the oscillator development already discussed. The chief differences between an oscillator and an amplifier are: (1) the amplifier's ability to utilize an input rf signal to initiate electron-beam bunching rather than rely upon the growth of rf noise arising from perturbations existing on the electron beam; and (2) the amplifier's output power, which is governed by a gain curve that is (usually) an increasing function of input power over a specified range, has a specified dependence upon operating frequency, and operates over a range of frequencies (instead of only at discrete resonant modes, as does an oscillator).

Our first goal in this program is to improve our ability to control the electron-beam optics needed for such devices. Because we want to produce higher powers in this amplifier than have been produced before, we must learn to control a high-power electron beam in a regime not well investigated in the past, at Los Alamos or elsewhere. Existing and proven rf source technology uses beams of 50–300 kV and currents of 100–500 A. While much rf source work also has been performed at multi-MV beam energies, this work has not proved useful for practical systems because of severe voltage hold-off constraints and the large x-ray fluxes produced by these beams that require costly and massive radiation shielding.

We are working with beams formed at an intermediate voltage, 600–700 kV, at currents of several kiloamps, for which the voltage handling and x-ray problems are much reduced. The combination of moderate beam potential, significant current, and electron space charge does, however, imply an effort to extend our capability in electron-beam optics to master this regime. Developing this new technology provides the foundation for other types of very high-power microwave sources in addition to the LOG amplifier, such as high-power magnetrons, klystrons, and gyroklystrons.

The first step in this effort has been a series of calculations of physical characteristics of the electron-beam diode that will enable the injection of a suitably large fraction of the original 4 kA of diode current (at least half initially) through a magnetic cusp, into the amplifier region downstream. These calculations were performed by the Pulsed Energy Applications Group X-10, using the PIC code ISIS. These calculations revealed that both the cathode position (with respect to the cusp and anode), and the emission radius, affect the beam dynamics in the gyrotron region very sensitively. These parameters affect the amount of current which propagates. In addition, they control the magnitude of a common behavior of improper design: the presence of radial oscillations in the beam as it propagates downstream. These oscillations draw the beam away from the optimum radial position for interaction with the rf structure, reducing the rf conversion efficiency.

The optimum beam designed by ISIS modeling, shown in Fig. 9.9, was found to be formed by a cathode emitter with a diameter of 14 cm, 3.5 cm from the anode plane. The equipotential surface, which includes the electron emission annulus, is conical, having an angle of 67.5° with respect to the system axis. For this configuration, the electron-beam voltage is 650 kV, the current injected is 2 kA, and the magnetic field cusp has the contour we presently employ in our existing experimental facility. The axial magnetic field in these studies was in the range of 500–600 G. The annular slot at the cusp position has a diameter of 12.5 cm and an annular width of 1 cm.

Having determined these beam characteristics from the modeling, we have designed and built experimental cathode hardware to explore a range of operating characteristics spanning the optimum conditions predicted by the code. These experiments were begun in the summer, 1990, and are continuing. The new cathode hardware allows us to vary the angle of the equipotential emitting surface in four steps of 70°, 67.5°, 66°, and 60°. Emission from this cathode will be provided by a field-enhanced sharp-edged ring, mounted to the equipotential field-shaping surface. The cathodes will be housed in a newly constructed diode vacuum chamber, which is large enough to comfortably contain the new cathode field shapers with minimal electron emission losses to the chamber. Two new magnetic field coils were also constructed for the chamber which allow us to control the field from each coil individually, providing added control of the magnetic field contour in the diode.

We utilize explosive emission to form a plasma on the ring's sharp edge. The surrounding field-shaping surface is scaled to minimize the geometric field enhancement factor in regions other than the emitting ring, thus reducing extraneous emission from the negative electrode surface. Since explosive emission begins at an electric field threshold of 100–300 kV/cm, and the field shaper has an electric field everywhere less than 100 kV/cm, the ring will emit much more readily than the field-shaping electrode holding it, allowing us to control the electron emission to come predominantly from the ring. The radius of the emitting ring can be varied in 2-mm increments with the hardware we have constructed.

Using a sharp-edged emitter is a departure from the computer design, which has the surface of a smooth, conical section as the emitter. We have attempted to minimize the effect of this departure by providing a large, suitably conical region with the proper equipotential contour, surrounding the emission edge. In addition, we have kept the extent of the protrusion by the

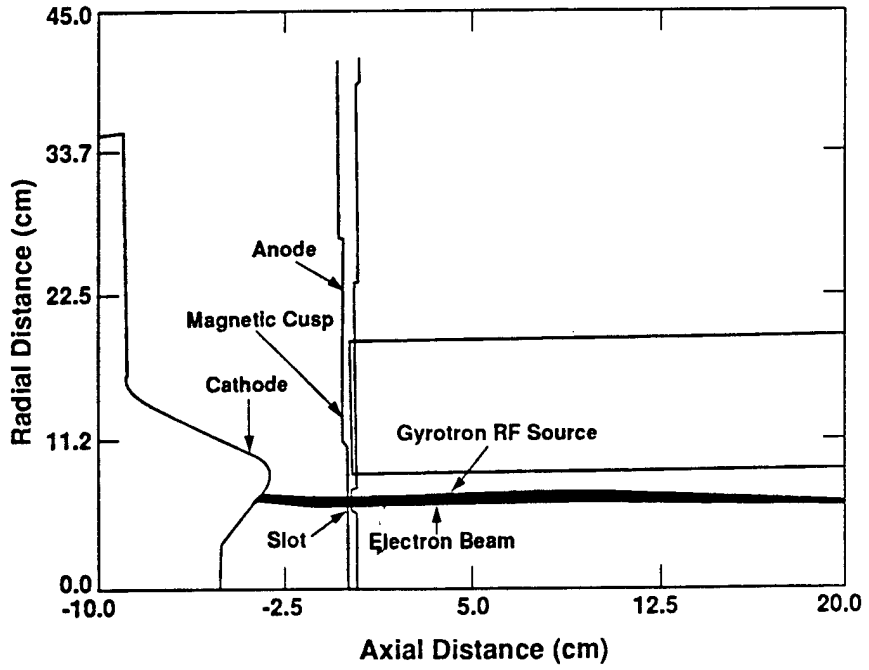

Figure 9.9. ISIS model of optimum diode configuration.

emission edge short (4 mm) so that the aspect ratio of the emission protrusion to the radial extent of the field-shaping surface is small (of order 10). As the electrons of the beam move toward the anode, the field perturbation caused by the emission edge falls off, and the equipotential surfaces merge with the contours dominated by the conically angled field shaper holding the emitting ring. Thus, the departure from conical equipotentials becomes small after the electron beam has moved across 20–30 percent of the acceleration-gap distance. We expect that by having field-shaping electrodes with various conical angles in the range of the code prediction, and by having the ability to control the emitter radius by replaceable field-enhanced rings of different radii, we can find an optimum diode configuration near that predicted by the computational modeling.

The first experiments in this series were performed during the summer, FY 1990. During these experiments, we developed current monitors which we will use to measure the electron-beam propagation efficiency through the cusp, and in the rf source region downstream. This effort required special care, since the helical electron beam and the rf in the resonator create unusual diagnostic problems not normally encountered in pulsed-power experiments. Special attention was required for us to develop confidence in these diagnostics.

Plans for Future Work

Experiments begun in the summer are continuing through the winter, FY 1991. Integration into the experiment of the recently designed field shapers and emitting rings is now underway, with utilization expected to begin in November 1990. This investigation will teach us to control the electron-beam position, current, and voltage in the device. Knowledgeably varying these parameters is a fundamental requirement for tuning the amplifier gain and stability.

Following completion of these electron-beam optics studies during the winter, FY 1991, we will design and construct the rf amplifier circuit. We have chosen an operating frequency of 1.3 GHz for this proof-of-principle experiment because of the availability of numerous rf input drivers at this frequency. Designing of the amplifier hardware includes several steps. The first of these is the evaluation of alternative design concepts, such as the choice between a monolithic integral device, in which the stages of operation are merged, or a discreetly staged device, which simplifies progressive improvement at the expense of added size and parts. We have decided on the staged device, which is illustrated in Fig. 9.10. Other issues include the merits of alternative input coupling schemes, such as iris or loop couplers, and alternative rf-extraction geometries, either in the axial or radial direction. This activity has been ongoing since the start of the program and will come to fruition in FY 1991.

In addition to the systems issues mentioned above, preliminary computer code modeling of the structure with the 3-dimensional electromagnetic code MAFIA has been performed. MAFIA modeling, in conjunction with experimental cold testing of simulated rf structures, will enable us to examine alternative input and output structures. Such a combined computational and experimental effort can guide the fine adjustment of structures, thus minimizing reflected energy and the conversion of rf into unwanted modes.

The first stage consists of an azimuthally periodic wall boundary in a resonant cavity with cylindrical symmetry. The helical electron beam now being developed will be injected into this cavity. The rf is injected by a loop or iris coupler, establishing a standing wave in the cavity which velocity modulates the rotating electron beam. By designing the cavity to be beyond cutoff for axial rf propagation, the rf is contained in this structure.

The beam, now with an azimuthal-velocity modulation, is transported by the axial magnetic field through a smooth, cylindrical section where azimuthal spatial bunching of the beam develops through the negative mass instability. This instability is started by a small initial spatial bunching induced by the original velocity modulation originated in the input cavity. Adjustment of the length of this drift section will optimize the degree of spatial bunching achieved at the end of the transport.

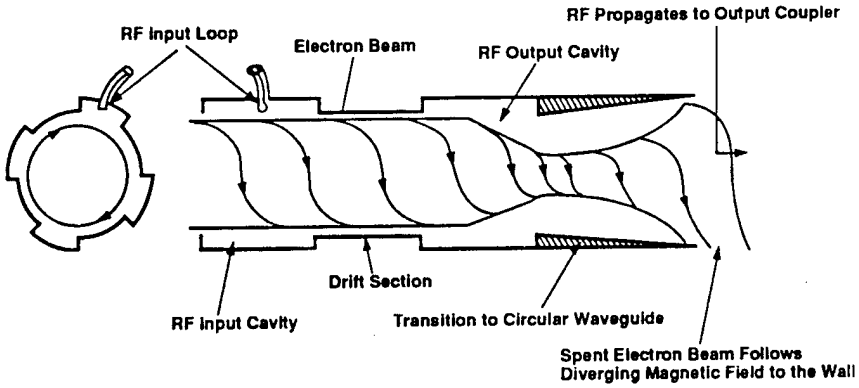

Figure 9.10. Conceptual layout of a LOG amplifier.

Downstream of the transport section, the beam enters a second periodic wall structure which converts the energy of the rotating, spatially bunched, beam into rf standing wave energy. This energy is then coupled into waveguides through either an axial or side-extraction coupler. A mode converter would pipe the output rf into an array of rectangular waveguides.

We have evaluated a number of alternative techniques to extract the rf into rectangular waveguides. Two of these are now under serious final consideration.[8,9] Both techniques first convert the resonator-mode pattern into the TE_{10} circular waveguide mode.[10] In the first scheme, this mode is converted by a gradual geometric transition into several rectangular waveguides operating in TE_{10} mode with a structure called a Marie transducer. The alternative extraction approach, called simply a coupled transmission-line transducer, is to couple from a slot at one position, or a series of positions on the wall of the circular waveguide into the narrow wall of rectangular waveguide, operated in the TE_{10}. By adjusting the axial length of the slot connecting the two waveguides, essentially all of the power in the fundamental mode of the circular waveguide can be transferred to the rectangular waveguide.

Evaluation of amplifier approaches is ongoing, with initial hardware designs expected to be completed in the summer, 1991. During the final year of the program we will merge the staged elements we have described above into an integrated amplifier for characterization. The rf input drive for the amplifier will be one of several 1.3-GHz sources we have available at power levels from 5 kW to 10 MW. Having such a large range of input powers will enable us to examine the gain linearity over a very wide range. Since the device is designed with discrete stages which are easily replaceable, we will be in a position, following the completion of this IRP, to shift operation of the device to other frequencies, thus fitting the needs of programmatic requirements which arise from the availability of this new frequency-flexible device.

Pulsed Power Research and Development

Wideband Pulse Capability

The wideband electromagentic pulse environment (WEMPE) capability for producing ultra-wideband video pulses has expanded to include a portable unit capable of 10 kV and 5-ns pulses with a rise time of ~150 ps. This unit can be repetitively pulsed at up to 5 kHz continuously, and at diminishing burst times up to 15 kHz. This pulser has been used to drive transverse electromagnetic test cells and a large guided wave impulse antenna called "JAWS." The "JAWS" antenna is shown in Fig. 9.11. At 10 m from the antenna, the radiated field has been measured to be ~1 kV/m peak with a rise time of 700 ps. The pulse sharpening technology used in this pulser was slower than what is currently available, so it should now be possible to make the rise time considerably faster. A wideband ridged-guide antenna smaller than "JAWS" has been evaluated for both microwave and fast rise time electromagnetic pulse (EMP) efforts. The incorporation of this new antenna will considerably miniaturize the overall system.

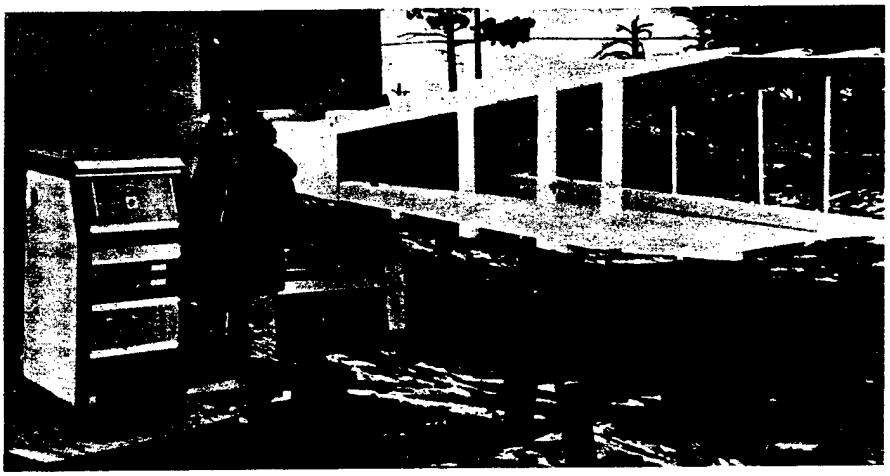

Figure 9.11. The "JAWS" wideband electromagnetic wave launcher.

The most recent design modification to the ridged-guide antenna is intended to achieve higher voltage operation. This modification has resulted in an antenna that covers the 100-MHz to 2-GHz frequency band for microwave pulses and also transmits fast rise time pulses with 10-kV peak voltage and a 250-ps rise time.

BANSHEE Modulator

The BANSHEE pulser is a thyratron-switched high-power modulator that extends the performance of current klystron-type modulator technology beyond the state-of-the-art to the megavolt and kiloampere level. BANSHEE was developed by AT-9 with help from CLS Division. It is engineered to be capable ultimately of routine operation at 5 Hz, 10 GW (1 MV, 10 kA) with a source impedance of 100 Ω in microsecond pulses. BANSHEE is well on its way to achieving the design specifications, and improvements are being made continuously. This pulser represents a unique capability that does not exist elsewhere in the US.

The BANSHEE design consists of four parallel lumped-element Blumleins switched by two high-power thyratrons. The output of the Blumleins drives a 10:1 step-up transformer to supply the hundreds of kilovolts needed for microwave source development. Until very recently, only one thyratron existed at Los Alamos National Laboratory (LANL), which is

why the microwave tube development to date has used a spark-gap switch.

BANSHEE is currently operated routinely at 500 kV, 5 kA, 2.5 GW, 1.5-μs duration in single-shot mode with an explosive field-emission diode load, either magnetized or unmagnetized. BANSHEE has been successfully operated during the last year for testing two relativistic electron-beam driven microwave sources: a relativistic klystron amplifier and a vircator. The modulator has been operated in the single-shot mode with the switching being done with a high-current spark gap while awaiting delivery of the second of two thyratrons. Pulses have been supplied to a field-emission diode at 450 kV producing an electron beam of 7–10 kA with a duration of ~1 μs. The peak power in this electron beam is about 4.5 GW.

In the spring of 1990, we achieved repetitive operation with one thyratron at 5 Hz into a resistive load. This accomplishment demonstrated that BANSHEE can be capable of routine operation at the 5-GW level at rep-rates of up to 5 Hz for several hours at a time. Over a 2-week period, approximately 250,000 shots were fired with this tube. The highest level of performance attained was 70 kV at 73 kA peak at a 1-Hz rate. This translates to a BANSHEE output of 700 kV and ~3.5 kA on the secondary of the output pulse transformer. With the addition of the second thyratron, the output current would be ~7.0 kA. The tube was also run at a 5-Hz rate and achieved 57 kV anode voltage and 61 kA peak current.

The key element of the system which facilitated this performance was the installation of a new thyratron switch developed by English Electric Valve specifically for this test (funded by the Strategic Defense Initiative Organization). This thyratron enabled us to operate at up to 2.5 GW, 5 Hz, at a final output impedance of 200 Ω. Permanent operation at these repetitive performance levels is planned for the fall, 1990, when two of these thyratrons will be incorporated into the BANSHEE pulse-forming network. The use of two of these thyratrons in parallel will enable 100-Ω operation at 5–10 GW and up to 5 Hz.

Vulnerability, Lethality, and Effects (VL&E) Testing

Summary

The VL&E Section was created this year in response to the growing amount of electromagnetic effects testing work which has come to AT-9. The Section is responsible for planning, executing, and documenting electromagnetic coupling tests for various sponsors. Data processing and analysis is an additional charter shared with X-10. The electromagnetic coupling tests provide AT-9 with the opportunity to continue the development of ultra-wideband video pulse sources (WEMPE pulsers), plus the contribution of critical coupling data to national committees such as the System Effects Assessment Team and the DOE Tri-Lab (Sandia, Livermore, Los Alamos) Committee. During the course of FY 1990, the VL&E Section within AT-9 conducted three testing programs in which one program investigated the coupling of HPM radiation into a contemporary Army antitank mine. The remaining two programs investigated the coupling of ultra-wideband electromagnetic pulses to a mobile command post and a complex, highly integrated field radio.

Mine Testing

Two years ago, AT-9 contracted with the US Army to perform an HPM coupling experiment on one of their robust antitank mines. The test would utilize the existing 1300-MHz high-power (20 MW) klystron source in Building MPF-14 in the AT Division complex at TA-53. The actual testing was fairly straightforward, but the pre-test preparations were nontrivial. One of the most challenging parts of this program was the construction of a device to simulate the various linear and rotational accelerations necessary to activate the arming mechanism within the mine. (This arming mechanism then activates the internal electronics for sensing the target and detonating the mine.) Personnel for AT-1 and MST-DO developed the arming device.

The toughest requirement for designing the arming device was the necessity to activate the electronics, remove the mine from the arming device, and position it within the test chamber before the electronic sensor began working. Less than 1 minute was available to perform these tasks. Once the sensor began working, any motion of the mine would result in the sensor generating a detonate signal and detonating a small primer charge (< 1 gram of high explosive). During microwave irradiation, the explosive charge served as an audible indicator that energy had been coupled into the electronics, possibly upsetting the logic used to sort real targets from decoys. Once the arming device was built and checked out, the testing proceeded very quickly, and the data gathered followed predictions made by staff at Livermore and Los Alamos.

This was a great achievement because it marked the first time that analytical calculations on HPM coupling to a fielded system had been corroborated by experimental work. This has led to a proposal to conduct a follow-up test on the same mine at another microwave frequency that has been shown analytically to have much better coupling to the mine. This next test will allow AT-9 to continue development of the LOG by using it as the HPM source for the test, with weaponization a final goal.

Field Testing of a Command Post and Communications Equipment

The data acquired during the electromagnetic coupling tests described in this section have been incorporated into a transfer-function database that is available to weapons designers so that they can tailor their weapons' output to capitalize on electromagnetic frequency coupling windows that exist on that particular system. Both tests were

conducted at the AT-9 Antenna Test and Calibration Range located at TA-49. This range is a 1-km-long area void of structures which would interfere with the propagation of electromagnetic energy.

The Test Range features a mobile instrumentation van which houses the data acquisition systems and the sources which drive the antennas, a commercial log periodic dipole (LPD), and a custom AT-9-built wave launcher known as "JAWS." These items, along with the mobile command post under test, are shown in Fig. 9.12. A Hewlett-Packard 8753B Network Analyzer, when connected to the LPD, generates broadband continuous-wave sweeps that measure the transfer function to a particular test point (an internal node of an electronic circuit or system under test). This data can be used to determine if a test point can be damaged by conventional or nuclear EMP. The "JAWS" antenna can be connected to a compact 10-kV pulse generator to create an ultra-wideband (frequency content up to 1.2 GHz) video pulse. The video pulse can be used to confirm the calculations done on the network analyzer data because the video pulse couples up to 1000 times as much energy into the same test point and will drive the natural resonant frequencies of the system under test. These frequencies and their amplitudes can be compared to the data collected by the network analyzer. Whereas the network analyzer collects data in the frequency domain, the ultra-wideband pulse generator collects data in the time domain. The frequency data and the time domain data can then be cross correlated through the Fourier transform. This data can also be used by the same committees identified in the "Mine Testing" earlier in this report.

The command post and the field radio were tested in several configurations with the most significant being the power on/off configuration. Taking data on a test point when its electrical power is off reveals the passive impedance of the circuit attached to the test point; however, when the power is turned on, active elements within the circuit can display nonlinear behavior and result in a large increase or decrease in the circuit impedance. The electromagnetic coupling community has always held the belief that the power on/off condition did not affect the coupling impedance at frequencies above 1 MHz but has never collected such data to confirm the belief. The data acquired in the recent testing has provided us an opportunity to analyze this aspect of coupling. Our data has shown that the power-on condition does not greatly change the circuit's impedance, and, therefore, does not significantly change the potential for damage. However, the tests revealed that when a system is powered up, the coupled pulse propagates through the system as an errant signal resulting in upset of the system. This could create an electronic condition known as "latch up," where a digital system achieves a state from which it cannot recover unless there is a complete power down and reboot of the system.

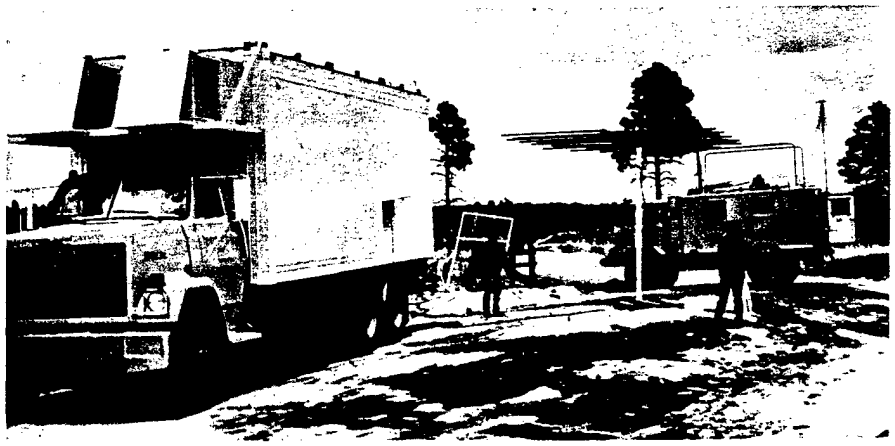

Figure 9.12. Electromagnetic vulnerability and effects testing at the AT-9 Antenna Test and Calibration Range located at TA-49. Shown is the mobile instrumentation van containing the microwave and wide bandwidth diagnostics, the LPD antenna, and the mobile command post under test.

Future Plans

Additional testing of more mines is currently under consideration by the Army and should be funded if budget cuts are not too deep. The final phase of testing the mobile command post will commence in January 1990 and will involve exposing the command post to the various electromagnetic pulse environments generated at the Defense Nuclear Agency's Advanced Research Electromagnetic Pulse Simulator Facility at Kirtland AFB in Albuquerque. The data acquired in this test will provide the final data necessary to confirm current extrapolation techniques used to scale low-level responses to high-level environments. Additional smaller effects tests will be performed to continue the development of ultra-wideband video pulsers and the appropriate antennas to propagate the new waveforms.

Microwave Diagnostics Development

AT-9 is actively involved in the development of state-of-the-art microwave diagnostics hardware and software to support ongoing microwave source development and field-testing programs within the group. These diagnostics must accurately characterize a variety of signals, ranging from high rep-rate, short-lifetime impulse radar signals to high-power single-shot microwave signals. A recent project

resulted in the development of the automated microwave instrumentation (AMI) system.

The AMI system was designed to be a user-friendly and comprehensive system, capable of performing measurements and characterization of any existing high-power microwave source while in the field at a remote location. This specification led to a 10-channel recording system coupled to a receiving antenna array. Each channel has a 1-GHz acquisition bandwidth for single-shot events, so that 10 channels can accurately monitor a 50-MHz to 10-GHz frequency band. This bandwidth also allows capture of subnanosecond width, impulse type signals. Each channel makes use of video-scan conversion hardware and custom, in-house software to allow single-shot data capture at a 10-shot-per-second rate. This repetitive, single-shot (i.e., nonsampling) capability is needed to accurately monitor the overall performance of many current high-power microwave sources, whose power output and freqeuncy may vary considerably from shot to shot. After the data is stored, corrections are performed to deconvolve the effects of cables, filters, and all other frequency dependent or nonlinear components in the signal path. The corrected data can then be displayed or printed for further analysis. A complete microwave calibration system is included with the AMI package to perform absolute phase and amplitude calibration measurements while in the field. A state-of-the-art microwave network analyzer serves as the cornerstone for this calibration setup.

The complete AMI system is installed in a 40' semitrailer for transfer to remote measurement sites. Upon arrival at the site, the measurement antennnas are unloaded and erected, signal cables are routed, and measurements can begin. The complete system was delivered in August 1990 and performed measurements in the field through September 1990. Currently, the AMI sytem is in use at LANL.

Antenna Design, Analysis, and Testing

AT-9 has improved its capability to design and test various antenna structures during the past year. We have an on-going program to design a broadband antenna system and to design wideband antenna and feed systems for our various rf and wideband pulse generators.

Antenna Modeling

A computer code has been acquired to model antennas and predict performance in free space as well as in the presence of surrounding structures, such as buildings. This past year marked the implementation of the GEMACS (General Electromagnetic Model for the Analysis of Complex Systems) antenna code in our group. This code can solve electromagnetic radiation and coupling problems using the method of moments, the geometric theory of diffraction, and finite difference techniques. Output options include a 3-D plot of the physical structure, the electric field in the far or near field, and the current distribution on the structure as well as input impedance at the drive point. Antennas that have been investigated and modeled include the LPD, the "bow tie," the cylindrical dipole, the asymptotic conical dipole, the ridged horn, and a parallel plate wave launcher. The ability to model nondispersive antennas (an antenna that faithfully reproduces the rf envelope applied to it) is of particular interest since some of our high-power video pulse generators have wideband spectral content.

In the coming year, broadband arrays will be modeled and designed along with a continuing investigation of nondispersive structures. A time domain code will be added to assist with this effort.

Broadband Antenna System Development

The goal of this effort is to build an antenna system with a 20-MHz to 550-MHz bandwidth capable of radiating several hundred watts of power, and to deliver the system in a short time frame. Due to the compressed schedule for this effort, commercial off-the-shelf components were used as much as possible. Several commercial broadband antennas were obtained and evaluated. These included a high-frequency log periodic, a high-frequency "bowtie", and a broadband horn structure. Radiation patterns were obtained for these antennas at the TA-49 antenna range using our mobile instrumentation laboratory equipped with network analyzers and high-speed digital waveform analyzers.

The system includes a novel broadband high-power (100 W) solid-state rf switch. The switch permits connecting two medium bandwidth antennas to a frequency-agile source to achieve a radiating bandwidth greater than either antenna has alone. Frequencies between 20 MHz and 550 MHz can be connected to the appropriate antenna with a switching time less than 1 ms. Isolation is greater than 55 dB and insertion loss less than 0.05 dB.

Future Directions

The development of the next generation of very high-power microwave tubes requires the advancement of technologies and physics on several fronts simultaneously. We need electron guns with the ability to repetitively generate intense, well-controlled beams for pulse durations of at least 1 ms. We also need to understand the beam physics associated with these space-charge dominated beams. Finally, we need to understand the mechanisms of rf breakdown in high-power structures.

Electron-Beam Diode and Electron Gun Development

Microsecond, rep-rated high-power rf sources will require major improvements in electron-beam diode performance to fully realize their potential. The current, nearly universal use of explosive emission cathodes in HPM sources limits the degree of control

over their performance because of electrode plasma closure and impedance collapse.

Thermionic Cathodes

The microsecond-duration electron guns used in the conventional microwave tube industry use thermionic emission or secondary emission cathodes. The best of the modern designs are believed to be capable, though marginally, of operation at the level of several guns and several kiloamps. While they should be able to provide the electron-beam current and beam quality required for higher-power microwave sources, only very limited experience with such cathodes (at truly high powers) has been acquired anywhere in the HPM community. Considerable additional experience will be needed to take full advantage of this technology. This is particularly true in regards to practical vacuum quality requirements, and cathode manufacturing and operation techniques which maximize cathode lifetime and facilitate the development of successful designs applicable to HPM needs.

AT-9 has been anticipating the needs of thermionic designs, has engineered BANSHEE to render feasible the inclusion of a thermionic cathode, and has maintained contact with such manufacturers as Varian and Spectromat, leaders in high-current thermionic cathode capability. When the need arises to implement a thermionic design, Los Alamos facilities are ready, requiring lead time only for the manufacture of the cathode assembly. Design specifications and the delivery time for such a device have already been discussed with the manufacturers.

Alternatives to Thermionic Cathodes

There are alternatives to conventional thermionic cathodes which offer the promise of simpler and less expensive designs. One of these is the Spindt cathode, developed at the Stanford Research Institute, now a product line under development by Coloray Display Technology. The other cathode technology is a plasma-enhanced lanthanum hexaboride cathode, under development by John De Groot at the University of California at Davis.

Spindt cathodes, which use microelectronic fabrication techniques to fashion micron-scale needle-shaped cathodes, emit electrons by Fowler-Nordheim emission with no plasma formation. This technology is at a stage where research can be performed on modulators such as BANSHEE.

The plasma cathodes being studied by UC Davis operate by retaining a low-pressure gas along the surface of the cathode. The gas is ionized by the low-density electron beam, forming a Langmuir sheath or double layer near the emission surface. This greatly raises the electric field there and leads to ion bombardment of the lanthanum hexaboride surface, heating it above the normal operating temperature of 1600°C to perhaps 2000°C. Both the higher temperature and the larger electric field raise the limiting current from the cathode to as much as 500–1000 A/cm^2. The high-current density achievable with this plasma cathode is very attractive for allowing small cathode structures to be constructed for more compact HPM sources than can be achieved with the state-of-the-art in conventional-dispenser cathode thermionic designs. These devices are at the stage where a prototype device could be installed in BANSHEE for evaluation.

Los Alamos has been in close communication with personnel in both of these programs for several years, and believes that both approaches offer promise for inclusion in future HPM sources. We have received a statement of interest from Coloray to collaborate in testing their cathodes, and we are interested in doing so if programmatic interest is expressed within the HPM community. A similar collaborative interest exists with the UC Davis team. Our pulse power source, BANSHEE, is ideally suited for testing the performance of these devices. Moreover, we can capitalize on the diagnostic resources of the many, diverse research programs at Los Alamos to characterize cathode performance. Such diagnostics include fast multiframing and streak cameras for testing temporal and spatial emission uniformity, and surface physics examinations of the cathodes after periods of use (to identify the nature of performance degradation with use and recommend ways to improve it).

References

1. M. Friedman, J. Krall, Y.Y. Law, and V. Serlin, "Externally Modulated Intense Relativistic Electron Beams," Journal of Applied Physics 64, 3353-3356 (1988).

2. M.V. Fazio, R.M. Stringfield, D.G. Rickel, J. Kinross-Wright, and R.F. Hoeberling, "High Power Microwave Source Development at Los Alamos," Fifth National Conf. on High Power Microwave Technology, West Point, N.Y., June 10-15, 1990, Los Alamos National Laboratory document LA-CP-90-235.

3. R.M. Stringfield, M.V. Fazio, D.G. Rickel, T.J.T. Kwan, A.L. Peratt, J. Kinross-Wright, F.W. VanHaaften, R.F.Hoeberling, R. Faehl, B.C. Carlsten, W.W. Destler, and L.B. Warner, "High Power Amplifiers For Accelerator Applications: The Large Orbit Gyrotron And The High Current, Space Charge Enhanced Relativistic Klystron," 1990 Linear Accelerator Conference, Albuquerque, NM, Sept. 10-14, 1990, Los Alamos National Laboratory document LA-UR-90-3099.

4. A.L. Peratt and T.J.T. Kwan, "Simulation of the Relativistic Klystron Experiment at Los Alamos," Fifth National Conf. on High Power Microwave Technology, West Point, N.Y., June 10-15, 1990.

5. W. W. Destler et al., "High-Power Microwave Generation from Large-Orbit Devices," IEEE Trans. on Plasma Science 16 (2) 71 (1988).

6. Y. Y. Lau and L. R. Barnett, "Theory of a Low Magnetic Field Gyrotron (Gyromagnetron)," International Journal of Infrared and Millimeter Waves 3, 619 (1982).

7. J. Y. Choe, K. Boulais, V. Ayres, W. Namkung, and H. Uhm, "Preliminary Study of Cusptron Amplifier," Microwave and Particle Beam Sources and Directed Energy Concepts, SPIE 1061, 132 (1989).

8. S. S. Saad, J. B. Davies, and O. J. Davies, "Analysis and Design of a Circular TE01 Mode Transducer," Microwaves, Optics, and Acoustics 1 (2), p. 58.

9. S. E. Miller, "Coupled Wave Theory and Waveguide Applications," Bell System Journal, 661 (1954).

10. S. E. Miller, "Waveguide as Communications Medium," Bell System Journal, 1209 (1954).

AT-10
GTA Installation, Commissioning, and Operations

Oscar Sander, Deputy Group Leader; David Schneider, Group Leader

Introduction

Group AT-10 has a broad range of capabilities and responsibilities focussing mainly on supporting the neutral particle beam (NPB) program. The group provides the hardware integration, installation, and checkout and the alignments for the ground test accelerator (GTA) components. It directs the planning, execution and analysis of the NPB application and GTA commissioning experiments. AT-10 designs, develops, and operates injectors capable of producing very intense ion beams for injection into the GTA radio-frequency quadrupole (RFQ). In support of NPB and other projects such as accelerator transmutation of wastes (ATW), the group is developing injectors for continuous-wave (cw) operation. AT-10 also provides the GTA facility support, such as cryogenic cooling, equipment and personnel safety interlocks, building power and water, equipment and signal wiring, and vacuum systems, as well as operator and safety training. A small fraction of the group's effort is directed to other small projects.

During the past year, AT-10 concluded the accelerator test stand (ATS) experimental program with the successful testing of a prototype 5-MeV H⁻ single-beam funnel. This single-beam demonstration explored the physics and engineering issues of a two-beam funnel. ATS is now moth-balled. The GTA injector was completed, commissioned, and mated to the RFQ in time for the initial RFQ beam tests. AT-10 provided the majority of the support systems and services for the first two GTA experiments, the commissioning of the injector (1A) and the commissioning of the RFQ (1B). In addition to the above-mentioned facility support, the group also provides the interface with most of the craft services and has primary responsibility for the two busiest AT division laboratory buildings. The detailed experimental plan for experiment 1B was completed and was the basis of the preparation for experiment 1B, which will start in the beginning of FY 1991. The pulsed

version (8X) of a cw surface plasma source (SPS) was operated. This operation demonstrated designed beam current and emittance, improved power, and gas efficiency. The 8X source has dimensions approximately eight times that of the SPS ATS source and incorporates improved engineering and cooling. In collaboration with Grumman Space Systems, we designed a cw version of the 8X source. Construction of the source will begin in FY 1991. A section of AT-10 operates the High-Power rf Structures Laboratory (HPSL) and has tested and conditioned radio-frequency (rf) structures for the beam funnel experiment, for cryogenic operation, and for evaluation of surface-preparation techniques that could improve rf efficiency at cryogenic operation.

Work continued at the one full-time equivalent level on two projects. A diagnostic, which uses photoabsorption and photodetachment, was assembled to measure the temperature and density of the H^- and H^0 components inside the source discharge. This measurement reveals the ultimate realizable brightness of the ion source and provides insight into the H^- production and transport mechanisms within the plasma. Initial measurements of the H atom density and temperature were made using this diagnostic. Design of the dual-axis radiograph hydro-test (DARHT) accelerator-beam transport continued using upgraded versions of injector/accelerator design TRACE and SCHAR codes.

Background

In mid-November 1989, group AT-2 was eliminated and AT-10 was formed in its place. A decade of beam experiments on the ATS came to an end with the conclusion of the funnel experiment, and new functions were needed to support the GTA. For the last two years of its existence, AT-2 had been a part of the GTA program, with primary responsibility for ion-injector development and accelerator experiments on both GTA and ATS. After the reorganization, AT-10 was given explicit responsibility for the installation, commissioning, and operations of GTA. The group retained its charter to develop ion injectors. The design, construction, and testing of the 8X source, which began in FY 1989, continued with a physics testing program. The commissioning section of AT-10 acts as the final "customer" for all GTA equipment and systems and has the responsibility of debugging and demonstrating proper beam operation of all GTA accelerating structures.

Achievements

Single-Beam Prototype Funnel

Accelerator concepts for heavy-ion fusion, the transmutation of nuclear waste, and GTA require small-emittance, high-current beams. Such applications include beam funneling in which high-current, like-charged particle beams are interlaced to double the beam current. The first experimental demonstration confirming the dynamics of the funnel principle (with contained emittance growth) began in FY 1989[1] and was completed on ATS during FY 1990. The objectives of this experiment were the control of emittance growth and the successful use of rf deflection and position control with 100% transmission. Figure 10.1 is a schematic of the funnel beam line mounted on separate plates (M1 through M4). A photograph of the funnel on ATS is shown in Fig. 10.2.

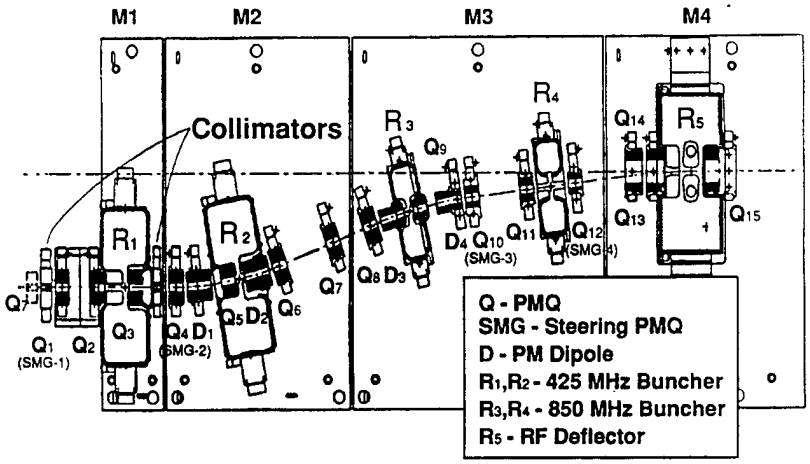

Figure 10.1. Schematic of the funnel beam line.

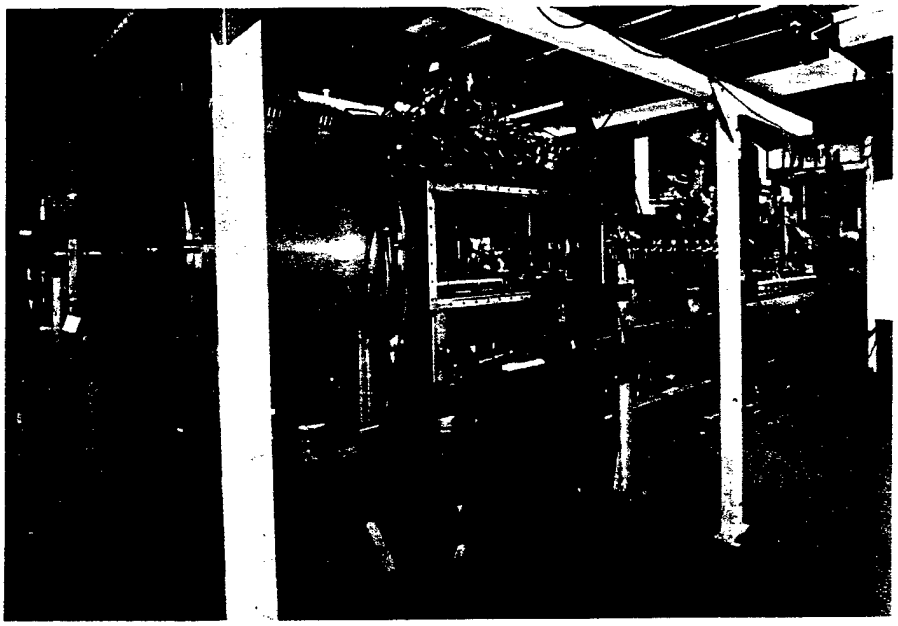

Figure 10.2. Photograph of the funnel on ATS.

Reference 1 gives a description of the beam line and the diagnostics. The diagnostics allowed measurement of beam intensity, position and angle centroids, transverse energy and phase centroids, transverse and longitudinal phase-space distributions. The operation of the M1 components and the characterization of the beam exiting the M1 plate were completed in FY 1989.

In FY 1990, we added the M2 and M3 plates. The steering model was experimentally verified; the model and experiments agreed within measurement errors of ±0.2 mm and ±1 mr. The phase set points of the remaining bunchers were determined using beam loading; the amplitude set points were determined using the laser-induced neutralization diagnostic approach to measure beam energy. We achieved good transmission (~100%) using the steering permanent-magnet quadrupoles (PMQs). The transverse and longitudinal emittance was measured in preparation for injection into M4 with its rf deflector. With M4 installed and the deflector energized, we measured the horizontal beam deflection and the relative emittances ε_x, ε_y, and ε_L as functions of deflector phase and cavity power. At the design deflector gap voltage (as determined by x-ray emission data[2]), the longitudinal emittance and the transverse emittance in the bend plane were minimized by adjusting the rf phase to 60°. At 60° the deflections were measured to be 36 ±2 mr; the simulation predicted a 38.4 mr deflection. Within the experimental error and the 5% uncertainty in the gap voltage, there was excellent agreement between measurement and simulation. The deflection scaled with rf power as expected. The observed ε_L emittance growth was 15–20%, whereas the simulated growth was approximately 5%. However, the simulations were based on the drift-tube linac (DTL) design emittance, which was four times greater than observed. As a result, the 20% emittance growth was not detrimental to the funnel's performance. The final transverse emittance, ε_x and ε_y at the exit of M4 (with optimal buncher and deflector settings), are consistent with simulations and with no growth. In conclusion, the dependence of the beam deflection, the transverse and longitudinal emittances on the deflector amplitude and phase was as expected. The desired amplitude and phase set points were easily determined, and the transverse and longitudinal emittance growth through the ATS single-beam funnel were controlled.

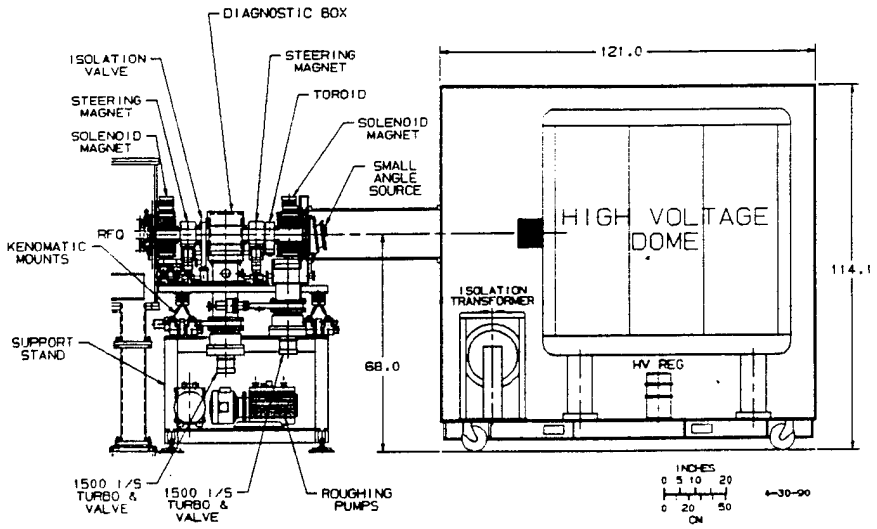

Figure 10.3. Schematic of the GTA injector.

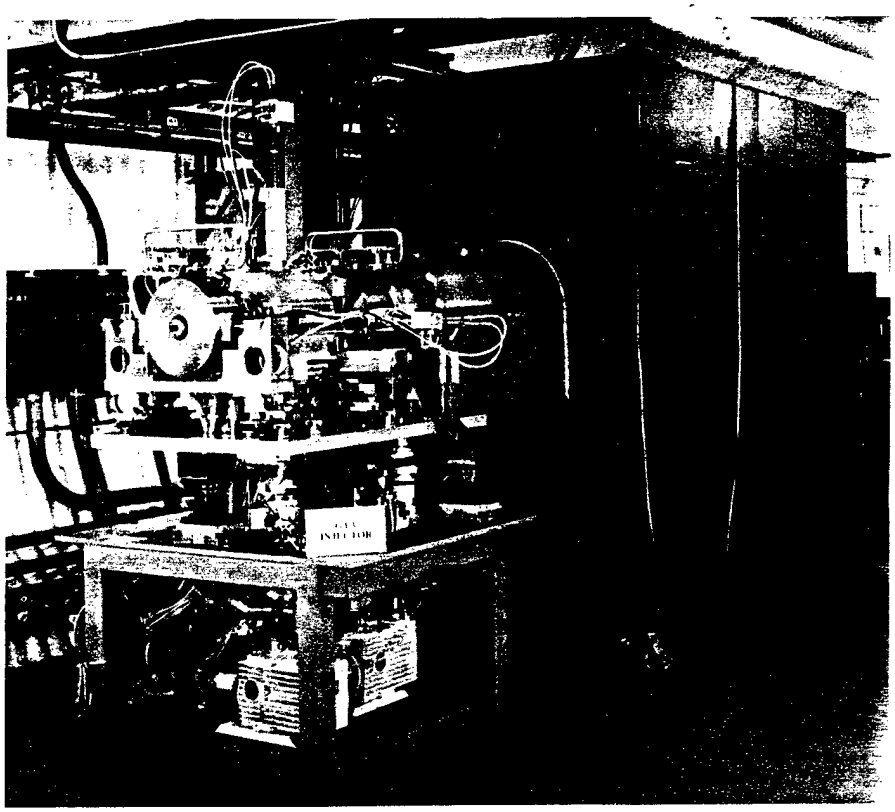

Figure 10.4. Photograph of the injector in the GTA tunnel.

GTA Injector

There were a number of major highlights in the GTA injector program. We moved the partially assembled and tested injector from the Building 18 assembly area to the GTA tunnel in Building 365. Its portable, modular design greatly facilitated this move. The construction of the entire assembly

(source, focussing solenoids, steering magnets, two diagnostic stations, vacuum system, electronic hardware, and control systems) was completed and tested. Figure 10.3 is a schematic of the GTA injector. Figure 10.4 is a photograph of the injector installed in the GTA beam tunnel. To verify and facilitate high-quality beam operation, we completed two sets of emittance scanners, associated data-taking and analysis codes, and calibration checks.

Measurements were taken over the range of discharge currents and extraction voltages of interest to GTA. Using these measurements, we set the ion-source operation parameters to minimize the extracted beam divergence and beam noise and to maximize the extracted current. Both high (~45–50 mA) and low (~12–18 mA) currents were obtained by varying the aperture of the extractor electrode. Using emittance measurements at the intended RFQ entrance, we produced tuning curves of Twiss parameters versus solenoid currents for future RFQ experiments. These experiments showed that the low-energy beam transport (LEBT) was capable of producing the matched Twiss parameters at the RFQ entrance for both low and high currents. Although the measured high-current emittance met the design specification at the diagnostic box (see Fig. 10.3), significant emittance growth was observed at the intended RFQ entrance.

We developed a video diagnostic technique[3] to monitor and characterize the two-dimensional beam-intensity profiles and the local angular divergence of the 25- to 35-keV injector beam. We placed a fluor screen downstream of the first solenoid in the injector's LEBT. A charged-coupled device camera and image-grabber board were employed to observe and record the beam image. The technique provides both real-time viewing of the beam shape and recorded data for further analysis. Figure 10.5 shows the digitized image of a single 35-keV beam pulse when the first LEBT solenoid was set to give a converging beam. To determine the beam profiles and investigate the accuracy of this visual diagnostic, we placed the fluor at the same axial position as the emittance scanner.[4] Figure 10.6 shows the horizontal profile of the data in Fig. 10.5 and the beam profile measured by the emittance scanner. The agreement between these profiles indicates the accuracy and the effectiveness of this visual technique.

Using measurements taken over many beam pulses, the standard emittance-scanner diagnostic provides two-dimensional phase space. By placing a shadowing wire grid upstream of the fluor, we can use the fluor diagnostic techniques to obtain four-dimensional phase-space information in a single beam pulse. Figure 10.7 is a digitized image of the injector beam with a grid of horizontal wires placed 5 cm upstream. For a given shadowing wire size, the relative depth of the wire shadows is related to the local divergence of the beam. After integrating the visual data over the vertical dimension, the local divergence measured by both methods was 6–8 mrads. The visual method did show that the local horizontal divergence had a vertical position dependence.

We incorporated a faster and improved version of the SNOW computer modeling code, which is used for designing our beam-extraction electrodes. The goal of these design studies is to produce a lower-divergence beam with lower beam-current fluctuations.

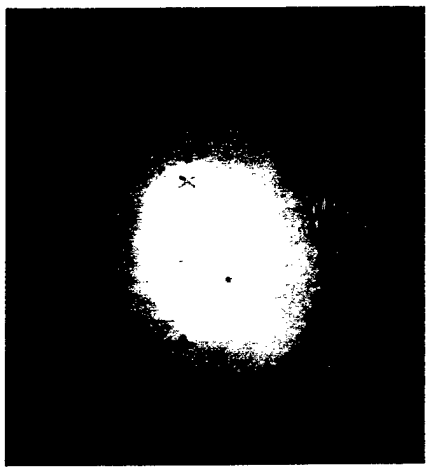

Figure 10.5. Digitized image of a 35-keV beam pulse. Darker colors indicate lower intensity.

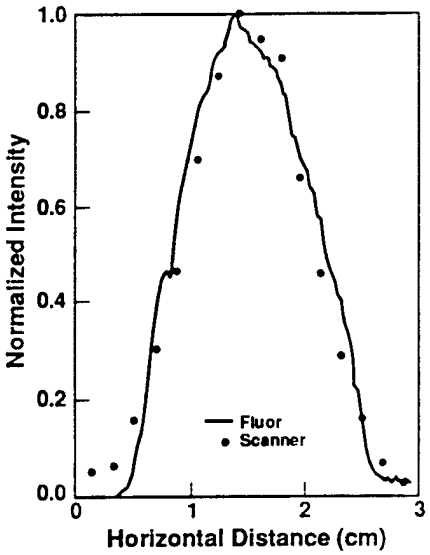

Figure 10.6. Horizontal profile of Figure 10.5 data.

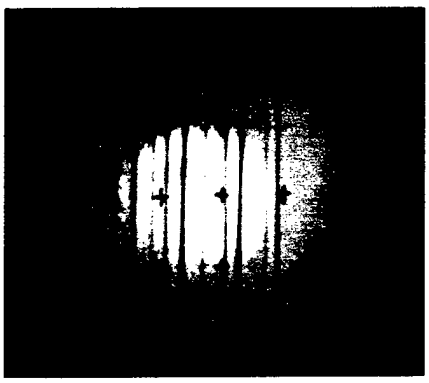

Figure 10.7. Digitized image of beam with upstream grid in place.

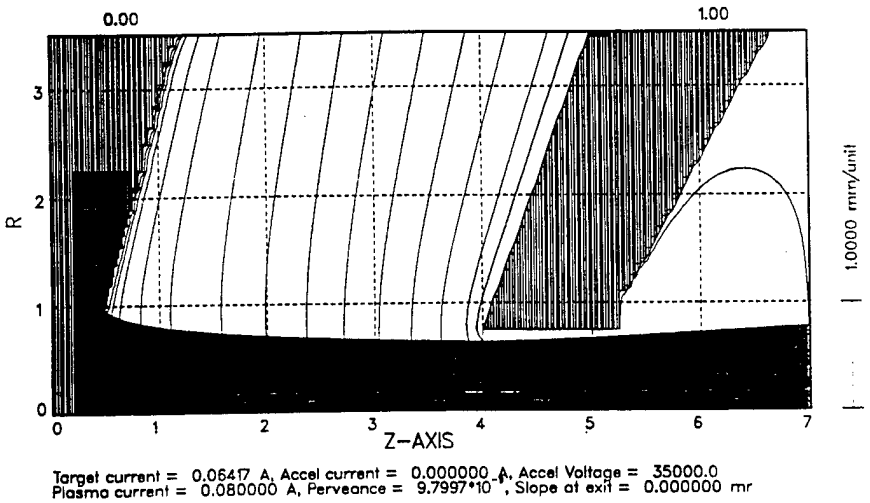

Figure 10.8. Simulated beam trajectories using a new H⁻ extractor design.

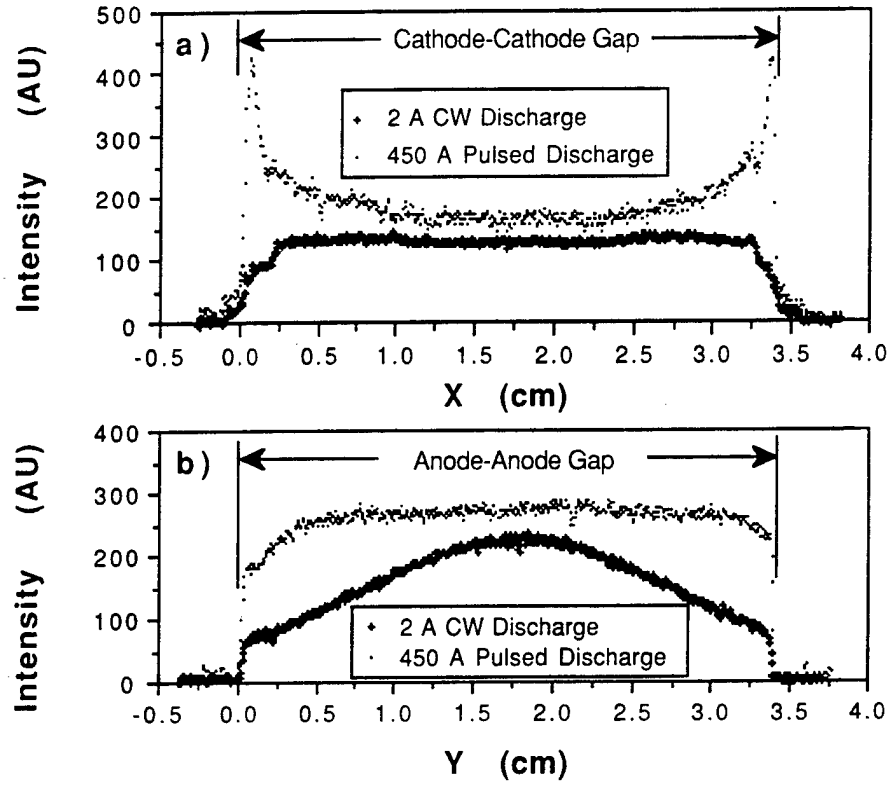

Figure 10.9. Total light emission from H⁻ source plasma region. (a) Emitted light distribution for a 2-A cw discharge (crosses) and a 450-A pulsed discharge (points) from cathode to cathode as measured with the video camera. (b) Emitted light distribution for a 2-A cw discharge (crosses) and a 450-A pulsed discharge (points) from anode to anode as measured with the video camera.

The lower divergence will result in a smaller diameter beam in the first solenoid, with resulting lower solenoid aberrations. Figure 10.8 shows the beam trajectories of a new H⁻ extractor design based on SNOW calculations.

8X Ion-Source Program

We checked the 8X plasma uniformity by measuring the total light emission through a diagnostic slit exposing a narrow strip of the entire discharge region, either from cathode to cathode or from anode to anode. Measurement results for a 2-A cw discharge (crosses) and for a 450-A pulsed discharge (points) are shown in Fig. 10.9a for the cathode-to-cathode measurements and in Fig. 10.9b for the anode-to-anode measurements. For the pulsed case, the discharge is uniform both from cathode to cathode and from anode to anode, with the exception of the near cathode region. In this region, the total light emission is increased because the species densities are higher (Fig. 10.10a and 10.10b). The cesium atoms and ions (Fig. 10.10b) and molybdenum atoms and ions are apparently trapped there by electron impact ionization.[5] Because the 8X source discharge is uniform near the center, the H⁻ emission current density is assumed to be uniform over the centrally-located 0.25- to 0.50-cm-diameter circular emitters used for the 8X source H⁻ beam extraction. Also, because the Cs atoms and ions are trapped near the cathode surfaces, the Cs flow through the emission aperture should be low and the Cs coverage on the cathode surfaces should be maintained at or near the optimum value when the source is operated in the cw mode.

By using the electrostatic sweep scanner to measure the angular distribution of the ribbon beam through the diagnostic slit, the H⁻ ion temperature kT_{H^-} in the 8X source plasma was determined.[6] In the aberration-free

central portion of the ribbon beam, the thermal energy of the H^- ions is, according to the thermal model,

$$kT_{H^-} = \phi_b(\theta_{FWHM}/2)^2/0.69$$

where ϕ_b is the beam energy and θ_{FWHM} is the full width at half maximum (FWHM) of the angular distribution. The kT_{H^-} is 0.18 eV for the 2-A cw discharge and 0.81 eV for the 450-A pulsed discharge. The spatial resolution of this slit-diagnostic technique is sufficient to allow kT_{H^-} to be measured along the whole discharge either from anode to anode or cathode to cathode. These measurements show that kT_{H^-} is uniform from cathode to cathode, but there is approximately a 20% increase from the anode surface with the H_2 gas feed to the other anode surface. The variation of kT_{H^-} with the various source parameters was studied. The dependence of kT_{H^-} on the H_2 gas feed rate is shown in Fig. 10.11a for the anode-to-anode slit orientation and in Fig. 10.11b for the cathode-to-cathode slit orientation. The decline of the temperature with gas flow (or pressure) is presently a result of the H^- ion cooling in collisions with the colder H_2 molecules. The observation that the H^- temperature is lower near the anode surface with the H_2 gas inlet is explained by the data in Fig. 10.11a; the higher the H_2 gas pressure, the lower the H^- temperature. The magnetic field is in the cathode-to-cathode direction. Based on these figures, we conclude that kT_{H^-} is independent of the magnetic field orientation.

H^- Density and Temperature Diagnostic

Work on the H^- density and temperature diagnostic, which began in 1989, continued with the successful operation of the vacuum ultraviolet (VUV) laser. The technique calls for passing a VUV laser beam, which has been tuned to the Lyman-series transition, through the source plasma. The attenuation of the laser beam yields the H-atom density. The H-atom temperature is found by stepping the

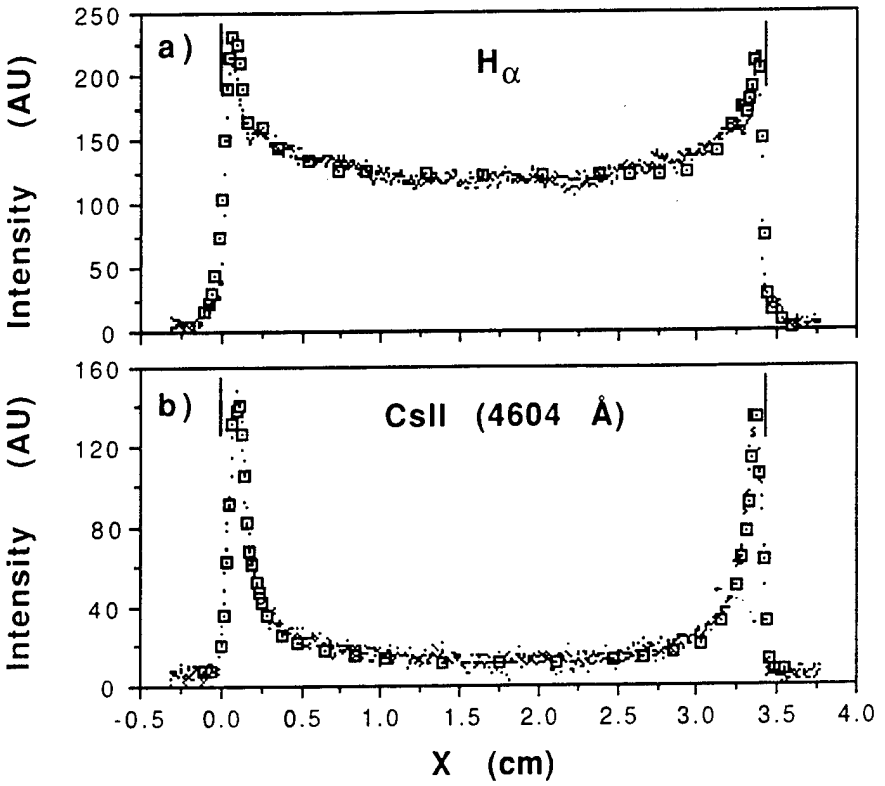

Figure 10.10. Species distribution in plasma region. (a) The emitted H_α light cathode to cathode recorded by the video camera when the filter monochromator is set at 6600 Å (dots). The 1-m monochromator H_α data (squares) are shown for comparison. The monochromator X scale is adjusted to place the peaks at the locations determined from the video camera work. The monochromator intensity scale is adjusted to make the average peak height the same as the average peak height of the video camera measurement. (b) The emitted CsII (4604 Å) light cathode to cathode recorded by the video camera when the filter monochromator is set at 4600 Å. Otherwise the same as (a).

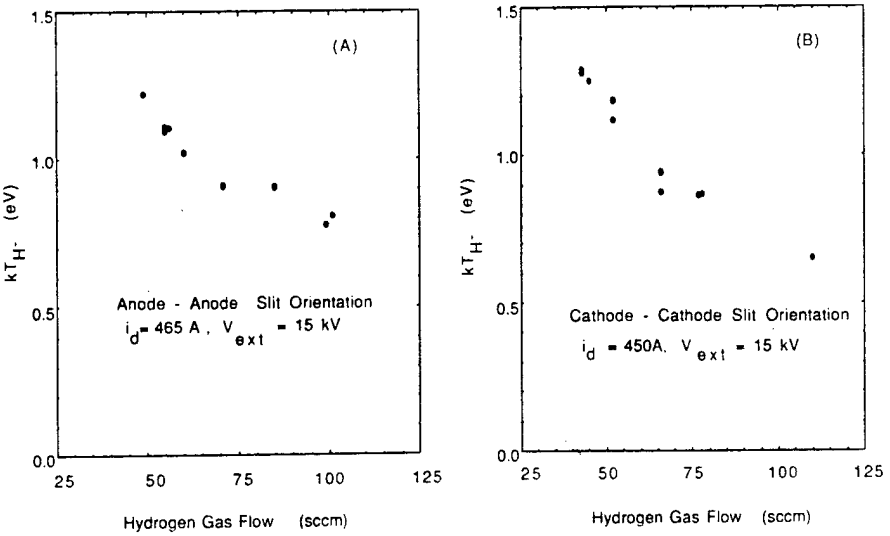

Figure 10.11. Ion temperature dependence on gas flow and position in plasma. Plots of averaged H^- temperatures vs. H_2 gas flow for the (A) anode - anode, and (B) cathode - cathode slit orientations.

VUV laser wavelength across the transition and measuring the Doppler-broadened line width.[7] By passing an intense yttrium aluminum garnet laser pulse through the probed channel, all H^- ions are neutralized by photo detachment. By measuring the H-atom density just after photodetachment and subtracting the equilibrium H-atom density, we reduce the equilibrium H^- density. Figure 10.12 shows the H-atom absorption profile over the Lyman-gamma transition. A Gausian

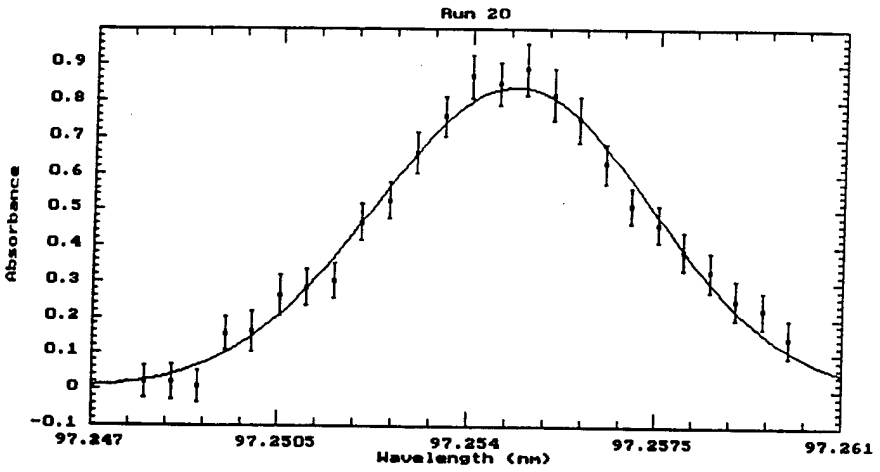

Figure 10.12. H-atom absorption in Lyman-gamma transition.

fit to the data yields a H-atom temperature of 0.66 eV and density of $1.8 * 10^{14}$ cm^{-3}. The system is presently capable of a 10% H-atom density measurement. Recent work is concentrating on improving the sensitivity to better than 1%.

DARHT Support

The DARHT machine will produce two 20-MeV, 3-kA, 60-ns electron-beam pulses from induction linacs. Each linac has 64 gaps of 250 kV. The output beams will be focussed to a 0.5-mm radius at the x-ray target. Solenoidal focussing will transport the beam through each linac and onto the target.

The linac dynamics were studied with the codes TRACE and ETRACE, which were upgraded for relativistic beams with solenoid misalignment. Beam centroid displacement drives deflecting modes in the cavities formed by the accelerating gaps; these modes lead to beam breakup (BBU) instabilities and consequent beam loss and emittance growth. It appears possible to limit BBU by using steering coils on each of the 64 solenoids to achieve an overall beam alignment of < 1 mm. Beam focussing on the target depends on beam emittance and energy spread. Low emittance has been achieved at the 4-MeV source. However, the difficult task for the pulsed power will be obtaining an energy spread of ±2% that computational studies show must be maintained along the machine. The code SCHAR was used to study the aberrations of the final focus lens. The use of a permanent magnet quadrupole may be useful because its small size permits placement closer to the target than is possible for a solenoid lens. Preliminary studies show that if the aberrations are small, the spot size could be halved by using this quadrupole.

High-current induction linacs are prone to BBU because large image currents can excite rf modes. The excitation can be reduced by reducing the impedance of the cells, but impedance measurements of low-Q cells have previously been difficult. Using the two-wire lumped-circuit model,[8] we made impedances of cells with Q~4. The method was verified on cells of known impedance. In collaboration with Lawrence Livermore National Laboratory personnel, we used the measurements to improve the code AMOS;[9] measurements and theory now agree.

High–Power rf Structures Laboratory (HPSL) Results

In support of the funnel experiment, we did considerable work to make the buncher cavities and their rf amplifiers operational. All of the rf drivelines were reconfigured to improve their maximum power transmission without producing radio-frequency interference to the sensitive, nearby beam diagnostics. We conditioned the cavities and, by measuring the end-point energy of the x-ray emission, determined the gap voltage-versus-power for the various cavities.

An experimental program was mounted to determine appropriate surface-treatment procedures for the GTA copper drift tubes, post couplers, and cavities. The method is based on measuring the Q-enhancement factor of a sample as it is cooled to cryogenic temperatures in the transverse electric-mode coaxial cavity. The optimal Q gain was found by following a procedure[10] of annealing, chemical polishing, and final electropolishing. Figure 10.13 shows Q versus temperature for a sample whose Q-enhancement factor is greater than 5.

To study the electric field stability of the envisioned GTA RFQ, we constructed the cryogenic RFQ sparker (CRFQS). This CRFQS has many of the characteristics of the GTA RFQ. During the mechanical assembly of the GTA RFQ, several technical challenges arose which required verification of engineering methods. The CRFQS provided a test-bed for evaluation of these methods. The first challenge was mechanically shifting the RFQ configuration during the temperature cycling for tuning. By measuring the CRFQS frequency versus assembly bolt torque, the required torque was identified which resulted in a stable structure. If the cryogenic cycling distorted the RFQ mechanical structure, dipole fields would most likely be produced. The local fields were measured by perturbing the field through the insertion of aluminum probes; the relative fields were determined by measuring the

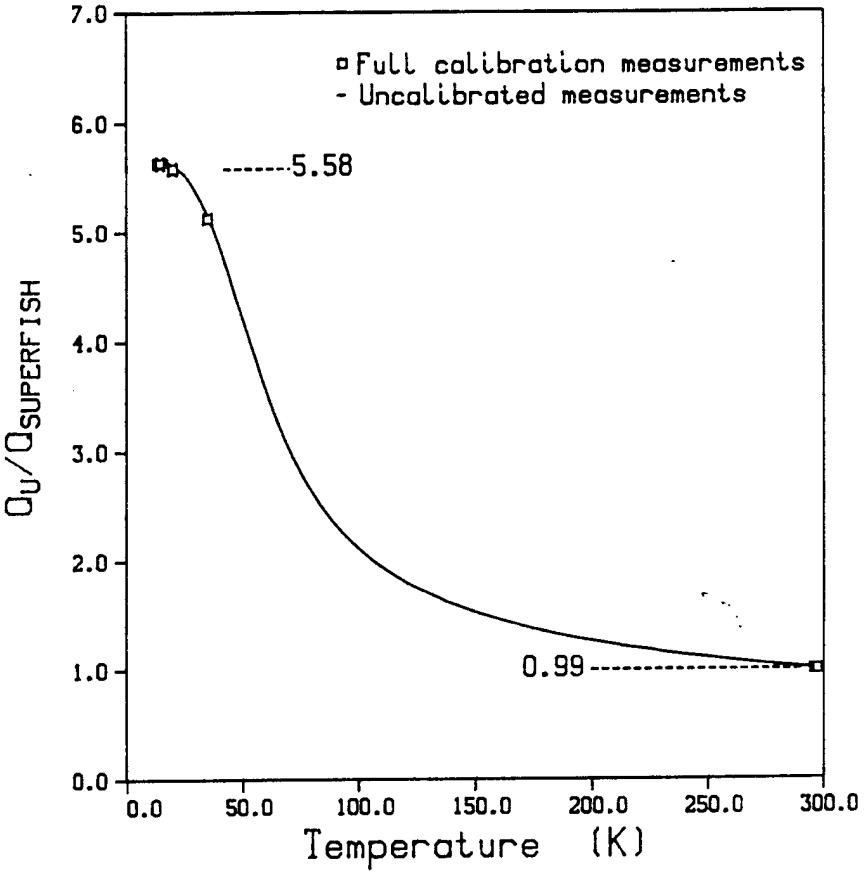

Figure 10.13. Q versus temperature for a sample that has been annealed and chemically polished with Shipley Chem-Polish 14.

corresponding resonant frequency shifts. The results showed that cryogenic cycling had little or no effect on the mechanical structure, because all dipoles fields shifted by less than 0.7%. *In situ* repair of the high-pressure helium coolant connections was also perfected on the CRFQS.

In preparation for the operation of the GTA, we first tested procedures on the CRFQS. The mechanical operation of the slug tuner was verified at cryogenic temperatures on the CRFQS. A method of setting the driveline coupling without perturbing the RFQ field configuration was evaluated and verified to be effective on the CRFQS. High-power conditioning of the CRFQS demonstrated that conditioning of the GTA RFQ can be done at cryogenic temperatures.

After the final field tuning of the GTA RFQ, we made room-temperature perturbation measurements of the GTA RFQ field configuration to verify the long-term stability of the GTA RFQ fields. If there are suspicions of field changes, these measurements can be made while the RFQ remains installed in the GTA beam line. Such field checks were desired but unavailable on the ATS.

Operations Support

The FY 1990 cooling requirements of the GTA program were successfully met by two 750-W helium refrigerators. A newly installed Model 1620S refrigerator became operational in February. The other refrigerator was installed in 1986 and was used to cool the CRFQS test structure to 20 K.

A 40-kW cryo cooling system (CCS) is being built to meet the needs of future experiments whose heat loads

exceed the capacity of a refrigerator. Unlike the compressor-driven refrigerator, which circulates helium through a liquid nitrogen precool heat exchanger and then reduces the gas temperature through isentropic work extraction in two expansion engines, the 40-kW CCS obtains its preliminary cooling through a LN_2/GHe heat exchanger and the primary refrigeration capability from a LH_2/GHe exchanger. Helium gas is first circulated by a compressor between the GTA and the liquid nitrogen heat exchanger until the helium gas temperature is lowered to approximately 80 K. The flow of gas is then redirected through a two-stage liquid hydrogen heat exchanger and the cooling process continues until the helium temperature reaches approximately 20 K.

At the beginning of the 1990, refurbishment of surplus LN_2 tankers was underway and fabrication of the large 40-kW CCS was in process at CVI. Because of the significant safety concerns of storing this amount of liquid hydrogen, there has been extensive documentation and involvement with safety review teams.

Facility Alignment

During the alignment of the various ATS funnel components, M-plates, and diagnostics plate, the theodolite system proved a fast and accurate technique for aligning relatively inaccessible components inside a vacuum tank. We used the theodolite system to map the GTA floor and wall monuments and to install and align the injector, RFQ, and D-plate in preparation for experiment 1B. The cooling apertures on the DTL were mapped for the final machining operation.

Facility Wiring

All the wiring for system control, signal monitoring, and diagnostics for the GTA must be documented. During this year, the program Wireflex (a relational database) was modified and upgraded to meet program needs for covering all wiring documentation. The database provides all information starting at the beam line device and includes the devices, connections, types of connectors, wire manufacturers, conduits, and cable tray paths. Over 20,520 wires have been recorded covering the RFQ and intertank matching section (IMS) functions. These wires represent 25 to 30% of the expected GTA entries.

Future Plans

The injector section of the group plans to set up and operate a cw (or dc) high-current test stand to develop new high-brightness ion sources and LEBT systems. Such a test stand will have application to the next phases of the NPB program and to other programs such as ATW and perhaps the accelerator production of tritium (APT). The injector section will continue providing beams for GTA with the required reduction of beam-current fluctuation and emittance and will test the cw 8X source when its fabrication is completed.

The beam experiments section of the group (responsible for installation, commissioning, and operations) will have an increasing involvement in GTA as more hardware becomes available for installing and testing with beams. The commissioning of the GTA RFQ, IMS, and tank #1 of the DTL is expected during FY 1991. Other developments will continue, in an effort to enhance the group's ability to tackle new ion accelerator projects.

Major cryogenic system support in the coming year will include providing flowing cryogens for all beam experiments, off-line testing of new accelerating structures, recertification and modification of a surplus 28 000-gallon LH2 Dewar, construction of a new equipment building, and installation and check-out of the entire new CCS.

The facility support section of the group will continue the installation and check-out of new GTA rf structures and diagnostics. This section will characterize and condition the IMS buncher cavities and DTL modules during FY 1990. Addition of wiring and power needs will be met as the installation of GTA progresses.

References

1. Accelerator Technology Division Annual Report, LA 11636-PR.

2. G. O. Bolme, Proceedings 1990 Linear Accelerator Conference, September 10-14, 1990.

3. K. Saadatmand, J. D. Schneider, C. Geisik, and R. R. Stevens, Jr., "Beam Structure Studies of Low-Energy Ion Beams," Eleventh International Conference on the Application of Accelerators in Research and Industry, November 5-8, 1990, LA-UR-90-3312.

4. Paul Allison, Joseph Sherman, and David Holtkamp, "An Emittance Scanner for Intense Low-Energy Ion Beam," IEEE Transactions on Nuclear Science, NS-30, No.4, 204–2206 (August 1983).

5. H. V. Smith, Jr., P. Allison, K. Saadatmand, and J. D. Schneider , "Spatial Distributions of the Emitting Species in a Penning Surface-Plasma Source," Proc. 2nd European Particle Accelerator Conf. (Editions Frontieres, Gif-sur-Cedex, 1990) pp 659-661.

6. J. D. Sherman, H. V. Smith, Jr., C. Geisik, and P. Allison, "H^- Temperature Measurements by a Slit Diagnostic Technique," Proc. 1991 Particle Accelerator Conf., San Francisco, 1991 (in press); AT-division technical note: AT-10 Technical Note:90-12.

7. H. V. Smith, "H^0 Temperature and Density Measurements in a Penning Surface-Plasma H^- Ion Source. I.," Rev. Sci. Instruments 61 (1990) 425-426.

8. L. Walling, P. Allison, A. Shapiro, "Transverse Coupling Impedance Measurement Studies of Low-Q Cavities," Proc. 1990 Linac Conf., Albuquerque, N. M. (in press).

9. J. F. DeFord, G. D. Craig, and R. McLeod, "The AMOS (Azimuthal Mode Simulator) Code," Proc. 1989 Particle Accelerator Conf., Chicago, Il., March 20-23, 1989, 2281-1183.

10. D. J. Liska and G. O. Bolme, "The Surface Treatment of Copper for High-Q Applications in Cryogenic RF Cavities," Second Neutral Particle Beam Technical Symposium, May 20-24, 1990, Los Alamos National Laboratory document LA-CP-90-214.

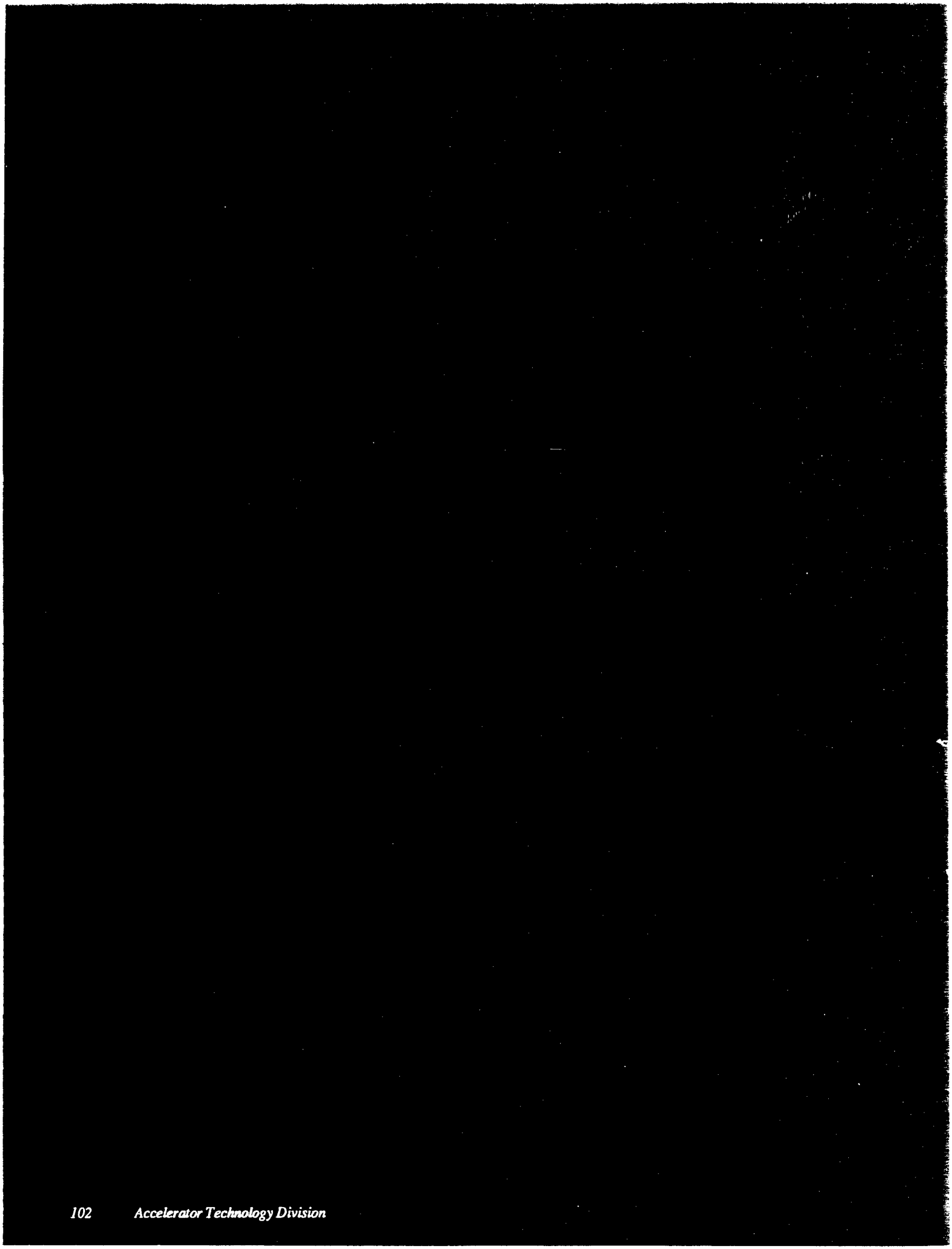

Appendix A
Publications

AT-1

E. Gray, "Tuning of PILAC Cavities," PILAC Technical Workshop, Los Alamos National Laboratory, September 9–11, 1990, Los Alamos National Laboratory document LA-UR-90-4132.

B. Rusnak, "Superconducting Cavity Development at LANL," PILAC Technical Workshop, Los Alamos National Laboratory, September 9–11, 1990, Los Alamos National Laboratory document LA-UR-90-4132.

G. Spalek et al., "A Coaxial Line Azimuthal Field Stabilizer for RFQs," 1990 Linear Accelerator Conference, Albuquerque, NM, September 10–14, 1990, Los Alamos National Laboratory document LA-UR-90-3095.

B. Rusnak et al., "Radio Frequency Superconducting Structures Development Laboratory Capability at Los Alamos National Laboratory," 1990 Linear Accelerator Conference, Albuquerque, NM, September 10-14, 1990, Los Alamos National Laboratory document LA-UR-90-3037.

T. Bhatia, "Error and Tolerance Estimates for the 425 MHz 2.5 MeV GTA RFQ," NPB Technical Symposium and Scientific Exchange, San Diego, CA, May 20-24, 1990, Los Alamos National Laboratory document LA-CP-90-46.

T. Bhatia, G. Neuschaefer, R. Garnett, K. Crandall, "Error and Tolerance Estimates for the SSC Coupled-Cavity Linac," (Poster) 1990 Linear Accelerator Conference, Albuquerque, NM, September 10-14, 1990, Los Alamos National Laboratory document LA-UR-90-1905.

T. Bhatia, G. Neuschaefer, R. Garnett, K. Crandall, "Error and Tolerance Estimates for the SSC Coupled-Cavity Linac," 1990 Linear Accelerator Conference, Albuquerque, NM, September 10-14, 1990, Los Alamos National Laboratory document LA-UR-90-3475.

B. Campbell, "Engineering the Intertank Matching Section for the Ground Test Accelerator," 1990 Neutral Particle Beam Technical Symposium and Scientific Exchange, San Diego, CA, May 20-24, 1990, Los Alamos National Laboratory document LA-CP-90-363.

R. Garnett, R. Mills, and T. Wangler, "Beam Dynamics Simulation of the LAMPF Linear Accelerator," 1990 Linear Accelerator Conference, Albuquerque, NM, September 10-14, 1990, Los Alamos National Laboratory document LA-UR-90-3100.

E. Gray, D. Cooke, and P. Arendt, "Power- and Magnetic Field Induced Microwave Absorption in T1-Based High-Tc Superconducting Films," Applied Physics Letter, LA-UR-90-3003.

J. Johnson, R. Maggs, and J. Plato, "The Demonstration of Automatic Cycling of a Surface Plasma Source," Grumman Corporation in Fulfillment of Contract No. DE-F104-90AL65039, Los Alamos National Laboratory document LA-UR-90-2758.

S. Nath and T. Wangler, "Superconducting CCL Design and Beam Dynamics Simulations," 1990 Neutral Particle Beam Technical Symposium and Scientific Interchange, San Diego, CA, May 20-24, 1990, Los Alamos National Laboratory document, LA-CP-90-260.

G. Neuschaefer, S. Nath, J. Billen, T. Bhatia, and J. Watson, "SSC Drift Tube Linac Physics Design," 1990 Linear Accelerator Conference, Albuquerque, NM, September 10-14, 1990, Los Alamos National Laboratory document LA-UR-90-3098.

B. Rusnak, G. Spalek, J. Rose, et al., "Measurement of Surface Conductivity at Cryogenic Temperatures using a Coaxial Resonant Cavity," 1990 Neutral Particle Beam Technical Symposium and Scientific Interchange, San Diego, CA, May 20-24, 1990, Los Alamos National Laboratory document LA-UR-90-385.

B. Rusnak, J. Rose, G. Spalek, G. Bolme, et al., "Evaluation of RF Seals for Resonant Cavity Applications," 1990 Linear Accelerator Conference, Albuquerque, NM, September 10-14, 1990, Los Alamos National Laboratory document LA-UR-90-3038.

D. Schrage, L. Young, P. Roybal, et al., "The 1300-MHz Photoinjector Linac for the LANL High-Brightness Accelerator FEL (HIBAF) Facility," December 1989, Los Alamos National Laboratory document LA-UR-89-4075.

D. Schrage, K. Christensen, L. Young, et al., "Design and Fabrication of a RFQ Cold Model for the CWDD Accelerator," 1990 NPB Technical Symposium and Scientific Interchange, San Diego, CA, May 20-24, 1990, Los Alamos National Laboratory document, LA-CP-90-392.

G. Spalek, G. Bolme, G. Boicourt, et al., "Measurement of Surface Conductivity at Cryogenic Temperatures Using a Coaxial Resonant Cavity," 1990 Neutral Particle Beam Technical Symposium and Scientific Interchange, San Diego, CA, May 20-24, 1990, Los Alamos National Laboratory document LA-CP-90-385.

G. Spalek, A. Klapetzky, J. Rose, "A Coaxial Line Azimuthal Field Stabilizer for Radio-Frequency Quadrupoles (RFQ's)," 1990 Linear Accelerator Conference, Albuquerque, NM, September 10-14, 1990, Los Alamos National Laboratory document LA-UR-90-3095.

G. Spalek, A. Klapetzky, J. Rose, "Azimuthal Stabilization of the Radio-Frequency Quadrupole with Loop-Coupled Tem Lines," 1990 Linear Accelerator Conference, Albuquerque, NM, September 10-14, 1990, Los Alamos National Laboratory document LA-UR-90-3080.

J. E. Stovall, "Commissioning Proton Linear Accelerators," 1990 Neutral Particle Beam Technical Symposium and Scientific Interchange, San Diego, CA, May 20-24, 1990, Los Alamos National Laboratory document LA-CP-90-404.

L. Walling, B. Campbell, G. Bolme, et al., "Design and Test Results of a Robust, High Field RF Deflector," Neutral Particle Beam Technical Symposium and Scientific Interchange, San Diego, CA, May 20-24, 1990, Los Alamos National Laboratory document LA-CP-90-201.

L. Walling, P. Allison, A. Shapiro, and M. Burns, "Transverse Impedance Measurements Studies of Low-Q Cavities for DARHT," 1990 Linear Accelerator Conference Albuquerque, NM, September 10-14, 1990, Los Alamos National Laboratory document LA-UR-90-3101.

T. Wangler and S. Nath, "Superconducting CCL Design and Beam Dynamics Simulation," 1990 Nuetral Particle Beam Symposium and Scientific Interchange, San Diego, CA, May 20-24, 1990, Los Alamos National Laboratory document LA-CP-90-260.

T. Wangler, G. Lawrence, T. Bhatia, J. Billen, et al., "Linac Physics Design for Accelerator Production of Tritium," Neutral Particle Beam Technical Symposium and Scientific Interchange, San Diego, CA, May 20-24, 1990, Los Alamos National Laboratory document LA-CP-90-181.

T. Wangler, G. Lawrence, T. Bhatia, J. Billen, et al., "Linear Accelerator for Production of Tritium: Physics Design Challenges," 1990 Linear Accelerator Conference, Albuquerque, NM, September 10-14, 1990, Los Alamos National Laboratory document LA-UR-90-3096.

L. Young, "Compact Photoinjector Accelerators for FEL's," Eleventh International Conference on the Applications of Accelerators in Research and Industry, Denton, Texas, November 5-8, 1990, Los Alamos National Laboratory document LA-UR-90-3332.

L. Young, and A. Cucchetti, "Design of a 10 MeV Photoinjector Accelerator for ELFA," 1990 Linear Accelerator Conference, Albuquerque, NM, September 10-14, 1990, Los Alamos National Laboratory document LA-UR-90-3078.

L. Young and J. Browman, "Coupled Radio-Frequency Quadrupoles as Compensated Structures," 1990 Linear Accelerator Conference, Albuquerque, NM, September 10-14, 1990, LA-UR-90-1574.

L. Young, B. Carlsten, B. McVey, and E. Svaton, "Magnetic Bunchers for the Generation of High Peak Current, Low Emittance Electron Pulses at Medium Energy," 1990 Linear Accelerator Conference, Albuquerque, NM, September 10-14, 1990, Los Alamos National Laboratory document LA-UR-90-1699.

L. Young, D. Schrage, K. Christensen, et al., "Design and Fabrication of a RFQ Cold Model for the CWDD Accelerator," 1990 Neutral Particle Beam Technical Symposium and Scientific Interchange, San Diego, CA, May 20-24, 1990, Los Alamos National Laboratory document LA-CP-90-392.

L. Young, "Tuning and Stabilization of RFQs," 1990 Linear Accelerator Conference, Albuquerque, NM, September 10-14, 1990, Los Alamos National Laboratory document LA-UR-90-3077.

AT-3

R. E. Shafer, "Beam Position Monitoring," Brookhaven Instrumentation Workshop, October 23-26, 1989, Los Alamos National Laboratory document LA-UR-89-3472.

Cliff Fortgang et al.,"Heavy Beam Loading Measurements of an rf Accelerating Cavity Under Amplitude and Phase Control," Review of Scientific Instruments Argonne Laboratory, Argonne, IL , November 1990, Los Alamos National Laboratory document LA-UR-89-4286.

Walter P. Lysenko, "The New Bedlam Optics Code," NPB Technical Symposium, May 21-24, 1990, San Diego, CA, Los Alamos National Laboratory document LA-CP-90-321.

P.L. Walstrom and H.L. Pallmeyer, "The GTA Steering Magnet-Scale Model and Full-Sized Magnet," NPB Technical Symposium, May 21-24, 1990, San Diego, CA, Los Alamos National Laboratory document LA-CP-90-342.

J. D. Gilpatrick, R. Connolly, K. F. Johnson, J. Power, and O. Sander, "Performance of the Single Beam Funnel Diagnostics, " NPB Technical Symposium, May 21-24, 1990, San Diego, CA, Los Alamos National Laboratory document LA-CP-90-366.

R.H. Kraus and B. Campbell, "A Variable-Field Permanent-Magnet Quadrupole for Application in the GTA Intertank and Optics Matching Sections," NPB Technical Symposium, May 21-24, 1990, San Diego, CA, Los Alamos National Laboratory document LA-CP-90-349.

D.B. Barlow, R. H. Kraus, C.T. Lobb, M.T. Menzel, P.L. Walstrom, "A Small-Bore High-Field Superconducting Quadrupole Magnet," NPB Technical Symposium, May 21-24, 1990, San Diego, CA, Los Alamos National Laboratory document LA-CP-90-351.

V. Yuan, R. Garcia, K. Johnson, K. Saasatmand, O. Sander, D. Sandoval, and M. Shinas, "Measurement of Longitudinal Emittance Growth in a Drift Space Following the ATS Drift-Tube Linac," NPB Technical Symposium, San Diego, CA, May 21-24, 1990. Los Alamos National Laboratory document LA-CP-90-401.

V. Yuan, R. Garcia, K. Johnson, K. Saasatmand, O. Sander, D. Sandoval, and M. Shinas, "Characterization of the ATS Drift-Tube Linac Using LINDA," NPB Technical Symposium, San Diego, CA, May 21-24, 1990, Los Alamos National Laboratory document LA-CP-90-402.

W. P. Lysenko and P.J. Channell, "New Bedlam," Conference on Codes and the Linear Accelerator Community, Jan. 22-25, 1990, Los Alamos, NM, Los Alamos National Laboratory document LA-UR-90-1247.

E.A. Wadlinger et al., "First, Second, and Third Order Achromatic Bend Systems (9/14-19/90) For Free-Electron Laser Application," 1990 LINAC Conference, Albuquerque, NM, September 14-19, 1990, Los Alamos National Laboratory document LA-UR-90-1689.

J. D. Gilpatrick et al., "Design and Performance of a Microstrip Beam Position Monitor Probe," 1990 LINAC Conference, Albuquerque, NM, September 14-19, 1990, Los Alamos National Laboratory document LA-UR-90-1903.

Barbara Blind, "Production of Uniform and Well-Confined Beams by Nonlinear Optics," 11th International Conference on the Application of Accelerators in Research and Industry, Denton, TX, November 5-8, 1990, Los Alamos National Laboratory document LA-UR-90-2180 .

R. H. Kraus, "Rare Earth Permanent Magnet Materials for Particle Accelerator Applications," Sixth International Symposium on Magnetic Anisotropy and Coercivity in Rare Earth Transition Metal Alloys, October 25,1990, Pittsburg, PA, Los Alamos National Laboratory document LA-UR-90-2605.

Walter Lysenko, "Moment Methods for Simulation and Design," 1990 LINAC Conference, Albuquerque, NM, September 14-19, 1990, Los Alamos National Laboratory document LA-UR-90-2739.

D. B. Barlow et al., "A Superconducting Quadrupole Magnet for Use In Superconducting Coupled-Cavity Linacs," 1990 LINAC Conference, Albuquerque, NM, September 14-19, 1990, Los Alamos National Laboratory document LA-UR-90-2740.

Barbara Blind, "Generation of a Rectangular Beam Distribution for Irradiation of the Accelerator Production of Tritium Target," 1990 LINAC Conference, Albuquerque, NM, September 14-19, 1990, Los Alamos National Laboratory document LA-UR-90-2759.

Darryl Sandoval, "Laser-Induced Neutralization Diagnostics Approach (LINDA)," Workshop on Accelerator Instrumentation, October 1-4, 1990, Batavia, IL, Los Alamos National Laboratory document LA-UR-90-2827.

J.F. Power, "Compact Cryogenic Toroid for Beam Current Measurements," Workshop on Accelerator Instrumentation, October 1-4, 1990, Batavia, IL, Los Alamos National Laboratory document LA-UR-90-2853.

P. Walstrom, F. Neri, T. Mottershead, "High Order Optics of Multipole Magnets," 1990 Linac Conference, Albuquerque, NM, September 9-14, 1990, Los Alamos National Laboratory document LA-UR-90-2888.

F. D. Wells and R. E. Shafer, "Log-Ratio Beam Position Detector," Workshop on Accelerator Instrumentation, October 1-4, 1990, Batavia, IL, Los Alamos National Laboratory document LA-UR-90-2890.

S.K. Brown and E. A. Wadlinger, "The Use of a Spreadsheet in the Design of Accelerator Components," 1990 LINAC Conference, Albuquerque, NM, September 14-19, 1990, Los Alamos National Laboratory document LA-UR-90-3043.

C. Fortgang, L. Dauelsberg, C. Geisik, D. Liska, and R. Shafer," Pulsed Taut-Wire Alignment of Multiple Permanent Magnet Quadropoles," 1990 Linac Conference, Albuquerque, NM, September 9-14, 1990, Los Alamos National Laboratory document LA-UR-90-3074.

Barbara Blind, "Production of Uniform and Well-Confined Beams by Nonlinear Optics," Eleventh International Conference on the Application of Accelerators in Research and Industry, Denton, Texas, November 5-8, 1990, Los Alamos National Laboratory document LA-UR-90-3293.

Darryl P. Sandoval et al., "Laser-Induced Neutralization for H^- Beam Emittance Measurement," Workshop on Accelerator Instrumentation, Batavia, IL, October 1-4, 1990, Los Alamos National Laboratory document LA-UR-90-3297.

F. D. Wells, R. E. Shafer, J. D. Gilpatrick, and R. B. Shurter, "Log-Ratio Circuit for Beam Position Monitoring," Workshop on Accelerator Instrumentation, October 1-4, 1990, Batavia, IL, Los Alamos National Laboratory document LA-UR-90-3340.

R. E. Shafer, "Diagnostics for High-Brightness Beams," 1990 Linac Conference, Albuquerque, NM, September 9-14, 1990, Los Alamos National Laboratory document LA-UR-90-3564.

F. D. Wells, R. E. Shafer, J. D. Gilpatrick, and R. B. Shurter, "Log-Ratio Circuit for Beam Position Monitoring," Workshop on Accelerator Instrumentation, Batavia, IL, September 1990, Los Alamos National Laboratory document LA-UR-90-3821.

Peter L. Walstrom, "Magnetic Fields and Inductances of Cylindrical Current Sheet Magnets," Los Alamos National Laboratory document LA-UR-90-4090.

AT-4

G. A. Bennett, "IR Surface Temperature Calibration," MAES National Convention, Albuquerque, NM, March 30, 1990, Los Alamos National Laboratory document LA-UR-90-365.

N. G. Wilson, W. W. Lemons, and C. Bridgman, "Rapid Energy Release in a Helium Refrigerator Cryogenic Vacuum Pump Used to Pump Hydrogen with Common Unbaked Vacuum System Residual Gases," 37th Annual AVS Symposium, Toronto, Canada, October 8-12, 1990, Los Alamos National Laboratory document LA-UR-90-1593.

H. W. Harris, N. K. Bultman, and G. Spalek, "E-Beam Accelerator Cavity Development for the Ground Based Free Electron Laser," 1990 Linac Conference, Albuquerque, NM, September 10-14, 1990, Los Alamos National Laboratory document LA-UR-90-1925.

W. Fox, N. Bultman, B. Campbell, R. Gentzlinger, K. Christensen, H. Kimerly, D. Liska, and H. Mignardot, "The Mechanical Engineering Design of the GTA 24-MeV Accelerator," 1990 Linac Conference, Albuquerque, NM, September 10-14, 1990, Abstract LA-UR-90-1927.

G. A. Bennett and T. H. Larkin, "Rotary Joint Thermal Test," Naval Research Laboratory, Radar Division, Los Alamos National Laboratory document LA-UR-90-451.

G. A. Bennett, "Electronics Survival in Hot Boreholes," Section of IEEE Book, High Temperature Electronics, Los Alamos National Laboratory document LA-UR-90-482.

N. G. Wilson and R. H. Kraus, Jr., "GTA Telescope Engineering," Second Neutral Particle Beam Technical Symposium, San Diego, CA, May 20-24, 1990, Los Alamos National Laboratory document LA-CP-90-267.

D. J. Liska and G. O. Bolme, "The Surface Treatment of Copper for High-Q Applications in Cryogenic RF Cavities," Second Neutral Particle Beam Technical Symposium, San Diego, CA, May 20-24, 1990, Los Alamos National Laboratory document LA-CP-90-214.

D. J. Liska, K. E. Christensen, and W. E. Fox, "Status Report on the Drift Tube Linac for the Ground Test Accelerator at Los Alamos," Second Neutral Particle Beam Technical Symposium, San Diego, CA, May 20-24, 1990, Los Alamos National Laboratory document LA-CP-90-215.

H. Mignardot, D. J. Liska, K. E. Chirstensen, D. R. Preecehtel, W. D. Purdy, and P. F. Smith, "GTA-24 Drift Tubes for Cryogenic Operation," Second Neutral Particle Beam Technical Symposium, San Diego, CA, May 20-24, 1990, Los Alamos National Laboratory document LA-CP-90-216.

B. Campbell, "Engineering the Intertank Matching Section for the Ground Test Accelerator," Second Neutral Particle Beam Technical Symposium, San Diego, CA, May 20-24, 1990, Los Alamos National Laboratory document LA-CP-90-363.

N. K. Bultman, "Mechanical Fabrication Aspects of the GTA RFQ," Second Neutral Particle Beam Technical Symposium, San Diego, CA, May 20-24, 1990, Los Alamos National Laboratory document LA-CP-90-391.

K. E. Christensen, D. L. Schrage, L. M. Young, A. G. Cimabue, J. W. Rathke, and E. G. Haas, "Design and Fabrication of a RFQ Cold Model for the CWDD Accelerator," Second Neutral Particle Beam Technical Symposium, San Diego, CA, May 20-24, 1990, Los Alamos National Laboratory document LA-CP-90-392.

W. E. Fox, "The Pros and Cons of Cryogenic Accelerators: An Engineering Point of View," 1990 Linac Conference, Albuquerque, NM, September 10-14, 1990, Los Alamos National Laboratory document LA-UR-90-3082.

AT-5

D. E. Rees and C. Friedrichs, "Increasing Output Power of a 850 MHz Tetrode with a Floating Deck Modulator," 1990 Linac Conference, Albuquerque, NM, September 10-14, 1990, Los Alamos National Laboratory document LA-UR-90-3046.

B. R. Cheo and S. P. Jachim, "Dynamic Interactions Between RF Sources and Linac Cavities with Beam Loading," Los Alamos National Laboratory document LA-UR-90-2347.

P. J. Talerico, "Recent Advances in RF Power Generation," European Particle Accelerator Conference, Los Alamos National Laboratory document LA-UR-90-2667.

P. J. Tallerico and C. R. Rose, "Progress on the GTA 850 MHz RF System," Los Alamos National Laboratory document LA-UR-90-231.

C. D. Ziomek, "Interfacing RF Control Electronics to the VXIbus for the Ground Test Accelerator," Los Alamos National Laboratory document LA-UR-90-217.

S. P. Jachim, A. H. Regan, W. D. Gutscher, E. F Natter, M. T. Curtin and P. M. Denney, "A Phase Stable Transport System," Los Alamos National Laboratory document LA-CP-90-213.

D. E. Rees and C. Friedrichs, "The Design and Test Result of a 425 MHz Tetrode Amplifier," Los Alamos National Laboratory document LA-CP-90-203.

AT-6

P. J. Channell and C. Scovel, "Symplectic Integration of Hamiltonian Systems," Nonlinearity, vol. 3, pp. 231-260, May 1990.

Rangarajan Chan, "Transient State of a Bunched Electron Beam Subject to Resistive-Wall Instability," Los Alamos National Laboratory document LA-UR-89-1853.

"Unbunched Beam Electron-Proton Instability in the PSR and Advanced Hadron Facilities," Los Alamos National Laboratory document LA-UR-89-2089.

D. V. Neuffer, "A Solution to Nonlinearity Problems," Los Alamos National Laboratory document LA-UR-89-2795.

K. C. D. Chan, "Minimized Emittance Growth with Elliptical Beam Pipes in Free-Electron Lasers," Los Alamos National Laboratory document LA-UR-89-2867.

H. Takeda and L. Thode, "The Electron Beam Quality Degradation in a Long Undulator," Los Alamos National Laboratory document LA-UR-89-3324.

B. Carlsten, L. Young, M. Jones, B. Blind, E. Svaton, K. C. D. Chan, L. Thode, "Accelerator Design and Calculated Performance of the Los Alamos HIBAF Facility," Los Alamos National Laboratory document LA-UR-89-3379B.

D. V. Neuffer, "Extended Methods and Applications in Nonlinear Correction," Los Alamos National Laboratory document LA-UR-89-4251.

K. C. D. Chan, L. Thode, M. Schmitt and J. Ostic, "Free-Electron Laser System-Design Code," abstract submitted to the American Physical Society for their Spring Meeting in April 1990, in Washington DC, Los Alamos National Laboratory document LA-UR-90-69.

G. Boicourt and J. Merson, "PARMILA Users and Reference Manual," produced for general distribution as a code manual LA-UR-90-127.

K. C. D. Chan , "Looking Back to 1989...," submitted to the Los Alamos Computer Codes and the Linear Accelerator Community Conference January 1990, Los Alamos National Laboratory document LA-UR-90-137.

J. Merson "PARMILA Documentation," submitted to the Los Alamos Computer Codes and the Linear Accelerator Community Conference in January 1990, Los Alamos National Laboratory document LA-UR-90-159.

K. Chan and R. Cooper, "Time-Domain Calculation of Sub-Nanosecond Pulse Launched by a Proton Beam," submitted to the First Los Alamos Symposium on Ultra-Wideband Radar, Los Alamos, NM, March 1990, Los Alamos National Laboratory document LA-UR-90-197.

K. C. D. Chan, "Beam-Induced Energy Spreads at Beam-Pipe Transitions," submitted to the Proceedings of the Impedance and Bunch Instability Workshop held at Argonne National Laboratory, October 31-November 1, 1989, Los Alamos National Laboratory document LA-UR-90-315.

K. C. D. Chan and R. K. Cooper, "Electromagnetic Modeling in Accelerator Designs," Los Alamos National Laboratory document LA-UR-90-1308.

K. C. D. Chan and R. K. Cooper, "Time Domain Calculation of Subnanosecond Pulse Launched by a Proton Beam," Los Alamos National Laboratory document LA-UR-90-1469.

L. Thode, K. C. D. Chan, M. Schmitt, R. McKee, J. Ostic, J. Elliott, and B. McVey, "Free-Electron Laser Physical Process Code FELPPC," Los Alamos National Laboratory document LA-UR-90-1483.

M. Jean Browman and Lloyd M. Young, "Coupled Radio-Frequency Quadrupoles as Compensated Structures," submitted to the 1990 Linear Accelerator Conference, Los Alamos National Laboratory document LA-UR-90-1574.

K. C. D. Chan, "Cumulative Beam Breakup of the Ground-Based Free-Electron Laser," submitted to 12th International FEL Conference, September 17-21, 1990, Paris, France, Los Alamos National Laboratory document LA-UR-90-1728.

R. Wallace and K. C. D. Chan, "Wakefield Effects of Auxiliary Beamline Elements," submitted to 12th International FEL Conference, September 17-21, 1990, Paris, France, Los Alamos National Laboratory document LA-UR-90-1729.

P. Schoessow and K. C. D. Chan, "Computer Simulations of New Dielectric Accelerator Devices," submitted to the 1990 Linear Accelerator Conference, Los Alamos National Laboratory document LA-UR-90-1730.

H. Takeda, "The Beam Quality Simulation of Boeing Photo-Injector Accelerator for the MCTD Project," submitted to 12th International FEL Conference, September 17-21, 1990, Paris, France, Los Alamos National Laboratory document LA-UR-90-1731.

H. K. Deaven and K. C. D. Chan, "Computer Codes Used in Particle Accelerator Design and Analysis: A Compendium," produced as a manual for general distribution, Los Alamos National Laboratory document LA-UR-90-1766.

L. S. Walling, B. M. Campbell, G. O. Bolme, and M. J. Browman, "Design and Test Results of a Robust, High-Field RF Deflector for Beam Funneling," submitted to the 1990 Linear Accelerator Conference, Los Alamos National Laboratory document LA-UR-90-1909.

Bruce E. Carlsten, Lloyd M. Young, M. Jean Browman, and H. Takeda, "INEX Simulations of Experimentally Measured Accelerator Performance at the Los Alamos HIBAF Facility," submitted to the 12th International FEL Conference, September 17-21, 1990, Paris, Los Alamos National Laboratory document LA-UR-90-1909.

T. Wangler, G. Lawrence, T. Bhatia, K. C. D. Chan, R. Garnett, F. Guy, D. Liska, M. Shubaly, S. Nath, G. Neuschaefer, "Linear Accelerator for Production of Tritium: Physics Design Challenges," submitted to the 1990 Linear Accelerator Conference, Los Alamos National Laboratory document LA-UR-90-1908.

Richard K. Cooper, K.C. Dominic Chan, Jean L. Merson, "Component Analysis and Simulation Results for a Beacon-Illuminator Accelerator," Los Alamos National Laboratory document LA-UR-90-2247.

AT-7

W. D. Joel Johnson, "Robust Control of Particle Accelerators," 1990 American Controls Conference, San Diego, CA, May 23-25, 1990, Los Alamos National Laboratory document LA-UR-90-751.

D. W. Feldman, W. D. Cornelius, S. C. Bender, B. E. Carlsten, R. L. Sheffield, and P. G. O'Shea, "Los Alamos High-Brightness Accelerator FEL (HIBAF) Facility," LASE 90', Los Angeles, CA, January 18-23, 1990, Los Alamos National Laboratory document LA-UR-90-997.

B. E. Carlsten, R. L. Sheffield, and B. D. McVey, "Photoelectric Injector Designs at Los Alamos National Laboratory," Bendor Workshop, Bendor, France, June 18-22, 1990, Los Alamos National Laboratory document LA-UR-90-3180.

R. L. Sheffield, "Progress in Photoinjectors for Linacs," 1990 Linear Accelerator Conference, Albuquerque, NM, September 10-14, 1990, Los Alamos National Laboratory document LA-UR-90-3296.

W. D. Joel Johnson, "Dual Klystron Modulator," 1990 Linear Accelerator Conference, Albuquerque, NM, September 10-14, 1990, Los Alamos National Laboratory document LA-UR-90-3440.

P. G. O'Shea, "Robust RF Control of Accelerators," 1990 Linear Accelerator Conference, Albuquerque, NM, September 10-14, 1990, Los Alamos National Laboratory document LA-UR-90-3474.

AT-8

W. H. Atkins, "Example of the Ease of Applying the GTA Control System," Second Neutral Particle Beam Technical Symposium, San Diego, California, May 21-24, 1990, Los Alamos National Laboratory document LA-CP-90-182.

W. H. Atkins, "Example of the Ease of Applying the GTA Control System," (Viewgraphs), Second Neutral Particle Beam Technical Symposium, San Diego, California, May 21-24, 1990, Los Alamos National Laboratory document LA-CP-90-332.

S. K. Brown and E. A. Wadlinger, "The Use of a Spreadsheet in the Design of Accelerator Components," Linear Accelerator Conference, Albuquerque, NM, September 10-14, 1990, Los Alamos Laboratory document LA-UR-90-3043.

S. K. Brown, "Description of a Spreadsheet that Provides for the Calculation of RFQ Parameters," Los Alamos National Laboratory document LA-UR-90-3598.

M. E. Zander, "Imagetool: Image Processing on the Sun," Los Alamos National Laboratory document LA-UR-90-3836.

AT-9

M.V. Fazio, R.M. Stringfield, D.G. Rickel, J. Kinross-Wright, and R.F. Hoeberling, "High Power Microwave Source Development at Los Alamos," Fifth National Conference on High Power Microwave Technology, West Point, NY, June 10-15, 1990, Los Alamos National Laboratory document LA-CP-90-235.

R.M. Stringfield, M.V. Fazio, D.G. Rickel, T.J.T. Kwan, A.L. Peratt, J. Kinross-Wright, F.W. VanHaaften, R.F.Hoeberling, R. Fachl, B.C. Carlsten, W.W. Destler, and L.B. Warner, "High Power Amplifiers For Accelerator Applications: The Large Orbit Gyrotron And The High Current, Space Charge Enhanced Relativistic Klystron," 1990 Linear Accelerator Conference, Albuquerque, NM, September 10-14, 1990, Los Alamos National Laboratory document LA-UR-90-3099.

M.V. Fazio, J. Kinross-Wright, B. Haynes, and R.F. Hoeberling, "The virtual cathode amplifier experiment," Journal of Applied Physics, 66, 2675-2678 (1989).

Fred Van Haaften, R.F. Hoeberling, and M.V. Fazio, "A High-Voltage, High-Current Electron Beam Modulator for Microwave Source Development," Fifth National Conference on High Power Microwave Technology, West Point, NY, June 10-15, 1990, Los Alamos National Laboratory document LA-CP-90-229.

M.V. Fazio, J. Farnham, B. Freeman, R.F. Hoeberling, J. Kinross-Wright, D.G. Rickel, and R.M. Stringfield, "A Long-Pulse, Frequency-Stabilized Virtual Cathode Oscillator Using A Resonant Cavity," 8th Intl. Conference on High Power Particle Beams, Novosibirsk, USSR, July 2-5, 1990, Los Alamos National Laboratory document LA-UR-90-2044.

AT-10

O. R. Sander, Transverse Emittance Workshop on Accelerator Instrumentation, 10/23-25/89 BNL, Los Alamos National Laboratory document LA-UR-89-3278.

H. Vernon Smith, Jr., Paul Allison, E. J. Pitcher, R. R. Stevens, Jr., G. J. Worth, G. C. Stutzin, A. T. Young, A. S. Schlachter, K. N. Leung, and W. B. Kunkel, "H° Temperature and Density Measurement in a Penning Surface-Plasma Ion Source II," 5th International Symposium on the Production & Neutralization of Negative Ions & Beams, 10/30/89 - 11/3/89, BNL, Los Alamos National Laboratory document LA-UR-89-3673.

G. O. Bolme, G. P. Boicourt, K. F. Johnson, R. A. Lohse, and O. R. Sander, "Measurement of rf Accelerator Cavity Field Levels at High Power from the Charasteristic X-Ray Emissions," NPB Technical Symposium, San Diego, CA, May 21-24, 1990, Los Alamos National Laboratory document LA-CP-90-382.

G. O. Bolme, G. P. Boicourt, L. Booth, N. K. Bultman, E. Foley, D. J. Liska, R. A. Lohsen, J. B. Niesen, B. Rusnak, G. Spalek, N. G. Wilson, and J. Rose, "Measurement of Surface Conductivity at Cryogenic Temperatures using a Coaxial Resonant Cavity," NPB Technical Symposium, San Diego, CA, May 21-24, 1990, Los Alamos National Laboratory document LA-CP-90-385.

V. Yuan, R. Garcia, K. F. Johnson, K. Saadatmand, O. R. Sander, D. Sandoval, and M. Shinas, "Measurement of Longitudinal Emittance Growth in a Drift Space Following the ATS Drift-Tube LINAC," NPB Technical Symposium, San Diego, CA, May 21-24, 1990, Los Alamos National Laboratory document LA-CP-90-401.

V. Yuan, R. Garcia, K, Saadatmand, O. R. Sander, D. Sandoval, and M. Shinas, "Characterization of the ATS Drift-Tube LINAC using LINDA," NPB Technical Symposium, San Diego, CA, May 21-24, 1990, Los Alamos National Laboratory document LA-CP-90-402.

Oscar R. Sander, "Transverse Emittance: its Definition, Applications, and Measurement," First Annual Accelerator Instrumentation Workshop, Brookhaven National Laboratory, Los Alamos National Laboratory document LA-UR-90-1476.

H. Vernon Smith, "Spatial Distributions of the Emitting Species in a Penning Surface-Plasma Source," Second European Particle Accelerator Conference, Kourosh Saadatmand, Nice, 1990, Los Alamos National Laboratory document LA-UR-90-1878.

K. Saadatmand, J. D. Schneider, C. Geisik, and R. R. Stevens, Jr., "Flour and Wire-Shadow Diagnostic for Low-Energy Ion Beams," 1990 Linear Accelerator Conference, Albuquerque, NM, September 1990, Los Alamos National Laboratory document LA-UR-90-3081.

D. B. Blackwell, W. L. Rogers, V. W. Brown, G. A. Ekeroth, and T. O. McGill, "Application of a Relational Database for Documenting the Ground Test Accelerator Cable Routing and Wiring Interconnections," 1990 Linear Accelerator Conference, Albuquerque, NM, September 1990, Los Alamos National Laboratory document LA-UR-90-3094.

K. Saadatmand, J. D. Schneider, C. Geisik, and R. R. Stevens, Jr., "Beam Structure Studies of Low-Energy Ion," Eleventh International Conference on the Application of Accelerators in Research and Industry, 11/5-8/1990, Albuquerque, NM, September 1990, Los Alamos National Laboratory document LA-UR-90-3312.

K. F. Johnson, O. R. Sander, G. O. Bolme, J. D. Gilpatrick, F. W. Guy, J. H. Marquardt, K. Saadatmand, D. Sandoval, and V. Yuan, "The Single-Beam Funnel Demonstration: Experiment and Simulation," 1990 Linear Accelerator Conference, Albuquerque, NM, September 1990, Los Alamos National Laboratory document LA-UR-90-3334.

G. O. Bolme, G. P. Boicourt, K. F. Johnson, R. A. Lohsen, O. R. Sander, and L. S. Walling, "Measurement of rf Accelerator Cavity Field Levels at High Power From the Characteristic X-ray Emissions," 1990 Linear Accelerator Conference, Albuquerque, NM, September 1990, Los Alamos National Laboratory document LA-UR-90-3410.

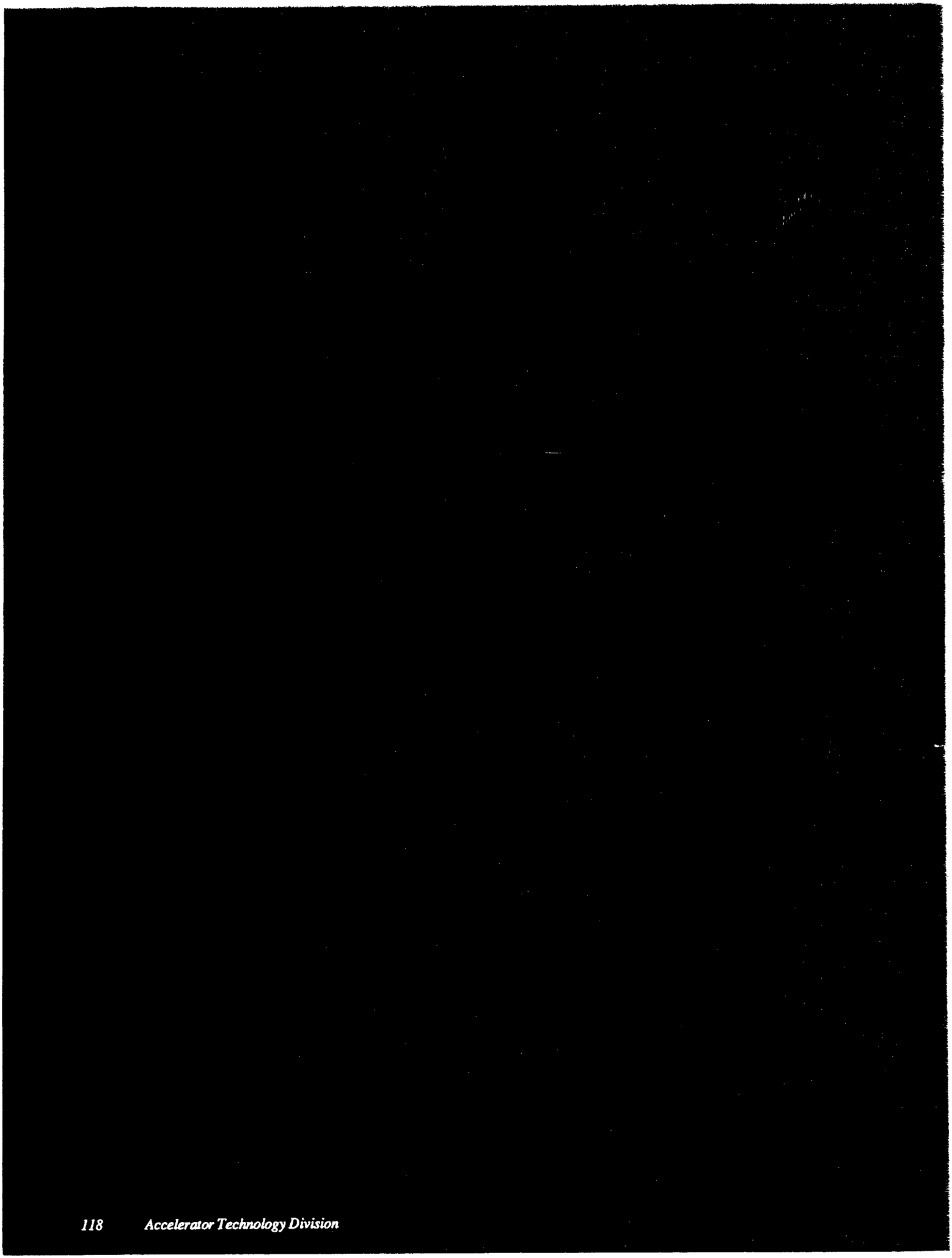

Appendix B
Glossary

A – Analysis and Assessment Division
AFEL – advanced free-electron laser
AK – anode-cathode
AMI – automated microwave instrumentation
AMOS – azimuthally symmetric mode simulator
APS – Argonne Photo Source
APT – accelerator production of tritium
ASAT – antisatellite
AT – Accelerator Technology
ATS – accelerator test stand
ATW – accelerator transmutation of nuclear waste

BBU – beam breakup
BEAR – Beam Experiment Aboard a Rocket

CCL – coupled-cavity linac
CCS – cryo cooling system
CCTB – cryogenic component test-bed
CERN – European Center for Nuclear Research
CFS – Central File System
CLS – Chemical and Laser Sciences
CORE – common run-time environment
CR – coaxial resonator
CRFQS – cryogenic radio-frequency quadrupole sparker
CTSS – CRAY time-sharing system
cw – continuous wave
CWDD – Continuous-Wave Deuterium Demonstrator

DARHT – dual-axis radiograph hydro-test
DoD – Department of Defense
DOE – Department of Energy
DTL – drift-tube linac

ELFA – Electron Linac for Acceleration
EMP – electromagnetic pulse
EMR – electromagnetic radiation
ERAB – Energy Research Advisory Board

FEL – free-electron laser
FELPPC – free-electron laser physical process code
FMIT – fusion materials irradiation test
FPAC – Fusion Power Advisory Committee

GBFEL – ground-based free-electron laser
GPIB – general purpose interface bus
GTA – Ground Test Accelerator

HIBAF – High-Brightness Accelerator Free-Electron Laser
HIF – heavy ion fusion
HPCTB – high-power cryogenic test-bed
HPM – high-power microwave
HPSL – High-Power rf Structures Laboratory

I/O – input/output
IOC – input/output controller
IMS – intertank matching section
INEX – integrated numerical experiment
INFN – National Institute of Nuclear Physics
IRP – independent research project
ISRD – Institutional Supported Research and Development
I&Q – in-phase and quadrative

LAACG – Los Alamos Accelerator Code Group
LAMPF – Clinton P. Anderson Meson Physics Facility
LANL – Los Alamos National Laboratory
LEB – low-energy booster
LEBT – low-energy beam transport
LEP_2 – large electron-positron collider
linac – linear accelerator
LINDA – laser-induced neutralization diagnostic approach
LLRF – low-level radio frequency
LOG – large periodic dipole
LPD – log periodic dipole
LSS – laser subsystem

M – Dynamic Testing Division
MCTD – Modular Concept Test Development
MMACS – multi-media access centers
MOPA – master-oscillator power-amplifier
MP – Medium Energy Physics Division
MST – Materials Science and Technology Division

N – Nuclear Technology and Engineering Division
NAS – National Academy of Science
NCLR – Netherlands Center for Laser Research
NERSC – The National Energy Research Supercomputer Center
NMT – Nuclear Materials Technology Division
NPB – neutral particle beam
NRL – Naval Research Laboratory

OPI – operator interface

P – Physics Division
PARMILA – phase and radial motion in linear accelerators
PEI – photoelectric injector
PFN – pulse-forming network
PIC – particle in the cell
PILAC – pion linac
PLC – programmable logic controller
PMQ – permanent-magnet quadrupole
PSD – power systems demonstrator

rf – radio-frequency
RFQ – radio-frequency quadrupole
RKA – relativistic klystron amplifier

SAIC – Science Application International Corporation
SAS – small angle ion source
SBFEL – space-based free-electron laser
SCR –
SCRF – superconducting radio-frequency
SDI – Strategic Defense Initiative
SDIO – Strategic Defense Initiative Organization
SPS – surface plasma source
SSC – Superconducting Super Collider
SSRI – Special Supporting Research Initiative
SST – Space Science and Technology Division

T – Theoretical Division
TA – Technical area

USASDC – US Army Strategic Defense Command

VME – Versa Module European
VUV – vacuum ultraviolet
VL&E – vulnerability, lethality, and effects

WEMPE – wideband electromagnetic pulse environment

X – Applied Theoretical Physics Division

U.S. GOVERNMENT PRINTING OFFICE: 1991 – 573-208/20051